# Bedrock Channel of the Par River: Its Forms and Processes

**A thesis submitted to**

**Tilak Maharashtra Vidyapeeth, Pune**

**For the Degree of Doctor of Philosophy (Ph.D.)**

**in**

## Geography

**Board of Moral, Social and Earth Sciences Studies**

**By**


## Archana Dilip Patil


**Under the Guidance of**

**Dr. Pramodkumar S. Hire**

**August 2017**

# Bedrock Channel of the Par River: Its Forms and Processes

**A thesis submitted to**

**Tilak Maharashtra Vidyapeeth, Pune**

**Board of Moral, Social and Earth Sciences Studies**

**For the degree of Vidyavachaspati (Ph.D.)**

**in**

## Geography

**By**


## Archana Dilip Patil


**Under the Guidance of**

**Dr. Pramodkumar S. Hire**


**Associate Professor and Head, Department of Geography**
**HPT Arts and RYK Science College**
**Nashik - 422 005.**


**August 2017**

## DECLARATION

I hereby declare that the thesis entitled "Bedrock Channel of the Par River: Its Forms and Processes" completed and written by me has not previously been formed as the basis for the award of any degree or other similar title upon me of this or any other Vidyapeeth or examining body. I understand that if my Ph.D. Thesis (or part of it) is found duplicate at any point of time my research degree will be withdrawn.

Place: Pune
Date: 31st August 2017

Archana D. Patil
(Research Student)

## CERTIFICATE

This is to certify that the thesis entitled "Bedrock Channel of the Par River: Its Forms and Processes" which is being submitted herewith for the award of the Degree of Vidyavachaspati (Ph.D.) in Geography of Tilak Maharashtra Vidyapeeth, Pune, is the result of original research work completed by Ms. Archana D. Patil under my supervision and guidance. To the best of my Knowledge and belief the work incorporated in this thesis has not formed the basis for the award of any degree or similar title of this or any other University or examining body upon him.

Place: Pune
Date: 31st August 2017

Dr. Pramodkumar S. Hire
(Research Guide)

# ACKNOWLEDGEMENTS

Foremost, I would like to express my sincere gratitude to my respected teacher Dr. Pramodkumar S. Hire, Head, Department of Geography, HPT Arts and RYK Science College, Nasik, for giving me an opportunity to work under his guidance. I am thankful to him, for his painstaking guidance, scholarly inputs, never-ending determination and many insightful conversations during the development of the ideas in this thesis. It was my privilege to get full benefit of his resounding knowledge and huge experience in the field. I am indebted to him not only for the academic guidance but also for giving proper direction in personal development. He will always remain as a source of motivation to me. Without his guidance and constant feedback this PhD would not have been achievable. I am grateful to him for giving me an opportunity to work on the research project of this topic, which was partially supported by Board of College and University Development (BCUD), Savitribai Phule Pune University (SPPU), Pune, Grant No. 14SCI000138. BCUD is gratefully acknowledged for the support given for the field work and data collection.

I would like to express my special thanks to Professor Vishwas S. Kale for his many critical and constructive comments and valuable suggestions during the field as well as during the course of this work.

I owe special thanks to all my teachers especially Professor Shrikant Karlekar, Dr. (Mrs.) Bhagyashree Yargop and Professor Veena U. Joshi for their academic guidance. My sincere thanks are due to all the authors whose work has been reproduced from their published research papers, reports and books.

This work would not have been possible without the help of Tilak Maharashtra Vidyapeeth, Pune and Savitribai Phule Pune University, Pune. I am grateful to authorities of these Universities. I convey special thanks to officials of India Meteorological Department (IMD), Central Water Commission (CWC), National Water Development Agency (NWDA), Irrigation Departments of Maharashtra and Gujarat States for supply of meteorological, hydrological and other data.

I am thankful to Professor S.R. Khadilkar, Dr. Rajendra Gunjal and Mr. Uttam Pawar for their everlasting support for completion of this work.

I am obliged to Ms. Snehal Kasar, Dr. Pradnya Ahirrao, Ms. Priyanka Hire, Mrs. Ujwala Hire, Mr. Ajit Babar, Mr. Laxman Shendge, Mr. Abhijit Borse, Mr. Prasad Patil, Mr. Vitthal Anwat and Mr.Vishal Pagare for their invaluable assistance in the field. Thanks are also due to Mr.

Nilesh Susware, Mr. Sandeep Pawar, Ms. Ketaki Joshi/Maste, Dr. Nikhil Shejwalkar for proving guidance in GIS applications.

I would like to thank Sir Dr. M.S. Gosavi, Secretary and Dr. (Mrs.) D.P. Deshpande, Zonal Secretary, Gokhale Education Society, Nashik, for their blessings and encouragement to complete this research work. I am grateful to Principal Dr. Ram Kulkarni, RNC Arts, JDB Commerce and NSC Science College, Nashik Road and Principal V.N. Suryavanshi, HPT Arts and RYK Science College, Nashik for their support for this work. I express thanks to Dr. V.N. Bhamare, Head, Department of Geography, Mr. Sudhakar Borse and Mr. Naresh Patil of RNC Arts, JDB Commerce and NSC Science College, Nashik Road and staff members of the Department of Geography of RNC Arts, JDB Commerce and NSC Science College, Nashik Road and HPT Arts and RYK Science College, Nashik for their support and well wishes to the work.

I am thankful to IAG (International Association of Geomorphologists) for awarding financial support to present part of this work in the International conference of International Association of Geomorphologists regional conference at Barnaul, Russia. I am indebted to INQUA (International Union for Quaternary Science) for hundred percent financial support to attend Intensive Field Course (IFC) for young Geomorphologists to Russian Altai.

I owe a lot to my parents, who encouraged, helped and supported me at every stage of my personal and academic life, and waited patiently to see my achievements.
I would also like to say a heartfelt thank you to my sister Dr. Pradnya, my brothers Mr. Dhananjay and Mr. Abhijeet and my brother-in-law Mr. Sanjay for always believing in me and encouraging me to follow my dreams.

Last but not the least, due to my beloved Swaranjali, because of her love and affection I could complete this work.

**Archana D. Patil**

ABSTRACT

**BEDROCK CHANNEL OF THE PAR RIVER: ITS FORMS AND PROCESSES**

**1) Rationale and significance of the study**

A river is a natural water channel, usually freshwater, flowing towards an ocean, a lake, a sea, or another river. On the basis of the bed and bank materials, rivers are classified mainly into two categories namely alluvial and bedrock rivers and the combination of both may be called mixed bedrock-alluvial rivers. A bedrock river is a river that typically has little to no alluvium mantling the bedrock over which it flows. Such rivers are common in upland and mountainous regions. They are formed by incision into bedrock by a combination of abrasion as sediment in the flow collides with the channel bed and removes bits of material, and "quarrying" or "plucking" as large blocks of bedrock are pulled from the bed (often near ledges and waterfalls) and transported downstream. Bedrock rivers form when the river downcuts through the sediments and into the underlying bedrock. This phenomenon occurs in regions that have experienced some kind of uplift or which have hard lithology. The Par River has been selected for studies on bedrock channels. The river has its source in the Northern Maharashtra particularly in the western part of the Nashik District. The river is deeply incised into the upland plateau namely the Jawhar Plateau. It is intact in terms of study of bedrock channels and the knowledge of the river is scanty. Therefore, in view of the insufficient existing knowledge of the bedrock channel of the Par River and in order to study various aspects of the bedrock channels in terms of its form and processes, it is decided to undertake a detailed study of the Par River.

**2) Introduction to the study area**

The Par River from western India has been selected for the present study. It has its source near Harantekadi at an elevation of 982 m ASL. The Par River flows to the west through Maharashtra (46.45% area) and Gujarat (53.55% area) States and drains into the Arabian Sea near Umarsadi in the Gujarat State. The length of the river is 142 km.

The Par Basin extends over an area of 1664 $km^2$. It lies between $20^0 15' 41''$ and $20^0 35' 32''$ North latitude and between $72^0 53' 14''$ and $73^0 43' 19''$ East longitude. Physiographically, upper Par River and its tributaries flow on the Jawhar Plateau through meandering path, whereas, lower river flows on the Kokan Plains. The Par Basin is bordered by, roughly east-west trending, Surgana and Peth Ranges to north and south respectively and by Western Ghats to the East. The Par River and its tributaries have collectively created a dendritic drainage pattern. There are 12 major tributaries of the river. The largest tributary, i.e. the Nar rises very close to the source of the Par River, at Kem Hill (1177 m), and flows in east-west direction. It accounts for almost 25% of the total area of the Par Basin. The Par River and its tributaries are south-west summer monsoon fed (June to September). The basin is situated in an environment classic of monsoonal tropics, with periodic high-magnitude rainfall. The average annual rainfall of the basin is 2094 mm and 98% of the annual rainfall occurs during south-west summer monsoon season. The basin occasionally receives heavy rains due to cyclonic storms and depressions originating over the Bay of Bengal or adjoining land. The entire basin is underlain by horizontally bedded Cretaceous-Eocene Deccan Trap basalts. However, quaternary alluvium has been observed at a small reach of the Par River.

**3) Research questions**

The present study attempted to seek the answers to the following questions on the basis of field surveys, available secondary data and suitable research techniques.

- What are the channel morphological features of the bedrock Par River?
- What are the erosional processes and the modes of entrainment and transport of large clasts?
- How lithology controls erosional processes and channel morphology? and how bedrock channel of the Par River gives response to the tectonic upliftment?
- What are the hydrometeorological, hydrological and geomorphological characteristics of floods of the Par River?

**4) Hypothesis**

The present study has been based on a hypothesis which has given the direction to the work. Following hypothesis is formulated for the present research work.

- Changes in channel morphology in bedrock streams occur rapidly and episodically during infrequent intense large magnitude floods in contrast to the more frequent floods of low magnitude.

**5) Main objectives of the study**

- To record and explain the longitudinal variations in the morphologic features of the Par River.
- To investigate the characteristics of the Par River in term of erosional processes and sediment transport.
- To understand the role of lithology and the variations in the hydraulic conditions along the river.
- To examine the rainfall regime of the basin and to study meteorological characteristics associated with floods in the river basin.

**6) Data and methodology**

In order to attain the objectives of the present study, the following methodology have been adopted.

Numerous straight as well meandering channel reaches have been identified and measured with the help of field surveys, satellite images and topographical maps. In addition to this, the above mentioned planform of river under review have been mapped using software Google Earth and ArcGIS 9.3. Traditional bend statistics such as meander wavelength ($\lambda$), meander length ($L_m$), mean radius of curvature ($Rc_m$), channel width (W) and amplitude (A) have been calculated for meanders of the Par River using ArcGIS tool. Sinuosity index (Si) was calculated by the ratio of meander length ($L_m$) to meander wavelength ($\lambda$). The relations between meander wavelength ($\lambda$) and mean radius of curvature ($Rc_m$), channel width (W) and amplitude (A) have been expressed by power regression equations. Channel forms have been studied in terms of width, depth and form ratio for the Par River. Sixteen cross-sectional surveys have been carried out to study the

form of the channel. The main purpose of the present section is to recognize physical characteristics of morphology of different landforms and their formation processes. Therefore, in order to study erosional landforms, an extensive field survey was carried out from source to mouth of the river under review. Erosional as well as depositional landforms were identified in the field, measured, analysed and mapped with the help of toposheets, ArcGIS 9.3 and Google Earth.

As stated by Wohl (1998), the bedrock substrate is dominantly eroded by processes of (i) corrosion, or chemical weathering and solution, (ii) corrasion, or abrasion by sediment in transport along the channel, and (iii) cavitation and other hydrodynamic forces associated with flow turbulence. Other processes such as shear detachment or fluid stressing, quarrying or plucking, hydraulic wedging and knickpoint migration may contribute for bedrock erosion. Notably little information is available regarding the concrete processes by which bedrock channels are eroded. Due to lack of quantitative hydraulic data of rare floods for the Par River, data of cross sectional surveys were used for quantification. In addition to this, channel slope data have been measured in the field. The aforementioned data have been used to procure hydraulic and hydrodynamics parameters such as unit stream power ($\omega$), shear stress ($\tau$), Froude number (Fr), Reynolds number (Re) and critical velocity (Vc) to understand geomorphic efficacy of rare flood events. In order to find out sediment transport rates, sediment entrainment and flow capacity of bedrock channel of the Par River, thresholds of shear and entrainment of boulders have been computed using William's equations.

The morphology of channel is predominantly function of fluvial forces applied and bedrock resistance offered. The rock resistance to flow dynamics noticeably varies with respect to lithological considerations. The erodibility of rocks relies on the lithology which strongly controls the erosional processes. In order to study the role of lithology and efficiency of processes to shape the channel, the Schmidt hammer rebound values (N) were derived by using 'N' type Schmidt hammer (SH). The SH rebound values (N) were used to estimate the Rock Mass Strength (RMS). Statistical parameters of RMS such as range, standard deviation ($\sigma$) and coefficient of variation (Cv) have been calculated. In order to semi-quantitatively assess rock erodibility between basalt and dykes, two

parameters namely SH rebound values (N) and RMS have been used. The comparison between these two substrate resistance has been represented with the help of box-whisker plots.

Quantification of geomorphic response to tectonic activity is an immensely complicated task. However, the commonly-used geomorphic indices of active tectonics (GAT) have been developed as basic reconnaissance tools to assess the relationship between tectonics and basin morphology on the regional or basin scale and to identify areas experiencing tectonic deformation. The Par River Basin is very appropriate for this type of morphotectonic analysis and for making significant appraisals between basins and fluvial systems. Quantification of a number of geomorphometric indices for the river under review were made possible by means of the analysis of Digital Elevation Model (DEM) of ca. 30-m resolution Advance Spaceborne Thermal Emission and Reflection Radiometer (ASTER) data. The digital elevation data were used to extract information about drainage basin, network and river profile. This was achieved by using standard procedures in ArcGIS 9.3.

River incision into bedrock is a significant erosion process that has an impact on the rate of landscape response to changes in rock uplift rate and climate (Howard et al., 1994). Rainfall, therefore floods, is one of the conspicuous climatic elements playing a significant role in landscape development, whose characteristics, predominantly, the distribution in space and time are important from the standpoint of flood generation in the monsoonal regions. In general, the causes behind occurrence of floods are extraordinary synoptic situations, responsible for more precipitation to a drainage basin in comparison with the capacity of basin to absorb and store it (Hirschboeck, 1991). In order to understand the meteorological causes of floods, the analyses of synoptic conditions connected with large floods in the Par Basin was carried out. This encompasses analysis of (i) rainfall; (ii) analysis of storm tracts and; (iii) evaluation of the correlation between El Niño and monsoon rainfall in the basin. Meteorological data of five stations located within and close to the Par Basin have been obtained from India Meteorological Department (IMD), Pune and analysed to identify the rainfall characteristics that produce large floods on the Par River.

The Par River, similar to other monsoonal rivers, also subjected to high-magnitude floods at regular intervals. Thus, it is of paramount significant to know the hydrologic characteristics of floods in terms of magnitude, frequency, and distribution. In order to comprehend the flood hydrological characteristics, the annual maximum series (AMS) /stage data were procured from Irrigation Department of Gujarat State for a gauging site namely Nanivahial on Par River for 45 years. The limited gauge records have been used to evaluate floods and flood flow frequencies. In flood geomorphology, the measurement and evaluation of the geomorphic effectiveness of flows of different magnitude has been one of the significant themes. Large floods can generate noteworthy geomorphic impact on channel morphology and landscape. Therefore, to determine the geomorphic effect of floods, the geometry of river channels is considered to be a significant factor (Kochel, 1988). Therefore, to assess the channel geometry/morphology of the Par River, the cross sectional surveys were carried out and cross-sectional parameters of all the stations at high flood level (HFL) have been derived, analyzed and tabulated. At-a-station hydraulic geometry have been established since data regarding hydraulic geometry variables associated with annual maximum series (AMS) are available for a site on the Par River, viz. Nanivahial. This data have been obtained from Gujarat Irrigation Department and used to derive the at-a-station hydraulic geometry equations to understand the nature of adjustments in the hydraulic variables with discharge.

**7) Major findings of the study**

On the basis of analyses and results of the present study following major findings can be outlined for the river under review.

1) The Par River displays all the classical morphological erosional as well as depositional features of the bedrock river.
2) The morphology of the bedrock channel reaches of the Par River dominated by erosional processes such as corrosion or abrasion, cavitation, shear detachment or fluid stressing, quarrying or plucking, hydraulic wedging and knickpoint migration. The river is supply limited, indicating unusually high ability to erode and transport coarse sediment.

3) The river shows substantial difference in erodibility between basalt and dykes. It is further proved by control of dykes on the channel of Par River. The basin indeed undergone significant uplift till recent times and the consequences of tectonic activity have left noticeable imprints.
4) The Par River falls in the class of extraordinary hydrometeorological, hydrologic and geomorphic characteristics of floods which in turn results into noteworthy erosional processes, channel morphological features and bedrock incision.

**8) Arrangement of the text**

The present work is separated into six chapters. The first chapter is devoted to the introduction to the topic and introduction to the study area. Besides this, the chapter contains the main objectives of the study, a concise review of previous work done in the field of form and processes of bedrock channels and methodology, and the outline of the work.

In second chapter, morphological features generated by the Par River have been studied thoroughly. It includes bedrock channel planforms, channel geometry, erosional as well depositional landforms shaped by the river.

The third chapter deals with the dominant erosional processes which incise the bedrock channel and are responsible for formation of different landforms. This chapter describes the parameters of flood hydraulics and hydrodynamics and the process of coarse sediment transport within the channel.

The fourth chapter is primarily addressed the response of bedrock channel of the Par River to lithology and tectonic upliftment, which play critical role to change the form of the channel.

The fifth chapter is devoted to flood hydrometeorological, hydrological and geomorphological aspects of the Par River. Flood hydrometeorological aspects such as rainfall characteristics and synoptic situation associated with monsoon floods, the short- and long-term changes in the annual rainfall have been mentioned. The flood

hydrological aspect contents magnitude, frequency and distribution of floods. The flood geomorphological aspects includes channel morphology, hydraulic geometry, stream power and sediment transport.

The last concluding chapter presents the principal findings of the study. In this chapter an attempt has been made to highlight on the characteristics of the Par River in terms of morphological features generated by the Par River, erosional processes and sediment transport, role of lithology and tectonics, and hydrometeorological, hydrologic and geomorphic characteristics of floods occurred on the river under review.

## CONTENTS


| | Topic | | Page No. |
|---|---|---|---|
| **Chapter I** | **Introduction** | | **1-18** |
| | 1.1 | Rationale and significance of the study | 1 |
| | 1.2 | Introduction | 2 |
| | 1.3 | Research questions | 9 |
| | 1.4 | Hypothesis | 9 |
| | 1.5 | Main objectives of the study | 9 |
| | 1.6 | Introduction to the study area | 10 |
| | 1.7 | Arrangement of the text | 18 |
| **Chapter II** | **Review of Literature** | | **19-43** |
| | 2.1 | Introduction | 19 |
| | 2.2 | Channel morphological features | 20 |
| | 2.3 | Erosional processes and sediment transport | 27 |
| | 2.4 | Role of lithology and tectonics | 32 |
| | 2.5 | Flood hydrometeorology, flood hydrology and flood geomorphology | 36 |
| **Chapter III** | **Research Methodology** | | **44-67** |
| | 3.1 | Introduction | 44 |
| | 3.2 | Research Methodology | 44 |
| **Chapter IV** | **Analysis and Interpretation** | | **68-205** |
| | 4.1 | Introduction | 68 |
| | 4.2 | Channel morphological features | 68 |
| | 4.3 | Erosional processes and sediment transport | 127 |
| | 4.4 | Role of Lithology and Tectonics | 148 |
| | 4.5 | Flood Hydrometeorology, Hydrology and Geomorphology | 162 |
| **Chapter V** | **Overview and Conclusions** | | **206-230** |
| | 5.1 | Introduction | 206 |
| | 5.2 | Summary of results | 207 |
| | 5.3 | Limitations of the study | 227 |
| | 5.4 | Major findings of the study | 229 |
| **References** | | | **231-253** |

## LIST OF TABLES


| Table No. | Title of the Table | Page No. |
|---|---|---|
| **Chapter I** | **Introduction** | **1-18** |
| 1.1 | Morphometric properties of the Par Basin | 15 |
| 1.2 | Morphometric characteristics of the major tributaries of the Par River | 16 |
| **Chapter II** | **Review of Literature** | **19-43** |
| 2.1 | Scales of erosional features | 24 |
| 2.2 | Geomorphic indices of active tectonics (GAT) and their calculations | 34 |
| **Chapter III** | **Research Methodology** | **44-67** |
| **Chapter IV** | **Analysis and Interpretation** | **68-205** |
| 4.1 | Length(s) of straight channel reaches of Par and Nar Rivers | 71 |
| 4.2 | Meander geometry of the Par River | 75 |
| 4.3 | Empirical relations between size parameters for meanders of the Par River | 79 |
| 4.4 | Channel cross section and reach variables used in the present study | 86 |
| 4.5 | Channel morphologic variables of some cross sections of the Par and Nar River | 86 |
| 4.6 | Selected locations for bedrock channel erosional (Meso-scale) and depositional features | 90 |
| 4.7 | Statistical parameters of the various geometric properties of the potholes | 91 |
| 4.8 | Top 10 potholes in terms of diameter (cm) | 100 |
| 4.9 | Top 10 potholes in terms of length (cm) | 101 |
| 4.10 | Top 10 potholes in terms of width (cm) | 101 |
| 4.11 | Top 10 potholes in terms of depth (cm) | 102 |

| | | |
|---|---|---|
| 4.12 | Frequency of prominent shapes | 102 |
| 4.13 | Empirical relations between size parameters for potholes of the Par River | 104 |
| 4.14 | Statistical parameters of the various geometric properties of the longitudinal grooves | 105 |
| 4.15 | Statistical parameters of the various geometric properties of the inner channel | 109 |
| 4.16 | Knickpoints of the Par River | 113 |
| 4.17 | Channel width (W) and height of expansion bars | 117 |
| 4.18 | Channel width (W) and length, width and height of longitudinal bars | 123 |
| 4.19 | Area occupied by point bars | 124 |
| 4.20 | Highest threshold values of the hydraulic parameters associated with depositional features | 127 |
| 4.21 | Hydraulic parameters of rare floods on the Par and Nar Rivers | 128 |
| 4.22 | Boulder dimensions and the associated theoretical entrainment values | 129 |
| 4.23 | Froude numbers at cross sectional sites | 130 |
| 4.24 | Critical velocity for inception of cavitation (Vc) | 135 |
| 4.25 | Detachment, entrainment and deposition of blocks | 138 |
| 4.26 | Dimensions of knickpoints and associated gorges | 143 |
| 4.27 | Parameters of Stream Power Incision Model (SPEM) | 143 |
| 4.28 | Boulder dimensions | 146 |
| 4.29 | Rock Mass Strength (RMS) (in $N/mm^2$) variations between cross-sectional sites | 149 |
| 4.30 | Dimension, position and control of dykes with regard to Par River | 151 |
| 4.31 | Rock mass strength (RMS in $N/mm^2$) for dykes | 153 |
| 4.32 | Results of geomorphic indices of active tectonics (GAT) | 156 |

| | | |
|---|---|---|
| 4.33 | Rainfall characteristics at selected stations in the Par Basin (Monthly and annual averages in mm) | 164 |
| 4.34 | Annual rainfall characteristics at selected stations in the Par Basin (between 1901 and 2004) | 166 |
| 4.35 | Synoptic conditions associated with major floods on the Par River | 170 |
| 4.36 | Conditional probabilities of the monsoon rainfall over the Par Basin given the SST index of ENSO (N = 104 years) | 179 |
| 4.37 | Nature of changes/trends in annual rainfall records based on Mann- Kendall test | 179 |
| 4.38 | Percent change required to identify statically significant change in AAR of the Par Basin | 180 |
| 4.39 | Flood flow characteristics of the Par River at Nanivahial | 183 |
| 4.40 | Unit discharges for the Par River and Nar River | 185 |
| 4.41 | Estimated discharges in $m^3/s$ for different return periods (Based on GEVI distribution) | 187 |
| 4.42 | Return period of Qm, Qlf and Qmax (Based on GEVI) | 187 |
| 4.43 | Return periods for high floods on the Par River at Nanivahial based on Weibull's method | 189 |
| 4.44 | Channel morphologic variables of cross sections of the Par and Nar River | 196 |
| 4.45 | Exponent values of at-a-station hydraulic geometry | 202 |

# LIST OF ILLUSTRATIONS


| Figure No. | Title of the Figure | Page No. |
|---|---|---|
| **Chapter I** | **Introduction** | **1-18** |
| 1.1 | Geomorphic Setting of the Par Basin | 12 |
| 1.2 | Drainage Network of the Par River | 13 |
| 1.3 | Rain Gauge stations and Isohyets of the Par Basin | 14 |
| 1.4 | Geological Setting of the Par Basin | 17 |
| 1.5 | Quaternary alluvial deposits at Nanivahial, Par River | 18 |
| **Chapter II** | **Review of Literature** | **19-43** |
| **Chapter III** | **Research Methodology** | **44-67** |
| 3.1 | Sketch to define terms used in describing geometric characteristics of a meandering channel | 45 |
| **Chapter IV** | **Analysis and Interpretation** | **68-205** |
| 4.1 | Location of straight reaches on Par and Nar Rivers | 69 |
| 4.2 | Perfectly straight channel of the Par River near Khirman; Source: Google image; See Figure 4.1 (4) for location of reach | 70 |
| 4.3 | Two adjacent perfectly straight channels with a hairpin bend on the Nar River near Chavra; Source: Google image; See Figure 4.1 (23 and 24) for location of reaches | 70 |
| 4.4 | Straight channel of the Par River near Mendha; See Figure 4.1 (10) for location of reach | 72 |
| 4.5 | View of straight channel of the Nar River near Chavra; See Figure 4.1 (24) for location of reach | 72 |
| 4.6 | Location of meanders on Par River; M1 to M23 - number of meanders | 74 |
| 4.7 | Meander Train in the bedrock channel of the Par River on the Jawhar Plateau; Source: Google image; See Figure 4.7 (M8) for location of reach | 75 |
| 4.8 | Relation between meander wavelength ($\lambda$) and channel width (W) | 78 |

| | | |
|---|---|---|
| 4.9 | Relation between meander wavelength (λ) and mean radius of curvature ($Rc_m$) | 78 |
| 4.10 | Relations between amplitude (Am) and channel width (W) | 79 |
| 4.11 | Bedrock anastomoising/multi-thread channel of the Par River near Panchlai; Potholes not to scale; See Figure 4.19 for the location of reach | 80 |
| 4.12 | Location of cross-sectional sites on Par and Nar Rivers | 82 |
| 4.13 | Cross sections: Par River; See Figure 4.12 for location of sites; P = Par River; F = Form ratio | 83 |
| 4.14 | Cross section at Mendha (P7) on the Par River; See Figure 4.4 and Figure 4.12 for location of site; F = Form ratio; LB = Left bank; RB = Right bank | 84 |
| 4.15 | Cross sections: Nar River; See Figure 4.12for location of sites; N = Nar River; F = Form ratio | 84 |
| 4.16 | Downstream changes in width and depth | 85 |
| 4.17 | Downstream changes in width-depth ratio with discharge | 87 |
| 4.18 | Channel width versus drainage area for bedrock reaches of Par River | 88 |
| 4.19 | Location of sites of morphological features on Par River | 89 |
| 4.20 | Miniature potholes at Dongrale, Par River; Potholes not to Scale; See Figure 4.19 for location of site | 93 |
| 4.21 | View of miniature potholes at Dongrale near source; See Figure 4.19 for location of site | 93 |
| 4.22 | Geomorphic map of Par River from Ghatalbari to Jahule reach; Potholes not to scale; See Figure 4.19 for location of reach | 94 |
| 4.23 | Largest circular (diameter 380 cm) pothole in terms of diameter upstream of Ghatalbari knick; See Figure 4.19 for location of site | 95 |
| 4.24 | Ghatalbari Knick (height 8.4 m) during rainy season; See Figure 4.19 for location of site | 95 |
| 4.25 | Geomorphic map of Kalmane site; Potholes not to scale; See Figure 4.19 for location of site | 96 |

| | | |
|---|---|---|
| 4.26 | Largest pothole in terms of length (730 cm) and width (530 cm) upstream of Kalmane knick; See Figure 4.19 for location of site | 97 |
| 4.27 | Long and narrow gorge downstream of knick at Kalmane; See Figure 4.19 for location of site) | 97 |
| 4.28 | Geomorphic map of Par River at Shingharpada; Potholes and grooves not to scale; See Figure 4.19 for location of reach | 98 |
| 4.29 | Pot holes and inner channels shaped in exposed bedrock at Parvas; Potholes not to scale; See Figure 4.19 for location of reach | 98 |
| 4.30 | Size and shape variance of potholes at Parvas; See Figure 4.19 for location of site | 99 |
| 4.31 | Second largest potholes in terms of length (640 cm) at steep reaches of Parvas; See Figure 4.19 for location of site | 100 |
| 4.32 | Relation between diameter (K) and depth of potholes (D*) | 105 |
| 4.33 | Relation between Length (L) and depth of potholes (D*) | 104 |
| 4.34 | Geomorphic map of Par River at Nanivahial; Potholes and grooves not to scale; See Figure 4.19 for location of reach | 106 |
| 4.35 | View of longitudinal grooves eroded into exposed bedrock of the Par River at Parchapada (near source); See Figure 4.19 for location of site | 107 |
| 4.36 | Geomorphic map of Par River at Mangdhe; Grooves not to scale; See Figure 4.19 for location of site | 108 |
| 4.37 | Inner channel with undulating walls, Shingharpada, Par River; See Figure 4.19 for location of site | 110 |
| 4.38 | Longest (690 m) and deepest (9.20 m) inner channel at Mohankavchali, Par River; See Figure 4.19 for location of site | 110 |
| 4.39 | Geomorphic map of Par River at Mohankavchali; Par River; See Figure 4.19 for location of reach | 111 |
| 4.40 | Longitudinal Profile of the Par River | 111 |
| 4.41 | Highest near vertical knick at Kalmane (40 m); Note persons standing for scale; See Figure 4.19 for location of site | 113 |
| 4.42 | Knickpoint at Manjarpada, Par River; See Figure 4.19 for location | 114 |

of reach

4.43 Vertical and Second highest knickpoint at Manjarpada (21 m); Note persons standing for scale in circle; See Figure 4.19 for location of site 114

4.44 Geomorphic map of Par River at Chikadi; Potholes not to scale; See Figure 4.19 for location of reach 115

4.45 Relation between distance (L) and slope (S) (VI/HE) 116

4.46 Largest expansion bar downstream to constricted reach of Mendha Gorge; See Figure 4.19 for location of reach 118

4.47 Constricted gorge at Mendha; Flow direction from top to bottom of figure; See Figure 4.19 for location of reach 118

4.48 Frontage of expansion bar downstream to constricted reach of Mendha Gorge. Flow direction from bottom to top of figure; Note person for scale; See Figure 4.19 for location of reach 119

4.49 Geomorphic map of Par River at Parchapada; See Figure 4.19 for location of reach 120

4.50 Expansion bar at Jhiri; See Figure 4.19 for location of reach 121

4.51 Front view of expansion bar at Jhiri; Flow direction from top to bottom of figure; Note person for scale; See Figure 4.19 for location of reach 121

4.52 Geomorphic map of Par River at Dhamni, Par River; See Figure 4.19 for location of reach 122

4.53 Geomorphic map of Par River at Makadban; See Figure 4.19 for location of reach 123

4.54 Geomorphic map of Par River at Kachurpada; See Figure 4.19 for location of reach 124

4.55 Geomorphic map of Par River at Borpada; See Figure 4.19 for location of reach 125

4.56 Geomorphic map of Par River at Dhamni; See Figure 4.19 for location of reach 125

4.57 Standing wave-train upstream of Ghatalbari Knickpoint; Flow direction from top to bottom; See Figure 4.19 for location of site 131

| | | |
|---|---|---|
| 4.58 | Broken standing waves upstream of Ghatalbari knickpoint; Flow direction from top to bottom; See Figure 4.19 for location of site | 131 |
| 4.59 | Hydraulic drop and hydraulic jump at Chikadi; Note cow inside the circle for scale; See Figure 4.19 for location of reach | 133 |
| 4.60 | Hydraulic drop and hydraulic jump at Kalmane (40 m); See Figure 4.19 for location of reach | 133 |
| 4.61 | Giant boulder with 6200 mm i-axis, downstream of Mendha Gorge; See Figure 4.19 for location of site | 135 |
| 4.62 | Polished rock surface at Parvas; See Figure 4.19 for location of site | 137 |
| 4.63 | Huge pothole with grinding tools (sand to boulders); Flow direction from top to bottom; See Figure 4.19 for location of site | 137 |
| 4.64 | Highly Plucked plain bed of Par River at Parchapada; Flow direction from bottom to top; See Figure 4.19 for location of site | 139 |
| 4.65 | Plucked dyke (63.5 m) at Borpada; Flow direction from left to right; See Figure 4.19 for location of site | 139 |
| 4.66 | Extremely quarried dyke (20.4 m) near Dhamni; Flow direction from right to left; See Figure 4.19 for location of site | 140 |
| 4.67 | Remnant of plucked dyke (10.6 m) at Panchlai; Flow direction from right to left; See Figure 4.19 for location of site | 140 |
| 4.68 | The dyke (4.9 m) cutting across the Par River at Parvas. It raises high from the bed showing prominent control on the channel due to its resistance; See Figure 4.19 for location of site | 141 |
| 4.69 | Wedging process leading to development of cracks at Manjarpada; See Figure 4.19 for location of site | 142 |
| 4.70 | Upright knickpoint (51 m) at Kelavan on river Bhimtas (tributary of Par River); See Figure 4.71 and Figure 4.82 for location of reach | 144 |
| 4.71 | Geomorphic map of Bhimtas Gorge; See Figure 1.2 for location of river | 145 |
| 4.72 | Width(s) versus distance(s) of Bhimtas Gorge downstream of the knickpoint | 146 |
| 4.73 | Huge transported boulder with 1100 mm i-axis at Panchlai; See Figure 4.19 for location of site | 147 |

| | | |
|---|---|---|
| 4.74 | Collapsed bridge across the Par River due to 2004 flood (21775 $m^3/s$); Note the piller with 11900 mm X 4000 mm dimensions; Flow direction from right to left | 148 |
| 4.75 | Longitudinal variation in RMS ($N/mm^2$) | 150 |
| 4.76 | Resistant dyke (21.4 m) at Nanivahial; Flow direction from right to left; See Figure 4.19 for location of site | 152 |
| 4.77 | Extensively eroded dyke (23 m) in the form of outcrop at Dhamni; Flow direction from right to left; See Figure 4.19 for location of site | 152 |
| 4.78 | Comparison of substrate resistance between basalt and dykes (Schmidt hammer values) | 154 |
| 4.79 | Comparison of substrate resistance between basalt and dykes (Rock Mass Strength) | 155 |
| 4.80 | Hypsometric curve of the Par River | 157 |
| 4.81 | Tectonic tilting of the Par Bain, 61% area of basin is right side to trunk stream | 158 |
| 4.82 | Par Bain; Knickpoints: 1 Dongrale; 2 Manjarpada; 3 Parchapada; 4 Chikadi; 5 Ghatalbari; 6 Kalmane (Par R.); 7 Shirada (Amti R.); 8 Ranpada; 9 Chiknalpada; 10 Tamchhadi (Nar R.); 11 Kelavan; 12 Bhendshet; 13 Bhutran (Bhimtas R.); 14 Haste (Vajri R.); 15 Nalshet (Manmora Nala) | 159 |
| 4.83 | Rain gauge stations in Par Basin | 163 |
| 4.84 | Average annual rainfall (AAR) of five stations in the Par Basin | 165 |
| 4.85 | Interannual variability of Station Balsad; See the location of station in Figure 4.83 | 167 |
| 4.86 | Interannual variability of Station Dharampur; See the location of station in Figure 4.83 | 167 |
| 4.87 | Interannual variability of Station Pardi; See the location of station in Figure 4.83 | 167 |
| 4.88 | Interannual variability of Station Peth; See the location of station in Figure 4.83 | 168 |
| 4.89 | Interannual variability of Station Surgana; See the location of station in Figure 4.83 | 168 |

| | | |
|---|---|---|
| 4.90 | Interannual variability for the Par Basin (from 1901 to 2004) | 169 |
| 4.91 | Mean track of Low Pressure System (LPS) | 172 |
| 4.92 | Tracks of Low Pressure System (LPS) associated with large floods in the Par Basin | 174 |
| 4.93 | Discharge (Nanivahial) and Rainfall (Average annual rainfall of the basin) departure from mean | 175 |
| 4.94 | Normalized Accumulated Departure from Mean (NADM) and Discharge (Nanivahial) Graph | 176 |
| 4.95 | Categories of annual rainfall and ENSO index of the Par Basin; AAR = Average Annual Rainfall; Data source: India Meteorological Department (IMD) | 178 |
| 4.96 | Rating curve of the Par River at Nanivahial | 181 |
| 4.97 | Time series plot, Nanivahial; See Figure 4.12 for location of site | 182 |
| 4.98 | Variability of Peak Floods, Nanivahial Site; See Figure 4.12for location of site | 184 |
| 4.99 | Catchment areas upstream of cross-sectional sites | 186 |
| 4.100 | Annual Maximum Series, GEVI distribution, Nanivahial, Par River | 188 |
| 4.101 | World Envelope Curve with reference to Par Basin; Data source: Baker, 1995; Gujarat Irrigation Department; Field surveys | 190 |
| 4.102 | Downstream changes in width and depth | 192 |
| 4.103 | Downstream variations in width-depth relation with discharge | 194 |
| 4.104 | Cross sections, Par River; See Figure 4.12 for location of sites; F = Form ratio; HFL = High flood level | 197 |
| 4.105 | Par River at Kalmane; See Figure 4.12for location of site | 198 |
| 4.106 | Idealized cross-section of Par River at Mendha; See Figure 4.12 and 4.47 for location of site | 198 |
| 4.107 | The Par River at Dhamni; See Figure 4.12 for location of site | 199 |
| 4.108 | The cross-section of Par River at Nanivahial; See Figure 4.12 for location of site | 200 |

| | | |
|---|---|---|
| 4.109 | The Par River at Nanivahial (gauging site); See Figure 4.12 for location of site | 200 |
| 4.110 | Cross sections, Nar River; See Figure 4.12 for location of sites; F = Form ratio; HFL = High flood level | 201 |
| 4.111 | The Nar River at Tamchhadi; See Figure 4.12 for location of site | 201 |
| 4.112 | Cross-section of Par River for bankful stage at Nanivahial, See Figure 4.12 for location of site | 202 |
| 4.113 | Changes in width, mean depth and mean velocity with discharge at Nanivahial | 203 |
| 4.114 | The divided b-f-m diagram showing plotting position of at-a-station hydraulic geometry exponents for Nanivahial site | 205 |

Chapter 1

# Introduction

## 1.1 Rationale and significance of the study

A river is a natural water channel, usually freshwater, flowing towards an ocean, a lake, a sea, or another river. On the basis of the bed and bank materials, rivers are classified mainly into two categories namely alluvial and bedrock rivers and the combination of both may be called mixed bedrock-alluvial rivers.

An alluvial river is a river in which, the bed and banks are made up of mobile sediment and/or soil. Alluvial rivers have channels and floodplains that are self-formed in unconsolidated or weakly-consolidated sediments. Alluvial rivers erode their banks and deposit material on bars and their floodplains. A bedrock river is a river that typically has little to no alluvium mantling the bedrock over which it flows. Such rivers are common in upland and mountainous regions. They are formed by incision into bedrock by a combination of abrasion as sediment in the flow collides with the channel bed and removes bits of material, and "quarrying" or "plucking" as large blocks of bedrock are pulled from the bed (often near ledges and waterfalls) and transported downstream. Bedrock rivers form when the river downcuts through the sediments and into the underlying bedrock. This phenomenon occurs in regions that have experienced some kind of uplift or which have hard lithology. Rivers that go through patches of bedrock and patches of deep alluvial cover are classified as mixed bedrock-alluvial.

In the last two decades investigation on bedrock channels and fluvial erosion has seen a noteworthy increase in interest. It was accepted that these channels play a crucial role in the development of the entire landscape. They set the base-level for hillslope response, control the relief of a region and are major agents of sediment transport (Whipple, 2004). An idea of a dynamic combination between climate-driven erosion and tectonics received wide interest in the nineteen nineties (Molnar and England, 1990; Willett, 1999), and triggered exhaustive research in bedrock channels and fluvial erosion. Fluvial geomorphologists have recognized importance of bedrock channels because they behave quite differently than alluvial channels, which river

research had focused on for many decades (Tinkler and Wohl, 1998; Wohl and Merritts, 2001; Richardson and Carling, 2006; Turowski, 2010).

Previous work on Bedrock channels has been scanty and frequently focused on small-scale features of rock surface such as potholes, or upon the single catastrophic floods (Tinker and Wohl, 1998). Bedrock channels came into the focus of geomorphic research in the recent decades. Despite new insights, many research questions remain open. The subject of bedrock channels has a large but scattered literature dating back over a century. The world distribution of studies in bedrock channels has been shown by Tinker and Wohl (1998). Their map indicates that most of the bedrock channels investigations are from USA and Australia. Studies of bedrock channels from rest of the world are very limited. Like other countries of the world, the research on bedrock channels in India is also inadequate though the bedrock channels are existing in many areas.

The Par River has been selected for studies on bedrock channels. The river has its source in the Northern Maharashtra particularly in the western part of the Nashik District. The river is deeply incised into the upland plateau namely the Jawhar Plateau. The river is intact in terms of study of bedrock channels and the knowledge of the river is scanty. In addition to this, in August 1968, July 1976 and August 2004, major floods were reported from the Par River. Such events are rare and meteorologically, hydrologically, and geomorphologically extremely important. Such floods provide an opportunity to examine the role of floods in shaping bedrock channels. Therefore, in view of the insufficient existing knowledge of the bedrock channel of the Par River and in order to study various aspects of the bedrock channels in terms of its form and processes, it is decided to undertake a detailed study of the Par River.

## 1.2 Introduction

### *1.2.1 Definition(s) of bedrock channels*

In concord with prior definitions of bedrock channels (Gilbert, 1877; Howard, 1980; Howard et al., 1994; Montgomery et al., 1996), Whipple (2004) wrote the definition as “bedrock channels lack a continuous cover of alluvial sediments, even at low flow, and exist only where transport capacity (*Qc*) exceeds sediment flux (*Qs*) over the long

term (Qs/Qc<1)". A second definition by Tinkler and Wohl (1998) identifies "bedrock channels as those reaches along which a substantial proportion of the boundary (≥50%) is exposed bedrock, or is covered by an alluvial veneer which is largely mobilized during high flows such that underlying bedrock geometry strongly influences patterns of flow hydraulics and sediment movement." Both statements define bedrock channels according to the extent of alluvial cover on the bed and equate scarce cover with a physical condition in the river. However, Turowski et al. (2008) propose to define fluvial bedrock channels as "channels that cannot substantially widen, lower or shift its bed without eroding bedrock".

Turowski et al. (2008) emphasised the twofold role of sediment in bedrock channels and introduced the tool and cover effect of sediment to define the bedrock channels. According to him, increasing sediment supply will boost the number of impacts per unit bed area and time and with it the erosion rate (i.e. the tools effect). Nonetheless, a further increase of sediment supply may result in increased bed cover, protecting the bed from impacts, and decreasing the erosion rate (i.e. the cover effect).

### *1.2.2 Morphological Features of the Par River*

The morphological features of the bedrock channels are different than that of alluvial channels. Extensive literature is available on morphological features of alluvial channels as compared to bedrock-dominated channels. However, earth scientists have shown growing interest in bedrock rivers research in last one and half decades. Bedrock channel morphology reflects the interactions between erosive processes and the resistance of the channel substrate (Wohl, 1998). Five classes of single flow path bedrock channels according to reach morphology have been proposed by Wohl (1998) and Wohl and Merritt (2001). Duckson and Duckson (1995); Wohl (1998), Wohl and Grodek, (1994); Wohl and Legleiter (2002) and Wohl and Merritt (2001) have identified plane bed, pool-riffle, and step-pool channels in bedrock. Besides, Wohl et al. (1999) and Wohl and Merritt (2001) have observed channels with undulating walls and with inner channels as separate morphologies. In channel planform, straight, meandering and anastomoising channels have been studied by Moore, 1926; Wohl, 1998; Baker and Kale, 1998; Kale, 2005 and Barbour, 2008. A variety of fluvially sculpted surfaces and erosional bedfroms were observed in bedrock channels, controlled by substrate type, flow regime and dominant erosional processes (e.g.,

Allen, 1971; Richardson and Carling, 2005; Springer and Wohl, 2002; Tinkler, 1997b). Wohl (1998) have identified the bedrock channel forms that result from erosional processes at various spatial scales (Table 2.1). Alluvial channels are self-formed through independent adjustments of the morphological variables comprising their hydraulic geometry (Leopold and Maddock, 1953; Maddock, 1976). Bedrock river channels present various thresholds to effective channel adjustments. Therefore, only relatively rare, high-magnitude flood discharges contribute to shaping their morphologies. Therefore, an attempt has been made to study the morphological features of bedrock channel of the Par River in detail.

Bedrock rivers are predominantly erosional, however, they exhibit abundant depositional features. Infrequent large magnitude floods are associated with the processes of extensive erosion and deposition in resistant-boundary channels. In bedrock channels erosion process takes place in the constricted reaches. These reaches of high flow energy and competence accelerate the amount of sediment transported and deposited by flood. Therefore, an attempt has been made to measure and map the depositional features of the Par River.

### *1.2.3 Erosional Processes and Sediment Transport*

The bedrock channels are supply limited (since the transport capacity of flow is greater than the supply of sediment) and the morphology of bedrock channels is dominated by the processes of erosion. The bedrock substrate is dominantly eroded by processes of (i) corrosion, or chemical weathering and solution, (ii) corrasion, or abrasion by sediment in transport along the channel, and (iii) cavitation and other hydrodynamic forces associated with flow turbulence (Wohl, 1998). Other processes such as shear detachment or fluid stressing, quarrying or plucking, hydraulic wedging and knickpoint migration may contribute for bedrock erosion. According to Hancock et al. (1998) the processes such as abrasion and quarrying appear to be very active in the erosion of bedrock channels, the process of cavitation is potentially important and other processes (e.g., chemical dissolution) are undoubtedly significant in some other bedrock channels, however, they appear to be less significant in the channels with hard lithology. Some evidences exhibit that bedrock channel dimensions also scale with flow notwithstanding the high erosional thresholds and substrate heterogeneity in bedrock channels (Montgomery and Gran 2001; Wohl and David, 2008). Local

bedrock properties, however, also influence channel morphology (Montgomery and Gran 2001). Thus, feedbacks between bedrock channel characteristics and hydraulic parameters expected to govern the balance between scaling of channel dimensions and spatial variability of channel forms by flow (Goode and Wohl, 2010).

Notably little information is available regarding the concrete processes by which bedrock channels are eroded. The reason may be very slow and infrequent bedrock erosion on a human time scale as efficiently prohibits direct measurement (Wohl, 1998). Due to above reasons bedrock erosion processes can be studied from indirect sources such as channel form. Scientists are gradually getting acquainted with the significance of rare events such as floods in shaping the landscape. These floods produce surprisingly spectacular geomorphic response (Baker and Costa, 1987). During such floods, the sediment particles lying on the channel bed of rivers are put in motion through continual impacts, they erode the exposed bedrock. Little quantitative hydraulic data on rare floods on the Par River are available. Therefore, the analysis of local flow hydraulics and its spatial variation were obtained by calculating the hydrodynamic variables within the different segments of cross-section. We used the parameters of flood hydraulics and hydrodynamics such as unit stream power, shear stress, Froude number, Reynolds number and critical velocity to understand geomorphic efficacy of floods. Critical unit stream power, boundary shear stress and mean velocity values necessary to entrain cobbles and boulders were estimated on the basis of empirical relationships for coarse sediment transport.

### *1.2.4 Role of Lithology and Tectonics*

The morphology of channel is predominantly function of fluvial forces applied and bedrock resistance offered. The rock resistance to flow dynamics noticeably varies with respect to lithological considerations. The erodibility of rocks relies on the lithology which strongly controls the erosional processes. In this standpoint rocks are frequently referred to as ‘hard’ or ‘resistant’ or ‘weak’ and ‘non-resistant’ to erosional processes (Goudie, 2004). The rock resistance refers to the inherent property of the rock to resist any changes in its shape or size. It is significant property of rock to find out the efficiency of various processes like weathering and erosion. In order to find out effects of rock strength/role of lithology in shaping the landforms, weathering phenomena and relative dating, the Schmidt hammer (SH) has now been adopted by

Geomorphologists (e.g. Ericson, 2004). The instrument was devised by E. Schmidt in 1948. Primarily Schmidt hammer has been used by civil engineers to test the strength of concrete. However, from last few decades, Geomorpologists and Geologists have started using SH to estimate the strength of rocks for numerous reasons (Goudie, 2006). SH measures the distance of rebound of controlled impact on a surface and represents a relative measure of surface hardness or strength (Goudie, 2006). There are three versions of the Schmidt hammer i.e. N-type, L-type, and P-type. The 'N' type SH has most commonly been used by Geomorphologists. It has been used to study a wide range of rock types from weak to very strong with compressive strengths ranging from c. 20 to 250 MPa.

Along with lithology, tectonic uplift has also significant role in controlling the efficiency of erosional processes ultimately shaping the channels. Geomorphometric description of the tectonic characteristics of a landscape is an immensely complicated task. It is well recognized, however, that the commonly-used geomorphic indices of active tectonics (GAT) have been developed as basic reconnaissance tools to assess the relationship between tectonics and basin morphology on the regional or basin scale and to identify areas experiencing tectonic deformation (Bull and McFadden, 1977; Keller, 1986; Keller and Pinter, 1996; Burbank and Anderson, 2001; Della Seta et al., 2004; Kale and Shejwalkar, 2008). The results of several geomorphic indices can be combined to provide an assessment of a relative degree of tectonic activity in an area (Keller and Pinter, 1996). Therefore, an attempt has been made to ascertain the morphotectonic characteristics of the Par River by deriving the commonly used geomorphic indices of active tectonics (GAT). The analysis primarily addressed the response of bedrock channel of the Par River to lithology and tectonic upliftment, which play critical role to change the form of the channel.

### *1.2.5 Flood Hydrometeorology, Hydrology and Geomorphology*

River incision into bedrock is a significant erosion process that has an impact on the rate of landscape response to changes in rock uplift rate and climate (Howard et al., 1994). According to Whipple (2004), bedrock rivers play a dominant role in erosional landscape progression, moreover, (i) they set the baselevel for hillslopes; (ii) they transport sediment to depositional basins and (iii) they commune changes in-between tectonic and climatic boundary setting all over the landscape. Rainfall, therefore

floods, is one of the conspicuous climatic elements playing a significant role in landscape development, whose characteristics, predominantly, the distribution in space and time are important from the standpoint of flood generation in the monsoonal regions. Consequently, the main objective of the present study is to analyze the available meteorological data and to identify the rainfall characteristics that produce large floods on the Par River. The Par River and its tributaries are rainfed. Therefore, all floods on the river are caused by heavy to very heavy rainfall during the southwest monsoon season. A variety of flood-generating meteorological conditions are responsible for producing excessive, widespread rainfalls. These comprise, (a) active to vigorous monsoon conditions, (b) low pressure systems (LPS) originating over the Bay of Bengal, and (c) land depressions. The characteristics of flood-producing rainfalls and the associated synoptic situations are described below. Rainfall data were available for five rain gauge stations located within and close to the basin (Figure 5.1). The data were available for more than 100 years except Surgana Station for which data were available for 50 years. The data were collected from India Meteorological Department (IMD), Pune.

According to Leopold et al. (1964) and Schumm (1977) the channel form and the processes of erosion and transportation in a river are closely associated with the river regimes specifically to the flows which they transmit. The regional hydro-climatic regime conditions strongly control the river regime (Beckinsale, 1969). Numerous case studies in the last four decades have showed that the geomorphic effects of a discharge of a given magnitude and frequency differ from one regime to another (Hire, 2000). For instance, Wolman and Miller (1960) revealed that the frequently occurring low and moderate flows largely determine the transfer of sediments and the channel size under humid temperate regime. On the contrary, infrequent large magnitude floods maintain and control the channel size of rivers in arid tropical regime (Wolman and Gerson, 1978). In semi-arid tropics the channel morphologic properties are not directed by a particular discharge but by a series of discharges taking place at different intervals (Pickup and Riger, 1979). Similar conclusion has been proposed by Gupta (1995a) he suggested that in seasonal tropics the rivers are not only controlled by the seasonality of discharge but also high-magnitude floods. Hire (2000) opines for the Tapi River that the low- or moderate-magnitude flows transport most of the fine-grained sediment (clay, silt and sand) and modify the

channel bedforms to some extent. However, the channel size and shape is maintained by large-magnitude floods that occur at long intervals. Considerable attention has been given to morphology of bedrock channels and dynamics and to fluvial erosional erosional processes in recent years (Turowski et al., 2008 and references therein). These studies, therefore, point out that a systematic understanding of the main features of the fluvial and flood regime of a river is essential for the estimation of the pattern of geomorphic work. In the present study, hence, an attempt has been made to inspect the mean annual flow pattern and the flood regime of the Par River through the analysis of streamflow/discharge data.

Floods play a dominant role in shaping the river channel and the landscape in certain hydro-geomorphic environments, such as the seasonal tropics (Wohl, 1992b; Gupta, 1995a). In accordance with Bakers (1988) view, flood geomorphology is concerned with the processes, forms, effects, and causes of floods. The frequency and hydraulic properties of the high flows play foremost important role to shape the channel and to carry the sediment. Infrequent large floods that occur at an interval of several decades are associated with much higher levels of power expenditure and thus are capable of producing major channel changes and movement of coarse sediments (Baker and Kale, 1998). In flood geomorphology, the measurement and evaluation of the geomorphic effectiveness of flows of different magnitude has been one of the significant themes. Efficacy of events in shaping landforms is measured by the magnitude of flows, by the frequency with which they occur, and by the amount of suspended sediment they transport (Wolman and Miller, 1960). Recently, the potential of flood flows has also been assessed in terms of the channel boundary shear stress and stream power per unit boundary area (Baker and Costa, 1987), as well as the flood flow duration (Costa and O'Connor, 1995).

The Par River is primarily flood-controlled. Nonetheless, whether a large discharge occurrence on the river is geomorphologically effective can be determined by understanding the channel geometry, the hydraulic characteristics of floods and the dynamics of coarse sediment transport. Thus, in the present study, an attempt has been made to describe and analyze the channel size, shape and coarse sediment characteristics of the Par River to recognize the relative significance of low and high flows. Besides, hydraulic geometry and energy exerted by floods have also been determined for some sites to evaluate the geomorphic effectiveness of flows of different magnitude and return period.

### 1.3 Research questions

The present study attempted to seek the answers to the following questions on the basis of field surveys, available secondary data and suitable research techniques.

- What are the channel morphological features of the bedrock Par River?
- What are the erosional processes? and what are the modes of entrainment and transport of large clasts?
- How lithology controls erosional processes and channel morphology? and how bedrock channel of the Par River gives response to the tectonic upliftment?
- What are the hydrometeorological, hydrological and geomorphological characteristics of floods of the Par River?

### 1.4 Hypothesis

The present study has been based on a hypothesis which has given the direction to the work. Following hypothesis is formulated for the present research work.

- Changes in channel morphology in bedrock streams occur rapidly and episodically during infrequent intense large magnitude floods in contrast to the more frequent floods of low magnitude.

### 1.5 Main objectives of the study

- To record and explain the longitudinal variations in the morphologic features of the Par River.
- To investigate the characteristics of the Par River in term of erosional processes and sediment transport.

- To understand the role of lithology and the variations in the hydraulic conditions along the river.
- To examine the rainfall regime of the basin and to study meteorological characteristics associated with floods in the river basin.

## 1.6 Introduction to the study area

### *1.6.1 Geomorphic setting*

The Par River from western India has been selected for the present study. It has its source near Harantekadi at an elevation of 982 m ASL. The Par River flows to the west through Maharashtra (46.45% area) and Gujarat (53.55% area) States and drains into the Arabian Sea near Umarsadi in the Gujarat State (Figure 1.1). The length of the river is 142 km. The Nar River, with the length of 87 km, is the major northern tributary of the Par River. Other tributaries of the Par River are the Keng, the Bhensdara, the Walandi, the Bhimtas, the Dholdo, the Jamul, the Vajri, the Mani, the Julwan, the Matuniya and the Manmora, etc. (Figure 1.2). The Par Basin extends over an area of 1664 $km^2$. It lies between 20˚15′41″ and 20˚35′32″ North latitude and between 72˚53′14″ and 73˚43′19″ East longitude. Physiographically, upper Par River and its tributaries flow on the Jawhar Plateau through highly meandering path, whereas, lower river flows on the Kokan Plains (Figure 1.1).

The Par Basin is bordered by, roughly east-west trending, Surgana and Peth Ranges to north and south respectively and by Western Ghats to the East (Figure 1.1). The altitude of Surgana and Peth Hills ranges from 450 to 750< m ASL. The Western Ghats (>900 m ASL) is higher in altitude than Surgana and Peth ranges. The basin relief, i.e. Kem Hill (1177 m), is located as offshoot of Western Ghats. The Par and the Nar Rivers are separated by a small Barhe Plateau which ranges in altitude between 450 and 750 m ASL. One of the tributaries of Bhimtas River (a tributary of the Par River) has breached the Barhe Plateau to the east of 73˚20′ E longitude and has developed a gap known as “Avalkhindi Gap” near village Avalkhindi (Figure 1.1).

### *1.6.2 Climate*

The Par River and its tributaries are south-west summer monsoon fed (June to September). The basin is situated in an environment classic of monsoonal tropics, with periodic high-magnitude rainfall. The average annual rainfall of the basin is 2094 mm and 98% of the annual rainfall occurs during south-west summer monsoon season. July is the rainiest month throughout the basin followed by August and both the months account for 39% and 27% the total annual rainfall of the basin respectively.

Spatially, the annual rainfall displays a marked variation within the basin. This variation has been represented by isohyetal map of the Par Basin (Figure 1.3). Geographical location, orographic effect of Barhe Plateau (interfluves of Par and its major tributary Nar) and the east-west trending ranges in the Par Basin play significant role in rainfall distribution. For instance, Peth Range, Surgana Range and other interfluves act as barrier for the rain bearing south-west monsoon clouds (Figure 1.1). It attributes to maximum amount of rainfall in the middle of the Par Basin (2200 mm to 2300 mm). Being distant from the coast, the amount of rainfall reduces towards the source of the Par and Nar Rivers. It ranges between 1700 mm and 1800 mm. However, due to proximity of the coast the amount of rainfall is more at the western part of the basin ranging from 2000 mm to 2200 mm. Most part of the basin receives about 1800 mm to 2200 mm rainfall with average annual rainfall of 2094 mm (Figure 1.3). The basin occasionally receives heavy rains due to cyclonic storms and depressions originating over the Bay of Bengal or adjoining land and traverse toward the basin. The flood generating hydrometeorological conditions in the Par Basin have been discussed in greater details in the fourth chapter.

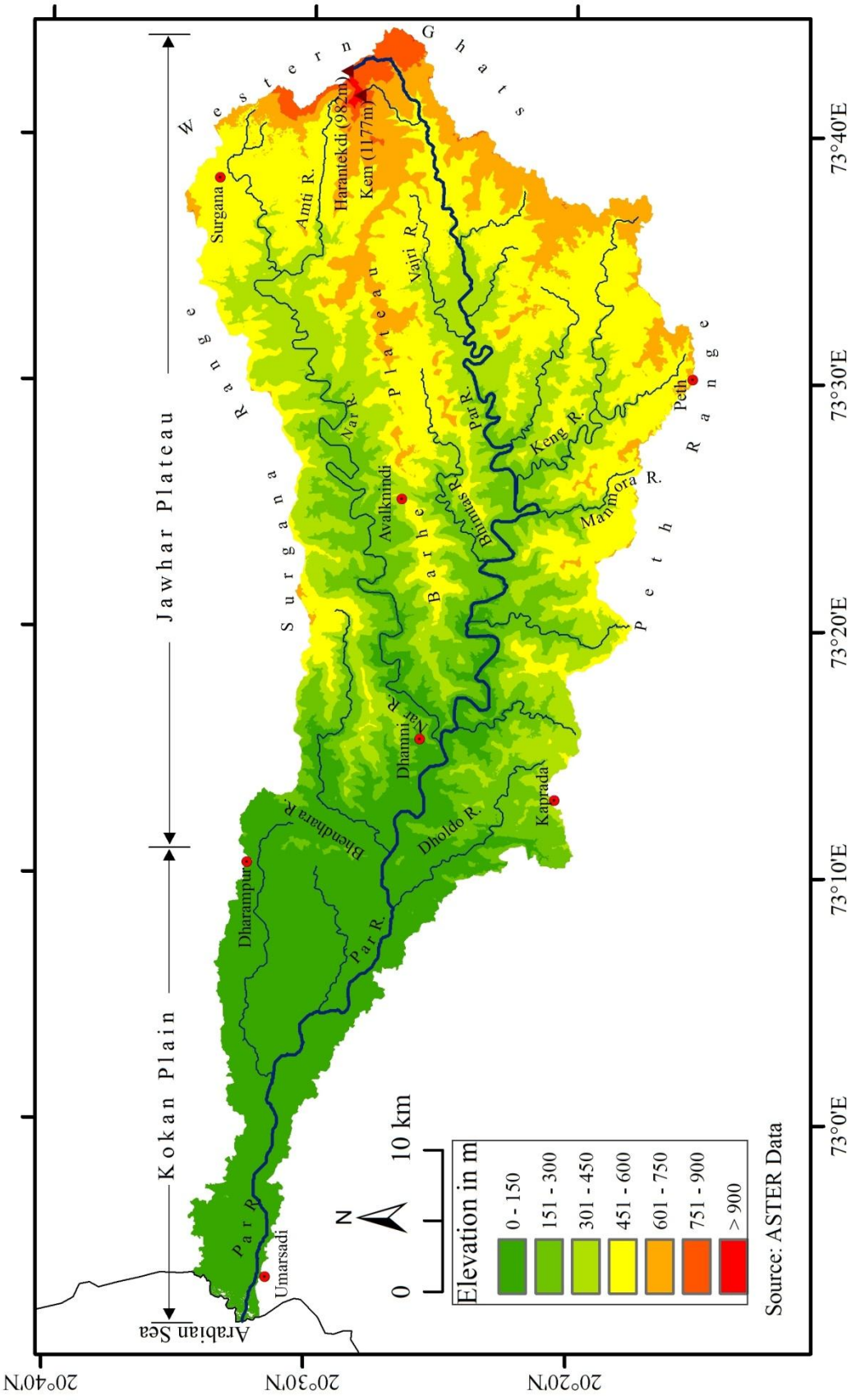


**Figure 1.1** Geomorphic Setting of the Par Basin

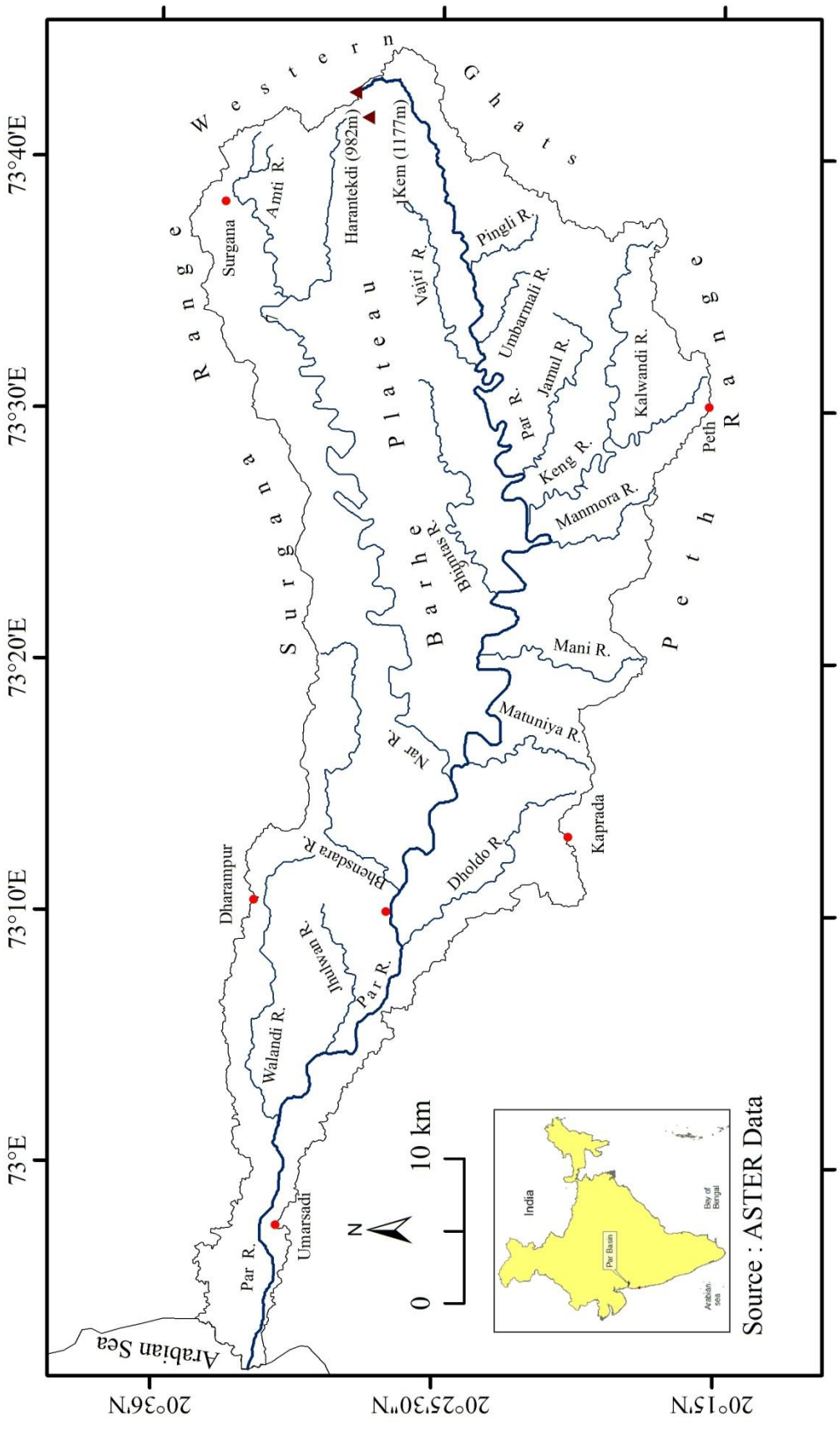


**Figure 1.2** Drainage Network of the Par River

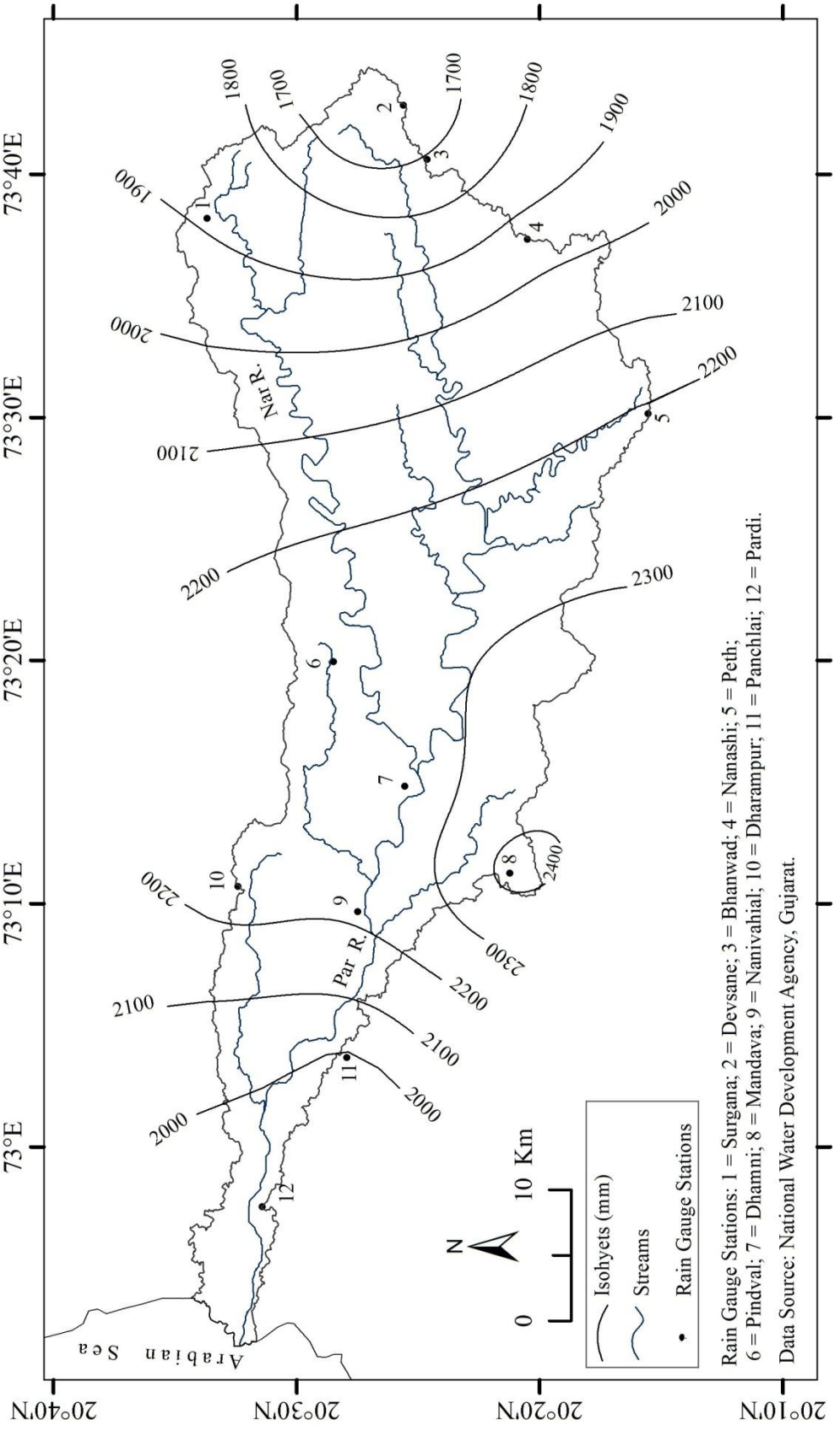


**Figure 1.3** Rain Gauge stations and Isohyets of the Par Basin

### *1.6.3 Drainage basin and network characteristics*

According to Schumm (1956), Morisawa (1962) and Leopold et al. (1964), the hydrological characteristics of a river are controlled to a large measure by the drainage basin and network characteristics. The drainage basin characteristics, for instance, basin relief, size, shape, drainage density, etc. play significant role in the generation of floods. Table 1.1 gives the primary basin and discharge characteristics of the Par Basin.

**Table 1.1** Morphometric properties of the Par Basin

| **Morphometric parameters** | **Values** |
|---|---|
| Basin area | 1664 $km^2$ |
| Basin relief | 1177 m |
| River length | 142 km |
| Average channel slope | 0.0069 |
| Elongation ratio | 0.49 |
| Form factor | 0.082 |
| Peak on record | 23820 $m^3/s$ (1968) |
| Unit discharge | 5.4 - 101 $m^3/s/km^2$ |

The Par River and its tributaries have collectively created a dendritic drainage pattern. There are 12 major tributaries of the river (Figure 1.2; Table 1.2). The largest tributary, i.e. the Nar rises very close to the source of the Par River, at Kem Hill (1177 m), and flows generally towards west. It accounts for almost 25% of the total area of the Par Basin. The Nar River flows in highly meandering path, before entering in the Par River at Dhamni (Figure 1.1). Some of the other main tributaries of the river such as the Keng, the Dholdo, the Mani, the Matuniya, and the Manmora head in the Peth Range and the Bhensdhara and Amti originate in the Surgana Range (Figure 1.2). Most of the left bank tributaries, for instance, the Keng, the Manmora, the Mani, the Matuniya and the Bhensdara meet the Par River almost at the right-angle (Figure 1.2). The left bank tributaries are comparatively smaller in length than right bank tributaries. The drainage network arrangement exhibits a strong control of geologic structure and tectonics.

**Table 1.2** Morphometric characteristics of the major tributaries of the Par River

| Name of the tributary | Elevation of the source in m | Length in km | Area in $km^2$ | Average Slope | Bank |
|---|---|---|---|---|---|
| Nar | 1177 | 87.0 | 407 | 0.01268 | Right |
| Keng | 600 | 30.8 | 135 | 0.01364 | Left |
| Bhensdara | 644 | 28.4 | 72 | 0.02126 | Right |
| Walandi | 850 | 26.0 | 72 | 0.03192 | Right |
| Bhimtas | 620 | 24.5 | 57 | 0.02041 | Right |
| Dholdo | 400 | 21.6 | 63 | 0.01573 | Left |
| Jamul | 600 | 19.2 | 46 | 0.02100 | Left |
| Vajri | 700 | 17.4 | 57 | 0.02064 | Right |
| Mani | 516 | 16.4 | 51 | 0.02533 | Left |
| Julwan | 140 | 14.4 | 20 | 0.00694 | Right |
| Matuniya | 300 | 13.8 | 32 | 0.01600 | Left |
| Manmora | 600 | 11.1 | 35 | 0.03949 | Left |

See Figure 1.2 for location of tributaries

### *1.6.4 Geology*

The entire basin is underlain by horizontally bedded Cretaceous-Eocene Deccan Trap basalts (Figure 1.4). However, quaternary alluvium has been observed at a small reach of the Par River particularly at Nanivahial (Figure 1.5). The river has single, sinuous, and well-defined channel, incised into bedrock. The channel floor is either of bedrock or covered by pebbly/cobbly material or boulders. The alluvial channel, with tidal effect, is seen only in lower reaches for seven km from the mouth. The basin is characterised by a number of lineaments. Some of prominent lineaments have been shown in Figure 1.4.

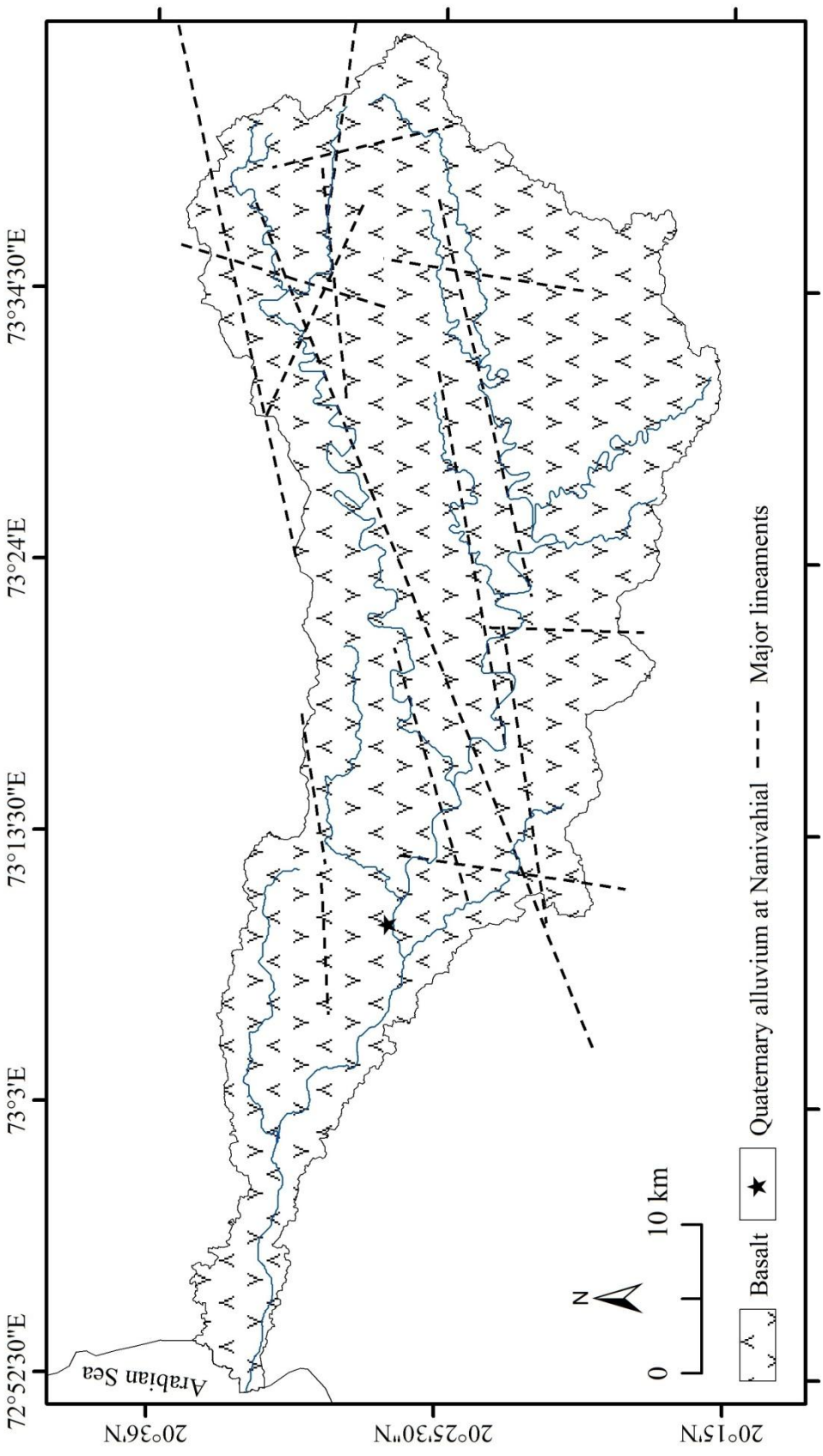


**Figure 1.4** Geological Setting of the Par Basin


**Figure 1.5** Quaternary alluvial deposits at Nanivahial, Par River; Flow direction is from right bottom to top left of the figure; Photograph by Prof. Vishwas S. Kale

## 1.7 Arrangement of the text

The present work is separated into five chapters. The first chapter is devoted to the introduction to the topic and introduction to the study area. Besides this, the chapter contains the research questions, hypothesis and main objectives of the study. The second chapter covers elaborative review of previous work done in the field of form and processes of bedrock channels. The third chapter deals with the methodology. The fourth chapter is of analysis and interpretation. The fifth chapter is devoted to major conclusions of the study.

Chapter 2

# Review of Literature

## 2.1 Introduction

In the last two decades investigation on bedrock channels and fluvial erosion has seen a noteworthy increase in interest. It was accepted that these channels play a crucial role in the development of the entire landscape. They set the base-level for hillslope response, control the relief of a region and are major agents of sediment transport (Whipple, 2004). An idea of a dynamic combination between climate-driven erosion and tectonics received wide interest in the nineteen nineties (Molnar and England, 1990; Willett, 1999), and triggered exhaustive research in bedrock channels and fluvial erosion. Fluvial geomorphologists have recognized importance of bedrock channels because they behave quite differently than alluvial channels, for which river research had focused on for many decades (Tinkler and Wohl, 1998; Richardson and Carling, 2006; Wohl and Merritts, 2001; Turowski, 2011).

Previous work on bedrock channels has been scanty and frequently focused on small-scale features of rock surface such as potholes or upon the single catastrophic floods (Tinker and Wohl, 1998). Bedrock channels came into the focus of geomorphic research in the recent decades. Despite new insights, many research questions remain open. The subject of bedrock channels has a large but scattered literature dating back over a century. The world distribution of studies in bedrock channels has been shown by Tinker and Wohl (1998). Their map indicates that most of the bedrock channel investigations are from USA and Australia. Studies of bedrock channels from rest of the world are very limited. Like other countries of the world, the research on bedrock channels in India is also inadequate though the bedrock channels are present in many areas. However, some work on the bedrock channels of the Narmada and Tapi Rivers have been carried out (Kale et al., 1994; Rajaguru et al., 1995; Ely et al., 1996; Kale et al., 1996; Kale and Gadgil, 1997; Baker and Kale, 1998; Hire, 2000; Kale et al., 2003; Kale and Hire, 2004; Kale, 2005).

There are three approaches to study bedrock channels namely basin-scale, reach-scale and experimental (Tinkler and Wohl, 1998).

Basin-scale approach, which generally focus on the evolution of channel longitudinal profile at time scales of centuries or longer (Weissel and Seidl, 1998). Studies may be field-based (Merritts et al., 1994; Pazzaglia et al., 1998). Some of the field-based studies are oriented towards computer modelling of basin evolution (Howard, 1987; Howard et al., 1994; Seidl et al., 1997; Howard, 1998; Sklar and Dietrich, 1998). However, the general focus is on long-term rates of profile lowering and the development of an erosion rate law (Tinkler and Wohl, 1998; Wohl and Merritts, 2001).

The reach-scale studies are associated with the processes of erosion and deposition, as these factors have influence on channel morphology for few square meters to several widths at spatial scale. At time scales, such studies include observable processes for days to decades (e.g. Toda, 1994; Tinkler and Parish, 1998; Tinkler and Wohl 1998; Hancock et al., 1998). An indirect approach of inferring processes from form, with the aid of palaeostage indicators and hydraulic simulation programs was adopted by O' Connor et al. (1986); Baker and Pickup (1987); Whol (1992a, b); Whol et al. (1993). Besides this, reach-scale studies include sophisticated mathematical flow modeling in bedrock channels (Miller and Cluer, 1998).

Experimental studies have used a variety of cohesive substrates to simulate either erosion of a specific feature, for instance, potholes (Alexander, 1932; Angeby, 1951) or knickpoints, (Holland and Pickup, 1976; Gardner, 1983) or general channel erosion under different conditions (Shepherd and Schumm, 1974; Wohl and Ikeda, 1997).

The literature review for the present work has been carried out on the basis of following points to match the objectives of the study and subsequent chapterization.

### 2.2 Channel morphological features

Straight channels, in fact, rarely exist or almost fictional among natural channels. However, exceptionally short sections or reaches of the channel are possibly straight. Nevertheless, in general, the reaches which are straight for distance more than ten times the channel width are rare in nature (Leopold and Wolman, 1957).

Meandering channels is a vast research area, covering a broad range of time and space scales, environmental dominions, and theoretical and practical approaches (Güneralp et al., 2012). A widespread review of the huge literature on alluvial river meanders is much more than that of bedrock river meanders. The research on alluvial meandering rivers had amplified to such extent by the latter part of the 20$^{th}$ century that in 1983 the conference namely Rivers' 83, sponsored by the American Society of Civil Engineers (ASCE), focused absolutely on meandering rivers (Elliot, 1984). Progress in research on river meandering during the 90s and at the commencement of the 21$^{st}$ century have focused exclusively on numerous topics such as (i) channel planform evolution; (ii) field-based or empirical research on the interactions of linking flow structure and bed morphology; (iii) research stand on experiment or laboratory on flow and sediment transport in winding channels and (iv) numerical modelling of meander morphodynamics (Güneralp et al., 2012). To analyze river-meander patterns thoroughly, two general approaches i.e. traditional approach and series approach has been given by Williams (1986). The traditional approach presumes and highlights on fundamental regularity of meander geometry (Inglis, 1947; Leopold and Wolman, 1960). However, by a thorough study of the meander trace, the series approach emphasize on the varying degrees of irregularity or quasi-randomness (Ferguson, 1976).

According to Güneralp et al. (2012) Studies on meandering river channels has mainly endeavored to explain the morphodynamic development of meandering rivers controlled by the interactions among water flow, sediment transport, channel planform and bed morphology. Güneralp et al. (2012) thoroughly introduced special issue of Geomorphology i.e. advances and challenges in meandering channels research, however, the subject matter of bedrock meanders remain ignored. Marked differences in dimensions of the alluvial and bedrock meanders have been noted by previous workers. Flows effective in meander formation may have a much larger recurrence interval than those of meandering alluvial channels (Tinkler, 1971). When meanders are observed in bedrock rivers they are classically interpreted as an antecedent feature. However, Hovius and Stark (2001) have found widespread evidence in Taiwan that this is not always the case and that instead bedrock rivers may actively meander.

In accordance with Leopold and Wolman (1960), the meander geometry has been the object of widespread statistical study and examples of that were given by Jefferson (1902), Inglis (1937; 1949), Bates (1939), and Leopold and Wolman (1957). Brice (1964) applied the Sinuosity index (Si) to differentiate straight river channels from sinuous and meandering river channels. Si ranges between 1.3 to one and four to one for the large majority of meandering rivers (Leopold and Langbean, 1966). A constant ratio between the meander wavelength and the radius of curvature has been noticed by Leopold and Langbean (1966) in a given series of meanders for the alluvial rivers. The appearance of regularity in meander depends in part on how constant this ratio is. The striking uniformity in dimensions of meanders in different physiographic settings is the result of certain geometric proportions appear common to all. For example, a nearly constant ratio of radius of curvature (Rc) to channel width (W) has been noticed by Leopold and Wolman (1960) and Williams (1986). The three empirical equations, for instance, meander wavelength ($\lambda$) and channel width (W), meander wavelength ($\lambda$) and mean radius of curvature ($Rc_m$) and amplitude (A) and channel width (W) have been given by Leopold and Wolman (1960) to show remarkable relationship between meander wavelength, channel width and radius of curvature for alluvial rivers.

Bedrock river channels mainly flow through single path. However, several workers have described multiple-flow path channels incised into bedrock in variety of environments. Such channels are known both bedrock anastomoising channels and scabland topography or scablands (Wohl, 1998). Heritage et al., (2000) used term bedrock anastomoising for multi-thread channels in bedrock. Garner (1974) follows Bretz (1923) and define anastomoising channel as “an erosionally developed network of channels in which the insular flow obstructions represent relict topographic highs and often consist of bedrock”. According to Wohl (1998) anomalous development of multiple channels in bedrock are attributed to one or more of the three processes namely (i) inadequate channel capacity; (ii) localized uplift along the channel and (iii) preferential erosion along lines of weakness, such as joints and fractures. Kale et al. (1996) and Gupta et al. (1999) described anastomoising channels along the Narmada River of India. Kale and Shingade (1987) illustrated the formation of multiple bedrock channels along the Indrayani River by coalescence of grooves and potholes along joints in basalt bedrock.

The form of a channel is primarily a function of (i) the discharge and its variations; (ii) the texture and quantity of sediments passing through the section and (iii) the nature of the bed and bank material (Leopold et al., 1964; Schumm, 1977; Petts and Foster, 1985). In accordance with Leopold and Maddock (1953) and Maddock (1976), the alluvial channels having sedimentary particles at banks and beds are mobile in nature; these channels are self-generated through the self-governing adjustment of the morphological variables encompassing their hydraulic geometry. Nevertheless, such channels may experience infrequent high-magnitude events, their morphology have a tendency to recover to the original dimensions at varying rates depending on the series of floods and other climatic-geomorphic causes (Wolman and Gerson, 1978). Baker and Kale (1998) considered high-energy processes that are less studied by previous workers and which occur during severe floods in highly resistant bedrock channel situations in their work. According to Schumm (1977), although, alluvial channel patterns can be systematically linked to sediment types (which forms channel banks), to sediment loads, and to moderate flood characteristics, the lofty thresholds for channel alteration in bedrock rivers (Baker, 1977) bring about a diverse range of channel types and patterns (Shepherd, 1979; Wohl, 1998).

The form ratio is the ratio of channel width and depth. It is primary index of channel shape and is related to the sediment transport and boundary resistance (Schumm, 1960). Generally two groups of aspects are considered to describe channel cross sectional form – i) channel size and ii) channel shape. Perimeter lithology is an important factor to determine channel shape. Rosgen (1994) used boundary composition as one of the basic criteria to classify river channels. It is the most elaborate classification schemes yet developed. He produced 41 channel types on the basis of boundary composition. The impact of floods depends not so much on the volume of water as on the energy exerted by it. The adjustments in the width-depth ratio and hydraulic variables with discharge have been shown to very useful concepts in evaluating the potential of flows to be geomorphologically effective (Kale et al., 1994; Gupta, 1995a). Montgomery and Gran (2001) derived a fundamental set of relationships between drainage area (A) (a surrogate for discharge) and channel width (W) for alluvial and bedrock rivers. In view of their research work for alluvial and bedrock rivers, an attempt has been made to highlight how classic concepts and

empiricisms of fluvial geomorphology are based on investigations of alluvial channel systems (Leopold et al., 1964).

As stated by Wohl (1998), the existence of exposed bedrock along a channel entails only limited and localized deposition along the channel. As a result, the morphology of many bedrock channels is dominated by erosional processes such as corrosion, solution, corrasion or abrasion, cavitation, etc. Wohl (1998) has classified bedrock erosional landforms at various spatial scales, for instance, micro-scale (mm to cm), meso-scale (cm to m) and macro-scale (m to km) (Table 2.1). The mainstreams of studies have focused on meso-scale erosional forms which are largely descriptive and empirical, as several researchers have executed experiments to compute erosive process (Wohl, 1998). As demonstrated by Blank (1958), the preliminary approach to meso-scale erosional features was 1) to illustrate a particular channel reach which have potholes or longitudinal grooves 2) to infer the erosive processes that produce these features 3) furthermore, to describe the position of the erosional features in relation to lithology, gradient, or other characteristics of reach-length exclusive to that site. Baker (1973) has developed another approach to study meso-scale erosional forms using paleostage indicators in combination with step-backwater hydraulic models to course a flood discharge along a reach of channel. A second fundamental approach towards erosive processes and channel form has been given by Wohl (1998), which focuses on modelling macro-scale channel evolution. The third approach, micro-scale studies mainly concentrate on longitudinal profile as a sign of the channel's capability to incise, or on development of channel network (Wohl, 1998).

**Table 2.1** Scales of erosional features

| **Scale** | **Erosional characteristics** |
|---|---|
| Micro-scale (mm to cm) | Abrasion, flaking, or plucking of individual grains or small pieces of rock |
| Meso-scale (cm to m) | Selective erosion of portions of the channel boundaries across a cross section or along a reach: produces potholes, longitudinal grooves, knickpoints, undulating walls, inner channel, pool-riffle or step-pool sequences |
| Macro-scale (m to km) | Reach- to basin-scale channel morphologies in planform (meandering, downstream alternations in width and gradient), and in gradient |

After Wohl (1998)

Richardson and Carling (2005) define potholes as being essentially round (in plan view), deep depressions, which are, or can be expected to be, eroded by vortices with approximately vertical axes by mechanisms other than plucking. According to them this is the most comprehensive definition because it takes into account both the process of formation and the morphological aspect. Potholes are meso-scale erosional landforms (cm to m scale) and are found in a variety of climates, lithologies and channel types (Wohl, 1998). These are formed by fluvial erosional processes like corrasion, abrasion and cavitation (Wohl, 1998; Kale and Gupta, 2001; Sengupta and Kale, 2011). Potholes are significant component of channel incision and, in turn, lead to distinctive form of bedrock channels (Kale and Shingade, 1987; Springer et al., 2006). Kale and Shingade (1987) stated that potholes are created as tiny depressions in the beginning. These small depressions trap more sediments and water, enhancing erosion through whirling movement of water and sediment. Later, the pit is abraded, deepened and widened to a typical pothole.

Longitudinal grooves parallel to flow result from longitudinal vortices and turbulent vortices during high-magnitude flood flows (Wohl, 1993). Longitudinal groove are associated with zones of enhanced erosion.

Shepherd and Schumm (1974) hypothesized that inner channels are formed by the high flow stresses generated during large floods in the steep reaches of the bedrock rivers. Further, investigations by Baker (1988), Wohl (1992a) and Wohl and Ikeda (1997) supported their explanation. Inner channels play significant role for incision of channels into resistant substrate, which maximize shear stress and unit stream power for a given stage.

Channel gradient is another important channel morphologic variable dictating the flood power and impact. Gradient is controlled by the lithology of a basin (Hack, 1973). Generally, areas of resistant bedrock exhibit steeper channel gradient. Such high-gradient channel reaches are efficient in terms of erosion and transportation of material during large floods. Channel boundary shear stress and unit stream power are vital parameters in determining geomorphic response. These parameters are greatly influenced by channel slope (Baker and Costa, 1987).

In open bedrock channels, Richardson and Carling (2005) projected a comprehensive explanation and an organized taxonomy for the typology of sculpted shapes. The dimensions of such sculpted marks are varied, and an extensive range of approaches have been applied to study them thoroughly (Velázquez et al., 2016). Wohl and Merritt (2001) and Wohl and Achyuthan (2002) have carried comprehensive reviews in this perspective, with regard to factors such as 1) hydraulic driving force, 2) physical resistances of the substrate and 3) morphological features.

As opined by Leopold and Maddock (1953); Schumm (1977) and Schumm and Winkley (1994), alluvial channels shape their channel in bed and bank sediment that can readily entrain and transported by rivers for a broad range of flows. Consequently, according to Leopold and Maddock (1953) and Hey (1982), these channels regulate their geometry, pattern, and gradient to frequent flows of low to moderate magnitude that transport the most sediment and that are close to bankfull conditions. Cenderelli and Cluer (1998) stated that, for large part, alluvial channels supply abundant sediment due to availability of sediment at the channel bottom and banks and because of the capability of the stream to readily entrain and transport this sediment. On the contrary, in resistant-boundary channels and valleys, coarse-grained deposition mainly cobbles and boulders and fine-grained deposition essentially sand and fine pebbles, usually remain in association with infrequent and extreme floods (Cenderelli and Cluer, 1998). Infrequent and extreme floods produce flows that are "out-of-bank" and extend across the whole valley bottom in the resistant-boundary valleys. Such flows are responsible for widespread geomorphic activities along the course of the flow (Cenderelli and Cluer, 1998). The process of erosion primarily takes place in constricted reaches where valley side slopes are embraced of coarse and unconsolidated sediment. Quite the reverse, according to Martini (1977); Baker (1978, 1984); Church and Jones (1982); Carling (1987, 1989, 1995); Wohl (1992) and O'Connor (1993), in general, deposition of coarse-grained material occurs at particular locations for instance (i) where the channel and/or valley widen; (ii) upstream and downstream of obstructions and; (iii) along the margins of channel bends. In resistant-boundary channels, the supply of coarse-sediment is spatially irregular (Baker,1988) and forcefully controlled by the factors like (i) the availability of sediment in constricted reaches; (ii) the capability of the flow to entrain and transport the sediment and; (iii) the number and closeness of depositional areas to the sediment source

(Cenderelli and Cluer, 1998). The situation of fine-grained sediment transport remains different in resistant-boundary channels. During frequent low to moderate flows, amount of fine-grained sediment are entrained transported and deposited (Cenderelli and Cluer, 1998). According to Schmidt (1990) and Cluer (1995) such phenomenon normally takes place immediately upstream and downstream of constricted reaches and beside the channel margins where flow recirculates. Two case studies, specifically (i) coarse-grained deposition in the Mt. Everest Region of Nepal due to infrequent and extreme flood and (ii) fine-grained deposition along the Colorado River in and near the Grand Canyon, U.S.A. owing to low to moderate floods have been examined by Cenderelli and Cluer (1998). The above-mentioned unique case studies assess the significance of sediment supply in influencing coarse as well as fine-grained deposition in resistant-boundary channels.

Substantial depositional features located at sudden expansions immediately downstream of constricted reaches are called as expansion bar or boulder delta (Baker, 1978, 1984; Elfstorm, 1987; O'Conner, 1993). Surfaces of this bar consist of multiple linear and lenticular bars separated by shallow channels. The bars are outcome of rapid reduction of flow energy and flow competence. Longitudinal bars are narrow, linear to curvilinear, elongated along the axis of channel that formed at local flow expansions along the valley margins. They are extended in the direction of flow. Sometimes, longitudinal bars form in the centre of the channel, typically where the channel is relatively wide. Longitudinal bars tend to taper off in a downstream direction (Robert, 2003). Point bars are plainly an accumulation of deposited material along the inner margins of channel bends where flow energy is reduced and secondary currents transport sediment from the main channel to this reduced flow region (Knighton, 1984; Dietrich and Smith, 1984; de Jong and Ergenzinger, 1995).

### 2.3 Erosional processes and sediment transport

The bedrock channels are supply limited (since the transport capacity of flow is greater than the supply of sediment) and the morphology of bedrock channels is dominated by the processes of erosion. As per Wohl (1998), the bedrock substrate is dominantly eroded by processes of (i) corrosion, or chemical weathering and solution; (ii) corrasion, or abrasion by sediment in transport along the channel and (iii) cavitation and other hydrodynamic forces associated with flow turbulence. Knighton

(1998) described that under conditions of very high flow velocity, sudden changes in pressure can cause the formation and implosion of vapour bubbles. The shock waves generated by implosion that weaken the bed by the process of cavitation. This effect is mainly caused by the abrupt collapse of vapour pockets within the flow. The cause behind the process of cavitation may be flow separation induced by joints, bedding planes, or other surface irregularities in bedrock (Barnes, 1956). The erosive potential of this process can be phenomenal, under sustained high flow (Eckley and Hinchliff, 1986). Erosional features such as flute marks, polished rock surfaces and pot holes are indicators of intense bedrock scouring, resulting from cavitating flow conditions (Baker, 1988; Kale et al., 1993b; Kale et al., 1994). Embleton and King (1968) opined that the process of cavitation may causes quarrying of the scablands. One of the crucial causes behind entrainment of particles is fluid stressing or shear detachment in which flowing water exerts a shear force upon the bed it overflows. It is distinguished that the sediment transport rates and sediment entrainment are driven by excess shear stress over a threshold value, and a similar mechanism can be predicted for bedrock erosion (Turowski, 2012). However, according to Howard (1998) this process is important only in weakly consolidated rocks and clays. The process of quarrying or plucking in bedrock erosion is the removal of loose blocks of rock from the bed of channels by drag and lift forces. It is dominant process of bedrock erosion (Hancock et al., 1998) rather than abrasion (Bretz, 1924). Chatanantavet and Parker (2009) introduced the concept of macro-abrasion, this process is major cause for formation of blocks. In this process the existing cracks, joins and plane of weakness in the material are enlarged by the impact of particles until individual blocks are loosened. These loose blocks of rocks can be separated by shear detachment and entrained. Only minute study and introductory laboratory work has been available regarding this process (Dubinski and Wohl, 2005), though quarrying is thought to be significant in joined rocks (Brez, 1926; Hartshorn et al., 2002).

Impact erosion or abrasion is the process of scraping or wearing. Moving sediment particles in the flow may strike the bed and remove small fragments of the impacted rock material, it also drives crack proliferation and weakens the substrate (and thus prepares for plucking) (e.g., Bitter, 1963; Wilson, 2009). The most rapid rates of abrasion perhaps take place during turbulent floods, along channels of weakly resistant bedrock, accompany with large and moderately coarse suspended sediment

loads. This process can initiate the development of potholes and deep circular scour features, these formations affect the flow and accelerate the rate of erosion. The accumulated coarse material in pothole swirled around by the flow and it deepens as well as enlarges the potholes through drilling process into the channel bed. Over the time the bed elevation lowers due to coalesce of potholes. The other forms such as longitudinal grooves, knickpoints, and similar erosional features along the channel bed and walls are indicators of abrasion dominated erosion.

Hancock et al. (1998) for the first time documented and termed the process of hydraulic wedging. According to them hydraulic wedging is the process which loosens and prepares blocks for quarrying through wedging fragments of rocks/clasts into fractures and joints. Channel bed with wider or various preliminary cracks and bedload sediment is requisite for this process to function. The clasts ranges in size from fine sand to boulders and are wedged very tightly into joints of bedrock in such a way that removal of clasts necessitates noteworthy force (Hancock et al., 1998). Two possibilities have been given by Hancock et al. (1998) for encroachment of clasts into joints (i) the clasts are either emplaced forcefully by very high flow velocities (ii) clasts passively accepted into a crack that was momentarily widen while sediment was nearby, however, there is scarcity of data and no experiments to validate this process.

Knickpoint are sudden break or irregularity in the gradient along the long profile of a river. The migration of knickpoint is not erosional process as such, but interplay of several processes mounted by a channel-spanning bedform (Turowski, 2012). There are several viewpoints regarding formation of knickpoints. According to Whipple and Tucker (1999) knickpoints can be formed by changes in the climate or local tectonics. Korup (2006) stated that blocking of the channel by material of landslide may be responsible. Miller's (1999) view proposes that lithologic contrasts may possibly form knickpoints. Chatanantavet and Parker (2009) opined that knicks can arise autogenically. The knickpoints play crucial role in the channel dynamics since these contribute information on base level through the channel network (Whipple and Tucker, 1999; 2002). Studies of Bishop and Goldrick (1992) described knickpoints for which pothole erosion at the lip is an important component of headward retreat. As flow approaches the lip of knickpoint, width decreases, but depth, velocity, and bottom shear stress increases (Gardner, 1983). As a result of this, the slope of the

incising channel reaches increases above the lip of knickpoints. Very few actual measurements exist for rates of bedrock knickpoint retreat.

Infrequent and large magnitude floods produce massive discharges into channels. The geomorphic works associated with such floods are variable, in some cases these floods generate minute geomorphic response (Costa, 1974), and in other cases magnificent effects are observed (Baker, 1977; Gupta, 1983). The geomorphic effectiveness of a flood, which relates to its ability to affect the form of the landscape (Wolman and Gerson, 1978), is commonly linked to flood power and the degree of turbulence (Baker and Costa, 1987; Wohl, 1993; Baker and Kale, 1998; Kale and Hire, 2004; Hire and Kale, 2006; Kale and Hire, 2007).

According to Baker and Costa (1987) the unit stream power and shear stress are measures of existing energy and have verified valuable notions in assessing the function of large floods in generating major channel changes along with movement of cobbles and boulders. The data collected by Baker and Costa (1987) for some large flash-floods as well as for some great historic and prehistoric floods exhibit that the power values coupled with such floods are a number of orders of magnitude upper than those produced in alluvial rivers. Furthermore, according to Baker and Costa (1987) and Baker (1988), these investigations specify that, very high values of actual energy consequence in cavitational erosion and erosionally efficient macroturbulence. Therefore, magnificent changes, yet in the resistant channel boundaries, have been credited to such high-energy flood conditions.

Tinkler and Wohl (1998) opined that, flows in bedrock systems usually have highly aerated and turbulent flow structure and in general show greater velocities and shear stresses than those in alluvial reaches, in addition, substantial sections of the flow are critical (Fr = 1 or close to 1) or supercritical (Fr > 1). However, flow remains unsteady and gradually varied i.e. subcritical for several locations. Supercritical flow is more common in bedrock channels and can be sustained for longer period of time (Baker and Costa, 1987). This flow move rapidly and efficiently through the channel due to less intensive turbulent mixing and less deviation from the main downstream direction of flow. Supercritical flow may overshoot tight bends and can also be highly erosive (Kay, 1998). Supercritical flow in general occurs when increase in channel slope increases the flow velocity, resulting in a reduction in depth (the hydraulic

drop). Standing waves forms in critical flow when the Froude number is 1 or close to 1. Normally standing waves form over deforming or non-deforming boundaries, however, form more easily over rough boundaries (Alexander, 2008). The frequent occurrence of unbroken standing waves is caused by the presence of boulders and cobbles in the channel bottom, as well as by a considerable increase in gradient of the channel in some of its parts, in addition, broken standing waves are formed in channel i.e. turbulent flow with foamy water and breaking wave crests, generally appears like 'white water' (Wiejaczka et al., 2014). Instability occurs in channel if Froude number exceeds a critical value (i.e. 1), and it gives rise to supercritical flow. Whenever the Froude number is in excess of 1.6, roll waves or slug flow appears (Hjalmarson and Phillips, 1997). In general, these waves more probably to be initiated on wide, shallow, steep systems, and over gravel surfaces (Tinkler and Wohl, 1998). Roll waves then travel downstream, and they sustain for periods of hours during peak flow. These waves appear like "walls of water" in channel (reported by eyewitness) and are almost certainly roll waves (Tinkler and Wohl, 1998).

Reynolds Number is the ratio of inertial and viscous forces acting on a body of fluid, it is dimensionless coefficient, Re number measures the degree of turbulence, or random changes in flow direction and/or velocity superimposed on the main downstream movement of water (Richards, 2004).

The process critical velocity for inception of cavitation (Vc) can occur only for certain critical conditions. According to Hjulstrom (1935) the minimum velocity necessary for cavitation to take place in river is about 12 m/s. However, this figure is applicable for relatively shallow and swift streams (Baker, 1973). The critical velocity for inception of cavitation in m/s is given by Baker (1973) and Baker and Costa (1987).

The upstream migration of knickpoints has been recognized as significant means of bedrock channel lowering, however, little is known about the mechanisms that control the shapes and migrations of knickpoints (Miller, 1991; Seidl and Dietrich, 1992; Seidl, 1993; Whipple et al., 2000 (a, b); Zaprowski et al., 2001). According to Baker (1988); Wohl (1992, 1998 and 2000) and Wohl and Ikeda (1997) headward migration of a knickpoint through resistant substrate can leave behind a deep and narrow gorge, it reflects the erosional resistance of the channel boundaries, and maximizes the shear stress and stream power per unit area of a given discharge and channel gradient.

Several equations and models have been developed by researchers to predict channel incision of a river into its bed. However, the comprehensive and most commonly used stream power erosion model (SPEM) is of great use since there are few variables and can be measured against topographical data (Howard and Kerby, 1983; Skylar and Dietrich, 2001). It is argued by Howard and Kerby (1983) that the Stream Power Law/model (SPEM) is most applicable because it is related to physics of erosion. The family of stream power models is based on the principle that bedrock channel incision rate can be estimated by a power law function of mean bed shear stress or stream power (Howard and Kerby, 1983; Howard et al., 1994; Whipple et al., 2000a; Kobor and Roering, 2004; Whipple 2004). Stock and Montgomery (1999) have applied stream power erosion model for Kaulaula and Waipao Rivers, which flow through basalt lithology.

The investigations of Leopold and Maddock (1953); Schumm (1977) and Schumm and Winkely (1994) reveals that alluvial channels shape their form in bed and bank sediment that the stream can readily entrain and transport for a wide range of flows. In contrary, according to Baker (1988), the resistant-boundary channels are supply-limited, coarse sediment entrainment and deposition is usually associated with infrequent and extreme floods, since, energy required to transport a particle of sediment increases with particle size.

### 2.4 Role of lithology and tectonics

The morphology of channel is predominantly function of fluvial forces applied and bedrock resistance offered. The rock resistance to flow dynamics noticeably varies with respect to lithological considerations. In accordance with Goudie (2004) the erodibility of rocks relies on the lithology which strongly controls the erosional processes. In this standpoint, rocks are frequently referred to as ‘hard’ or ‘resistant’ or ‘weak’ and ‘non-resistant’ to erosional processes. In order to find out effects of rock strength/role of lithology in shaping the landforms, weathering phenomena and relative dating the Schmidt hammer (SH) has now been adopted by Geomorphologists (e.g. Ericson, 2004). The instrument was devised by E. Schmidt in 1948. Primarily Schmidt hammer has been used by civil engineers to test the strength of concrete. However, from last few decades, Geomorpologists and Geologists have started using SH to estimate the strength of rocks for numerous reasons (Goudie, 2006). SH

measures the distance of rebound of controlled impact on a surface and represents a relative measure of surface hardness or strength (Goudie, 2006). Yasar and Erdogan (2004) stated that, several studies on the investigation of efficacy of the Schmidt hammer test on diverse rock types have been made by numerous investigators. Goudie (2004) used the Schmidt hammer rebound values (N) to estimate the Rock Mass Strength (RMS) i.e. the specific properties of the rock mass that control its strength and subsequent slope stability.

The commonly-used geomorphic indices of active tectonics (GAT) have been developed as basic investigation tools to assess the relationship between tectonics and basin morphology on the regional or basin scale and to identify areas experiencing tectonic deformation (Table 2.2) (Bull and McFadden, 1977; Keller, 1986; Keller and Pinter, 1996; Burbank and Anderson, 2001; Della Seta et al., 2004; Kale and Shejwalkar, 2008). According to Keller and Pinter (1996) the results of several geomorphic indices can be combined to provide an assessment of a relative degree of tectonic activity in an area. Geomorphic indices can be obtained easily from topographic maps or aerial photos (Strahler, 1952). The analysis of Kale and Shejwalkar (2008) and Troiani and Della Seta (2008) states that, in recent decades, the increasing usefulness of GIS software has made it possible to undertake quick and detailed processing of data. Recently, in morphotectonic studies, traditional geomorphic analysis has been integrated with morphometric analysis of landforms and with geostatistical topographic analysis (Keller et al., 1982; Mayer, 1990; Cox, 1994; Merritts et al., 1994; Lupia et al., 1995; Lupia et al., 2001; Currado and Fredi, 2000; Pike, 2002; Della Seta, 2004; Della Seta et al., 2004; Kale and Shejwalkar, 2008; Troiani and Della Seta, 2008; Figueroa and Knott, 2010; Dehbozorgi et al., 2010; Font et al., 2010; Jayappa et al., 2012). Geomorphic indices appropriate to fluvial systems in different regions and of varying size (Strahler, 1958), associate with independently derived uplift rates (Rockwell et al., 1985; Merritts and Vincent, 1989; Kirby and Whipple, 2001) and are applicable to a variety of tectonic settings where topography is being changed (Bull and McFadden, 1977; Wells et al., 1988; Azor et al., 2002; Figueroa and Knott, 2010).

**Table 2.2** Geomorphic indices of active tectonics (GAT) and their calculations

| Sr. No. | Index | Formula | Variables | Reference |
|---|---|---|---|---|
| 1 | Hypsometric Integral (HI) | HI = (Em − Emin)/ (Emax − Emin) | Em = mean elevation<br>Emax = maximum elevation<br>Emin = minimum elevation | Bull and McFadden (1977) |
| 2 | Valley width-height Ratio (Vf) | Vf = Vfw/(((Eld-Esc)+ (Erd-Esc))/2) | Vfw = width of valley floor<br>Eld = elevation of the left valley divide<br>Erd = elevation of the right valley divide<br>Esc = elevation of the valley Floor | Bull and McFadden (1977) |
| 3 | Asymmetry Factor (AF) | AF = 100(Ar/At) | Ar = area of the basin to the right of the trunk stream<br>AT = total area of the drainage basin | Keller and Pinter (1996) |
| 4 | Stream Length-Gradient Index (SL) | SL = (H1 − H2)/ (ln L2 − lnL1) | H1 and H2 are the elevations of each end of a given reach L1 and L2 are the distances from each end of the reach to the source | Hack (1973) |
| 5 | Basin elongation ratio (Re) | Re = (2√A :√π)/LB | A = basin area<br>LB = length of the basin | Bull and McFadden (1977) |

Hypsometric analysis (or area-altitude analysis) is the study of the distribution of horizontal cross-sectional area of a landmass with respect to elevation (Strahler, 1952). Classically, hypsometric analysis has been used to differentiate between erosional landforms at different stages during their evolution (Strahler, 1952; Schumm, 1956; Strahler, 1964). Hypsometric Integral (HI) is a relief variable which is widely used to measure the degree of fluvial landscape erosion and describes the distribution of elevations across the drainage basin area (Strahler, 1952). Hypsometric Curve (HC) of a catchment represents the relative area below (or above) a given altitude (Strahler, 1952). Hypsometric curve can also be used to infer the stage of development of the drainage network and can be considered as a powerful tool to differentiate between tectonically active and inactive areas (Keller and Pinter, 1996).

Vf is basically an index of the form or shape of the valley cross-section. The Vf ratio is a good measure that indicates whether the river is actively downcutting and incising (Bull and McFadden, 1977). The Vf index reflects the difference between V-shaped valleys that are down cut in response to active uplift (low values of Vf) and broad-

floored valleys that are eroding laterally into adjacent hill slopes in response to base level stability (high values of Vf) (Bull, 1978).

The effect of tectonics on the drainage pattern is also reflected by the asymmetry of drainage basins (Molin et al., 2004). AF can be used to evaluate tectonic tilting at the regional or basin scale (Hare and Gardner, 1985; Keller and Pinter, 2002).

The Stream Length-Gradient Index (SL Index) is considered as one of the quantitative geomorphic parameters incorporated in morphotectonic analysis (Hack, 1973). In tectonically active regions, and/or at the basin scale of investigation, the SL Index can be a useful tool to detect tectonic displacements (Keller and Pinter, 1996; Chen et al., 2003; Zovoili et al., 2004; Kale and Shejwalkar, 2008, Troiani and Della Seta, 2008; Monteiro et al., 2010). Nevertheless, the effectiveness of the parameter in detecting local active structures has not been confirmed for small catchments and/or in regions where tectonic activity is subtle (Chen et al., 2003 and references therein; Verrios et al., 2004; Troiani and Della Seta, 2008). In small river basins the contribution of the lithological effect to anomalous values of the SL Index seems indistinguishable from the tectonic one (Troiani and Della Seta, 2008). However, in spite of all the difficulties, SL index has been widely used as a proxy to identify areas of anomalous uplift within a landscape (Kale and Shejwalkar, 2008).

Basin elongation ratio (Re) is an areal morphometric variable that quantitatively describes the planimetric shape of a basin and, thus, indirectly provides information about the degree of maturity of the basin landscape (Kale and Shejwalkar, 2008). Basins draining tectonically active areas are more elongated and become more circular with the ending of uplift (Bull and McFadden, 1977). Elongated basin shapes are also associated with high local relief and steep valley slopes (Molin et al., 2004).

An idea of a dynamic combination between climate-driven erosion and tectonics received wide interest in the nineteen nineties (Molnar and England, 1990; Willett, 1999), and triggered exhaustive research in bedrock channels and fluvial erosion. River incision into bedrock is a significant erosion process that has an impact on the rate of landscape response to changes in rock uplift rate and climate (Howard et al., 1994). Considerable attention has been given to morphology of bedrock channels and dynamics and to fluvial erosional processes in recent years (e.g. Turowski et al., 2008;

Howard, 1994; Wohl et al., 1994; Tinkler and Wohl, 1998a; Stock and Montgomery, 1999; Whipple et al., 2000a, b; Wohl and Merritt, 2001; Finnegan et al., 2005; Stark, 2006; Wobus et al., 2006a, b; Whittaker et al., 2007).

## 2.5 Flood hydrometeorology, flood hydrology and flood geomorphology

### (i) Flood hydrometeorology

As stated by Wohl (1992b) and Gupta (1995a), floods play a dominant role in shaping the river channel and the landscape in certain hydro-geomorphic environments, such as the seasonal tropics. In accordance with Baker's (1988) view, flood geomorphology is concerned with the processes, forms, effects, and causes of floods. The frequency and hydraulic properties of the high flows play foremost important role to shape the channel and to carry the sediment. Infrequent large floods that occur at an interval of several decades are associated with much higher levels of power expenditure and thus are capable of producing major channel changes and movement of coarse sediments (Baker and Kale, 1998). The major reason of occurrence of floods was given by Hirschboeck (1991), according to her, floods are produced due to extraordinary synoptic situations that deliver more precipitation to a drainage basin than that can be readily stored or absorbed in the basin. In the humid and seasonal tropics, large floods are mostly associated with high-magnitude rainfall caused by synoptic events ranging in force from lows to cyclones (Gupta, 1988; 1995a). Almost 80-90% of the annual rain over most parts of the country falls during the period of summer monsoon season i.e. from June to September due to the monsoon circulation. During this period cyclonic disturbances from the Bay of Bengal and the Arabian Sea produce widespread and heavy rainfall which often causes severe floods in Indian rivers (Rakhecha, 2002). As per earlier and recent studies of the synoptic situations associated with the rainstorms, flood-generating rainstorms are connected with (Abbi and Jain, 1971; Ramaswamy, 1985) -

(1) Bay of Bengal depressions moving westwards
(2) General active monsoon conditions over Madhya Pradesh and Gujarat
(3) Land depressions moving westwards

It is well known that the monsoon rainfall of the same region goes through variations from one year to another. However, departures of rainfall from its long-term mean in any two years are not same (Gadgil, 2002). The year to year fluctuations in rainfall of the region cause complexity in recognition of the direction of change in the rainfall. Thus, some effective statistical methods are to be applied to identify the nature of long-term variability in monsoon rainfall. The frequently used method to study the variability of rainfall is Normalized Accumulated Departure from mean (NADM). Successive properties within long-term data can be merely resolved by NADM method (Riehl et al., 1979; Mooley and Parthasarathy, 1984; Probst and Tardy, 1987; Kale, 1999b). Consequently, the NADM plotting method has been used to emphasize the long-term variability by minimizing short-term fluctuations in the monsoon rainfall.

According to earlier studies, based on data for rivers from around the world, floods are not randomly distributed. Nevertheless, there is a tendency for periods of high and low floods to match with periods of high and low rainfall (Burn and Arnell, 1993; Chiew and McMohan, 1993; Kale, 1999b).

El Niño is a phenomenon in which episodic warming of the ocean occurs in the central and eastern Pacific, and Southern Oscillation is the seesaw pattern of atmospheric pressure change that takes place between the eastern and western Pacific (Lutgens and Tarbuck, 1995). The ENSO event was discovered by Gilbert Walker with ascertaining the fact that Indian monsoon was not an isolated system but had strong teleconnections with the global climate (Kelkar, 2009). Numerous studies evaluated the probable linkages between the ENSO and Indian summer monsoon rainfall (ISMR) and revealed diverse aspects of the relationship between ISMR and ENSO (Khandekar, 1979; Sikka, 1980; Rasmusson and Carpenter, 1983; Shukla and Paolino, 1983; Ropelewski and Halpert, 1987; Kane, 1989; Simpson et al., 1993; Khole, 2004; Lutgens and Tarbuck, 2007; Ihara et al., 2007) after Walker (1924). These studies have deduced that usually, ISMR is inversely correlated with Sea Surface Temperature (SST) of the Pacific Ocean. Lutgens and Tarbuck (2007) observed that El Niño is indeed a part of the global circulation and influences the weather at great distances from the Pacific Ocean. Additionally, it is marked by an anomalous weather patterns. Indian monsoon is more prone to drought situations

during El Niño events, on the contrary, wet monsoons are more likely to prevail, during the La Niña events. (Krishnan and Sugi, 2003). Similar relationship between them has also been recognized by Saha et al. (2007).

Long-term changes in seasonal and annual rainfall have been evaluated using Mann-Kendall test by Hollander and Wolfe, 1973. In accordance with Subramanian et al. (1992), Mann-Kendall test is a powerful statistical technique for randomness against trend. Numerous workers have reported the use of Mann-Kendall test in trend analysis of meteorological parameters, particularly of rainfall. Krishnakumar et al. (2009) established the long-term changes in seasonal and annual rainfall over Kerala by Mann-Kendall trend test. Several workers have also applied this non-parametric method for quantifying the direction and magnitude of trends in the streamflow and rainfall records (Chiew and McMahon, 1993; Kale, 1998; Hire, 2000; Marengo, 1995; Probst and Tardy, 1987; Gunjal and Hire, 2007). Moreover, some other workers (Sahu (2004), Seetharam (2003), Lal et al. (1993) and Suresh et al. (1998)) used this test for detection of the nature of changes in the rainfall of the small regions or stations.

The important question to rainfall studies in India is whether the future is likely to see the condition of rainfall decreased, unchanged or exacerbated. Even though, it is complex to envisage the direction and magnitude of change, it is possible to approximate the percentage change required in the future data series before it can be considered to be statistically significant (Kale, 1998). Student's t-test has been used by Chiew and McMohan (1993) and Marengo (1995) to find out the percentage change essential in the mean of the future rainfall data series prior it can be considered to be appreciably different from the historical gauge record.

**(ii) Flood hydrology**

It is obvious from the above discussion that monsoon regime plays an important role to determine the river regime conditions of the river under study. Nonetheless, the efficacy of discharge regime characteristics is inadequate for geomorphological purposes since it is based on monthly or ten-daily means. The extensive work on some large Indian rivers designate that the channel forms and processes are associated to very large, but relatively infrequent flood events (Goswami, 1985; Kale et al., 1994; Gupta, 1995a; Gupta et al., 1999).

According to Rostvedt et al. (1968) and Ward (1978), in a broad intellect, rise in the water level/stage or discharge that result in overtopping of natural or artificial banks of a stream is known as flood. In hydrology, a flood perhaps any relatively high water level or discharge above a pre-determined flood level or discharge magnitude (Ward, 1978). From the geomorphic standpoint, a flood has been defined as a high flow for which the stream channel is clearly inadequate transportation system and whose passage occupies at least the lower part of the valley flat (Gupta, 1988). Moreover, in India for meteorological functions, flood is recognized with reference to a danger level (DL). For instance, Ramaswamy (1985) considers a flood as 'severe' if the highest flow level is at least 2 m above the danger level. Large floods are often expressed in terms of return period or recurrence interval (100-yr, 500-yr or 1000-yr flood).

The definitions given above are usually accepted, however, they are neither applicable across the world nor to the study area since, the river under review is deeply incised in bedrock. Due to which even high flows are incapable to fill the entire channel, and overtopping is infrequent. At the same time, there is little uncertainty that significant positive departures from mean flows occur, and such flows cannot be treated as just high flows (Hire, 2000). Thus, there is a need to have an alternative definition of flood for the study area.

In general, for hydrologists and geomorphologists, the single maximum instantaneous discharge for every year of gauge record is of great interest. Consequently, the simplest and most suitable definition of flood for an incised river should be based on the statistical parameters such as mean and standard deviation of the annual peak discharges (Hire, 2000). According to Petts and Foster (1985), in fluvial geomorphology flows having a recurrence interval of 2.33 years to about 5 years are considered to be significant from the standpoint of geomorphic work (Petts and Foster, 1985). For the river under review none of the definitions given by earlier workers are applicable. However, Hire (2000) has defined floods on the basis of recurrence interval. According to him, a discharge having a recurrence interval of 2.33 years is the same to the mean annual peak discharge (Qm), whereas, a flow having a return period of 5 years is close to mean plus one standard deviation ($Qm+1\sigma$), which has a recurrence interval of 6.93 years. The above depictions given by Hire (2000)

seem to be appropriate for the Par River. Moreover, annual maximum series data are available for about 50 years for a gauging site on the river. Therefore, floods are defined as under;

- *Floods* (Qf): all annual peak discharges above mean annual peak (Qm), but below mean plus one standard deviation (i.e. $Qm<Qm+1\sigma$).
- *Large floods* (Qlf): all floods that exceeds mean plus one standard deviation ($>Qm+1\sigma$).
- *Peak on record* (Qmax): highest annual peak flood discharge on record during the gauge period. This is the highest Qlf.

The measured instantaneous peak flood discharges encompass one of the most important datasets for hydrologists, engineers and geomorphologists. According to hydrologist annual peak discharge series or annual maximum series (AMS) is highest peak discharge recorded in each year for a series of years at a gauging site (Ward, 1978).

In general sense, in hydrology, stage discharge curve or rating curve is a graph of discharge versus stage/gauge for a given point on a stream, normally at gauging stations, where the stream discharge is measured across the stream channel with a flow meter. According to Giovanni (2008), the empirical as well as theoretical relationship exist between the water-surface stage (i.e. the water level) and the concurrent flow discharge in an open channel, this relationship is known as stage-discharge relation or rating curve, or just rating. Numerous measurements of stream discharge are made over a range of stream stages.

An evaluation of the effectiveness of flows depends much on the magnitude and frequency of the events than mean discharges. Magnitude-frequency analysis is one method that identifies the hydrological and geomorphological importance of these events quantitatively, particularly the frequency of flood events of various magnitudes (Chow, 1964; Leopold et al., 1964; Morisawa, 1968). In flood hydrology, flood frequency analysis (FFA) is a statistical measure and is considered to be an effective tool to interpret past records of gauge data in terms of future probabilities of occurrences (Mutreja, 1995). One of the most familiar means to indicate the probability of a flood event is to assign return period or recurrence interval to the

event. In general sense, the recurrence interval or return period is defined as "an annual maximum event having a return period or recurrence interval of T years, if its magnitude is equalled or exceeded once, on the average, every T years. The reciprocal of T is the exceedance probability of the events i.e. the probability that the event is equalled or exceeded in any one year" (Bedient and Huber, 1989). Floods are analyzed and explained in a probabilistic sense because of their inherent randomness.

There are numerous probability distributions that are used in flood hydrology. The most commonly used probability distributions are Lognormal, Gamma (Pearson type III), Log Pearson type III (LP III), Gumbel extreme value type I (GEVI) etc. Since the objective of the present study is not to find out the most appropriate probability distribution(s) for the river under study, but to estimate the recurrence interval of high flows, the FFA is mainly based on the GEVI distribution. GEVI probability distribution have been selected mainly on the basis of its applicability to the monsoon-dominated Indian rivers. On the basis of analysis of long records available for 92 gauging stations, Garde and Kothyari (1990), have proposed GEVI distribution for the AMS data from Indian catchments. Therefore, in order to understand the hydrological characteristics of floods in terms of size and frequency, the GEVI probability distribution has been applied to the AMS data.

E. J. Gumbel put forward the concept of extreme-value, in which he conceived that the largest daily discharge in a year was the upper extreme of the 365 daily flows, and this value of a year formed part of an extreme-value series (Petts and Foster, 1985).

According to Costa and O'Connor (1995), the maximum discharge is typically considered as a measure of the potential of flow to be an effective geomorphic agent. Large discharges indexed by area or recurrence interval are supposed to generate large forces to cause enduring changes in the channel and valley morphology. Nonetheless, given the hydro-climatic conditions there is an upper physical limit to the magnitude of floods that can be produced (Enzel et al., 1993), and consequently the maximum possible force that can be generated. Thus, to assess the potential of a region to produce a maximum possible peak discharge, regional envelope curves encompassing the maximum flood peaks experienced in a region have often been used to define the natural upper bounds to flood magnitudes (Enzel et al., 1993). This graphical and empirical approach is based on two assumptions: (1) that there are physical limits to

supply of precipitation to a basin (Enzel et al., 1993), and (2) the maximum flood per unit drainage area in one basin is likely to be experienced in nearby basins having similar hydro-geomorphic conditions (Mutreja, 1995).

**(iii) Flood geomorphology**

In flood geomorphology, the measurement and evaluation of the geomorphic effectiveness of flows of different magnitude has been one of the significant themes. Efficacy of events in shaping landforms is measured by the magnitude of flows, by the frequency with which they occur, and by the amount of suspended sediment they transport (Wolman and Miller, 1960). Recently, the potential of flood flows has also been assessed in terms of the channel boundary shear stress and stream power per unit boundary area (Baker and Costa, 1987), as well as the flood flow duration (Costa and O'Connor, 1995). Channel morphology is the dimensions of a river channel in cross section and in plan (Petts and Foster, 1985). The morphologic properties of a channel vary in different reaches throughout the course of a river and are governed by the factors given below (Morisawa, 1985);

- The interaction of the hydraulic of flow (velocity, discharge, roughness, and shear stress),
- The channel configuration at the reach and immediately upstream (width, depth, shape, slope and pattern),
- Sediment load entering the reach (caliber and amount), and
- The composition of bed and bank material.

Therefore, according to Morisawa (1985) the river channel morphology is an expression of equilibrium between stream power and the resistance of material comprising the channel perimeter. The appearance of a river can be divided into following categories.

- Channel size and shape: The size includes channel width (W), mean depth (d), cross sectional area ($A_C$), wetted perimeter (Wp), and hydraulic radius (R), and the shape of the channel is characterized by the width-depth (w/d) ratio.
- Channel slope or gradient
- Channel pattern: i.e. the form of the channel in two dimensions.

The form of the channel is a function of the energy available to erode or deposit materials of different caliber along the bed and banks at different flood stages. The channel form is function of bed and bank material texture, fluctuations in discharge, sediment load, the balance between aggradation and degradation and the resulting pattern, rates of bank erosion and deposition at any cross-section or along any reach (Fryirs and Brierley, 2009).

The literature review indicates that a few studies have highlighted on meteorological, hydrological and geomorphological aspects of floods on bedrock rivers.

Chapter 3

# Research Methodology

## 3.1 Introduction

Research methodology is employed in every research to systematically solve the research problem. It is a process of dealing with research problem scientifically. The following section includes various steps that are adopted in the present work to study research problem along with the logic behind it.

## 3.2 Research Methodology

In order to attain the objectives of the present study given in section 1.5, the following methodology has been adopted.

### *3.2.1 Channel morphological features*

#### (i) Bedrock channel planform

River planform is the form or shape of a river channel as viewed from above. Three channel planforms namely straight, meandering and anastomoising channels have been identified for the river under review. The straight channel reaches have been identified on Par and Nar Rivers with the help of field surveys, satellite images and topographical maps. In addition to this, the straight reaches of river under review have been mapped using software Google earth and ArcGIS 9.3.

Brice (1964) applied the Sinuosity index (Si) to differentiate straight river channels from sinuous and meandering river channels. If the Si <1.05 the channel is straight; Si between 1.05 and 1.5 is sinuous; and if Si> 1.5 the river channel is meandering. These values have been used for the river under review. Quantification of bend statistics for the river was made possible by means of ca. 30 m resolution Advance Spaceborne Thermal Emission and Reflection Radiometer (ASTER) data, by means of topographical maps and numerous field surveys. In addition to this, Google Earth Images have been used to represent and quantify meandering channel of the Par River. Traditional bend statistics such as meander wavelength ($\lambda$), meander length ($L_m$), mean radius of curvature ($Rc_m$), channel width (W) and amplitude (A) (Figure

3.1) have been calculated for 23 meanders of the Par River using tools of ArcGIS 9.3. Sinuosity index (Si) was calculated by the ratio of meander length ($L_m$) to meander wavelength (λ).

$$Si = L_m / \lambda \qquad \text{Equation}\ldots\ldots 3.1$$

The relations between meander wavelength (λ) and mean radius of curvature ($Rc_m$), channel width (W) and amplitude (Am) have been expressed by power regression equations as under. Where a and b are constants.

$$\lambda = aW^b \qquad \text{Equation}\ldots\ldots 3.2$$

$$\lambda = aRc_m^{\ b} \qquad \text{Equation}\ldots\ldots 3.3$$

$$Am = aW^b \qquad \text{Equation}\ldots\ldots 3.4$$

Leopold et al. (1964) proposed that meander wavelength (λ) is empirically associated with square root of effective or dominant discharge for alluvial rivers. Since channel width (W) is also allied to discharge, it has been proposed that there is fundamental relation between channel width (W) and meander wavelength (λ). Although the Par River is not the alluvial river, an attempt has been made to show relationship between channel width (W) and meander wavelength (λ).

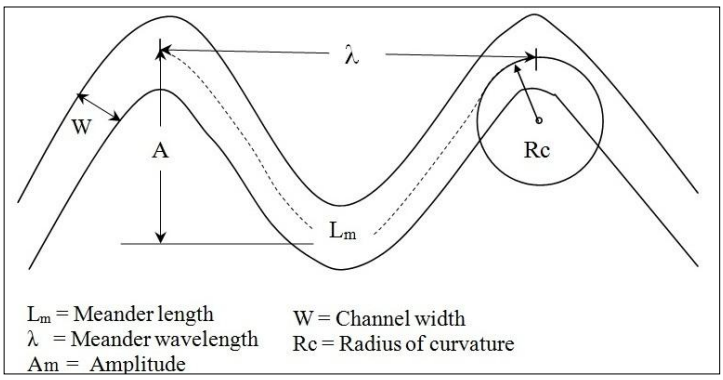


**Figure 3.1** Sketch to define terms used in describing geometric characteristics of a meandering channel

Like the other bedrock rivers, the Par River also flows through single flow path from its source to mouth. However, extensive bedrock outcrops in the form of multi-thread channels have been identified near Panchlai, furthermore, with the help of field surveys, topographical maps and google images and essential measurements have been taken. Besides, the multi-thread pattern of Par River channel has been mapped. In addition to this, an attempt has been made to find out the formation process of bedrock anastomoised channel near Panchlai.

**(ii) Channel form/channel geometry**

Channel forms have been studied in terms of width, depth and form ratio for the Par River. Sixteen cross-sectional surveys have been carried out to study the form of the channel. Generally two groups of aspects are considered to describe channel cross sectional form – i) channel size and ii) channel shape. Perimeter lithology is an important factor to determine channel shape. Rosgen (1994) used boundary composition as one of the basic criteria to classify river channels. He produced 41 channel types on the basis of boundary composition. Similar scheme have been applied to classify the channels of the Par as well as its major tributary i.e. the Nar.

The adjustments in the width-depth ratio and hydraulic variables with discharge have been shown to very useful concepts in evaluating the potential of flows to be geomorphologically effective (Kale et al., 1994; Gupta, 1995a). Therefore, an attempt has been made to find out width-depth ratio(s) and hydraulic variables of the Par River.

In order to examine the relationship between width and discharge (Q) or drainage area (A), it is necessary to define reference discharge. However, due to scarcity of data for river under review, such discharges were not available. The width of most bedrock channels can be more readily defined on the basis of the zone of active scour, as indicated by the limit of established perennial vegetation (Montgomery and Gran, 2001). Therefore, an attempt has been made to examine the relation between channel width and drainage area, as they are relatively unambiguous to determine even for bedrock reaches (Montgomery and Gran, 2001). Several field surveys have been carried out to measure width of the active channels on the Par River. Drainage areas have been measured with the help of ASTER DEM data, toposheets (1:50000 and

1:250000) and GIS applications. Ultimately, the relation between channel width (W) and drainage area (A) is expressed as positive power function for the river as under;

$$W = cA^b \qquad \text{Equation } \ldots..3.5$$

Where c and b are constants.

(iii) **Erosional features of bedrock channel**

The main purpose of the present section is to recognize physical characteristics of morphology of different landforms and their formation processes. Therefore, in order to study erosional landforms, an extensive field survey was carried out from source to mouth of the Par River. Following erosional landforms have been identified in the field, measured, analysed and mapped with the help of toposheets, ArcGIS 9.3 and Google Earth.

- The locations of potholes in the Par River channel have been identified from source to mouth and careful measurements of size and shape of potholes have been carried out. The statistical parameters of various geometric properties of the potholes have been obtained and presented in tabular format. The coefficient of skewness ($\mathbf{C_s}$) is one of the most commonly used moments in statistical analyses. It is the measure used to find out the degree of asymmetry of a statistical distribution. Therefore, analysis of coefficient of skewness of the morphometric parameters of the potholes of the Par River has been carried out. Coefficient of kurtosis ($\mathbf{C_k}$) is a measure used to find out the degree of peakedness of a statistical distribution. In addition to this, the potholes have been categorised according to their prominent shapes. Furthermore, the empirical relationship between diameter (K) and depth of potholes (D*) has been established for the Par River as under;

  $$K = aD^{*b} \qquad \text{Equation } \ldots..3.6$$

  Where, K (cm) is Diameter of potholes and D* (cm) is Depth of potholes (cm), a and b are constants. The relationship between length (L) and depth of pothole (D*) has been expressed for the river under review as follows;

$$L = aD^{*\,b} \qquad \text{Equation } \ldots..3.7$$

Where, L (cm) is length of potholes and D* (cm) is depth of potholes, a and b are constants.

- The locations of grooves in the Par River channel have been identified from source to mouth and careful measurements of the dimensions of grooves have been taken in the field. The statistical parameters of various geometric properties of the grooves have been obtained and represented in tabular format.

- Eight prominent inner channels of the Par River were identified in the field and measurements of dimensions were carried out to find out possible mechanism of their formation.

The downstream changes in the gradient have been shown by its longitudinal profile, which is a graph of elevation against distance along the channel. The elevations of the knickpoints have been measured in the field.

The channel distance (L) and slope (S) are correlated by a power function and attempt has been made to establish the relation between distance (L) and slope (S). The channel distance (L) and slope (S) are correlated by a power function as under;

$$S = kL^{n} \qquad \text{Equation } \ldots..3.8$$

Where S is slope of channel and L is distance, k and n are steepness and concavity variables respectively.

Numerous expansion bars have been formed at abrupt expansions downstream of constricted reaches of the Par River. In order to find out expansion, the Expanded reaches (Er)/Constricted reaches (Cr) ratio has been established. In addition to this, longitudinal bars and point bars have been identified in the field. The dimensions of bars such as width, length and height have been measured in the field and areas occupied by bars have been measured by means of satellite images and GIS applications. Moreover, depositional features have been mapped using ArcGIS 9.3.

An attempt has been made to find out hydraulic parameters such as bed shear stress, unit stream power, and mean velocity necessary to transport coarse-grained sediment.

Using the empirical relationships developed by Williams (1983), the threshold values of unit stream power, bed shear stress, and mean velocity necessary to transport the boulders were calculated.

### *3.2.2 Erosional processes and sediment transport*

#### (i) Flood hydraulics and hydrodynamics

In order to find out effect of infrequent and large magnitude floods on the Par River, parameters of flood hydraulics and hydrodynamics such as unit stream power, bed shear stress, Froude number, Reynolds number and critical velocity for inception of cavitation were computed. Critical unit stream power, boundary shear stress and mean velocity values necessary to entrain cobbles and boulders were estimated on the basis of empirical relationships for coarse sediment transport.

#### a. Parameters of flood hydraulics and hydrodynamics

Due to lack of quantitative hydraulic data of rare floods for the Par River, sixteen cross-sectional surveys were carried out for the river under review. In addition to this, channel slope data have been constructed in the field. The aforementioned data have been used to procure hydraulic and hydrodynamics parameters such as unit stream power, boundary shear stress, Froude number, Reynolds number and critical velocity to understand geomorphic efficacy of rare flood events. The geomorphic effectiveness of a flood, which relates to its ability to affect the form of the landscape (Wolman and Gerson, 1978), is commonly linked to flood power and the degree of turbulence (Baker and Costa, 1987; Wohl, 1993; Baker and Kale, 1998; Kale and Hire, 2004, Hire and Kale, 2006, Kale and Hire, 2007). Therefore, for the known rare flood events, boundary shear stress, unit stream power per unit boundary area, Froude number, Reynolds number were computed (Leopold et al., 1964; Baker and Costa, 1987).

#### aa. Shear stress ($\tau$)/fluid stressing/shear detachment

Shear stress ($\tau$) is a measure of the frictional force from a fluid acting on a body in the path of that fluid. It is one of the critical causes behind entrainment of particles. In the case of open channel flow, it is the force of moving water against the bed of the

channel. Shear stress increases with flow depth and channel steepness. It is calculated as;

$$\tau = \gamma RS \qquad \text{.....Equation. 3.9}$$

where, $\tau$ (shear stress is represented by the Greek letter tau, ($\tau$)) is boundary shear stress expressed in Newton per square meter ($N/m^2$), $\gamma$ (gamma) is specific weight of clear water (9800 $N/m^2$), R is hydraulic radius or mean depth of water in m, S is channel slope.

**ab. Unit stream power (ω)**

Unit stream power (ω) is the capacity of a given flow to transport sediment. It represents the work done by a flow on a unit area of channel bed (Bangnold, 1980). Unit stream power is calculated as;

$$\omega = \gamma QS/w \qquad \text{.....Equation 3.10}$$

where, ω (lower-case omega, ω) is unit stream power expressed in watts per square meter ($W/m^2$), Q is discharge in $m^3/s$, w is the water surface width in m.

In order to find out sediment transport rates, sediment entrainment and flow capacity of bedrock channel of the Par River, the shear stress and unit stream power for 16 cross-sectional sites have been calculated. To compute thresholds of shear and entrainment, boulders located at seven cross-sections have been analysed using William's equations (Equation 3.15 to 3.17).

**ac. Froude number (Fr)**

To study flow characteristics of the Par River, Froude numbers (Fr) have been calculated and classified. Froude number (Fr) is the ratio between inertial and gravitational forces.

$$Fr = \bar{v} / (gR)^{0.5} \qquad \text{.....Equation 3.11}$$

where, Fr is Froude number, $\bar{v}$ is mean flow velocity in m/s, g is acceleration due to gravity (9.8 $m^2/s$), R is hydraulic radius or mean depth of water in m. Three possibilities of flow exist according to the range of Fr (i) If Froude number is less than one (Fr < 1), the flow is said to be subcritical and gravitational force dominates (ii) on the contrary if value of Fr is more than one (Fr > 1), the flow is supercritical and inertial forces govern the flow. (iii) the value of Fr is equal or close to one (Fr = 1), in such case the flow is critical or transitional.

**ad. Reynolds number (Re)**

In order to measures the degree of turbulence, or random changes in flow direction and/or velocity superimposed on the main downstream movement of water of the Par River, Reynolds number (Re) were calculated.

$$Re = \bar{v}R / \nu \qquad \text{.....Equation 3.12}$$

Re is Reynolds number, $\bar{v}$ is mean velocity, R is hydraulic radius or mean depth of water in m, $\nu$ (Greek small letter Nu) is kinematic viscosity ($1 \times 10^{-7}$ $m^2/s$ for water temperature of $20^o$ C) (Leopold et al., 1964; Petts and Foster, 1985). The values of Re are efficient to find out whether the flow is laminar or turbulent. At low Re numbers (<500) viscous forces dominate and the flow is laminar. High Re numbers (>2100) indicate turbulent flow; transitional flow is observed between Re values of 500 and 2,100.

**ae. Critical velocity for inception of cavitation (Vc)**

In order to find out intense bedrock scouring which results from cavitating flow condition, critical velocity required for inception of cavitation (Vc) have been calculated for the cross-sectional sites of the Par River as follows.

$$Vc = 2.6\ (10+D)^{0.5} \qquad \text{.....Equation 3.13}$$

Where, Vc is the critical velocity for the inception of cavitation in m/s and D is flow depth.

**af. Hydraulic plucking**

Numerous crisscross dykes have been observed in the Par Basin, of which, majority of dykes are highly dissected due to plucking. The plucked blocks of such dykes have been identified in the field and the distances of plucked blocks from the dykes (source) have been measured. The plucking has also been observed other than dykes in the channel of the Par River.

**ag. Knickpoint migration and river incision**

The upstream migration of knickpoints has been recognized as significant means of bedrock channel lowering, however, little is known about the mechanisms that control the shapes and migrations of knickpoints (Miller, 1991; Seidl and Dietrich, 1992; Seidl, 1993; Whipple et al., 2000 (a, b); Zaprowski et al., 2001). Therefore, attempts have been made to find out examples of knickpoint migration and to estimate rate of incision for the Par River. According to Baker (1988); Wohl (1992, 1998 and 2000) and Ikeda (1997), headward migration of a knickpoint through resistant substrate can leave behind a deep and narrow gorge, it reflects the erosional resistance of the channel boundaries, and maximizes the shear stress and stream power per unit area of a given discharge and channel gradient. Similar observations have been noted for the Par River as well as its tributaries, where, deep and narrow gorges are observed immediately downstream of knickpoints. Several equations and models have been developed by researchers to predict channel incision of a river into its bed. The comprehensive and most commonly used stream power erosion model (SPEM) is of great use, since, there are few variables and can be measured against topographical data (Howard and Kerby, 1983; Skylar and Dietrich, 2001). It is argued by Howard and Kerby (1983) that the Stream Power Law/model (SPEM) is most applicable because it is related to physics of erosion. Therefore, to estimate the incision rate and migration of knickpoints of the Par River stream power erosion model has been applied. The stream power erosion model has been applied as follows;

$$\varepsilon = KA^m S^n \qquad \text{..... Equation 3.14}$$

where, ε is (Greek small letter epsilon) vertical erosion rate (m/yr); K is coefficient of erosion (m/yr); A is upstream drainage area ($m^2$); S is channel bed gradient/local slope; m and n are exponents.

The major controls on the equation are that of slope, discharge/upstream drainage area and erodibility of the rock. The constant K in the stream power model is a dimensional coefficient of erosion incorporating effects due to lithology, climate, channel width, hydraulics, sediment load (Sklar and Dietrich, 2001), rock strength and the erosional capabilities of the fluvial system (Whipple, 2001). Stock and Montgomery (1999) have applied stream power erosion model for Kaulaula and Waipao Rivers, which flow through basalt lithology. For the above-mentioned rivers they have used K values as $6.7 \times 10^{-6}$ and $7.3 \times 10^{-6}$ respectively. Being similar lithology, average of above values (i.e. $7 \times 10^{-6}$) has been calculated and used to compute the model for the Par River. Howard and Kerby (1983) recommended that for construction of stream power erosion model, upslope drainage area can be used as a surrogate for dominant discharge. Howard et al. (1994) and Dietrich and Seidl (1994) opined that the proxy is possible since the average long term incision rate is proportional to the sheer stress exerted by the dominant discharge within the channel. Thus, upstream drainage area has been substituted for dominant discharge for construction of SPEM for the Par River. By using topographical maps, channel slope (S) has been calculated for Kalmane (0.0068) and Bhimtas (0.0304) reaches. In SPEM, m and n are area and slope exponents respectively (Whipple and Tucker, 1999). Stock and Montgomery (1999) recognize the exponent m as the account of the discharge drainage area interaction which is weighted by the significance of discharge on the process incision. Conversely, little information is available on the slope exponent (n), probably due to the process involved not being entirely understood. Fewer studies have reported the values for the exponent m and n. For construction of SPEM for the Par River, exponents given by Gardner (1983) and Howard et al. (1994) have been used, according to which if bedrock incision is proportional to shear stress, m = 0·3 and n = 0·7. Gilbert (1877) and Gannet (1893) hypothesized that the rate of bedrock river incision should be a function of rock resistance river, discharge (surrogate by area) and slope. The parameters given by Gilbert (1877) and Gannet (1893) have been derived in order to run SPEM and to estimate incision rate for the Par River.

Unfortunately, the above analysis does not provide any information about upstream propagation of knickpoints. However, the Bhimtas River, a tributary of the Par River, has developed an excellent gorge downstream of the Bhimtas Knickpoint. It appears that the gorge widens proportionately for about 4.5 km downstream from the knickpoint. Therefore, an attempt has been made to find out correlation between the distance and the width of the gorge from the knickpoint. The width(s) and the distances of the gorge have been measured for 38 sites for 4.5 km of the knickpoint (Figure 4.70; Figure 4.71). The simple regression equation has been applied for the above data and plotted.

**b. Coarse sediment transport**

The resistant-boundary channels are supply-limited, coarse sediment entrainment and deposition is usually associated with infrequent and extreme floods (Baker, 1988). The channel of the Par River is dominated by resistant bed and coarse sediment. Therefore, large boulders were identified and intermediate-axis (i-axis) of boulders has been measured to evaluate the tendency and mobility of coarse sediment from sixteen sites (285 coarse sediment samples). In order to evaluate the mobility of these coarse sediment theoretically, the sediment-transport equations developed by Williams (1983) were applied, and the approximate minimum critical values of bed shear stress ($\tau$), unit stream power ($\omega$), and mean velocity ($\bar{v}$) that could initiate coarse sediment movement were estimated with the help of following formulae;

$$\omega = 0.079\ dg^{1.27} \qquad \text{.....Equation 3.15}$$

$$\tau = 0.17\ dg \qquad \text{.....Equation 3.16}$$

$$\bar{v} = 0.065\ dg^{0.5} \qquad \text{.....Equation 3.17}$$

where, dg is the intermediate diameter of the grain in mm.

### *3.2.3 Role of lithology and tectonics*

**(i) Rock mass strength of resistant boundary channel of the Par River**

In order to study the role of lithology and efficiency of processes to shape the channel, the Schmidt hammer rebound values (N) were derived by using ‘N’ type Schmidt

hammer (SH). 371 N values were obtained for 12 cross sectional sites on the Par and two cross sectional sites on the Nar River. For each site 20 to 30 rebound values were procured. Two cross sectional sites have been excluded namely Jhiri, which exhibit mainly depositional material and very sensitive proposed dam site of Chachpada (See location in Figure 4.12). The N values were used to estimate the Rock Mass Strength (RMS) i.e. the specific properties of the rock mass that control its strength and subsequent slope stability (Goudie, 2004). Several testing procedures were given by different researchers (Goktan and Gunes, 2005) mainly with regard to the number of impacts used to obtain Rock Mass Strength (RMS) values. According to recommendation of International Society for Rock Mechanics (ISRM) (1978), average of upper 10 values as of 20 rebound values from single impacts separated by at least a plunger diameter should be considered. Matthews and Shakesby (1984) suggested that from 15 rebound values for each sample 5 most deviating values from the mean being discarded. Katz et al. (2000) performed 32 to 40 individual impacts and averaged the upper 50%. In order to find out RMS for the Par River, method given by Katz et al. (2000) has been applied i.e. from 20 to 30 rebound values of each cross sectional site, upper 50% values have been used. 181 unusual low values of rebound (N) have been excluded to calculate RMS due to various reasons such as i) they may relate to the fact that the rock was weakened by the actual impact of the hammer on the rock surface ii) small rock flaws that were not spotted visually before the impact was applied (Goudie, 2006). The rebound values or impact values (N) derived by Schmidt hammer were converted into standard averages of RMS ($N/mm^2$) by calculating a statistical power-law relationship (Goudie, 2006). The following conversion curve was used to convert N values into RMS (Sengupta and Kale, 2011);

$$RMS = 0.1152\ N^{1.6348} \qquad \text{....Equation 3.18}$$

where, RMS is Rock Mass Strength or rock resistance in $N/mm^2$; N is Schmidt rock hammer rebound value. The RMS values obtained from the N values were averaged in order to get the mean rock resistance of all cross sectional sites. The mean RMS of every cross sectional sites have been used to calculate average RMS of the Par river. Statistical parameters of RMS such as range, standard deviation ($\sigma$) and coefficient of variation (Cv) have been calculated.

The area under review is characterised by numerous crisscross lineaments and dykes. Thirty prominent dykes on Par River have been identified and measured. The position of dykes with respect to direction of flow has carefully been observed and attempts have been made to find out the control of dykes on path of channel. It could not become possible to measure the N values of all the dykes, nevertheless, 44 similar values of five dykes have been obtained from different cross sectional sites to get RMS values. By following the method given by Katz et al. (2000), 50% anomalous low values of rebound (i.e. 22 N values) have been excluded and upper 50% values have been used to calculate average RMS as well as other statistical parameters for dykes.

In order to semi-quantitatively assess rock erodibility between basalt and dykes, N and RMS values of basalt (167) and similar values of dykes (22) have been analysed. The comparison between these two substrate resistance has been represented with the help of box-whisker plots. It is hypothesised that there are differences in rock erodibility between basalt and dykes.

**(ii) Geomorphic Indices of Active Tectonics (GAT) in morphotectonic analysis**

The Par River Basin is very appropriate for this type of morphotectonic analysis and for making significant appraisals between basins and fluvial systems. Quantification of a number of geomorphometric indices for the river under review were made possible by means of the analysis of Digital Elevation Model (DEM) of ca. 30-m resolution Advance Spaceborne Thermal Emission and Reflection Radiometer (ASTER) data. Normally, 30-m resolution ASTER DEM with relative accuracy can be used effectively to assist mapping, geomorphic, geologic, tectonic, landform, and a range of environmental studies in remote areas of rugged terrain (Lang and Welch, 1999; Hirano et al., 2003; Figueroa and Knott, 2010). The digital elevation data were used to extract information about drainage basin, network and river profile. This was achieved by using standard procedures in ArcGIS 9.3 (Kale and Shejwalkar, 2007; Huasm, 2008; Kale and Shejwalkar, 2008; Wiltschko et al., 2010; Dehbozorgi et al., 2010).

The morphotectonic analysis of the river under review is based on the calculation of five commonly used geomorphic indices of active tectonics (GAT) such as the

hypsometric integral (HI), the basin asymmetry factor (AF), the valley width-height ratio (Vf), the stream gradient-length ratio (SL), and the basin elongation ratio (Re). The mountain front sinuosity, one of the widely used geomorphic indices, is not evaluated in the present study. In addition to hypsometric integral, hypsometric curve has been derived for the basin under investigation. The procedures adopted to calculate the GAT indices are defined in Table 2.2. The indices were then assessed by field observations of the occurrence of knickpoints, incised meanders, gorges, etc., as markers of active tectonics.

It is pertinent to mention here about the longitudinal profile extracted from the ASTER-DEM data. Because of stepping in adjacent elevations on the ASTER-DEM and the effect of water bodies such as ponds and dams, the recognition of substantial breaks and knick zones in the longitudinal profiles is not a very simple and straightforward task especially for low-gradient reaches (Kale and Shejwalkar, 2008). A running mean (aka moving average) of 11 consecutive elevation values used for smoothing the long profile partially reduces the problem but does not remove it completely (Kale and Shejwalkar, 2008). Therefore, zones of steeper reaches (knickpoints or zones) could not be identified. Hence, the knickpoints identified in the field have been mapped and discussed.

### *3.2.4 Flood Hydrometeorology, Hydrology and Geomorphology*

#### (i) Flood hydrometeorology

In order to understand the meteorological causes of floods, the analyses of synoptic conditions connected with large floods in the Par Basin was carried out. This encompasses analysis of (i) rainfall; (ii) analysis of storm tracts and; (iii) evaluation of the correlation between El Niño and monsoon rainfall in the basin.

Meteorological data of five stations located within and close to the Par Basin have been obtained from India Meteorological Department (IMD), Pune and analysed to identify the rainfall characteristics that produce large floods on the Par River. The data were available for more than 100 years except Surgana Station for which data availability is for 50 years. The general rainfall characteristics, for instance, monthly

and annual averages of rainfall, monsoonal rainfall and non-monsoonal rainfall, etc. for the five stations in the Par Basin have been calculated and shown graphically.

**a. Rainfall regime characteristics**

The average rainfall characteristics for the five stations in the Par Basin have been shown graphically and given in tabular format. Annual rainfall data of the above-mentioned five stations were averaged to obtain annual rainfall of the basin and displayed in Figure 4.90. Like other parts of the monsoon tropics, there is variability in the annual as well as monsoon rainfall between years. The interannual variability of selected stations and for the whole Par Basin have been calculated and represented graphically.

**b. Flood-generating meteorological conditions**

In the humid and seasonal tropics, large floods are mostly associated with high-magnitude rainfall caused by synoptic events ranging in force from lows to cyclones (Gupta, 1988; 1995a). Therefore, the tracks of the low pressure system, that affect the basin, have been identified using software eAtlas and analysed with the help of ArcGIS 9.3.

In general, during the passage of LPS, it causes heavy falls of rain along and near their tracks (Dhar at al., 1984). The LPS (Bay or land depressions) which follow a westward track through Tapi Basin are more effective in causing heavy rainfall and floods in the Par Basin. Therefore, an attempt has been made to identify and analyse the mean track of such LPS using software eAtlas (procured from IMD, Chennai) and ArcGIS 9.3. The software eAtlas contains data regarding tracks of LPS from year 1891 to 2007, thus, similar range have been adopted for further analyses. In general tropical cyclones range in diameter from 100 to well over 1000 km (Glossary of American Meteorological Society, 1959). Hence, a circle having thousand kilometre of diameter has been plotted from the centre of the basin and those LPS tracks which pass through the circle, as shown in Figure 4.92, have been identified and analysed. The latitudinal and longitudinal positions of such cyclones were taken into consideration for each day of their life span (Mooley and Shukla, 1987). Using these data the mean latitudinal and longitudinal positions were calculated. The above-

mentioned methodology has been adopted by Hire (2000), who has prepared mean LPS track for the Tapi Basin. As the areal extent of Tapi Basin (65145 $km^2$) is much greater than that of Par, those LPS tracks which range within five-hundred kilometres from the peripheral area of the Tapi basin have been selected by him. Being small in size, a circle drawn from the centre has been used instead of aforementioned method for Par Basin.

**c. Normalized accumulated departure from mean (NADM) method**

The year to year fluctuations in rainfall of the region cause complexity in recognition of the direction of change in the rainfall. Thus, some effective statistical methods are to be applied to identify the nature of long-term variability in monsoon rainfall. The frequently used method to study the variability of rainfall is Normalized Accumulated Departure from mean (NADM). Consequently, the NADM plotting method has been used to emphasize the long-term variability by minimizing short-term fluctuations in the monsoon rainfall. According to Thomas (1993), the NADM is the Accumulated Departure from Mean (ADM), divided by the largest number (absolute) in order to plot between -1 and +1. Therefore, the normalized ADM allows apparent as well as statistical association of dissimilar data (Thomas, 1993). Periods featured by above-average state are usually shown by positive slopes of the graph and vice-versa (Gregory, 1989b; Thomas, 1993). In contrast with other methods used for similar purpose, such as running means, the ADM clearly shows the difference between periods of high and low rainfalls (Probst and Tardy, 1987).

**d. Long-period fluctuations in monsoon rainfall and floods**

In order to further estimate the fluctuations in monsoon rainfall and floods, the long-term annual rainfall data of the Par Basin, has been compared with the fifty years flood data available for Nanivahial gauging site and represented graphically.

The Indian southwest monsoon is teleconnected with the ENSO events. Therefore, an attempt has been made to recognize natural variability in annual rainfall (and therefore floods) in the Par Basin and its correlation with ENSO events. The annual rainfall data for the period of 104 years (1901-2004) of the basin have been used to establish the relationship with ENSO events.

In order to detect future changes in the rainfall, the non-parametric Mann-Kendall test has been used. The Mann-Kendall's Tau (τ) has been obtained by following equation;

$$\tau = \frac{\text{Actual total of scores (ATS)}}{\text{Maximum possible total}} \quad \text{…… Equation 3.19}$$

Where, actual total of scores (ATS) is the total of all sum(s) as calculated by the method adopted by Gunjal, (2016).

The maximum possible total has been acquired with following equation;

$$\text{Maximum possible total} = N\,(N\text{-}1) / 2 \quad \text{..…… Equation 3.20}$$

Where, N = Number of observations. The Mann-Kendall's τ is obtained by putting values in Equation 3.19.

The trend derived by Mann-Kendall test is practically significant or not is to be tested by testing the significance of Tau (τ). The method delineated for testing the significance of τ becomes extremely burdensome for the large *N*. Nevertheless, Kendall (1955) has revealed that when *N* is greater than 8, the theoretical distribution of all probable values of τ approaches the normal distribution. The τ may be transformed into a normal standard deviate as follows;

$$z = \frac{\tau}{\sqrt{2(2N+5)/9N(N-1)}} \quad \text{..….. Equation 3.21}$$

The value of the *z* can be obtained while substituting the calculated value of τ. For large number of observations ($N > 30$), *z* value has to be greater than 2.32 at 0.01 level and 1.64 at 0.05 level for the sample to be statistically significant.

This exercise mainly proposed to observe the change/trend over the basin scale, hence, Mann-Kendall's τ and *z* scores are obtained for the whole basin and the results

are given in tabular format. The application of this non-parametric test to the annual rainfall data of the basin designates no significant trend at 0.01 and 0.05 level.

Student's t-test has been used (Chiew and McMohan, 1993; Marengo, 1995) to find out the percentage change essential in the mean of the future rainfall data series prior it can be considered to be appreciably different from the historical gauge record. The percentage change can be estimated as;

$$t = \sigma * t\alpha \sqrt{\left(\frac{1}{nh} + \frac{1}{nf}\right)} \quad \text{…….. Equation 3.22}$$

$$\text{Change} = (\ t / \text{AAR}) \text{ x } 100 \quad \text{……. Equation 3.23}$$

Where,

t = Student's t value

σ = standard deviation of the historical gauge data

nh = length of historical rainfall series

nf = length of future rainfall data

tα = the critical value of the t-statistics at 95% level of significance and

AAR = average annual rainfall

**(ii) Flood hydrology**

**a. Flood hydrology of the Par River**

The Par River, similar to other monsoonal rivers, also subjected to high-magnitude floods at regular intervals. Thus, it is of paramount significant to know the hydrologic characteristics of floods in terms of magnitude, frequency, and distribution.

**aa. Annual flood series data and analysis**

In order to comprehend the flood hydrological characteristics, the annual maximum series (AMS)/stage data were procured from Irrigation Department of Gujarat State for a gauging site namely Nanivahial on Par River for 45 years specifically from 1960

to 2005. Moreover, based on Qm (Mean annual peak discharge) and Qm+1σ, AMS data have been estimated for years 2006 to 2009.

**ab. Stage discharge curve/rating curve**

In order to find out relation between stage and discharge for the Nanivahial site, rating curve has been plotted with the help of forty-five datasets of stage and corresponding discharge (Figure 4.96). The limited gauge records have been used to evaluate floods and flood flow frequencies. Primarily the AMS data have been presented in the form of time series plots to understand the interannual variations in the annual peak flood magnitudes. Second, to reduce and summarize the characteristics of floods, simple statistical analyses of AMS data have been carried out. The statistical parameters that are expressed in terms of the moments such as central tendency, variability and skewness as well as coefficient of variation have been calculated. In addition to this, flash flood magnitude index (FFMI) and unit discharges have been derived to evaluate the variability and the potential of large floods on the Par River.

**ac. Flood regime characteristics**

The temporal pattern of variation in the annual peak discharges at Nanivahial site on the Par River is demonstrated graphically. Interannual variability in annual peak discharges and average magnitude and variability for Nanivahial Site on Par River have been constructed. The Qmax/Qm ratio has been calculated to find out the credibility of floods to cause remarkable geomorphic changes and to generate discharges many times beyond the mean flows experienced by a river. Besides the Qmax/Qm ratio, the coefficient of variation (Cv) is another useful measure of variability in the annual peak discharges. It is the ratio between standard deviation and the mean. In order to further highlight the extent of variability in peak discharges from one year to other, deviations from mean annual peaks has been shown graphically for Nanivahial site (Figure 4.98).

Numerous workers have used the Beard's flash flood magnitude index (FFMI) to estimate the variability of flood frequency measured as an index of flood flashiness (Baker, 1977). The FFMI values are calculated from the standard deviation of logarithms of AMS as given below:

$$FFMI = \sqrt{\frac{\sum X^2}{N-1}} \quad \text{..... Equation 3.24}$$

where, X = Xm-Qm, Xm = annual maximum event, Qm = mean annual peak discharge, N = number of years of record (X, Xm, and Qm expressed as logarithms to the base of 10).

Skewness is one of the most commonly used moments in the flood hydrology. Since most of the AMS data are not normally distributed, it is important to find the skewness of the data. Therefore, the coefficient of skewness ($C_s$) of the AMS data has been calculated. To verify the degree of skewness, the ratio between skewness and coefficient of variation has also been used by some hydrologists (Shaligram and Lele, 1978).

Unit discharge is another useful measure of the potential of large floods on a river (Gupta, 1988). It is the ratio between maximum annual peak discharge (Qmax) and the upstream catchment area (A). It gives discharge (or water yield) per unit drainage area ($m^3/s/km^2$).

**b. Flood frequency analyses**

**ba. Magnitude-frequency analysis**

FFA necessitates a good quality, long and continuous records. Typically the AMS data have been more frequently used for the analysis. In case of the study area, the AMS data of flood stage and magnitude are available for Nanivahial site on the Par River for the last 49 years (since 1961). This data have been used for magnitude-frequency analysis. The return periods of the Nanivahial flood data have been estimated by applying Weibull's method. In order to estimate discharges of a given return period, a frequency distribution is compiled from a data series of extreme events. By using Gumbel extreme value type I (GEVI) probability distribution, peak flows have been estimated for different return periods such as 2, 5, 10, 25, 50, and 100 years. The distribution has also been employed to estimate the recurrence interval of mean annual peak discharge (Qm), large flood (Qlf) and actually observed maximum annual peak discharge (Qmax). A visual inspection of the fit of the

frequency distribution is possibly the best way in determining how fine an individual distribution fits the AMS dataset or which distribution fits "best" (Bedient and Huber, 1989). Therefore, flood frequency of the Nanivahial site is represented graphically (Figure 4.100) which fairly represents the Par Basin.

**bb. Gumbel extreme value type I (GEVI) distribution**

Assuming the GEVI distribution for the AMS data of the selected site, an estimate of flows for a desired recurrence interval were obtained by using the following equation (Shaw, 1988).

$$Q_T = Qm + [K(T) * \sigma Q] \qquad \text{.....Equation 3.25}$$

where, $Q_T$ = discharge of required return period, Qm = mean annual peak discharge, $\sigma Q$ = standard deviation of AMS, and K(T) = frequency factor and is the function of the return period T. K(T) values were obtained from tables provided in the standard books on Applied Hydrology.

The recurrence intervals (T) of given discharges (X), such as mean annual peak discharge (Qm), large flood (Qlf) and peak on record (Qmax), have been estimated by applying the following equation (Shaw, 1988).

$$\frac{1}{T} = 1 - F(X) = 1 - \exp[-e^{-b(X-a)}] \qquad \text{.....Equation 3.26}$$

where, T = recurrence interval for a given discharge, F(X) = probability of an annual maximum $Q \leq X$, and a and b are two parameters related to the moments of population of Q values. The parameters a and b were determined by the following equations.

$$a = Qm - \frac{\gamma}{b} \qquad (\gamma = 0.5772) \qquad \text{.....Equation 3.27}$$

$$b = \frac{\pi}{\sigma Q \sqrt{6}} \qquad \text{.....Equation 3.28}$$

where, Qm = mean annual peak discharge, and σQ = standard deviation of annual peak discharge. The return periods of required discharges have been calculated by applying Equation 3.27.

In the GEVI analysis, the observed annual peak discharges have been plotted against the return period or F(X) values (plotting positions) on the Gumbel graph paper, designed for GEVI probability distribution. Several formulae have been used to calculate plotting positions, however, of the several formulae in use, the best is due to Gringorten since the outliers fall into line better than other plotting positions (Shaw, 1988). The F(X) values have been calculated as follows;

$$P(X) = 1 - F(X) = \frac{r - 0.44}{N + 0.12} \qquad \text{.....Equation 3.29}$$

where, r = flood magnitude rank and N = the number of years of records.

A line can be drawn by eye to fit the scatter, especially using the Gringorten plotting positions. However, it is sensible to draw the line mathematically. Additionally, since most of the AMS data are available for short period of time, it is essential to construct confidence limits about the fitted line relationship between the AMS and the linearized probability variable (Shaw, 1988). Shaw (1988) has given procedure to fit the line mathematically and to construct the confidence limits. The same procedure has been followed in this study.

**bc. Weibull's method**

In addition to above probability distribution, the recurrence interval of high-magnitude flood events that have occurred on the Par River at Nanivahial were predicted by using the following Weibull formula.

$$T = \frac{N + 1}{r} \qquad \text{.....Equation 3.30}$$

where, N = the number of years of record, and r = flood magnitude rank. The results obtained with the help of above equation are presented in Table 4.43.

**c. Discharge-area envelope curve**

The envelope curve for the Par Basin has been prepared with the help of data regarding estimated peak discharges (Qmax) and calculated drainage areas (A) for 15 sites and gauged data of a site in the Par Basin. The curve is shown in Figure 4.101. Further, for comparison, the envelope curve prepared by Baker (1995) for the world has been plotted on the same figure.

**(iii) Flood geomorphology**

In flood geomorphology, the measurement and evaluation of the geomorphic effectiveness of flows of different magnitude has been one of the significant themes. Large floods can generate noteworthy geomorphic impact on channel morphology and landscape. Therefore, to evaluate the geomorphic significance of floods of different magnitude and frequency, the following methodology has been adopted.

To determine the geomorphic effect of floods, the geometry of river channels is considered to be a significant factor (Kochel, 1988). Therefore, to assess the channel geometry/morphology of the Par River, the cross sectional surveys were carried out and fifteen cross-sections were constructed from field surveys and a cross-section has been obtained from Gujarat Irrigation Department. Furthermore, cross-sectional parameters of all the stations at high flood level (HFL) have been derived, analyzed and tabulated.

In order to derive the downstream hydraulic geometry equations, the values of width, depth and velocity for mean annual discharge data along the river are required. Due to unavailability such data, it is not possible to evaluate the downstream hydraulic geometry of the Par River. However, at-a-station hydraulic geometry has been established since data regarding hydraulic geometry variables associated with annual maximum series (AMS) are available for a site on the Par River, viz. Nanivahial. This data have been obtained from Gujarat Irrigation Department and used to derive the at-a-station hydraulic geometry equations to understand the nature of adjustments in the hydraulic variables with discharge. Moreover, the hydraulic geometry exponents (b, f, and m) of the Nanivhahial gauging station were plotted on Rhodes' (1977) ternary

diagram. According to whom ternary diagram is a tool for interpretation of hydraulic geometry.

***a. Changes in hydraulic variables with discharge***

Hydraulic geometry refers to the geometric rate of change of hydraulic variables, namely width (w), mean depth (d), and mean velocity (v), as discharge (Q) increases (Leopold and Maddock, 1953). These changes in the three variables are elementary to hydraulic geometry. The functions derived for a given cross section and among numerous cross sections along the river vary only in numerical values of coefficients and exponent. These functions are;

$$w = aQ^b \quad \text{....Equation 3.31}$$

$$d = cQ^f \quad \text{....Equation 3.32}$$

$$v = kQ^m \quad \text{....Equation 3.33}$$

where, w = width; d = mean depth; v = mean velocity; Q = water discharge in cubic meter per second ($m^2/s$); a, c, k, b, f and m are numerical constants.

Hydraulic geometry of alluvial channel does not applicable to highly variable bedrock channels (Wohl, 1998). Nonetheless, attempts have been made to establish hydraulic geometry equations for the river under review based on available data. The highest discharges of given site flows over the bank, this work is not concerned with discharges above bankful stage (Leopold and Maddock, 1953) the extreme values of overbank flooding for year 1968, 1976, 2004 and 2005 have been excluded and the values of HFL below gauge 8.45 m have been used for construction of at-a-station hydraulic geometry equations (Figure 4.113). The data of hydraulic variables, such as mean depth and mean velocity were not available, these variables were procured through stage and discharge data of AMS. The results of changes in hydraulic variables are given in Table 4.45 and comparison, width, depth, and velocity are plotted on logarithmic scales against discharge in Figure 4.113. The hydraulic geometry exponents (b, f, and m) of the Nanivhahial gauging station were plotted on Rhodes (1977) ternary diagram (Figure 4.114).

Chapter 4

# Analyses and Interpretation

## 4.1 Introduction

This chapter deals with analyses and interpretation of data in accordance with the present study in the following manner.

## 4.2 Channel morphological features

### *4.2.1 Bedrock channel planform*

#### (i) Straight channel

Channels with a sinuosity index (Si) less than 1.05 are called as straight channels**.** Straight channels are rare in nature, most single-channel rivers and streams follow a winding path. Normally, rivers, as simple straight open channels, exist only over short reaches while long, straight rivers rarely occur in nature. Thirty straight channel reaches having length more than 500 m have been identified on Par and Nar Rivers (Figure 4.1; Figure 4.2; Figure 4.3; Figure 4.4; Figure 4.5; Table 4.1). The maximum length of perfectly straight channel reach is 2192 m at Chavra 3 and minimum length is 502 m at Payarpada 1 on Nar River. The average length of straight reaches is about 1161 m. Unfortunately, the formation processes of the straight channels are not known for the river under review.

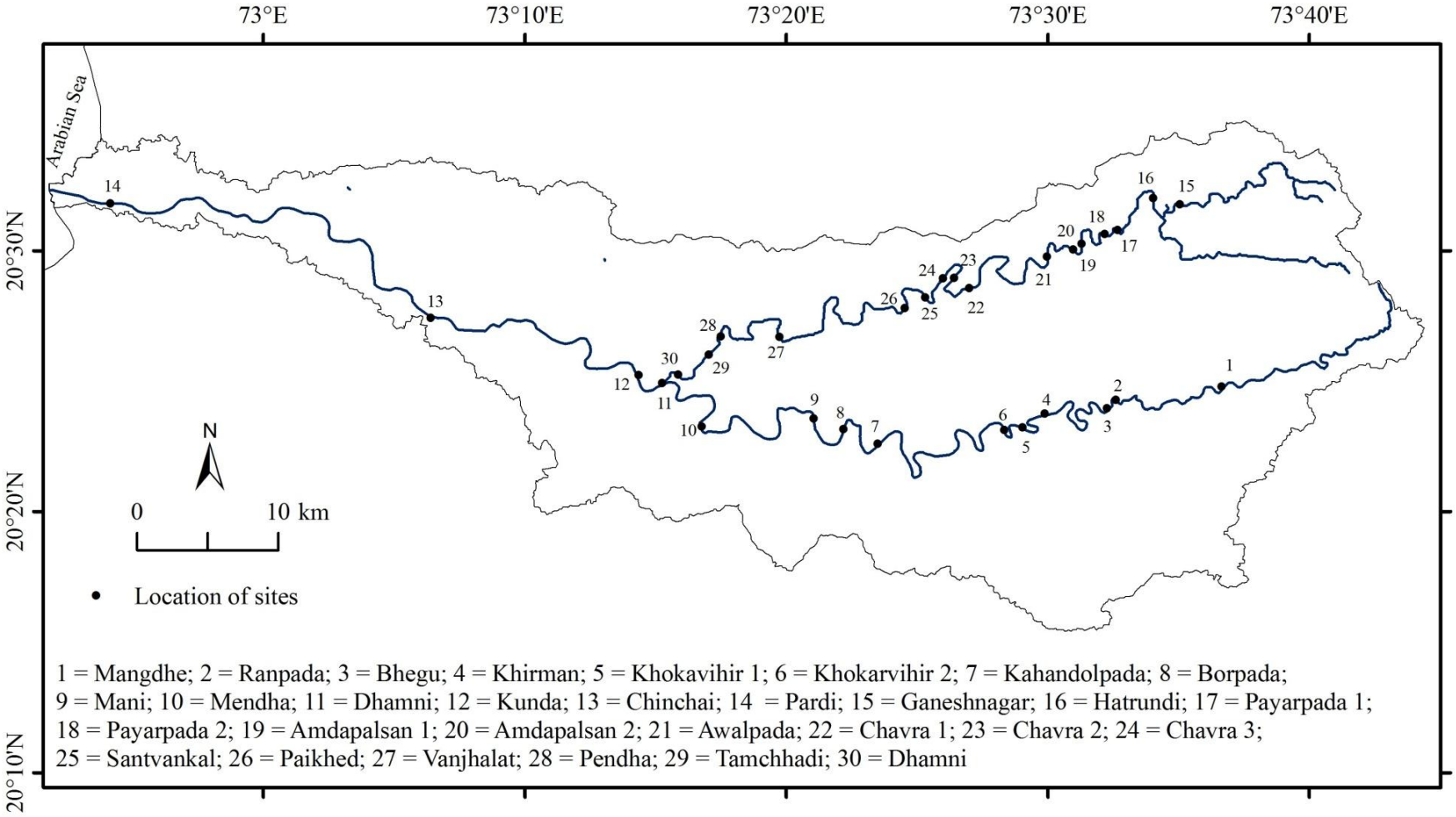


**Figure 4.1** Location of straight reaches on Par and Nar Rivers


**Figure 4.2** Perfectly straight channel of the Par River near Khirman; Source: Google image; See Figure 4.1 (4) for location of reach


**Figure 4.3** Two adjacent perfectly straight channels with a hairpin bend on the Nar River near Chavra; Source: Google image; See Figure 4.1 (23 and 24) for location of reaches

**Table 4.1** Length(s) of straight channel reaches of Par and Nar Rivers

| Sr. No | Name | Length (m) |
|---|---|---|
| **Par River** | | |
| 1 | Mangdhe | 851 |
| 2 | Ranpada | 560 |
| 3 | Bhegu | 670 |
| 4 | Khirman | 1482 |
| 5 | Khokarvihir 1 | 1138 |
| 6 | Khokarvihir 2 | 1037 |
| 7 | Kahandolpada | 1953 |
| 8 | Borpada | 1546 |
| 9 | Mani | 1075 |
| 10 | Mendha | 695 |
| 11 | Dhamni | 1156 |
| 12 | Kunda | 1757 |
| 13 | Chinchai | 1460 |
| 14 | Pardi | 1914 |
| **Nar River** | | |
| 15 | Ganeshnagar | 600 |
| 16 | Hatrundi | 1140 |
| 17 | Payarpada 1 | 502 |
| 18 | Payarpada 2 | 600 |
| 19 | Amdapalsan 1 | 1343 |
| 20 | Amdapalsan 2 | 1077 |
| 21 | Awalpada | 1240 |
| 22 | Chavra 1 | 921 |
| 23 | Chavra 2 | 1586 |
| 24 | Chavra 3 | 2192 |
| 25 | Santvankal | 1103 |
| 26 | Paikhed | 743 |
| 27 | Vanjhalat | 852 |
| 28 | Pendha | 1149 |
| 29 | Tamachhadi | 1664 |
| 30 | Dhanmi | 810 |
| | **Minimum** | **502** |
| | **Maximum** | **2192** |
| | **Average** | **1161** |

See Figure 2.1 for location of sites

**Figure 4.4** Straight channel of the Par River near Mendha; See Figure 2.1 (10) for location of reach

**Figure 4.5** View of straight channel of the Nar River near Chavra; See Figure 2.1 (24) for location of reach

**(ii) Meandering channel**

The river has single, sinuous, and well-defined channel, incised into bedrock (Figure 4.6; Figure 4.7). The results of analyses of meander geometry have been given in table 4.1.

**a. Meander Geometry**

**aa. Meander length ($L_m$)**

Meander length is the distance of one meander along the thalweg of channel (Figure 3.1). The minimum length is 580 m for bend M5, maximum length is 5900 m for bend M23 and the mean meander length is 3233 m (Figure 4.1; Table 4.1).

**ab. Meander wavelength (λ)**

The distance between two successive crests or troughs of a meander loop is known as meander wavelength (λ) (Figure 3.1). The minimum meander wavelength is 390 m for bend M5, maximum meander wavelength is 5140 m for bend M23 and the mean meander wavelength ($\lambda_m$) is 2010 m (Figure 4.6; Table 4.2).

**ac. Amplitude (Am)**

It is the width of the meander bends measured perpendicular to the valley (Figure 3.1). The minimum amplitude is 190 m for bend M5, maximum amplitude is 3700 m for bend M15 and the mean amplitude ($A_m$) is 1085 m (Figure 4.6; Table 4.2).

**ad. Sinuosity index (Si)**

Sinuosity index (Si) was calculated by the ratio of meander length ($L_m$) to meander wavelength (λ). The Si ranges from 1.12 to 2.88 (Table 4.2). Analysis indicates that the average Si value for the channel is 1.74. Since the average value is greater than 1.5, the channel is said to be meandering. Almost all the values of sinuosity indices lie within 1.3 to one and four to one (given by Leopold and Langbean, 1966 for alluvial rivers), thereby indicating no difference between the bedrock Par River channel and other alluvial rivers.

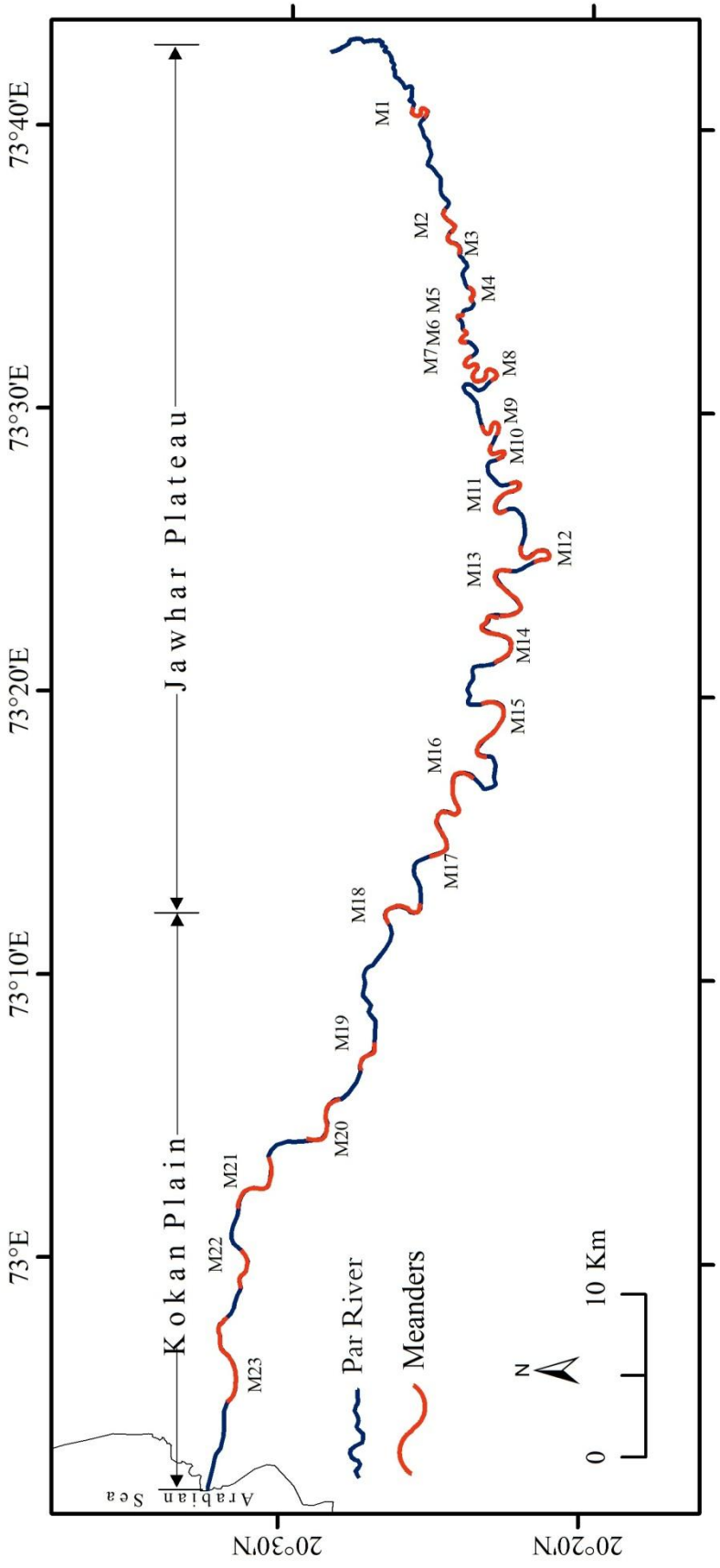


**Figure 4.6** Location of meanders on Par River; M1 to M23 - number of meanders


**Figure 4.7** Meander Train in the bedrock channel of the Par River on the Jawhar Plateau; Source: Google image; See Figure 2.6 (M8) for location of reach

**Table 4.2** Meander geometry of the Par River

| M. No. | Meander length ($L_m$) (m) | Meander wavelength (λ)(m) | Amplitude (Am)(m) | Sinuosity index (Si) | Mean radius of curvature ($Rc_m$) (m) | | Mean width (W) (m) | λ/ $Rc_m$ | $Rc_m$/W | Channel Form |
|---|---|---|---|---|---|---|---|---|---|---|
| M1 | 2000 | 880 | 550 | 2.27 | 264.70 | 194.25 | 80.45 | 3.83 | 2.85 | Meandering |
| M2 | 1920 | 1490 | 540 | 1.29 | 232.85 | 215.50 | 76.09 | 6.65 | 2.95 | Sinuous |
| M3 | 1780 | 1450 | 430 | 1.23 | 290.44 | 335.89 | 84.81 | 4.63 | 3.69 | Sinuous |
| M4 | 1250 | 930 | 290 | 1.34 | 318.69 | 111.06 | 97.70 | 4.33 | 2.20 | Sinuous |
| M5 | 580 | 390 | 190 | 1.49 | 80.27 | 55.09 | 81.58 | 5.76 | 0.83 | Meandering |
| M6 | 1400 | 800 | 590 | 1.75 | 72.13 | 92.92 | 76.88 | 9.69 | 1.07 | Meandering |
| M7 | 2200 | 1070 | 700 | 2.06 | 192.30 | 162.64 | 88.10 | 6.03 | 2.01 | Meandering |
| M8 | 3100 | 1100 | 1090 | 2.81 | 268.09 | 328.60 | 109.47 | 3.69 | 2.73 | Meandering |
| M9 | 2530 | 1140 | 750 | 2.22 | 160.15 | 180.62 | 114.01 | 6.69 | 1.49 | Meandering |
| M10 | 2140 | 960 | 710 | 2.23 | 241.98 | 137.66 | 111.15 | 5.06 | 1.71 | Meandering |
| M11 | 3970 | 1650 | 2230 | 2.41 | 184.98 | 361.31 | 136.70 | 6.04 | 2.00 | Meandering |
| M12 | 3810 | 1320 | 910 | 2.88 | 369.26 | 252.92 | 164.50 | 4.24 | 1.89 | Meandering |
| M13 | 5320 | 2890 | 1630 | 1.84 | 481.52 | 408.63 | 203.30 | 6.49 | 2.19 | Meandering |
| M14 | 5410 | 2740 | 1880 | 1.97 | 485.54 | 663.89 | 192.70 | 4.77 | 2.98 | Meandering |
| M15 | 5530 | 3280 | 3700 | 1.69 | 726.50 | 364.29 | 202.80 | 6.01 | 2.69 | Meandering |
| M16 | 4420 | 2570 | 1730 | 1.72 | 554.25 | 257.32 | 248.80 | 6.33 | 1.63 | Meandering |
| M17 | 4100 | 2900 | 1320 | 1.41 | 534.22 | 624.03 | 237.30 | 5.01 | 2.44 | Sinuous |
| M18 | 3550 | 2300 | 1740 | 1.54 | 283.76 | 676.56 | 293.30 | 4.79 | 1.64 | Meandering |
| M19 | 2230 | 1930 | 590 | 1.16 | 431.00 | 636.33 | 299.40 | 3.62 | 1.78 | Sinuous |
| M20 | 4000 | 3190 | 1300 | 1.25 | 740.50 | 669.51 | 357.30 | 4.52 | 1.97 | Sinuous |
| M21 | 4540 | 3710 | 990 | 1.22 | 740.41 | 931.70 | 323.00 | 4.44 | 2.59 | Sinuous |
| M22 | 2680 | 2400 | 500 | 1.12 | 873.88 | 287.80 | 335.30 | 4.13 | 1.73 | Sinuous |
| M23 | 5900 | 5140 | 590 | 1.15 | 1351.60 | 1948.62 | 352.60 | 3.11 | 4.68 | Sinuous |
| **Min** | 580 | 390 | 190 | 1.12 | 55.09 | | 76.09 | 3.11 | 0.83 | |
| **Max** | 5900 | 5140 | 3700 | 2.88 | 1948.62 | | 357.3 | 9.69 | 4.68 | |
| **Mean** | 3233 | 2010 | 1085 | 1.74 | 429.92 | | 185.53 | 5.21 | 2.25 | |

M1 to M23 = Meander Numbers

**ae. Radius of curvature (Rc)**

It is the distance measured perpendicular to the down-valley axis intersecting sinuous axis at the apex (Figure 3.1). The minimum radius of curvature (Rc) is 55.09 m for bend M5, maximum radius of curvature (Rc) is 1948.62 m for bend M23 and the mean radius of curvature ($Rc_m$) is about 430 m (Figure 4.6; Table 4.2).

**af. Meander width (W)**

Meander width is defined as the distance between two banks of a meander (Figure 3.1). It has been observed that the minimum width is 76.09 m for bend M2 and maximum width is 357.3 m for bend M20 and mean width (W) is about 185 m (Figure 4.6; Table 4.2).

**b. Meander wavelength (λ) /radius of curvature (Rc) ratio**

The minimum value of meander wavelength (λ)/radius of curvature (Rc) for the river under review is three to one, maximum value is 10 to one. However, both the values are in contrast with minimum and maximum values of the ratio given by Leopold and Langbean (1966) for the alluvial rivers. It is, therefore, evident that the minimum and maximum values of this ratio for bedrock meanders of the Par River differ markedly as compared to meanders in alluvial valleys. However, the average value of this ratio is about 5.2 to one, which is close to the average value (4.7 to one) given by Leopold and Langbean (1966).

**c. Radius of curvature (Rc)/channel width (W) ratio**

The computed arithmetic mean value of Rc/W is 2.1 and median value is 2.01. The range is from 0.83 to 4.68 or about 1 to 5. The data of Williams (1986) have this range from 1 to 7 whereas the data of Leopold and Wolman (1960) have a wider range namely from 1 to 10. About more than 90% of the values lie between 1.5 and 4.3. About $2/3^{rd}$ of the cases of this value lie between this range (Leopold and Wolman, 1960). About 50% of the values recline between 2.0 and 3.0 whereas about 25% of the values of Leopold and Wolman's 1960s data stretch out between this range. The range of values in case of bedrock meanders of the Par River differ from the data given by Leopold and Wolman (1960) and Williams (1986). About $1/3^{rd}$ of

the values given by Williams (1986) is less than 2 whereas about ½ (50%) of the values are less than 2 in case of the Par River. This, therefore, suggests perhaps a more common occurrence of such lower values than might until now have been expected. Williams (1986) has arrived to similar conclusion. Although there is substantial difference in values of the ratio, there are no radical departures from Leopold and Wolman (1960) and Williams (1986) results.

**d. Empirical relations between size parameters for meanders**

All river channels show remarkable relationship between meander wavelength, channel width and radius of curvature. The empirical relations between meander wavelength and channel width and radius of curvature; amplitude to channel width have been shown for the bedrock Par River and compared with alluvial river because such relations are not available for bedrock rivers.

**da. Empirical relation between meander wavelength (λ) and channel width (W)**

Due to variability in the dimensions of meanders of the Par River, substantial scatter of plotted data is expected for the relation between meander wavelength (λ) and channel width (W) (Figure 4.8). Despite the scatter, relations among the factors appear to hold. The meander wavelength (λ) is directly proportional to the channel width (W). The exponent in the regression equation for the relation is close to unity (0.93) (Figure 4.8; Table 4.3). It, therefore, shows that the relation is considered linear. However, there is no radical departure from Leopold and Wolman's (1960) results for the relationship between meander wavelength (λ) and channel width (W) ($\lambda = 10.09\ W^{1.01}$) for alluvial rivers.

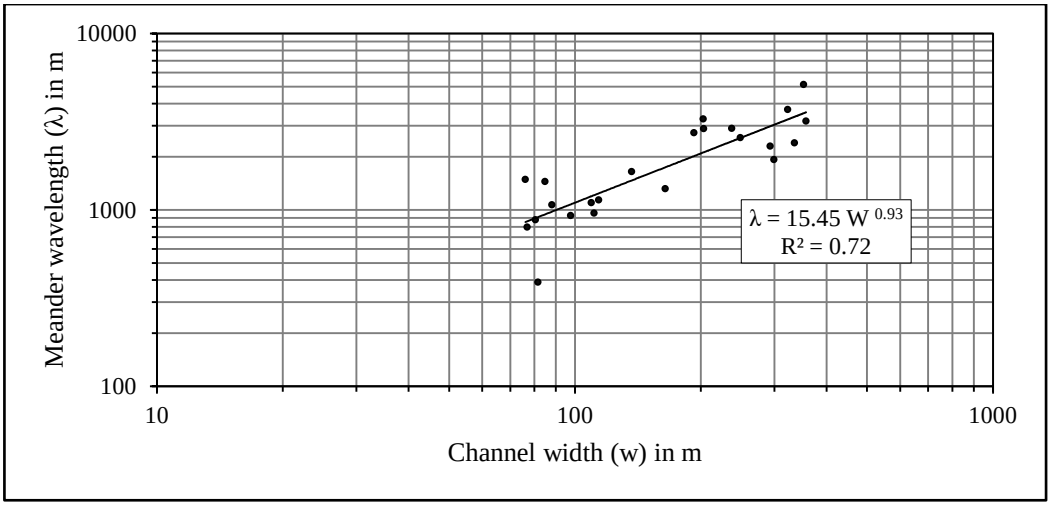


**Figure 4.8** Relation between meander wavelength (λ) and channel width (W)

### db. Empirical relation between meander wavelength (λ) and mean radius of curvature ($Rc_m$)

The relation between meander wavelength (λ) and mean radius of curvature ($Rc_m$) is very strong ($R^2$ = 0.79). However, the value of exponent is not the unity but 0.71 (Figure 4.9; Table 4.3). It indicates that the rate of change in the meander wavelength is comparatively slower as the mean radius of curvature increases. The value of exponent for the relation proposed by Leopold and Wolman (1960) is 0.98 ($\lambda = 4.7\ Rc_m^{0.98}$). This difference is perhaps due to variation in types of channel that are alluvial and bedrock.

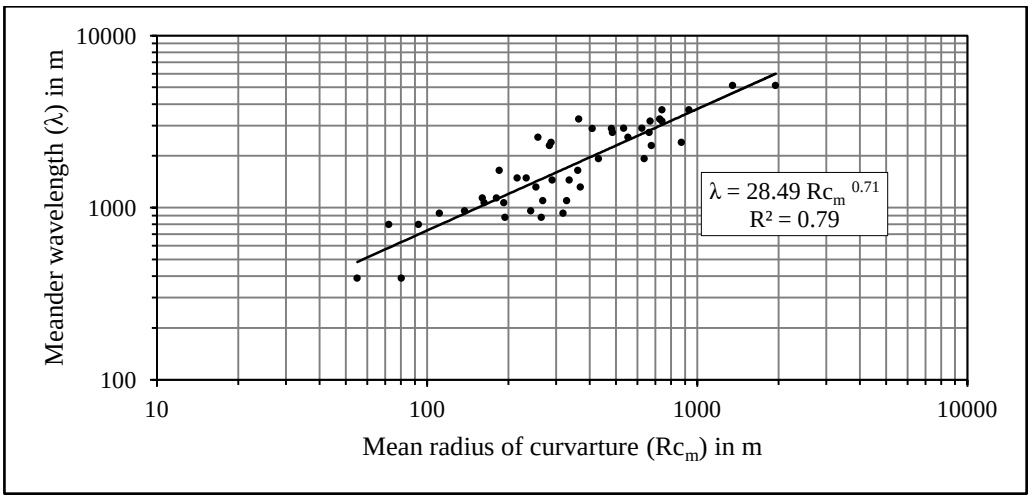


**Figure 4.9** Relation between meander wavelength (λ) and mean radius of curvature ($Rc_m$)

**dc. Empirical relation between amplitude (Am) and channel width (W)**

Amplitude (Am) correlates only poorly with channel width (W) ($R^2$ = 0.21) (Figure 4.3; Table 4.3). The empirical relationships established by Leopold and Wolman (1960) and others reveal that the values of exponents are very close to unity (1.11) for alluvial rivers. The value of exponent for the Par River is 0.37. Therefore, the relationship between amplitude (Am) and channel width (W) is in contract to the previous relationships in terms of value of exponents.

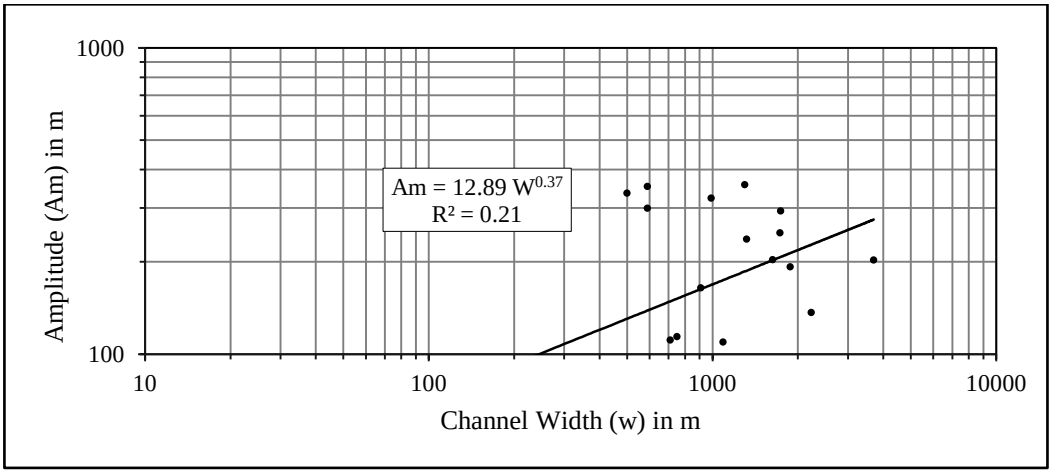


**Figure 4.10** Relations between amplitude (Am) and channel width (W)

**Table 4.3** Empirical relations between size parameters for meanders of the Par River

| Meander wavelength (λ) to channel width (W) | Meander wavelength (λ) to radius of curvature($Rc_m$) | Amplitude (Am) to channel width (W) |
|---|---|---|
| $\lambda = 15.45\ W^{0.93}$<br>$R^2 = 0.72$ | $\lambda = 28.49\ Rc_m^{0.71}$<br>$R^2 = 0.79$ | $Am = 12.89\ W^{0.37}$<br>$R^2 = 0.21$ |

The spatial scale analyses of bedrock meanders of the Par River show that almost all the values of sinuosity indices lie within the range of 1.3 to one and four to one, thereby indicating no difference, although the Par River channel is bedrock in nature. The minimum and maximum values of the meander wavelength and mean radius of curvature ($Rc_m$) ratio for the river differ markedly as compared to meanders in alluvial valleys. Although there is substantial difference in values of mean radius of curvature ($Rc_m$) and channel width (W) ratio, there are no radical departures from values given by previous workers for the alluvial channels. The best fitting empirical relations are

those between meander wavelength (λ) and channel width (W) and meander wavelength (λ) and mean radius of curvature ($Rc_m$). The equations, perhaps, approximate the true relations between the variables and are good for prediction. However, amplitude (Am) correlates only poorly with channel width (W). The main conclusion that emerges from the analyses is that, though not radical, bedrock channels of the river under review show marked difference in meander geometry as compared to alluvial channels.

**(iii) Bedrock anastomoising/multi-thread channels**

The average width of the bedrock anastomoised reach at Panchlai is 330 meters and the length is 1500 meters (Figure 4.11). The width upstream and downstream of it is 167 and 156 meters respectively. The process of formation of bedrock anastomoised channel near Panchlai is attributed to insufficient channel capacity. The other two formation processes namely localised uplift along the channel and joint control weathering given by Wohl (1998) are not applicable to anastomoised channel of the Par River.

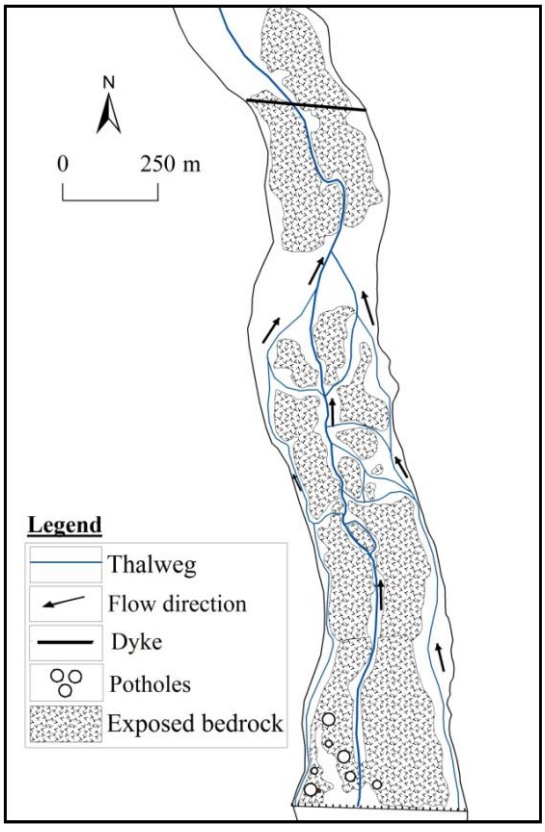


**Figure 4.11** Bedrock anastomoising/multi-thread channel of the Par River near Panchlai; Potholes not to scale; See Figure 4.19 for the location of reach

### *4.2.2 Channel form/channel geometry*

#### (i) Channel Width (W)

The channel width is the distance across a stream or channel as measured from bank to bank at bankfull stage. Figure 4.12 shows the locations of cross sectional sites on the Par and Nar River. In addition to this, Figure 4.13 to Figure 4.15 show the cross sections. Cross sections are either trapezoidal or saucer shaped. The average channel width of the Par River is about 164 m and that of the river Nar is 110 m. The channel width varies from 42 m at Mendha in the gorge section (Figure 4.46; Figure 4.47) to 371 m at Panchlai (Figure 4.13; Table 4.5). In the upper reaches, the rocky channel of the Par River is typically narrow. In the middle reaches, it is moderately wide (Figure 4.12). However, the channel exceptionally becomes narrow at the Mendha Gorge (Figure 4.46; Figure 4.47) and the width decreases to 42 m (Figure 4.47). Downstream, the channel width increases abruptly after Nar River confluence i.e. from Dhamni (184 m) to Pardi (290 m) (Figure 4.13) near the mouth of the river. The channel is widest at Panchlai (371 m) (Figure 4.13). By and large, in spite of the local variations in the channel width, there is a gradual increase in the width with an increase in the distance from the source (Figure 4.12, Figure 4.13; Figure 4.15).

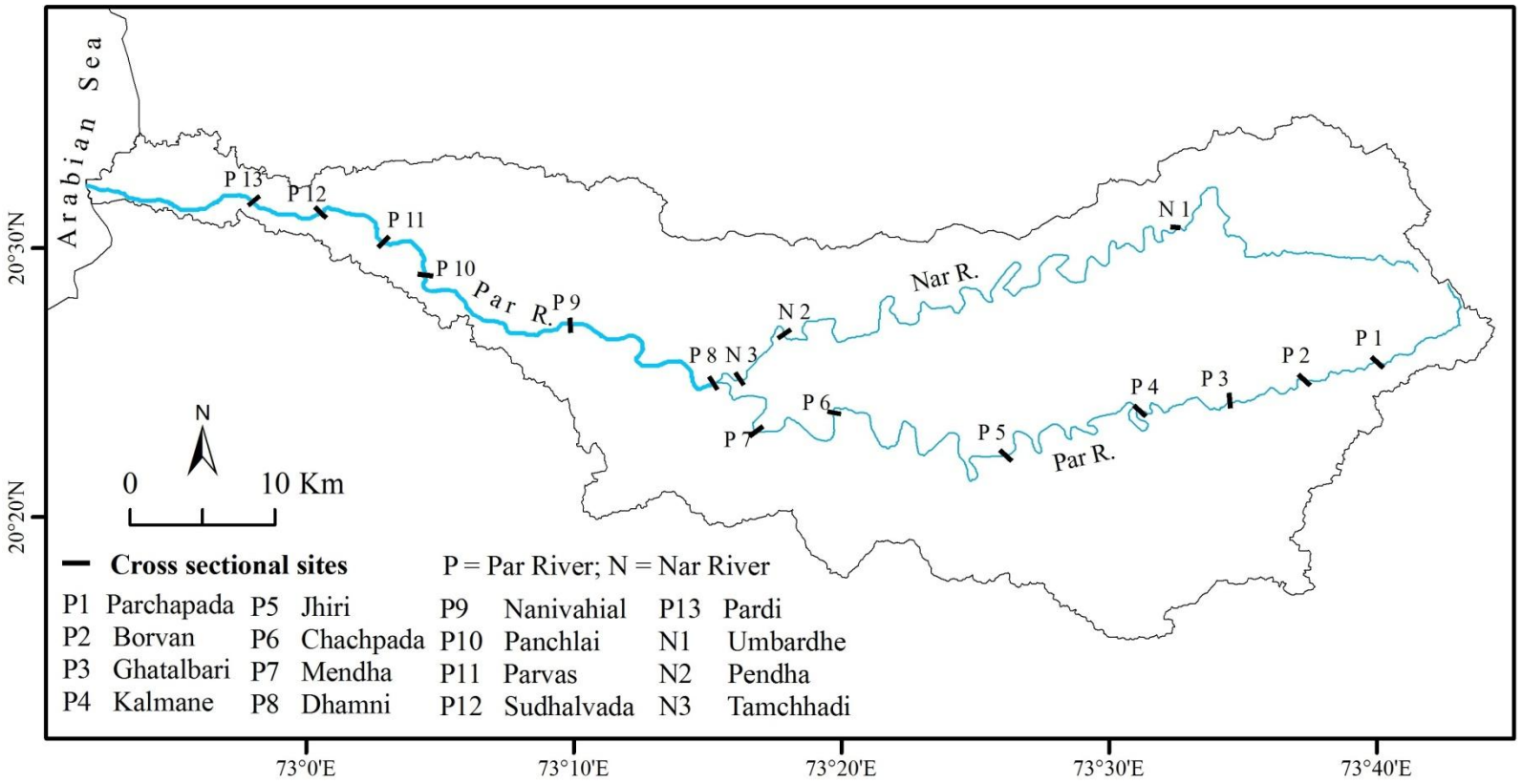


**Figure 4.12** Location of cross-sectional sites on Par and Nar Rivers

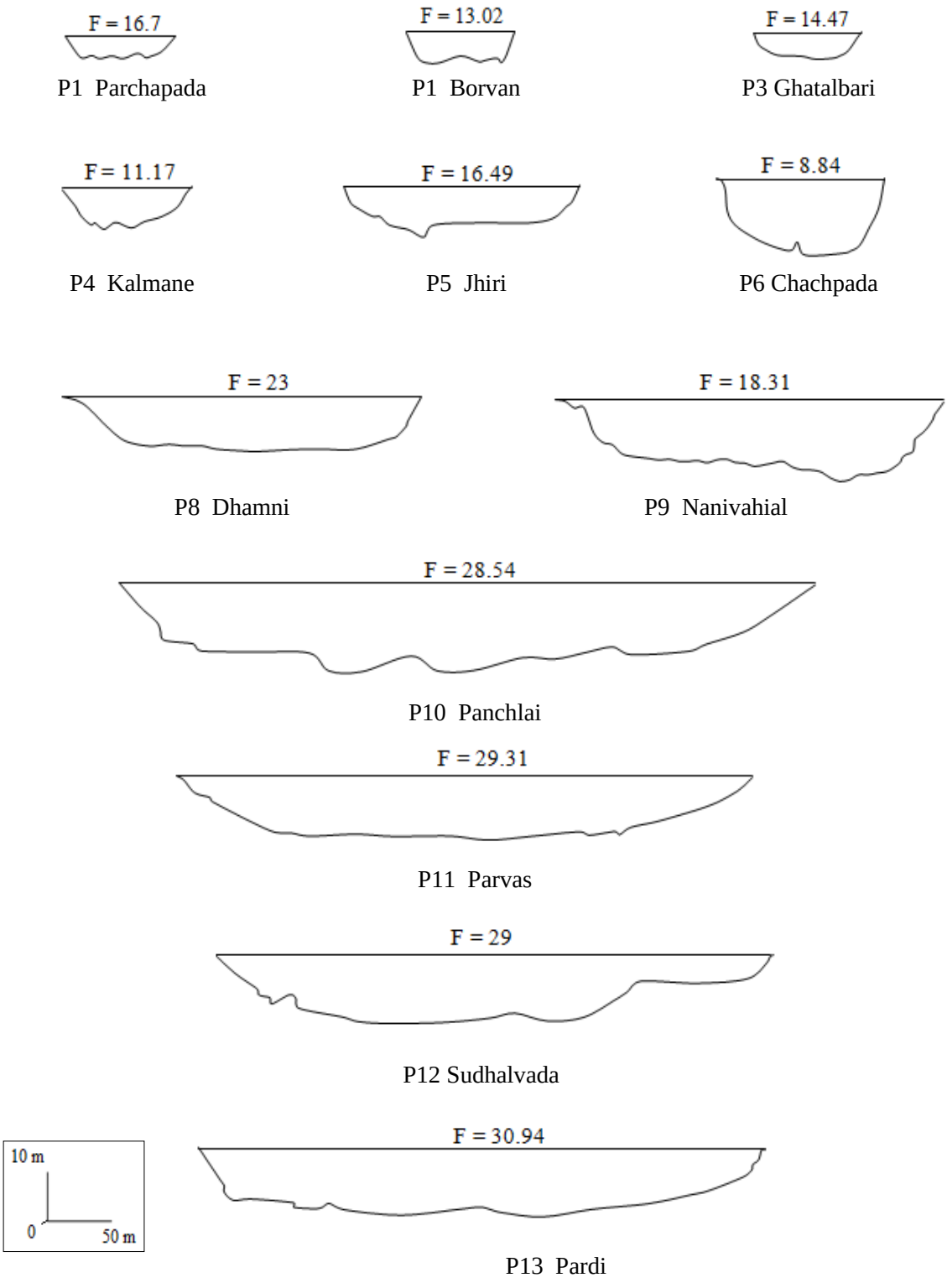


**Figure 4.13** Cross sections: Par River; See Figure 4.12 for location of sites; P = Par River; F = Form ratio

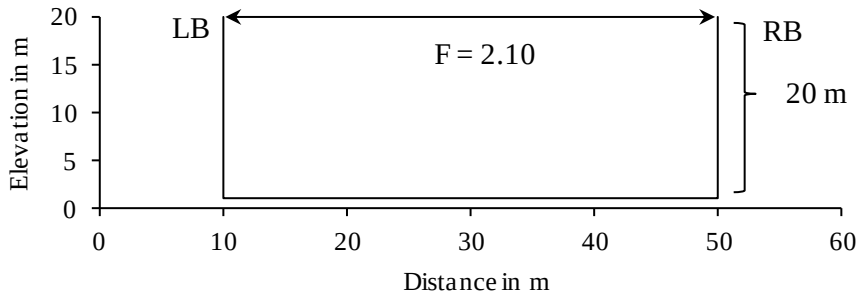


**Figure 4.14** Cross section at Mendha (P7) on the Par River; See Figure 2.4 and Figure 2.13 for location of site; F = Form ratio; LB = Left bank; RB = Right bank

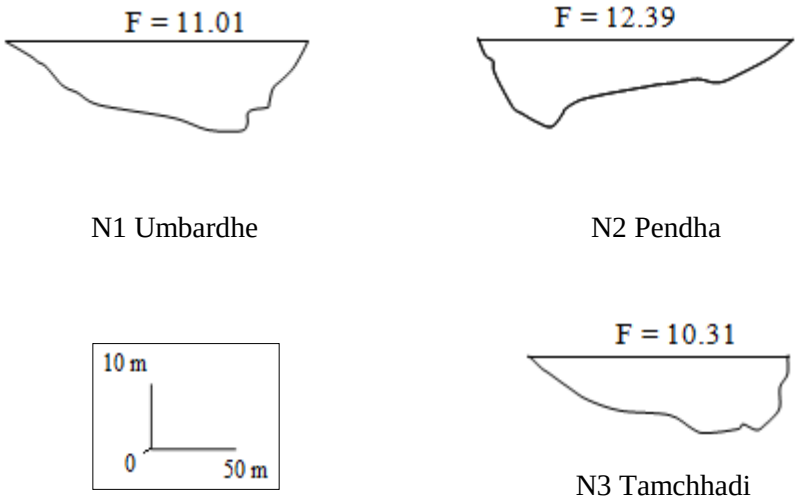


**Figure 4.15** Cross sections: Nar River; See Figure 2.13 for location of sites; N = Nar River; F = Form ratio

### (ii) Channel depth (D)

Channel depth is an important parameter that determines the power per unit area and boundary shear stress at a cross section. The average depth of the Par River is 9.02 m. It ranges between 4 m and 20 m. Figure 4.13; Figure 4.14 and Figure 4.15 illustrate that there is gradual increase in depth in the downstream direction. However, unlike width, the rate of increase in the depth is lower (Figure 4.16).

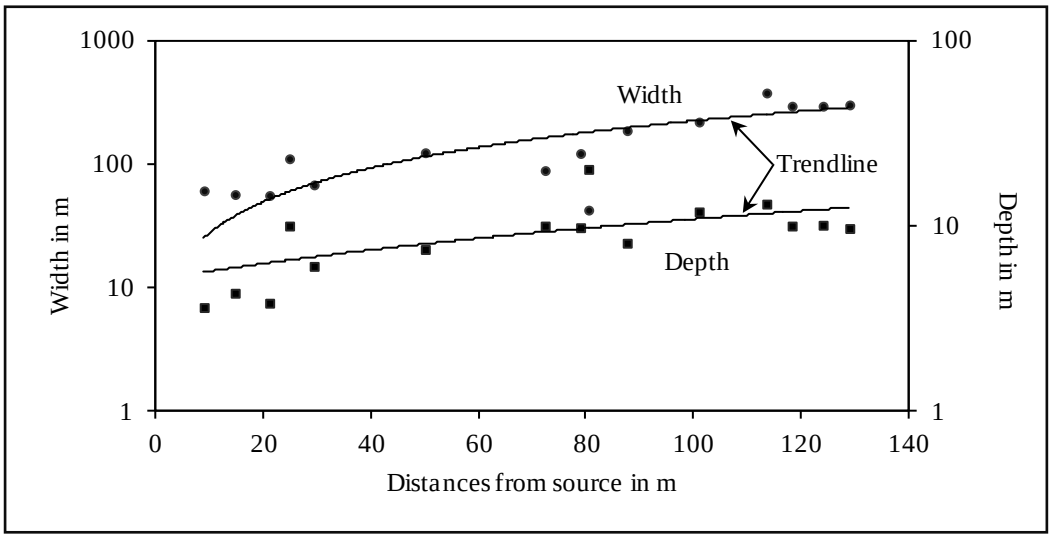


**Figure 4.16** Downstream changes in width and depth

**(iii) Form ratio (F)**

In case of the Par River the form ratio varies from 2 to 30. The width-depth ratio was found to be highest at Pardi due to wide channel and lowest at Mendha due to narrow gorge (Figure 4.14; Figure 4.47; Table 4.5).

By using channel classification used by Rosgen (1994), the Par as well as the Nar River channel reaches at the cross sections surveyed fall in types of A to C, representing relatively straight (A) (sinuosity < 1.2; W/D ratio < 12 ), low sinuosity (B) (sinuosity > 1.2 to < 1.4; W/D ratio > 12), meandering (C) (sinuosity > 1.4; W/D ratio > 12). Accordingly three cross sections on the Par River (Figure 2.13) namely Kalmane (P4), Chachpada (P6) and Mendha (P7) and Umbardhe (N1) and Tamchhadi (N3) on the Nar River belong to category A, representing relatively straight bedrock channels. The rest of the channel cross sections on both rivers fall either in type B or in type C categories of channel classification.

**Table 4.4** Channel cross section and reach variables used in the present study

| Parameter | Symbol | Unit |
|---|---|---|
| Maximum width | W | m |
| Water surface width | w | m |
| Maximum depth | D | m |
| Mean depth | d | m |
| Wetted perimeter | Wp | m |
| Hydraulic radius | R | m |
| Channel capacity | Ca | $m^2$ |
| Width-depth ratio | W/D | - |
| Channel slope | S | - |
| Flow velocity | v | m/s |
| Catchment area | A | $km^2$ |
| Channel length (from source) | L | km |

**Table 4.5** Channel morphologic variables of some cross sections of the Par and Nar River

| No. | Site | A | L | W | D | W/D |
|---|---|---|---|---|---|---|
| Sites on Par River | | | | | | |
| 1 | Parchapada | 35.64 | 8.82 | 60.00 | 3.60 | 16.67 |
| 2 | Borvan | 66.50 | 14.60 | 56.00 | 4.30 | 13.02 |
| 3 | Ghatalbari | 108.11 | 21.01 | 55.00 | 3.80 | 14.47 |
| 4 | Kalmane | 201.95 | 29.30 | 67.00 | 6.00 | 11.17 |
| 5 | Jhiri | 424.46 | 50.00 | 122.00 | 7.40 | 16.49 |
| 6 | Chachpada | 628.72 | 72.32 | 87.50 | 9.90 | 8.84 |
| 7 | Mendha | 655.63 | 80.42 | 41.90 | 20.00 | 2.10 |
| 8 | Dhamni | 1108.85 | 87.59 | 184.00 | 8.00 | 23.00 |
| 9 | Nanivahial* | 1252.31 | 100.99 | 216.00 | 11.80 | 18.31 |
| 10 | Panchlai | 1354.21 | 113.57 | 371.00 | 13.00 | 28.54 |
| 11 | Parvas | 1400.23 | 118.30 | 290.20 | 9.90 | 29.31 |
| 12 | Sudhalvada | 1501.49 | 124.07 | 290.00 | 10.00 | 29.00 |
| 13 | Pardi | 1528.07 | 129.03 | 297.00 | 9.60 | 30.94 |
| Sites on Nar River | | | | | | |
| 14 | Umbardhe | 177.17 | 24.72 | 109.00 | 9.90 | 11.01 |
| 15 | Pendha | 387.84 | 78.91 | 120.20 | 9.70 | 12.39 |
| 16 | Tamchhadi | 404.85 | 84.64 | 100.00 | 9.70 | 10.31 |
| | **Min** | | | 41.90 | 3.60 | |
| | **Max** | | | 371.00 | 20.00 | |
| | **Mean** | | | 154.18 | 9.16 | |

Sources: Field surveys and Gujarat Irrigation Department*; A = Catchment area in $km^2$; L = Distance from source in km; Refer Table 4.4 for notations; See Figure 4.12 for location of the sites

**a. Change in the width-depth ratio with discharge**

The form of the Par River is variable at different reaches, ranging from deep narrow to wide open. Therefore, during the dry season and during low flows the water spreads at few cross sections, and the width is high and depth is low. Therefore, the width-depth ratio is high and the channel reflects all the characteristics of a shallow, wide channel. However, in response to heavy rainfall as the stage and discharge increases, there is an increase only in the depth of flow in deep narrow channels. As a result, the width-depth ratio decreases, and the hydraulic efficiency increases dramatically. Figure 4.17 shows the plot of width-depth ratio(s) for low flows as well as high flows for different cross sections along the Par River. There is a noteworthy drop in the ratio(s), because of the wide nature of the channel of the Par in these sections (Figure 4.17). However, drop in the ratios is medium at Kalmane, Jhiri, Chachpada and lowest at Mendha, due to narrow, deep channel (Figure 4.17). It, therefore, suggests greater hydraulic efficiency of bedrock Par River.

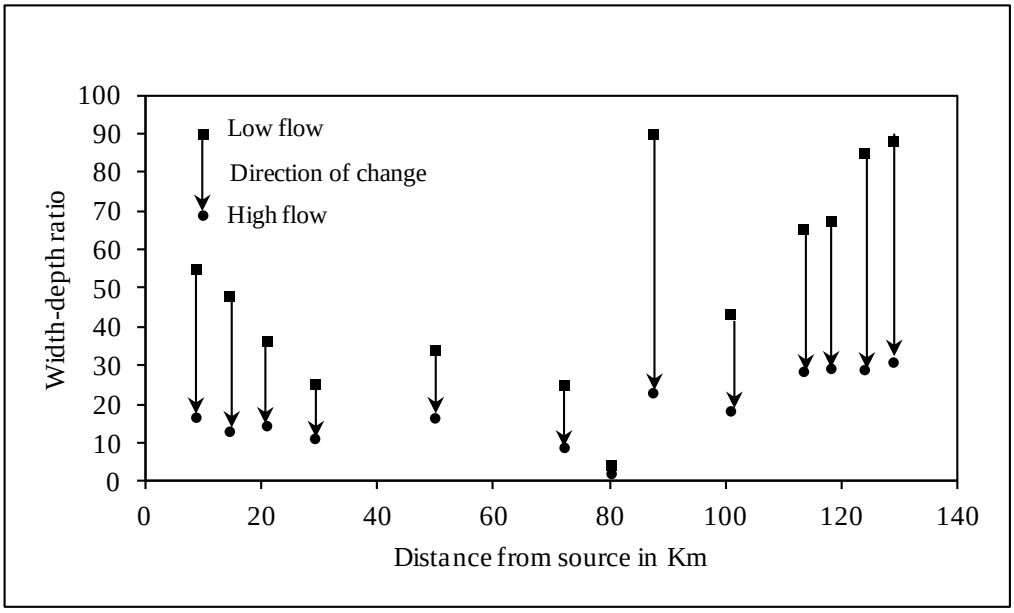


**Figure 4.17** Downstream changes in width-depth ratio with discharge

**iv. Relations between channel width (W) and drainage area (A)**

This relation is similar to the classical hydraulic geometry of alluvial channels. The value of the b coefficient is 0.46 for bedrock channels of the Par River. The value of $R^2$ is 0.61 suggesting very good positive relations between width and drainage area (Figure 4.18). Montgomery and Gran (2001) suggest that an alluvial hydraulic relationship where b = 0.3 to 0.5 holds also bedrock channel systems. It is concluded that downstream variation in the width of the bedrock channels generally follow classic hydraulic geometry relations, although there is substantial local variation in the channel width. Montgomery and Gran (2001) have also arrived to similar conclusions for bedrock channel systems.

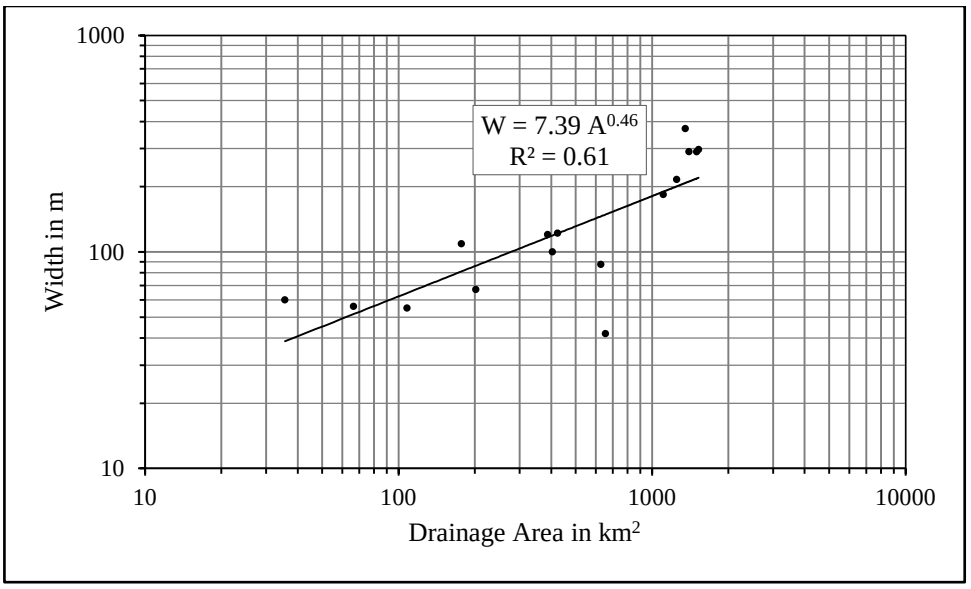


**Figure 4.18** Channel width versus drainage area for bedrock reaches of Par River

### *4.2.3 Erosional features of bedrock channel*

An attempt has been made to identify, analyse and map the erosional landforms of the Par River (Figure 4.19; Table 4.6).

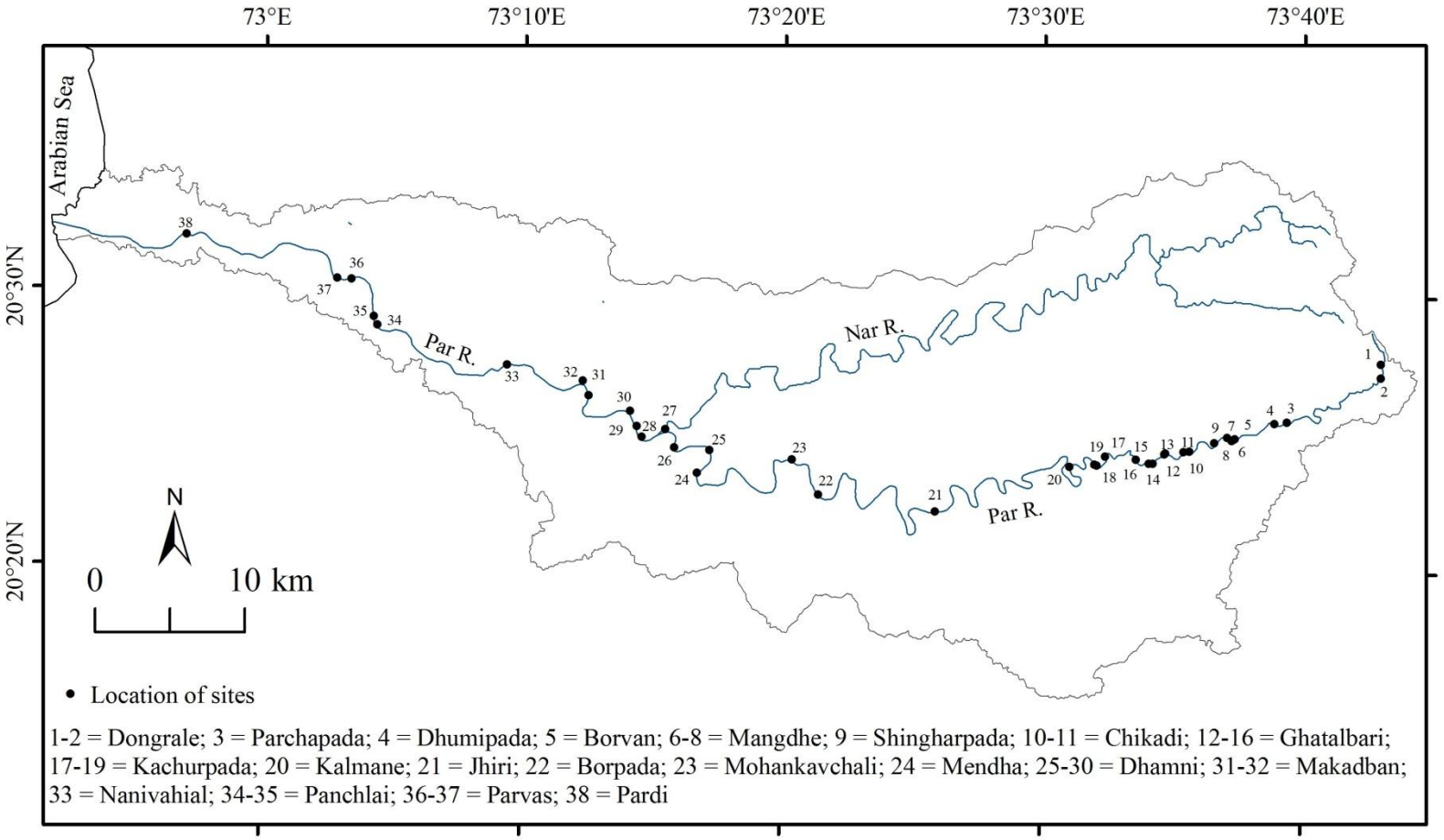


**Figure 4.19** Location of sites of morphological features on Par River

**Table 4.6** Selected locations for bedrock channel erosional (Meso-scale) and depositional features

| Sr. No. | Location | Morphological features |
|---|---|---|
| 1 | Dongrale | Potholes |
| 2. | Dongrale | Knickpoint |
| 3. | Parchapada | Knickpoint |
| 4. | Dhumipada | Expansion bar |
| 5. | Borvan | Grooves |
| 6. | Mangdhe | Inner channel |
| 7. | Mangdhe | Expansion bar |
| 8. | Mangdhe | Longitudinal bar |
| 9. | Shingharpada | Grooves, potholes, inner channel |
| 10. | Chikadi | Expansion bar |
| 11. | Chikadi | Knickpoint, potholes, inner channel |
| 12. | Ghatalbari | Knick |
| 13. | Ghatalbari | Expansion bar |
| 14. | Ghatalbari | Potholes |
| 15. | Ghatalbari | Expansion bar |
| 16. | Ghatalbari | Knick |
| 17. | Kachurpada | Potholes |
| 18. | Kachurpada | Point bar |
| 19. | Kachurpada | Longitudinal bar |
| 20. | Kalmane | Knickpoint, potholes |
| 21. | Jhiri | Expansion bar |
| 22. | Borpada | Point bar |
| 23. | Mohankavchali | Inner channel |
| 24. | Medha | Expansion bar |
| 25. | Dhamni | Point bar |
| 26. | Dhamni | Point bar |
| 27. | Dhamni | Expansion bar |
| 28. | Dhamni | Point bar |
| 29. | Dhamni | Longitudinal bar |
| 30. | Dhamni | Point bar |
| 31. | Makadban | Expansion bar |
| 32. | Makadban | Point bar |
| 33. | Nanivahial | Inner channel, potholes, grooves |
| 34. | Panchlai | Potholes |
| 35. | Panchlai | Anastomoising channel |
| 36. | Parvas | Potholes, inner channel |
| 37. | Parvas | Potholes |
| 38. | Pardi | Channel avulsion |

Meso-scale (cm to m); See Figure 4.19 for location of sites

**(i) Potholes**

The statistical parameters of various geometric properties of the potholes have been obtained and represented in Table 4.7.

**Table 4.7** Statistical parameters of the various geometric properties of the potholes

| Dimensions (cm) | No. Obs. | Min (cm) | Max (cm) | Range | Mean | σ | Cv (%) | $C_s$ | $C_k$ |
|---|---|---|---|---|---|---|---|---|---|
| Diameter | 116 | 0.60 | 380 | 379 | 50.36 | 47.43 | 94.18 | 3.56 | 20.33 |
| Length | 138 | 8.50 | 730 | 722 | 114.50 | 104.72 | 91.45 | 3.27 | 13.83 |
| Width | 138 | 7.00 | 550 | 543 | 78.81 | 75.30 | 95.54 | 3.52 | 16.22 |
| Depth | 252 | 0.80 | 600 | 599 | 68.22 | 64.50 | 94.55 | 4.01 | 24.86 |

No. Obs. = Number of observations; Min = Minimum; Max = Maximum; σ = Standard deviation; Cv = Coefficient of variation; $\mathbf{C_S}$ = Coefficient of skewness; $\mathbf{C_k}$ = Coefficient of kurtosis

The Table 4.7 to Table 4.12 reveal that potholes of the river under review are of various sizes and shapes. The minimum diameter of a pothole is 0.60 cm has been found in the source of the Par River near Dongrale (Figure 4.20; Figure 4.21; Table 4.7) and the maximum value is 380 cm just upstream of Ghatalbari waterfall (Figure 4.22; Figure 4.23; Figure 4.24; Table 4.7). Majority of large diameter potholes have been located upstream of knickpoints thereby indicating most prominent incision and erosion in bedrock (Table 4.8 to Table 4.12). The mean diameter of potholes is 50.36 cm. The minimum length of an elongated pothole is 8.5 cm, observed at Dongrale (Figure 4.20) and maximum length is 730 cm which is located upstream of knickpoint in the steep, narrow gorge near Kalmane (Figure 4.26; Figure 4.27; Table 4.9). The mean length of potholes is 114.50 cm. The minimum width of pothole is 7 cm and maximum width is 550 cm, which is also found at upstream of knickpoint near Kalmane (Figure 4.26; Table 4.10). The mean width is 78.81 cm. The minimum depth of a pothole is 0.80 cm at Parvas (Figure 4.19) and the maximum value of depth is 600 cm just upstream of Kalmane knickpoint (Figure 2.27; Table 2.12). Like the diameter of potholes, majority of deep potholes have been located upstream of knick points thereby signifying most prominent incision and erosion in bedrock. The values of coefficient of variations (Cv) of all the morphometric parameters of potholes are >90% specifying very high variability in morphometry of potholes (Table 4.7).

Majority of potholes with higher morphometric parameters have been located upstream of knickpoints namely Chikadi, Ghatalbari and Kalmane and in steep reaches such as Shingharpada (Figure 2.29), Panchlai (Figure 2.12) and Parvas

(Figure 2.30; Figure 2.31; Figure 2.32) thereby representing most prominent incision and erosion in bedrock.

The statistical parameters of various geometric properties of the potholes have been carried out according to that all the values of $C_s$ are positive, ranging between 3.27 and 4.01. The values of skewness are statistically significant as they are calculated on the basis of more than 100 observations (i.e. number of potholes) (Viessman and Lewis, 2003). The positive values propose the occurrence of one or two or a few very large potholes in terms of diameter, length, width and depth (Table 4.7). Like analysis of coefficient of skewness, analysis of coefficient of kurtosis ($\mathbf{C_k}$) for the morphometric parameters of the potholes of the Par River has been carried out. All the values of $\mathbf{C_k}$ are very high, ranging from 13.83 to 24.86. The high values suggest that the degree of peakedness is said to be leptokurtic. It further indicates that the morphometric parameters of the potholes of the Par River are close to the mean values (Table 4.7).

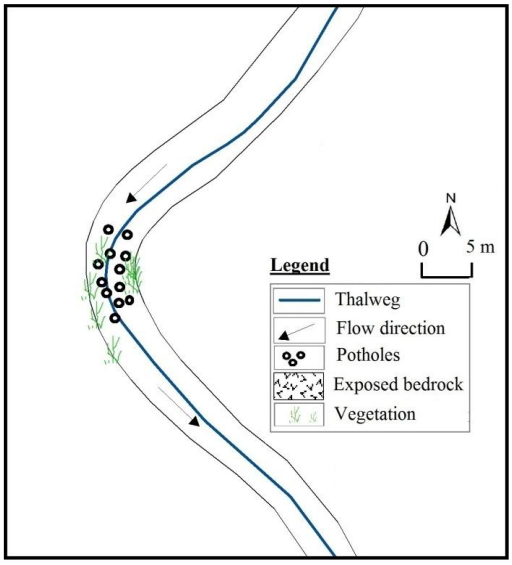


**Figure 4.20** Miniature potholes at Dongrale, Par River; Potholes not to Scale; See Figure 4.19 for location of site

**Figure 4.21** View of miniature potholes at Dongrale near source; See Figure 4.19 for location of site

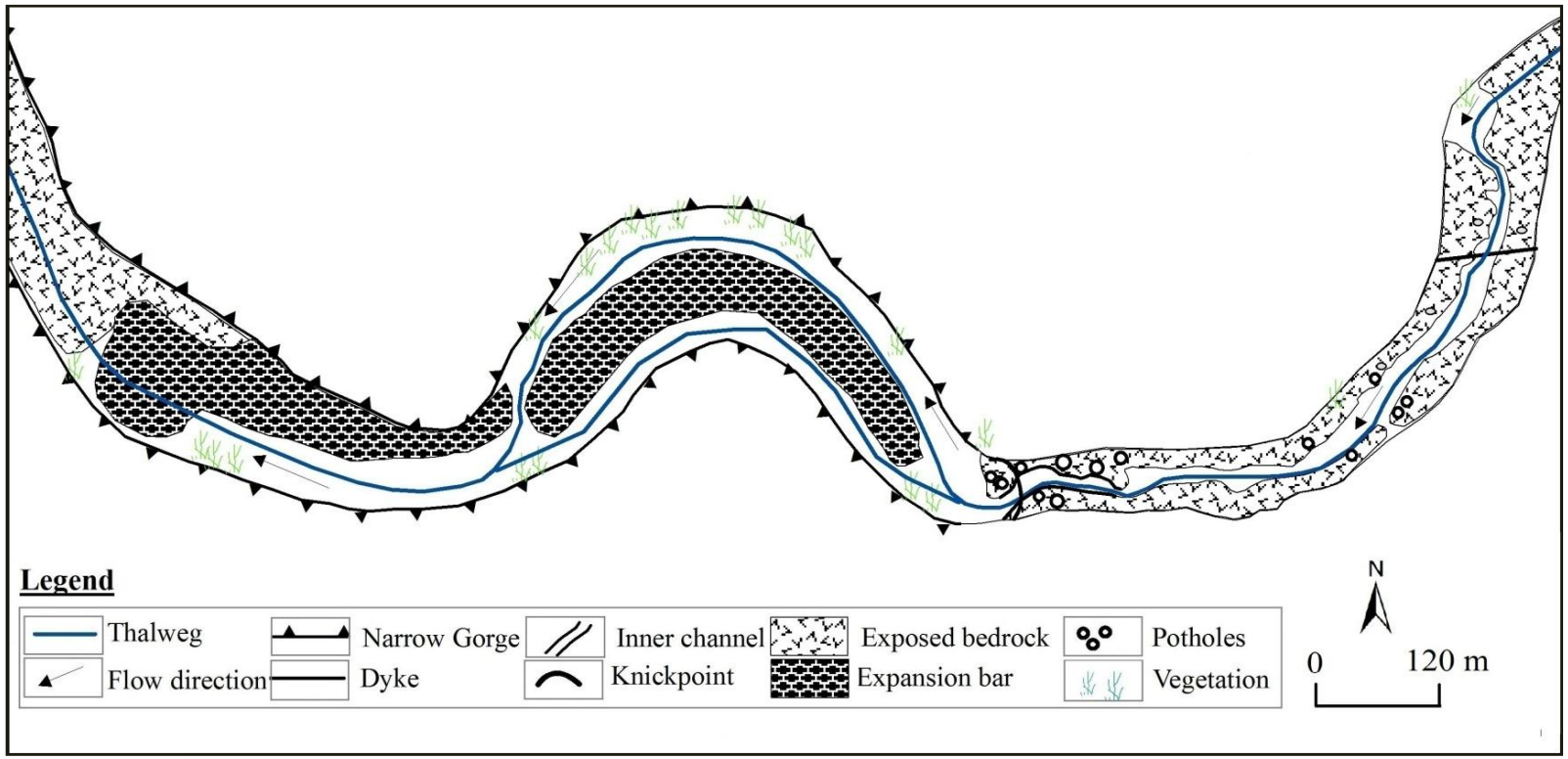


**Figure 4.22** Geomorphic map of Par River from Ghatalbari to Jahule reach; Potholes not to scale; See Figure 4.19 for location of reach

**Figure 4.23** Largest circular (diameter 380 cm) pothole in terms of diameter upstream of Ghatalbari knick; See Figure 4.19 for location of site

**Figure 4.24** Ghatalbari Knick (height 8.4 m) during rainy season; See Figure 4.19 for location of site

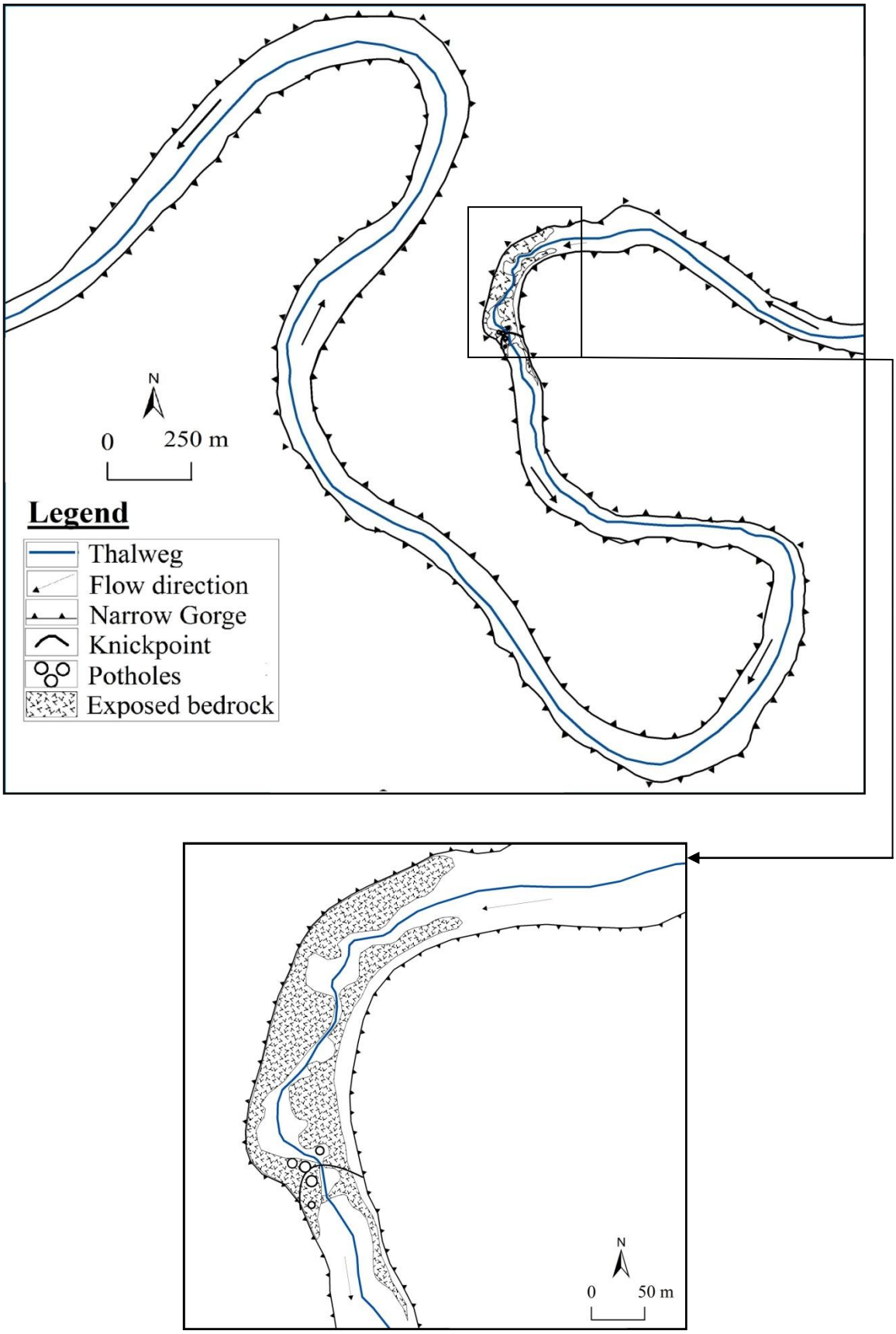


**Figure 4.25** Geomorphic map of Kalmane site**;** Potholes not to scale; See Figure 4.19 for location of site

**Figure 4.26** Largest pothole in terms of length (730 cm) and width (530 cm) upstream of Kalmane knick; See Figure 4.19 for location of site

**Figure 4.27** Long and narrow gorge downstream of knick at Kalmane; See Figure 4.19 for location of site)

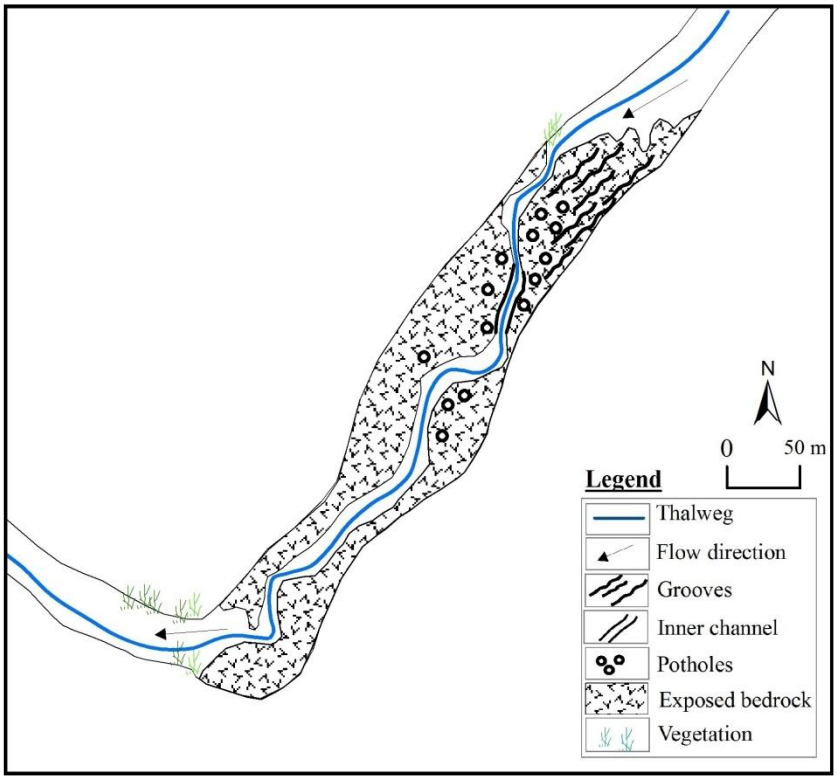


**Figure 4.28** Geomorphic map of Par River at Shingharpada; Potholes and grooves not to scale; See Figure 4.19 for location of reach

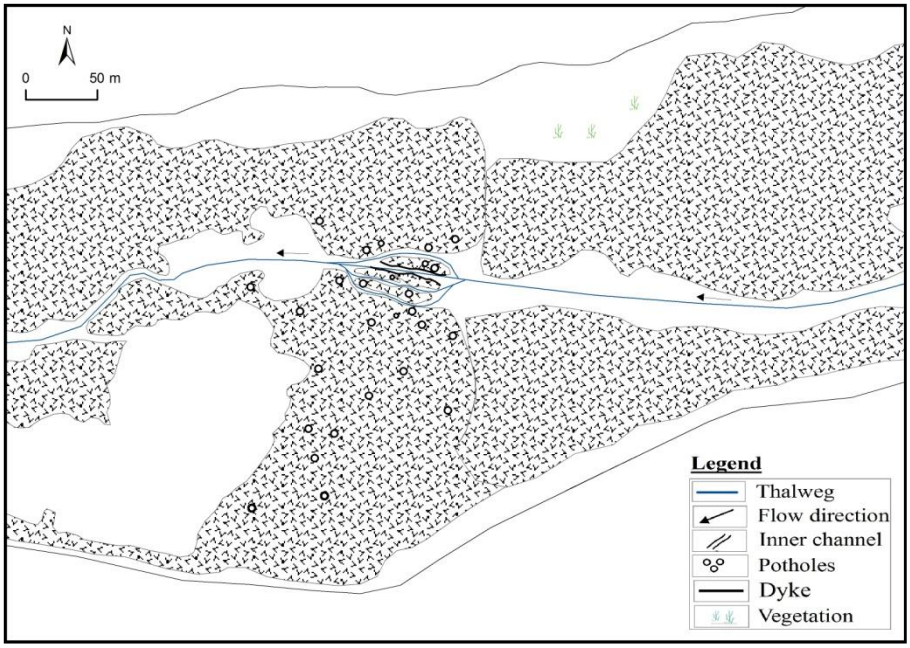


**Figure 4.29** Pot holes and inner channels shaped in exposed bedrock at Parvas; Potholes not to scale; See Figure 4.19 for location of reach

**Figure 4.30** Size and shape variance of potholes at Parvas; See Figure 4.19 for location of site

**Figure 4.31** Second largest potholes in terms of length (640 cm) at steep reaches of Parvas; See Figure 4.19 for location of site

**Table 4.8** Top 10 potholes in terms of diameter (cm)

| **Diameter (cm)** | **Shape** | **Material** | **Location** | **Remark** |
|---|---|---|---|---|
| 380 | Circular | Gravels to boulders | Upstream of Ghatalbari knick | Largest circular |
| 210 | Circular | Sand to cobbles | Upstream of Ghatalbari knick | Joints |
| 156 | Circular | Gravels | Upstream of Ghatalbari knick | Joints |
| 150 | Circular | Sand to cobbles | Upstream of Ghatalbari knick | $4^{th}$ largest circular |
| 130 | Circular | Pebbles to cobbles | Panchlai | Joints, regional slope = 0.00102 |
| 130 | Circular | Pebbles to boulders | Parvas | Regional slope = 0.00102 |
| 125 | Circular | Cobbles to boulders | Upstream of Ghatalbari knick | $7^{th}$ largest circular |
| 110 | Circular | Pebbles to cobbles | Parvas | Regional slope = 0.00102 |
| 110 | Circular | Pebbles to cobbles | Parvas | Cracks, regional slope = 0.00102 |
| 100 | Circular | Sand to cobbles | Parvas | Joints, regional slope = 0.00102 |
| 100 | Circular | Pebbles to cobbles | Upstream of Kalmane knick | $10^{th}$ largest circular |

See Figure 4.19 for location of sights

**Table 4.9** Top 10 potholes in terms of length (cm)

| Length (cm) | Shape | Material | Location | Remark |
|---|---|---|---|---|
| 730 | Oval | - | Upstream of Kalmane knick | Largest length |
| 640 | Elongated | No material | Parvas | Twin potholes, regional slope = 0.00102 |
| 490 | Elongated | Cobbles to boulders | Upstream of Ghatalbari knick | 3rd largest length |
| 420 | Elongated | Pebble to cobble | Upstream of Kalmane knick | Twin potholes |
| 400 | Elongated | Cobbles to boulders | Upstream of Kalmane knick | Horizontal beds |
| 400 | dumbbell | Cobbles to boulders | Upstream of Ghatalbari knick | 6th largest length |
| 330 | Oval | Sand to cobbles | Upstream of Chikadi knick | Joints |
| 260 | Oval | Sand to Boulders | Shingharpada | Joints, huge boulder- I axis – 56 cm regional slope = 0.008547 |
| 210 | Irregular | Sand to cobbles | Upstream of Ghatalbari knick | Joints connected at base |
| 210 | Oval | Pebbles to boulders | Parvas | Regional slope = 0.00102 |

See Figure 4.19 for location of sights

**Table 4.10** Top 10 potholes in terms of width (cm)

| Width (cm) | Shape | Material | Location | Remark |
|---|---|---|---|---|
| 550 | Oval | - | Upstream of Kalmane knick | Largest width |
| 400 | Twin | Pebble to cobble | Upstream of Kalmane knick | 2nd largest width |
| 300 | Elongated | Cobbles to boulders | Upstream of Ghatalbari knick | Horizontal beds |
| 225 | Oval | Sand to cobbles | Upstream of Chikadi knick | Joints |
| 210 | Oval | Sand to Boulders | Shingharpada | Joints, huge boulder, I axis – 56 cm regional slope = 0.008547 |
| 200 | Dumbbell | Cobbles to boulders | Upstream of Ghatalbari knick | 6th largest width |
| 200 | Elongated | Cobbles to boulders | Upstream of Ghatalbari knick | 7th largest width |
| 200 | | No material | Parvas | Twin potholes, regional slope = 0.00102 |
| 160 | Irregular | Fine sand to Boulders | Shingharpada | Joints, I axis – 80 cm regional slope = 0.008547 |
| 150 | Oval | Sand to Cobbles | Shingharpada | Fine Joints, regional slope = 0.008547 |

See Figure 4.19 for location of sights

**Table 4.11** Top 10 potholes in terms of depth (cm)

| Depth (cm) | Shape | Material | Location | Remark |
|---|---|---|---|---|
| 600 | Oval | | Upstream of Kalmane knick | Deepest pothole |
| 450 | Dumbbell | Cobbles to boulders | Upstream of Ghatalbari knick | 2nd deepest |
| 400 | circular | Fine to cobbles | Upstream of Ghatalbari knick | Joints, largest do far |
| 242 | Elongated | Cobbles to boulders | Upstream of Ghatalbari knick | Horizontal beds |
| 215 | Elongated | Cobbles to boulders | Upstream of Ghatalbari knick | 5th deepest |
| 210 | Circular | Pebble to cobble | Upstream of Kalmane knick | 6th deepest |
| 200 | Irregular | Fine to cobbles | Upstream of Ghatalbari knick | Joints |
| 200 | Circular | Fine to cobbles | Upstream of Ghatalbari knick | 8th deepest |
| 200 | Circular | Gravels | Upstream of Ghatalbari knick | joints |
| 200 | Oval | Gravels to boulders | Upstream of Ghatalbari knick | 10th deepest |
| 200 | Oval | Sand to Boulders | Shingharpada | Joints, huge boulder, I axis – 56 cm regional slope = 0.008547 |
| 200 | Circular | Sand to Boulders | Shingharpada | JointsJoints, connected below regional slope = 0.008547 |
| 200 | Oval | Sand to Cobbles | Shingharpada | Regional slope = 0.008547 |

See Figure 4.19 for location of sights

The potholes have been categorised according to their prominent shapes. According to that the frequency of circular and oval shaped potholes is highest than that of elongated, dumbbell and irregular shaped potholes (Table 4.12).

**Table 4.12** Frequency of prominent shapes

| Prominent shapes | Frequency | Total (%) |
|---|---|---|
| Circular | 117 | 46.25 |
| Oval | 100 | 39.5 |
| Irregular | 21 | 8.3 |
| Elongated | 11 | 4.35 |
| Dumbbell | 4 | 1.6 |

**a. Relation between diameter (K) and depth of potholes (D*)**

The exponent in the regression equation for the relation between diameter of potholes (K) and depth of potholes (D*) is close to unity (0.93) (Figure 4.32; Table 4.13). It shows that the relation between diameter of potholes (K) and depth of potholes (D*) is considered linear. The value of explained variance is 0.79 indicating very strong relationship between both the variables.

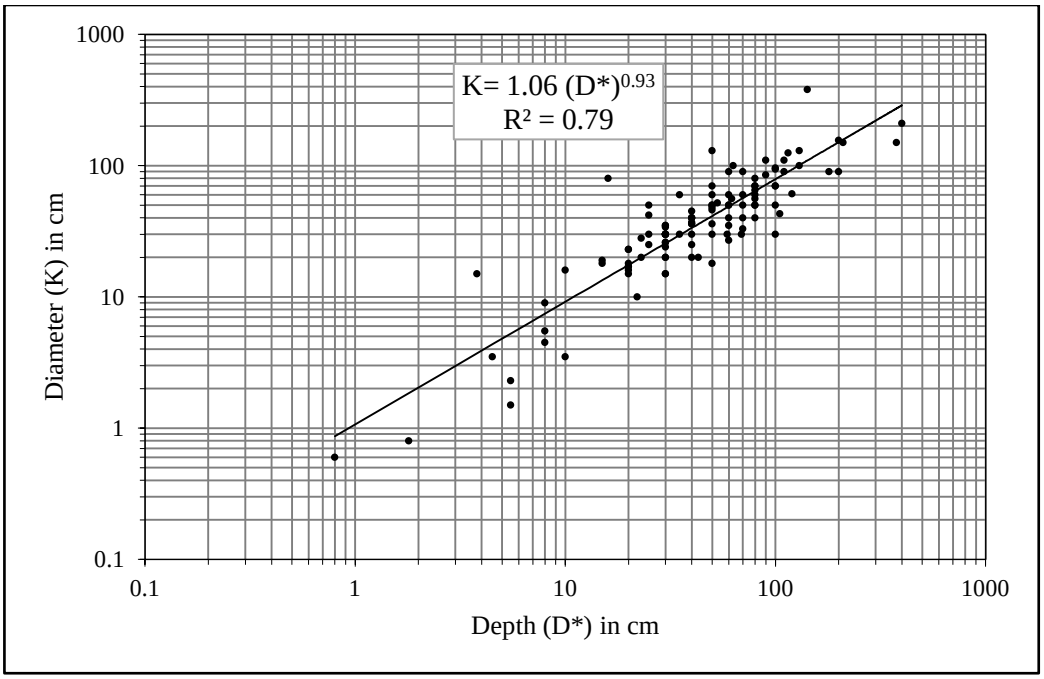


**Figure 4.32** Relation between diameter (K) and depth of potholes (D*)

**b. Relation between Length (L) and depth of potholes (D*)**

The plot of relation between Length (L) and depth of potholes (D*) shows considerable scattered points away from the regression line. Therefore, the value of $R^2$ is 0.52 (Figure 4.33; Table 4.13) indicating moderate relationship. However, there is no radical departure from Kale and Shingade's (1987) results for the relationship between depth of potholes (D*) to diameter (K) ($K = 3.7670\ (D^*)^{0.7138}$) and length of potholes (L) ($L = 3.4206\ (D^*)^{0.7737}$) for Indrayani River in Western India. The above equations can illustrate that the diameter and length of potholes increase on an average proportional to 0.93 and 0.71 respectively. In other word there is a rapid increase in diameter with depth than that of length with depth.

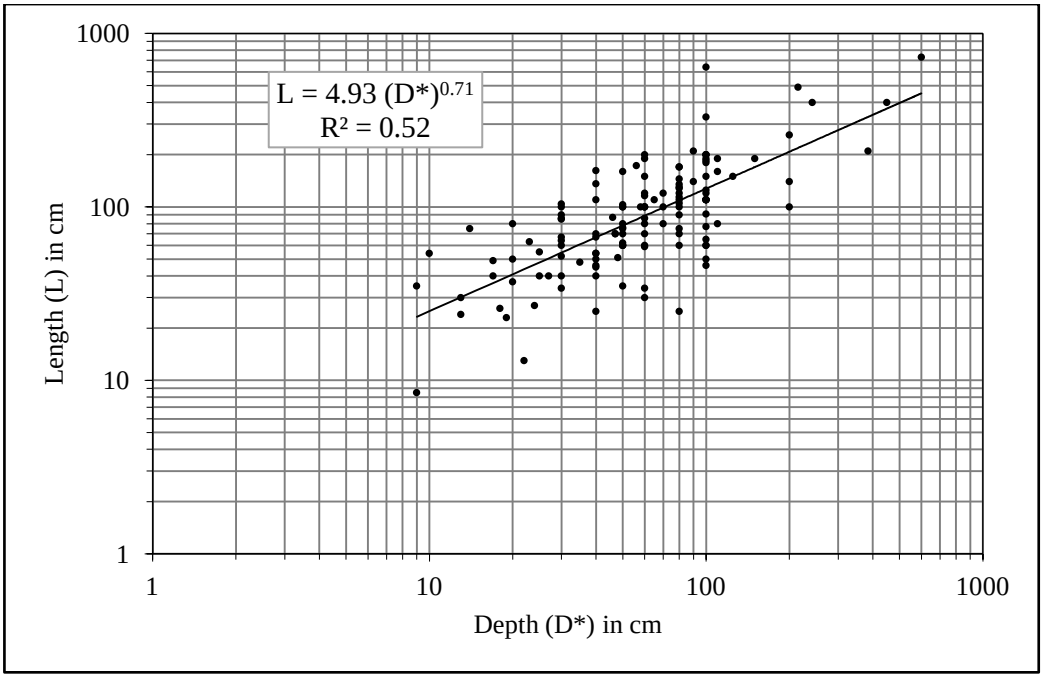


**Figure 4.33** Relation between Length (L) and depth of potholes (D*)

**Table 4.13** Empirical relations between size parameters for potholes of the Par River

| Diameter (K) and depth of potholes (D*) | Length (L) and depth of potholes (D*) |
|---|---|
| $K= 1.06 (D^*)^{0.93}$<br>$R^2 = 0.79$ | $L = 4.93 (D^*)^{0.71}$<br>$R^2 = 0.52$ |

**(ii) Longitudinal grooves**

The Table 4.14 shows the dimensions of longitudinal grooves. The minimum length of longitudinal groove is 340 cm and maximum length is 2200 cm, both extremities have been observed at Nanivahial (Figure 4.34; Table 4.14). The mean length is about 911 cm. The minimum width of longitudinal groove is 10 cm observed at Nanivahial and maximum width is 90 cm, which is observed near source of the Par River at Parchapada (Figure 4.35; Table 4.14). The mean width is about 38 cm. The minimum depth of a longitudinal groove is 6 cm observed upstream of inner channel near Mangdhe (Figure 4.36; Table 4.14) and the maximum value of depth is 55 cm near Parchapada (Figure 4.35).

The values of coefficient of variations (Cv) of all the morphometric parameters of grooves ranges from 48.52 to 55.19 indicating moderate variability in morphometry

of grooves. All the values of $C_s$ are positive, ranging between 0.86 and 1.62. The positive values intend the occurrence of one or two or a few very large grooves in length, width and depth. The value of $C_k$ for length (3.26) and depth (1.14) are higher. The high values of $C_k$ suggest that the degree of peakedness is said to be leptokurtic. It further indicates that the morphometric parameters of the grooves for length and depth of the Par River are close to the mean values. However, the value of $C_k$ for the width (0.09) is low. It, therefore, suggests that the distribution is said to be platykurtic. It further indicates that the width of the grooves does not vary much.

**Table 4.14** Statistical parameters of the various geometric properties of the longitudinal grooves

| Dimensions (cm) | No. Obs. | Min (cm) | Max (cm) | Range | Mean | σ | CV (%) | $C_S$ | $C_k$ |
|---|---|---|---|---|---|---|---|---|---|
| Length | 12 | 340 | 2200 | 1860 | 910.83 | 502.66 | 55.19 | 1.62 | 3.26 |
| Width | 100 | 10 | 90 | 80 | 37.94 | 18.62 | 49.07 | 0.86 | 0.09 |
| Depth | 100 | 6 | 55 | 49 | 21.10 | 10.24 | 48.52 | 1.09 | 1.15 |

No. Obs. = Number of observations; Min = Minimum; Max = Maximum; σ = Standard deviation; Cv = Coefficient of variation; $C_S$ = Coefficient of skewness; $C_k$ = Coefficient of kurtosis

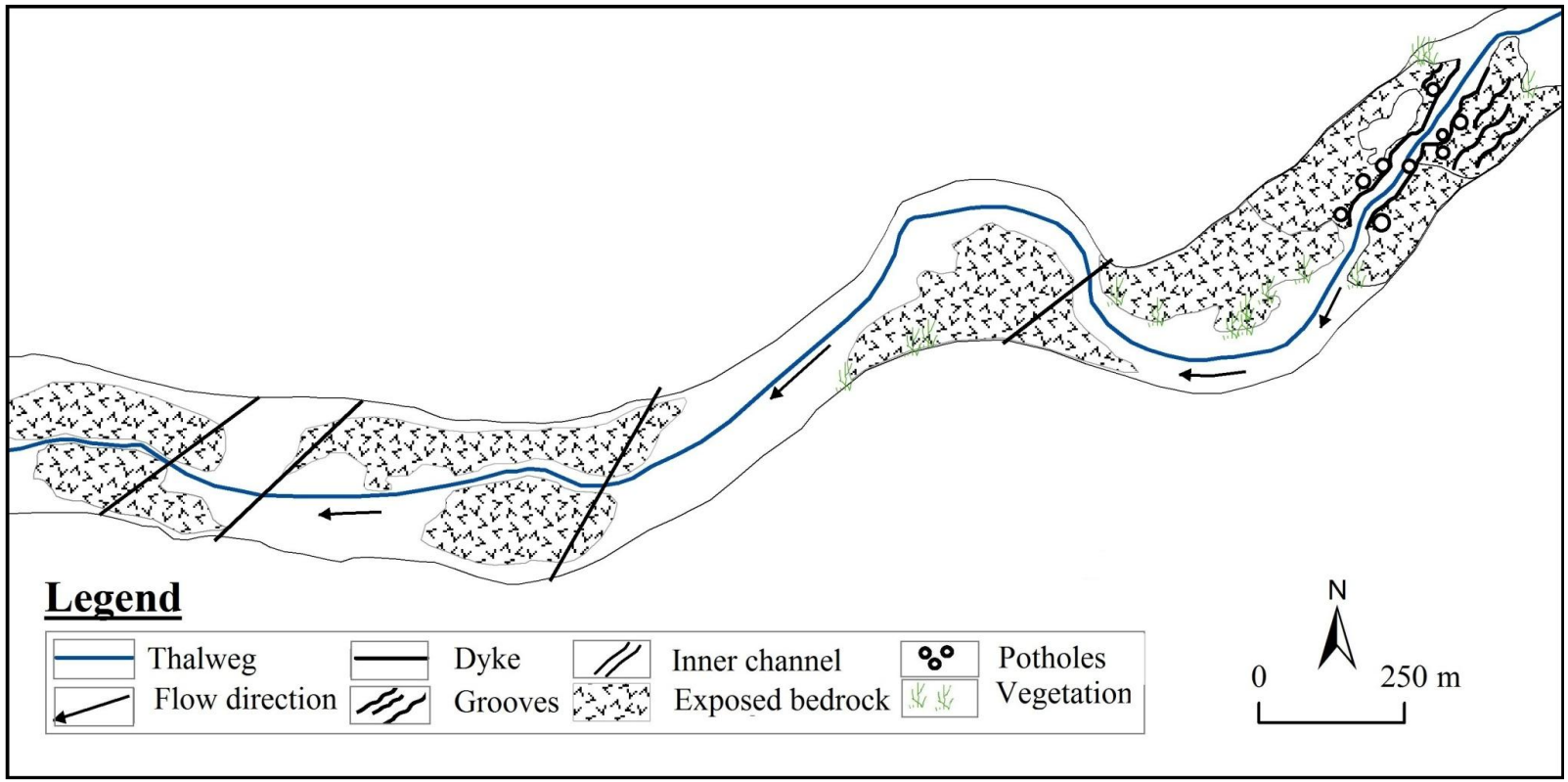


**Figure 4.34** Geomorphic map of Par River at Nanivahial; Potholes and grooves not to scale; See Figure 4.19 for location of reach

**Figure 4.35** View of longitudinal grooves eroded into exposed bedrock of the Par River at Parchapada (near source); See Figure 4.19 for location of site

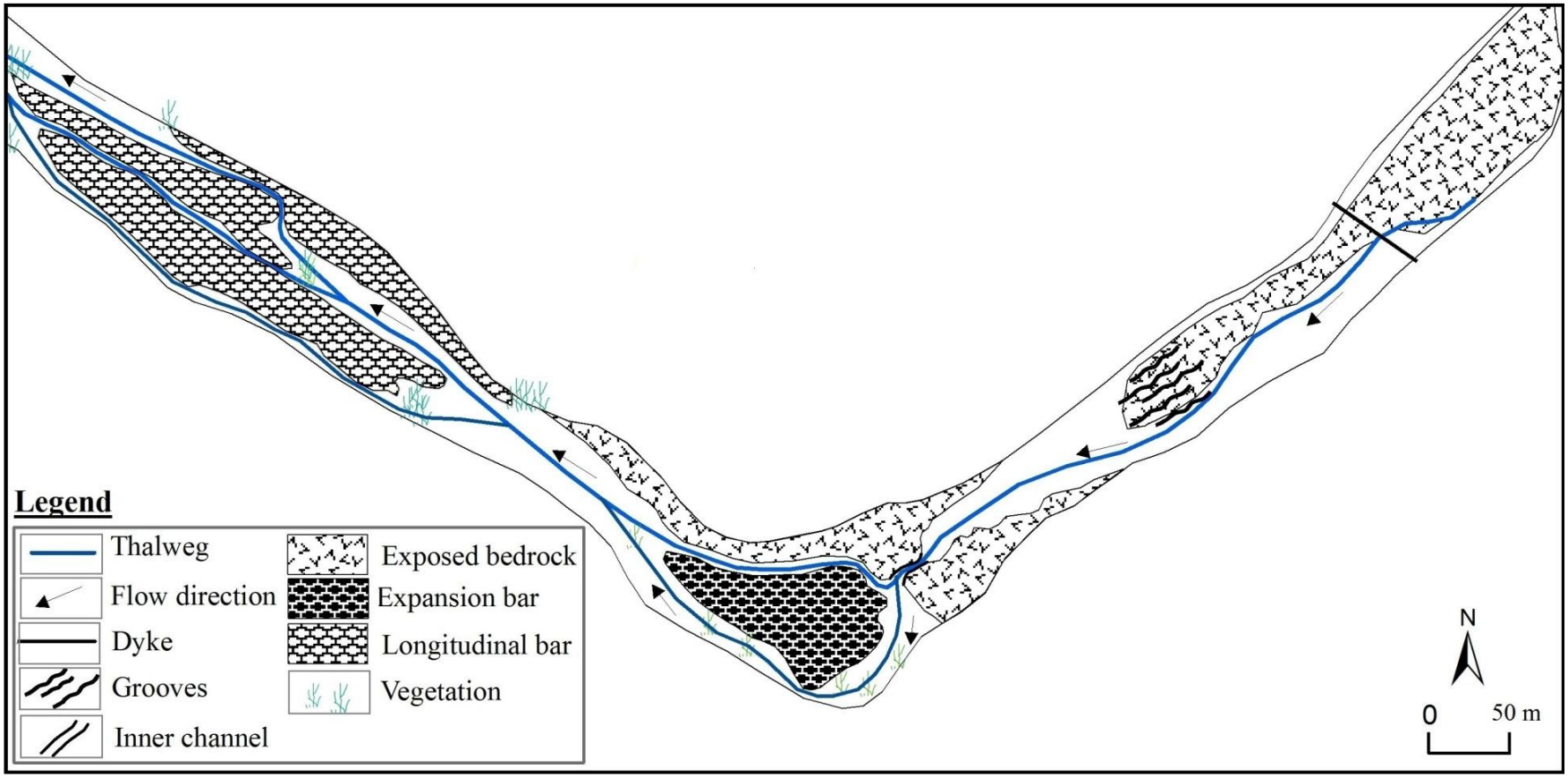


**Figure 4.36** Geomorphic map of Par River at Mangdhe; Grooves not to scale; See Figure 4.19 for location of site

**(iii) Inner channel**

The Table 4.15 shows the dimensions of inner channel. The minimum length of inner channel is about 28 m observed near Shingharpada (Figure 4.37) and maximum length is about 690 m near Mohankavchali (Figure 4.38; Figure 4.39). The mean length is 171.51 m. The minimum width of inner channel is 5.55 m which is found near Mangdhe (Figure 4.36) and maximum width is 32.30 m at Nanivahial (Figure 4.34). The mean width is 37.94 m. The minimum depth of inner channel is 1.5 m found near Nanivahial (Figure 4.34) and the maximum value of depth is 9.20 m near Mohankavchali (Figure 4.38; Figure 4.39). The mean depth is 3.98 m. Although, the role of high magnitude floods in the formation of the inner channels of the Par River is not known, very high values of stream power per unit area and bed sheer stress (e.g. 52125 $W/m^2$ and 3320 $N/m^2$ respectively) must have resulted high-energy erosional processes such as cavitation and microturbulent plucking and must have formed inner channels of Par River.

**Table 4.15** Statistical parameters of the various geometric properties of the inner channel

| Dimensions (m) | No. Obs. | Min (m) | Max (m) | Range | Mean |
|---|---|---|---|---|---|
| Length | 8 | 27.83 | 689.45 | 661.62 | 171.51 |
| Width | 8 | 5.55 | 32.30 | 26.76 | 12.39 |
| Depth | 8 | 1.50 | 9.20 | 7.70 | 3.98 |

No. obs. = Number of observations; Min = Minimum; Max = Maximum

**Figure 4.37** Inner channel with undulating walls, Shingharpada, Par River; See Figure 4.19 for location of site

**Figure 4.38** Longest (690 m) and deepest (9.20 m) inner channel at Mohankavchali, Par River; See Figure 4.19 for location of site

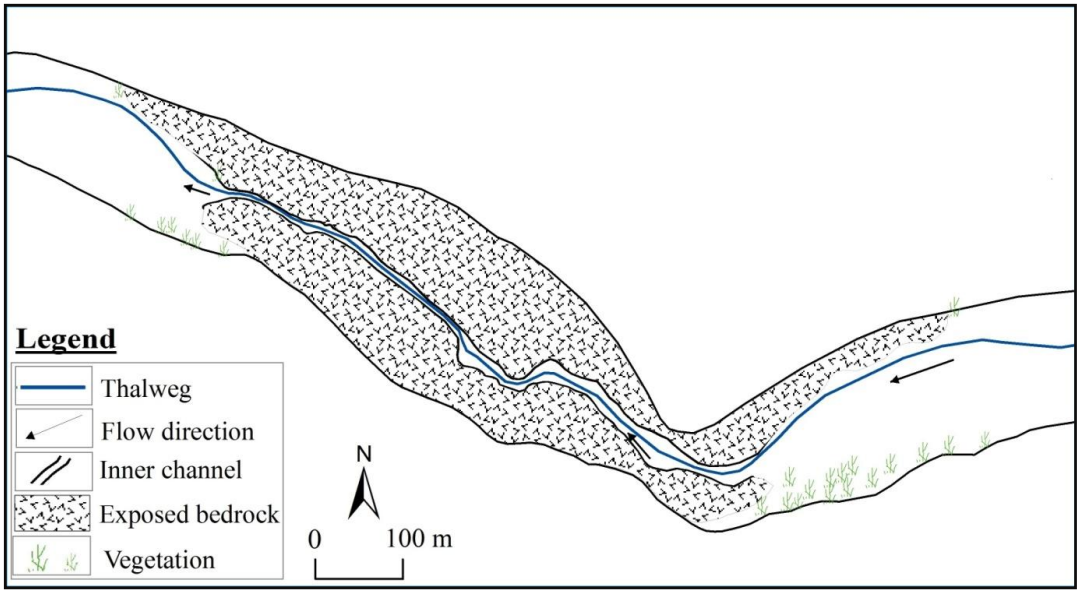


**Figure 4.39** Geomorphic map of Par River at Mohankavchali; Par River; See Figure 4.19 for location of reach

### *4.2.4 Longitudinal profile*

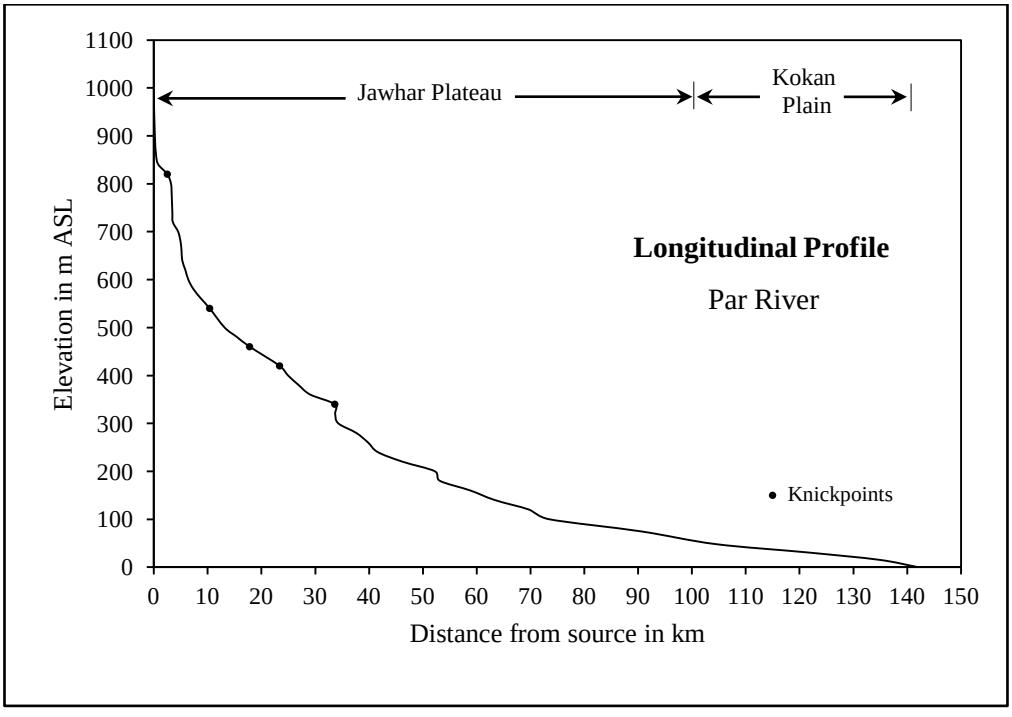


**Figure 4.40** Longitudinal Profile of the Par River

The longitudinal profile of the Par River shows a concave upward curve (Figure 4.40). The concavity reveals progressive decrease in gradient in the downstream direction.

The average gradient of the channel is 0.0069. When compared to other adjoining rivers, the average channel gradient is higher. As expected, the gradient is steeper at waterfalls and rapids. From the source, for about 103 km, the river flows over Jawhar Plateau having a slope of 0.0095. The channel gradient decreases in the Kokan Coastal Plains as 0.0026. The rate of decrease in the slope is higher in the upper reaches (up to the end of Jawhar Plateau) and low in the lower reaches of the river (in the Kokan Plain) (Figure 4.40). The channel of a Par River is characterised by five major knickpoints along its course (Table 4.16). The bedrock channel of the Par River may have downstream variability as a result of knickpoints. All the knick points were measured. The highest knick is at Kalmane (Figure 4.19) having height of 40 meters is within Kalmane Gorge (Figure 4.25; Figure 4.27); however, it is near vertical fall (Figure 4.41; Table 4.16). The 2$^{nd}$ highest waterfall of the river is situated about 2.5 kms from the source having the height of 21 meters (Figure 4.42; Figure 4.43; Table 4.16). The rest of the knickpoints have heights less than 10 meters. Such knickpoints are the locations of the higher concentration of energy dissipation along the course of the Par River. As flow approaches the lip of knickpoint, width decreases, but depth, velocity, and bottom shear stress increases (Gardner, 1983). As a result of this, the slope of the incising channel reach increases above the lip of knick points. Studies of Bishop and Goldrick (1992) described knickpoints for which pothole erosion at the lip is an important component of headward retreat. Similarly, a few knickpoints namely Chikadi (Figure 4.44), Ghatalbari (Figure 4.22; Figure 4.24) and Kalmane (Figure 4.19; Figure 4.41) have potholes at the lip of knickpoints. Pothole erosion at the lip of these knickpoints, are therefore, considered significant factor for headward erosion. Holland and Pickup (1976) subdivided a knickpoint system into four major components (i) an aggraded reach upstream from each knickpoint, (ii) an over steepened reach just above the knickpoint face, (iii) the knickpoint face, and (iv) an incising reach partially covered by moving sediment between successive knickpoints. It is observed at the Chikadi, Ghatalbari and Kalmane reaches that the first component of an aggraded reach upstream from knickpoint is missing. It is due to steeper gradient of the river in general. However, the remaining three components of a knickpoint system are present at these channel reaches.

**Table 4.16** Knickpoints of the Par River

| Sr. No. | Distance from source (km) | Height (m) | Location | Remark |
|---|---|---|---|---|
| 1. | 2.52 | 21.00 | Manjarpada | Upstream of Manjarpada dam wall |
| 2. | 9.86 | 6.00 | Parchapada | Downstream of Parchapada XS site |
| 3. | 19.30 | 10.40 | Chikadi | Downstream of Borvan XS site |
| 4. | 23.38 | 8.40 | Ghatalbari | Downstream of Ghatalbari XS site |
| 5. | 33.64 | 40.00 | Kalmane | Near vertical, downstream of Kalmane XS site |

XS = Cross section; See Figure 4.19 for location of sites

**Figure 4.41** Highest near vertical knick at Kalmane (40 m); Note persons standing for scale; See Figure 4.19 for location of site

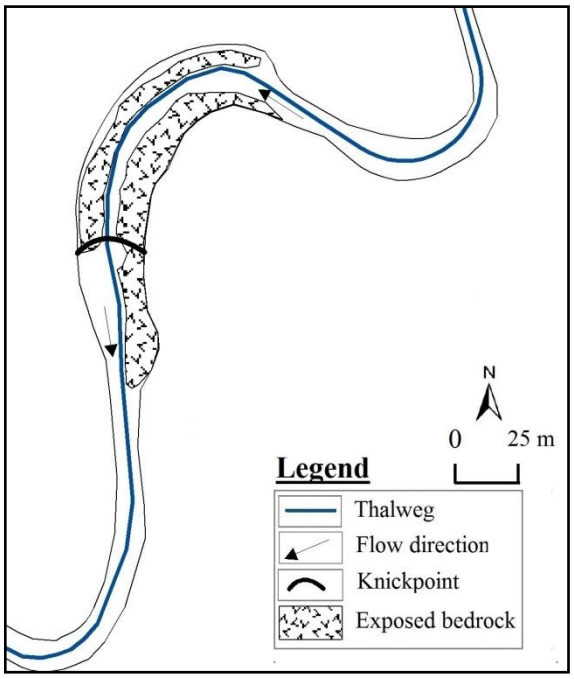


**Figure 4.42** Knickpoint at Manjarpada, Par River; See Figure 4.19 for location of reach

**Figure 4.43** Vertical and Second highest knickpoint at Manjarpada (21 m); Note persons standing for scale in circle; See Figure 4.19 for location of site

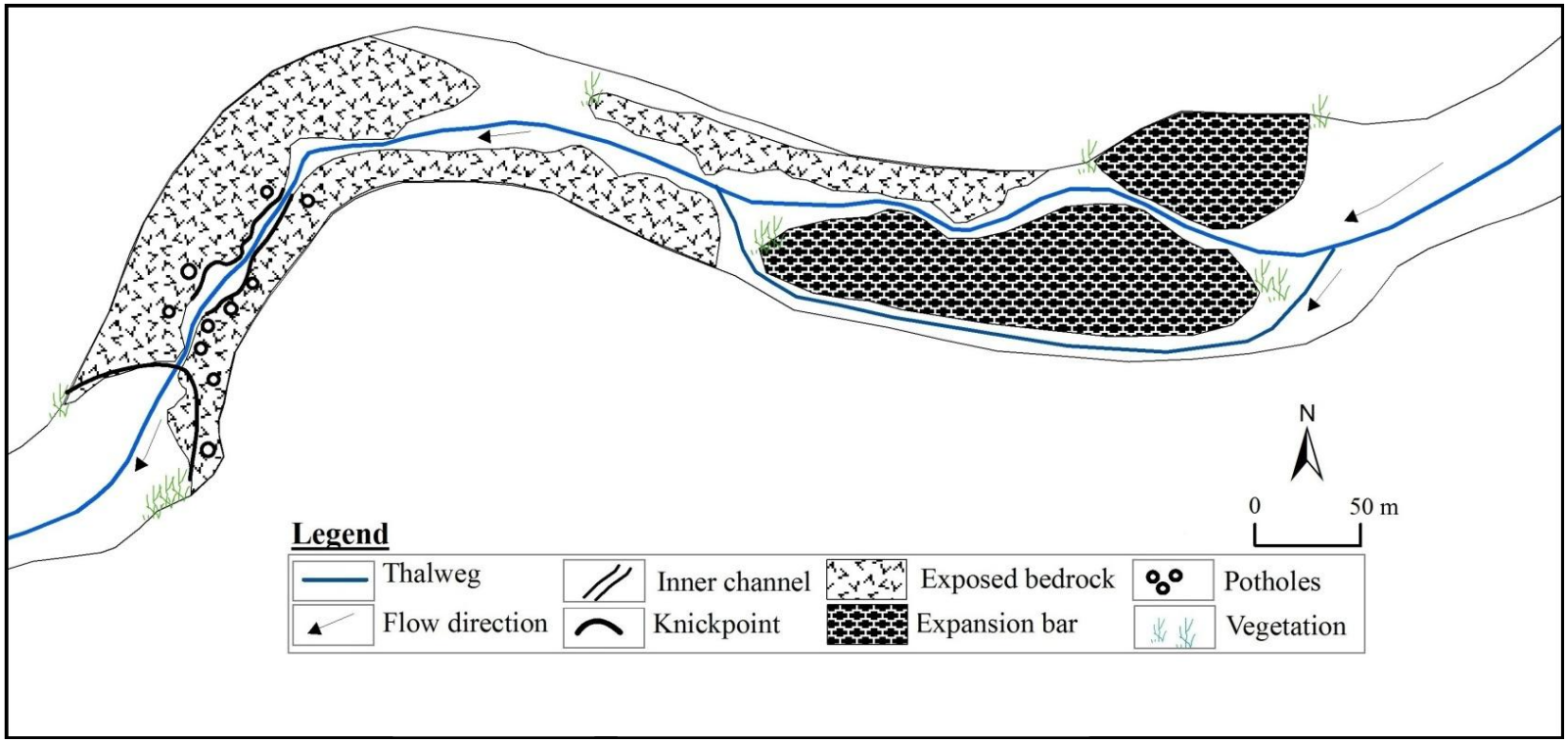


**Figure 4.44** Geomorphic map of Par River at Chikadi; Potholes not to scale; See Figure 4.19 for location of reach

**(i) Relation between distance (L) and slope (VI/HE)**

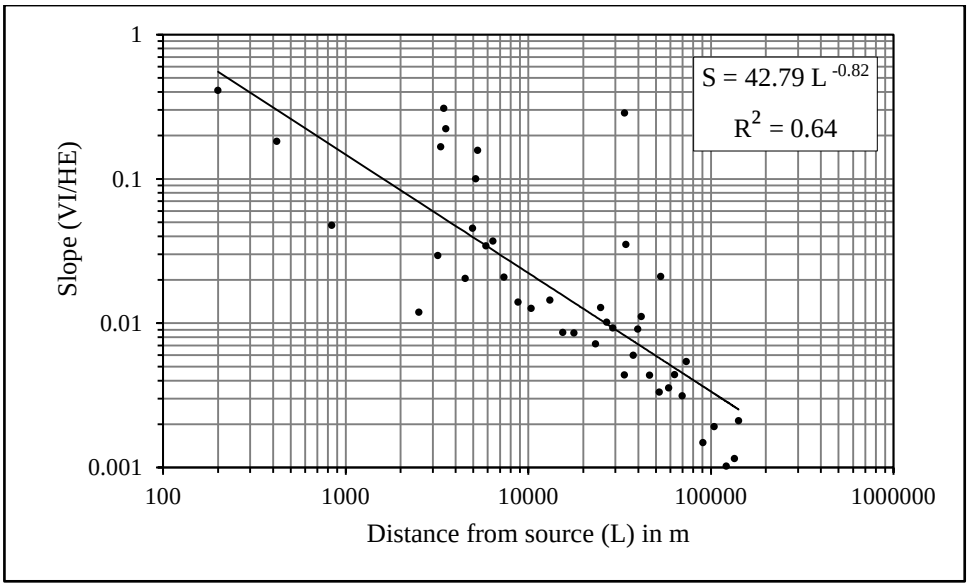


**Figure 4.45** Relation between distance (L) and slope (S) (VI/HE)

The relation between distance (L) and slope (S) is strong ($R^2 = 0.64$). The exponent in the regression equation is very close to unity (-0.82) (Figure 2.45). It shows inverse power law relationship between distance (L) and slope (S) of channel whereby as distance (L) increases from the head of river towards mouth the slope decreases proportionately. However, few outliers indicate sudden decrease or increase in slope with increasing distance. Such reaches are geomorphologically significant for erosion and deposition of coarse sediment in bedrock channels.

### *4.2.5 Depositional features of bedrock channel*

**(i) Expansion bar**

The Table 4.17 indicates that for all the sites the Er/Cr ratio ranges from 1.56 to 6.59. It shows that the maximum expansion of channel is about 7 times after the constricted reach of Mendha Gorge (Figure 4.46; Table 4.17). Manifold expansion boulder bars separated by parallel swales (troughs) have been observed in the Par River. The depth of swales ranges between two to five meters than the adjacent crests of bar. The expansion bar deposits are up to five meter thick. Due to high flow depth in swales the flow energy during deposition accelerates at depression than that of adjacent bar crests.

**Table 4.17** Channel width (W) and height of expansion bars

| Sr. No. | Location | Reference figures | Channel width (w) at constricted reach (Cr) (m) | Channel width (w) at expanded reaches (Er) (m) | Increase in width (m) | Er/Cr ratio | Height of Eb (m) |
|---|---|---|---|---|---|---|---|
| 1. | Parchapada | Figure 4.49 | 34.20 | 82.52 | 48.32 | 2.41 | 2.38 |
| 2. | Mangdhe | Figure 4.36 | 44.64 | 107.72 | 63.07 | 2.41 | 1.91 |
| 3. | Chikadi | Figure 4.44 | 56.33 | 88.11 | 31.78 | 1.56 | 3.02 |
| 4. | Ghatalbari | Figure 4.22 | 49.56 | 125.65 | 76.09 | 2.54 | - |
| 5. | Jhiri | Figure 4.50, Figure 4.51 | 135.35 | 227.92 | 92.57 | 1.68 | 1.61 |
| 6. | Mendha | Figure 4.46 Figure 4.47, Figure 4.48 | 42.77 | 281.69 | 238.92 | 6.59 | 4.83 |
| 7. | Dhamni | Figure 4.52 | 106.70 | 223.29 | 116.59 | 2.1 | 1.61 |
| 8. | Makadban | Figure 4.53 | 148.52 | 298.42 | 149.90 | 2.01 | 3.70 |
| 9. | Makadban | - | - | - | - | - | 4.00 |

Cr = Constricted reaches; Er = Expanded reaches; Eb = expansion bar; See Figure 4.19 for location of reach

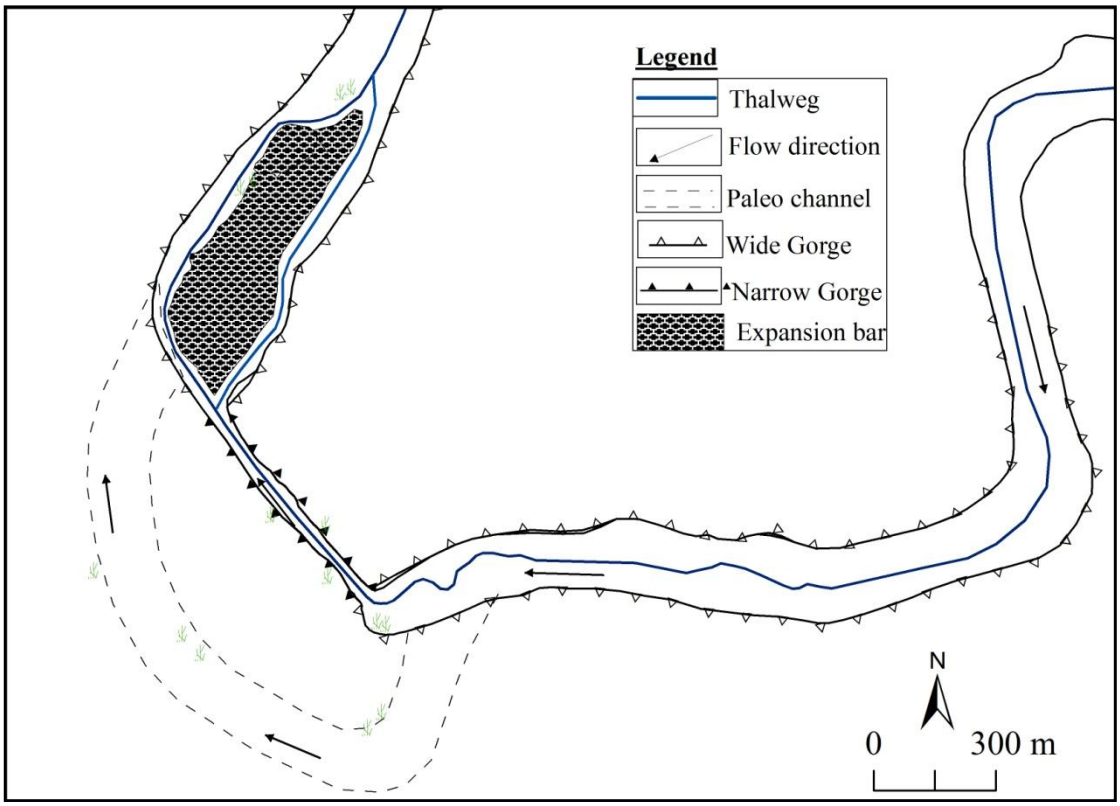


**Figure 4.46** Largest expansion bar downstream to constricted reach of Mendha Gorge; See Figure 4.19 for location of reach

**Figure 4.47** Constricted gorge at Mendha; Flow direction from top to bottom of figure; See Figure 4.19 for location of reach

**Figure 4.48** Frontage of expansion bar downstream to constricted reach of Mendha Gorge. Flow direction from bottom to top of figure; Note person for scale; See Figure 4.19 for location of reach

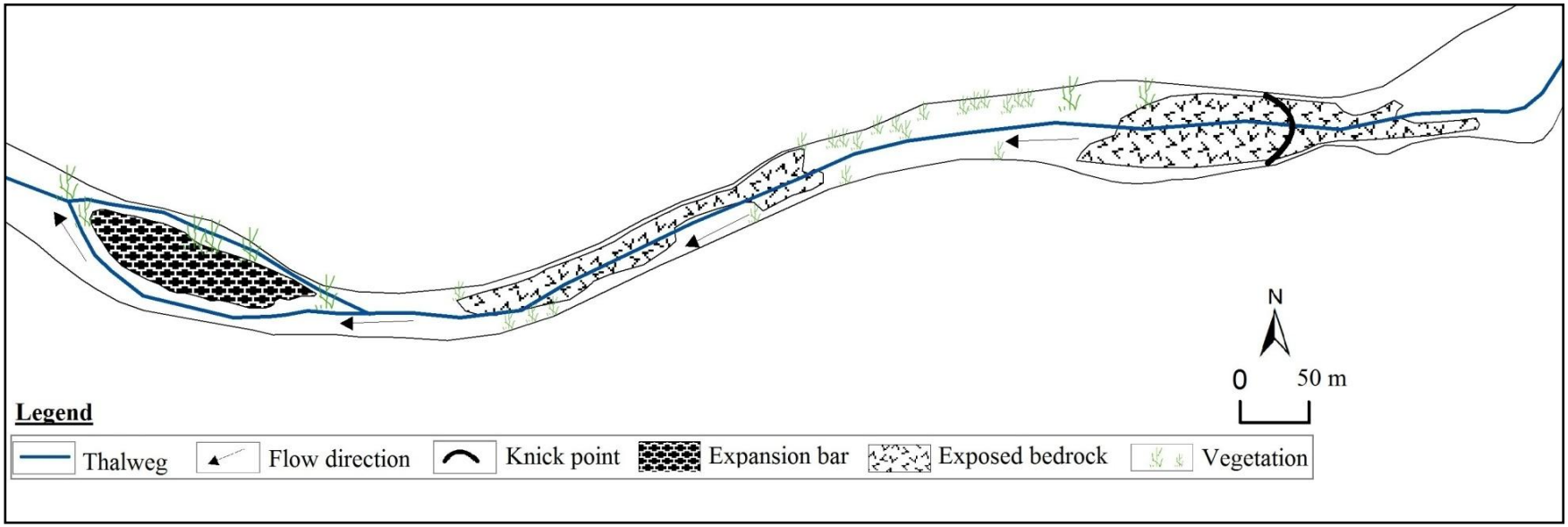


**Figure 4.49** Geomorphic map of Par River at Parchapada; See Figure 4.19 for location

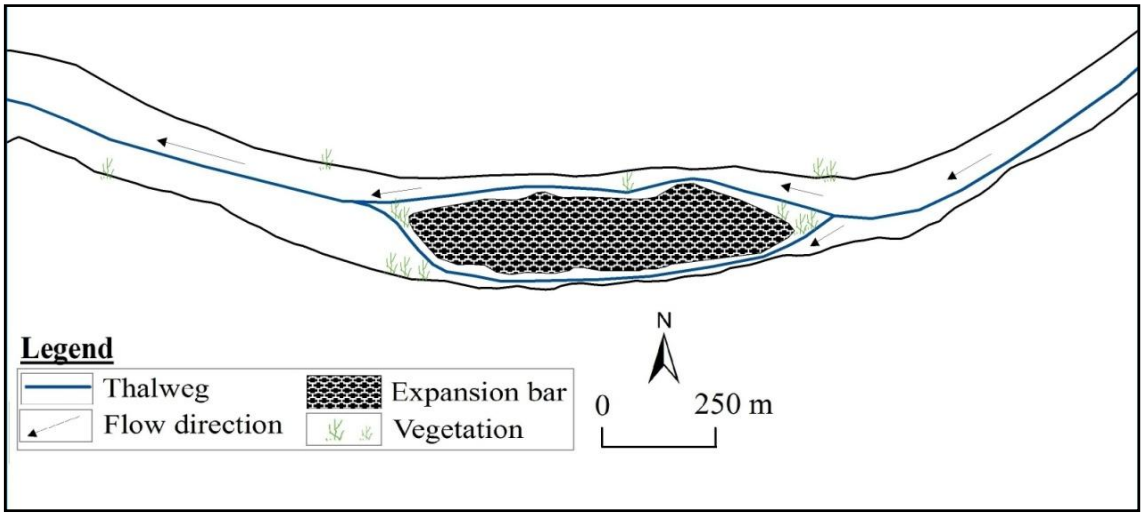


**Figure 4.50** Expansion bar at Jhiri; See Figure 4.19 for location of reach

**Figure 4.51** Front view of expansion bar at Jhiri; Flow direction from top to bottom of figure; Note person for scale; See Figure 4.19 for location of reach

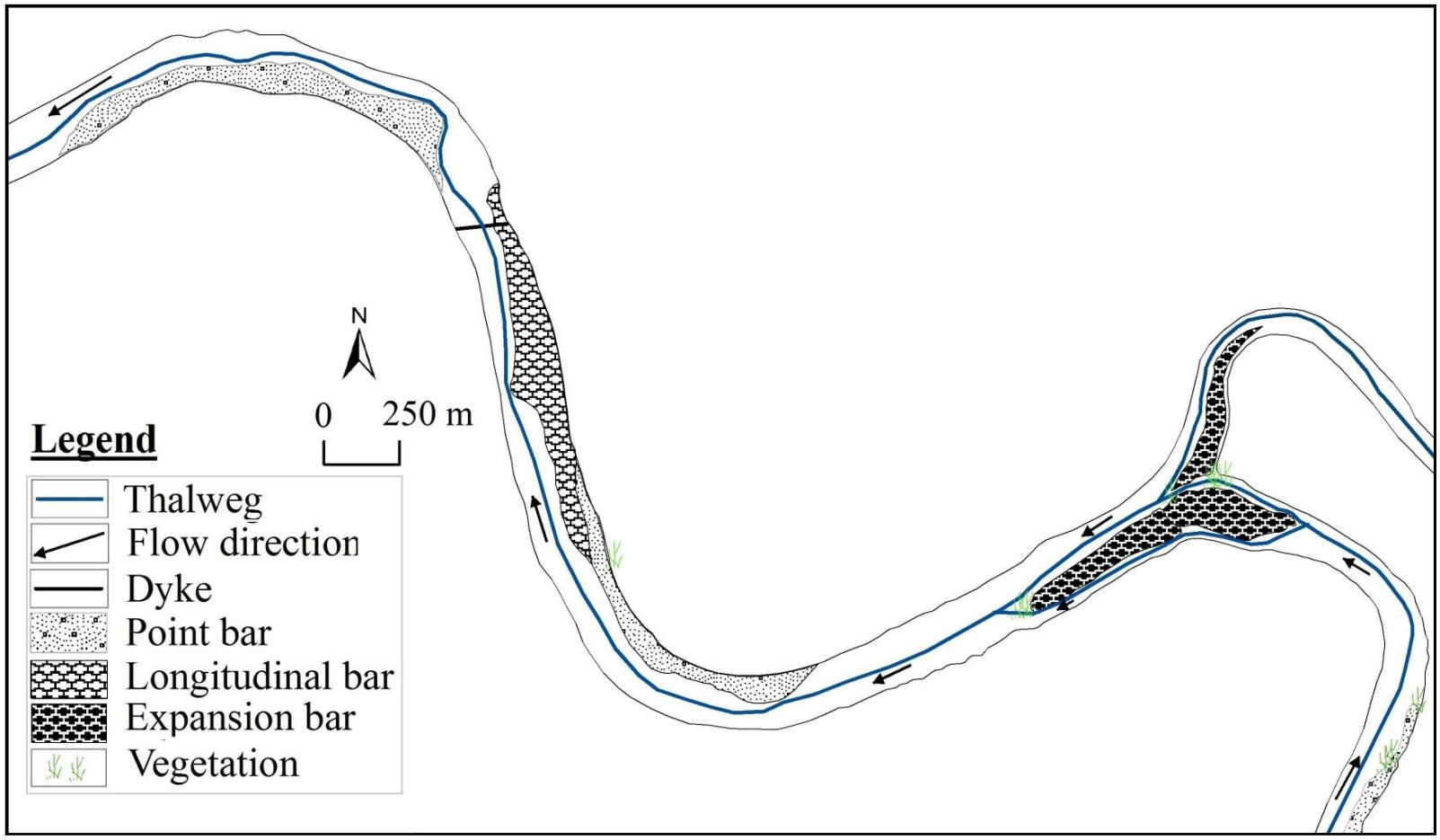


**Figure 4.52** Geomorphic map of Par River at Dhamni, Par River; See Figure 4.19 for location

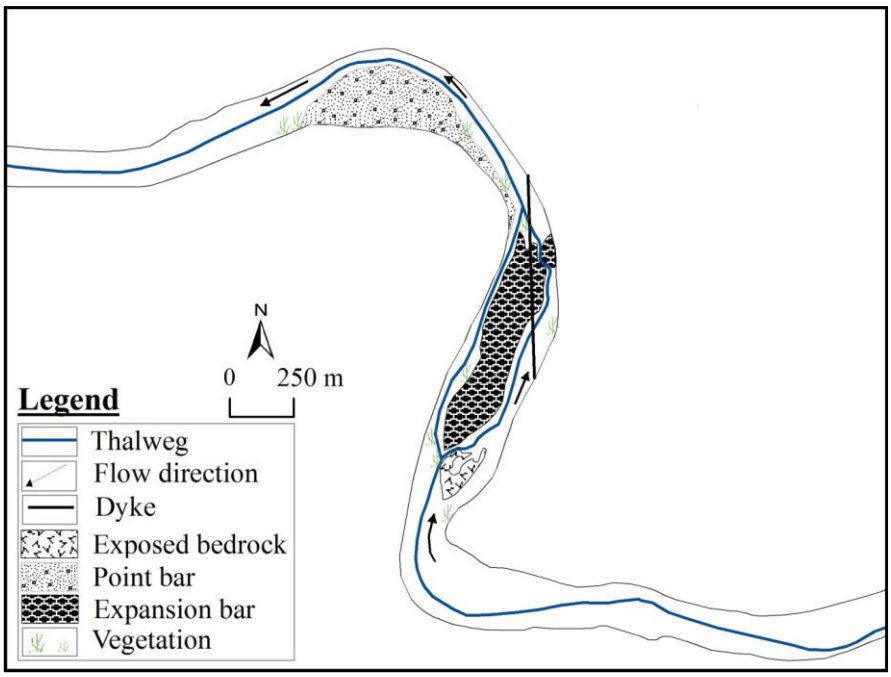


**Figure 4.53** Geomorphic map of Par River at Makadban**;** See Figure 4.19 for location of reach

### (ii) Longitudinal bar

The length to width ratio of longitudinal bars of the Par River ranges between four and ten (Table 4.18), which states that they are at least four times and at the most ten times longer than they are wide. Table 4.18 shows the dimensions of longitudinal bars at different locations of the Par River.

**Table 4.18** Channel width (W) and length, width and height of longitudinal bars

| Sr. No. | Location | Reference figure | Channel width (W) (m) | Length of Lb (m) | Width of Lb (m) | Length of Lb/ Width of Lb ratio | Height of Lb (m) |
|---|---|---|---|---|---|---|---|
| 1. | Mangdhe | Figure 4.36 | 87.27 | 279.51 | 34.62 | 8.07 | - |
| 2. | Mangdhe | Figure 4.36 | 87.27 | 201.71 | 29.94 | 6.74 | - |
| 3. | Mangdhe | Figure 4.36 | 87.27 | 258.83 | 25.08 | 10.32 | - |
| 4. | Kachurpada | Figure 4.54 | 98.16 | 199.83 | 36.00 | 5.55 | - |
| 5. | Kachurpada | Figure 4.54 | 98.16 | 88.02 | 22.34 | 3.94 | - |
| 6. | Dhamni | Figure 4.52 | 193.81 | 1265.28 | 162.67 | 7.78 | 2.85 |

Lb = Longitudinal bar; See Figure 4.19 for location of sites

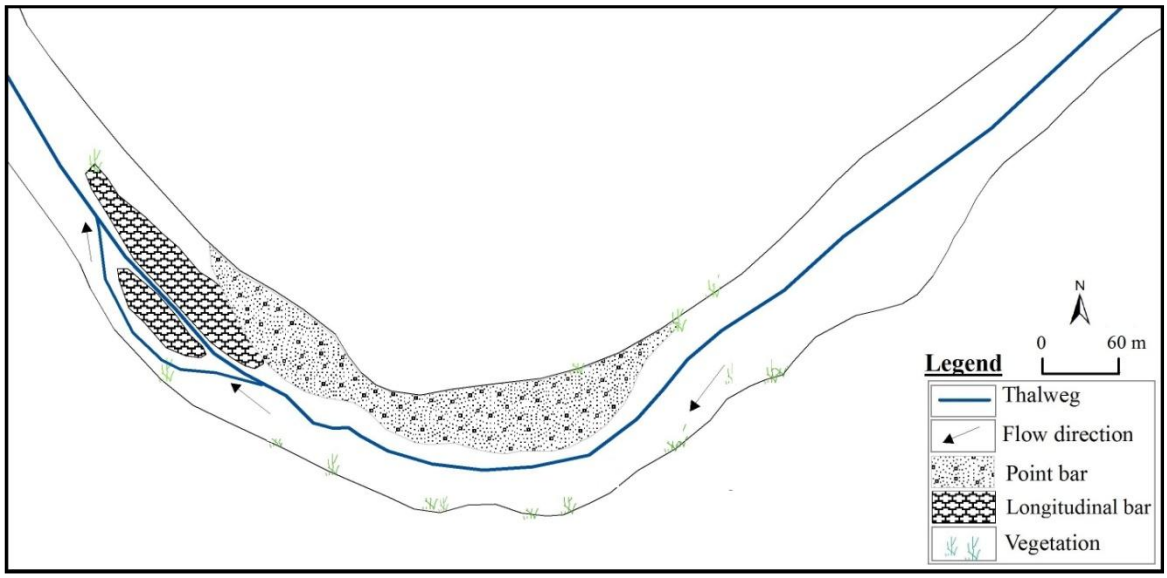


**Figure 4.54** Geomorphic map of Par River at Kachurpada; See Figure 4.19 for location of reach

**(iii) Point bar**

Well developed point bars have been observed along the inner margins of channel bends of the Par River (Figure 4.52 to Figure 4.56). The Table 4.19 shows the area occupied by the point bars. The maximum accumulation in the form of point bar is found at Borpada which covers 0.24 $km^2$ area. Point bar sediment ranges from cobbles to boulders. However, sediment of majority of point bars is in the form of cobbles.

**Table 4.19** Area occupied by point bars

| Sr. No. | Location | Reference figure | Area of point bar ($Km^2$) |
|---|---|---|---|
| 1. | Kachurpada | Figure 4.54 | 0.017 |
| 2. | Borpada | Figure 4.55 | 0.24 |
| 3. | Dhamni | Figure 4.52 | 0.112 |
| 4. | Dhamni | Figure 4.52 | 0.081 |
| 5. | Dhamni | Figure 4.56 | 0.067 |
| 6. | Dhamni | Figure 4.56 | 0.112 |
| 7. | Makadban | Figure 4.53 | 0.133 |

See Figure 4.19 for location of sites

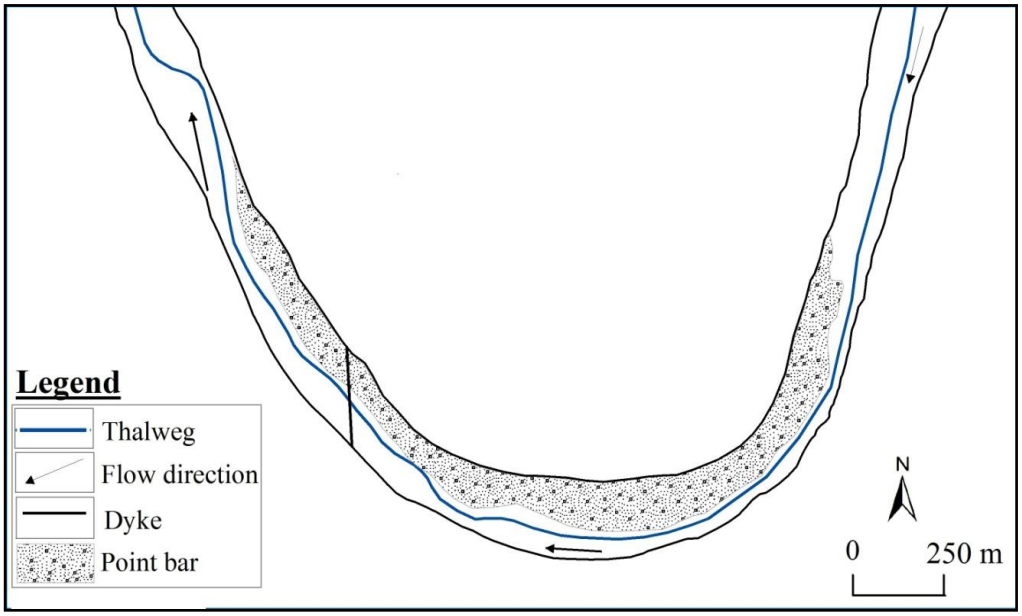


**Figure 4.55** Geomorphic map of Par River at Borpada; See Figure 4.19 for location of reach

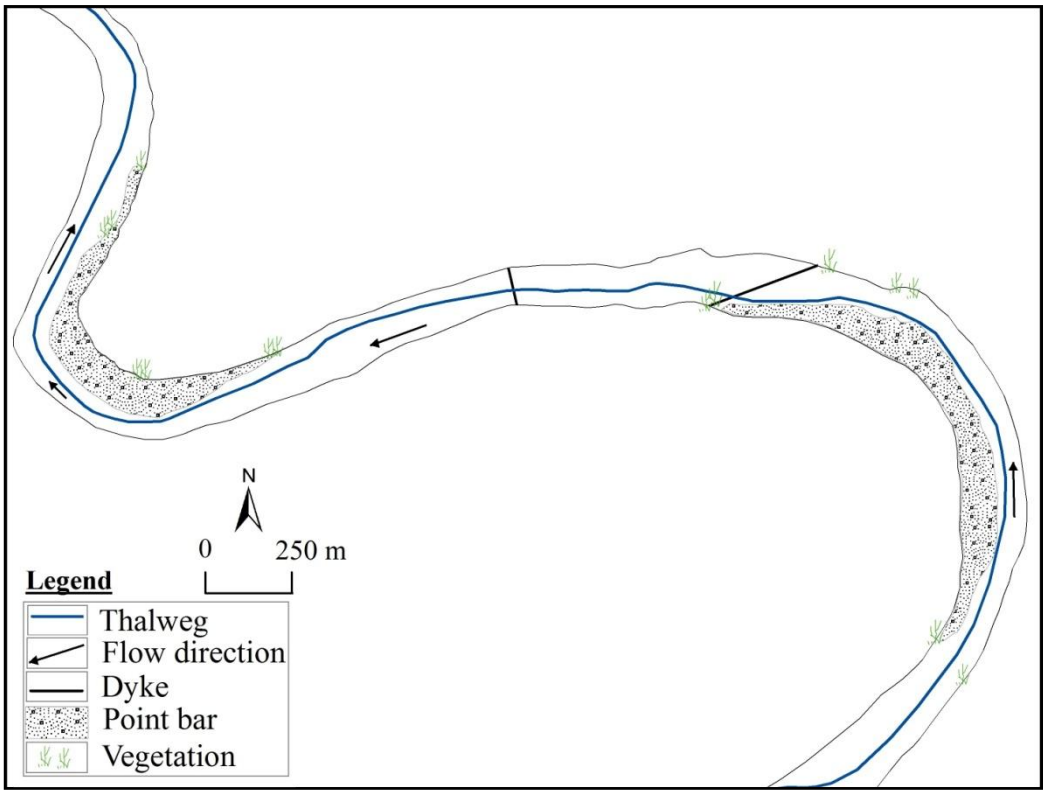


**Figure 4.56** Geomorphic map of Par River at Dhamni; See Figure 4.19 for location of reach

### *4.2.6 Hydraulic parameters associated with depositional features*

From the calculated hydraulic data of the Par River, these values stream power range between 616 and 52125 W/m$^2$, bed shear stress between 125 and 3320 N/m$^2$, and mean velocity from 4.91 to 16.62 m/s (Table 4.21). The estimated values, when compared with the values of unit stream power, bed shear stress, and mean velocity generated by reconstructions of flows in the constricted reaches in vicinity of the depositional features, reveal that the river flows are several orders of magnitude higher than the threshold values for the entrainment of boulders. These values show unusually high ability of the river to erode and transport sediments. These estimates and the hydraulic characteristics of the Par River further suggest that high flows can easily move cobbles in suspension, and large boulders as bedload (Baker and Costa, 1987) and make it available in downstream reaches for deposition. However, the values of hydraulic parameters associated with depositional features are much lower (Table 4.20) than the actual values estimated for rare floods in vicinity of depositional features. For instance, estimated values of hydraulic parameters such as unit stream power, bed shear stress, and mean velocity to entrain the giant boulder with 6200 mm i-axis located downstream of Mendha Gorge are 38322 W/m$^2$, 2306 N/m$^2$ and 16.62 m/s respectively. These values reduce to several orders of magnitude lower than the values associated with the deposition of the coarse sediment that are 5176 W/m$^2$, 1054 N/m$^2$ and 5.12 m/s respectively. It is, therefore, concluded that rapid reduction in flood energy and competence result in extensive deposition in the form of expansion bars, longitudinal bars and point bars. It is presumed that the deposited coarse-grained sediment are made available from constricted reaches located upstream of the depositional features.

**Table 4.20** Highest threshold values of the hydraulic parameters associated with depositional features

| Sites | Depositional features | i-axis of largest sediment mm | Stream Power ($\omega$) $W/m^2$ | Shear stress ($\tau$) $N/m^2$ | Mean velocity $\bar{v}$ m/s |
|---|---|---|---|---|---|
| Parchapada | Elongated bar | 580 | 255 | 99 | 1.57 |
| Mangdhe | Elongated bar | 1200 | 643 | 204 | 2.25 |
| Chikadi | Elongated bar | 1050 | 543 | 179 | 2.11 |
| Ghatalbari | Elongated bar | 2200 | 1388 | 374 | 3.05 |
| Kachurpada | Point bar, Longitudinal bar | 1600 | 927 | 272 | 2.60 |
| Kahondolpada | Point bar | 1150 | 609 | 196 | 2.20 |
| Jhiri | Elongated bar | 1900 | 1153 | 323 | 2.83 |
| Mendha | Elongated bar | 6200 | 5176 | 1054 | 5.12 |
| Dhamni | Elongated bar | 850 | 415 | 145 | 1.90 |
| Dhamni | Longitudinal bar | 500 | 212 | 85 | 1.45 |
| Makadban | Elongated bar | 580 | 255 | 99 | 1.57 |

See Figure 4.19 for location of sites

## 4.3 Erosional processes and sediment transport

### *4.3.1 Flood hydraulics and hydrodynamics*

Infrequent and large magnitude floods produce massive discharges into channels. The discharges for these rare floods on the Par River range from 2427 to 38006 $m^3/s$ (Table 4.21). These are large rainfall-runoff floods measured by indirect methods. These discharges stand out as high outlier of maximum floods per unit drainage area when compared with those recorded in the world.

**Table 4.21** Hydraulic parameters of rare floods on the Par and Nar Rivers

| Site | Discharge (Q) $m^3/s$ | Width (W) m | Depth (D) m | Slope (S) | Velocity $\bar{V}$ m/s | Shear stress ($\tau$) $N/m^2$ | Unit Stream Power ($\omega$) $W/m^2$ | Fr | Re x $10^7$ | Vc m/s |
|---|---|---|---|---|---|---|---|---|---|---|
| Parchapada | 3614 | 110 | 7.16 | 0.01294 | 6.99 | 596 | 4166 | 1.03 | 33 | 10.77 |
| Borvan | 2708 | 113 | 6.31 | 0.00883 | 6.16 | 381 | 2082 | 0.93 | 27 | 10.48 |
| Ghatalbari | 2427 | 109 | 6.64 | 0.00326 | 5.05 | 141 | 713 | 0.77 | 22 | 10.61 |
| Kalmane | 9710 | 95 | 9.73 | 0.05204 | 15.70 | 3320 | 52125 | 1.96 | 102 | 11.54 |
| Jhiri | 3955 | 154 | 9.43 | 0.00244 | 4.91 | 125 | 616 | 0.69 | 26 | 11.47 |
| Chachpada | 5954 | 88 | 11.70 | 0.00560 | 9.22 | 405 | 3734 | 1.08 | 68 | 11.22 |
| Mendha | 20056 | 42 | 28.80 | 0.00816 | 16.62 | 2306 | 38322 | 0.99 | 479 | 16.12 |
| Dhamni | 21775 | 240 | 14.00 | 0.00115 | 6.46 | 159 | 1024 | 0.55 | 91 | 13.77 |
| Nanivahial$^+$ | 23820 | 600 | 16.83 | 0.000654 | 5.3 | 47.98 | 254.45 | 0.62 | 39.7 | 13.48 |
| Panchlai | 35785 | 371 | 12.90 | 0.01097 | 10.67 | 972 | 10370 | 1.13 | 96 | 12.43 |
| Parvas | 38006 | 372 | 18.90 | 0.00269 | 7.20 | 374 | 2693 | 0.61 | 102 | 14.04 |
| Sudhalvada | 10699 | 290 | 9.98 | 0.00375 | 5.86 | 232 | 1356 | 0.75 | 37 | 11.60 |
| Pardi | 25732 | 390 | 15.90 | 0.00111 | 5.60 | 128 | 717 | 0.64 | 66 | 13.24 |
| Umbardhe* | 4438 | 68 | 12.00 | 0.008923 | 9.0 | 638.35 | 5745.2 | 1.06 | 65.70 | 12.19 |
| Pendha* | 2088 | 174 | 16.78 | 0.0000741 | 1.26 | 6.88 | 8.71 | 0.131 | 11.99 | 13.44 |
| Tamchhadi* | 14414 | 100 | 20.30 | 0.0092567 | 11.58 | 1134.9 | 13141.8 | 1.05 | 145 | 14.3 |

$^+$ = Gauging site * = Sites on Nar River; Fr = Froude number; Re = Reynolds number; Vc = Critical velocity for inception of cavitation

### (i) Shear stress ($\tau$)/fluid stressing/shear detachment

From the calculated hydraulic data of the Par River, unit stream power and bed shear stress ranges between 616 and 52125 $W/m^2$, and 125 and 3320 $N/m^2$ respectively (Table 4.21). These values indicate unusually high ability of the river to erode and transport coarse sediment. It is notable that the sediment transport rates and sediment entrainment are driven by excess shear stress over a threshold value (Turowski, 2012). In case of Par River the actual values of shear stress and unit stream power exceed the theoretical values (Table 4.22), thereby indicating capability of flows to entrain largest boulders.

**Table 4.22** Boulder dimensions and the associated theoretical entrainment values

| **Site** | **Shear stress (τ)** | **Unit stream power (ω)** | **Velocity** ($\bar{v}$) | **i-axis** | **W's T Shear stress (τ)** | **W's T Stream power (ω)** | **W's T Velocity** ($\bar{v}$) |
|---|---|---|---|---|---|---|---|
| | $N/m^2$ | $W/m^2$ | m/s | mm | $N/m^2$ | $W/m^2$ | m/s |
| Borvan | 380.79 | 2345.68 | 6.16 | 800 | 136 | 384.19 | 1.84 |
| Jhiri | 125.41 | 615.75 | 4.91 | 540 | 92 | 233 | 1.51 |
| Mendha | 2305.76 | 38321.7 | 16.62 | 6200 | 1054 | 5175.64 | 5.12 |
| Dhamni | 159 | 1024 | 6.46 | 400 | 68 | 159 | 1.30 |
| Panchlai | 971.854 | 10369.68 | 10.67 | 1100 | 187 | 575 | 2.20 |
| Parvas | 374.07 | 2693.35 | 7.20 | 660 | 112 | 301 | 1.66 |
| Sudhalvada | 231.525 | 1355.81 | 5.86 | 800 | 136 | 384 | 1.84 |

i-axis = intermediate axis; W's T = William's Threshold value of entrainment; See figure 4.19 for location of sites

**(ii) Froude number (Fr)**

The Fr numbers range from 0.13 (at Pendha on the Nar River) to 1.96 (at Kalmane on the Par River). Observations of Grant (1997) and Tinkler (1997a and 1997b), propose extremely frequent existence of critical flow in bedrock channels, although it is generally restricted to part of the channel. Large scale spatial variability in channel morphological features (e.g. longitudinal grooves, inner channels, etc.) reflect and control spatial variability in hydraulic forces (Tinkler and Wohl, 1998). The reach upstream of Ghatalbari knickpoint shows spatial variability in hydraulics along the bedrock channel of the Par River. This reach has undulating thalweg and shows standing waves (Fr = 1) (Figure 4.57) of water with critical waves system, which is of similar wavelength to the bed undulations. Such reaches are incised rapidly and therefore, express very localised but persistent hydraulic forces expended on the resistant boundary channels. Broken standing waves have also been observed in channel in the form of turbulent flow with foamy water (white water) and breaking wave crests near Ghatalbari (Figure 4.58). The flow may remain critical with increasing stage and velocities may stabilise without increasing, as energy is dissipated across the entire channel width (Tinkler, 1997a; Tinkler, 1997b) or depth. This is, in particular, possible to happen if the channel boundaries at high stages (water levels) are strongly confined or are especially rough (Tinkler and Wohl, 1998). The Mendha gorge on the Par River is pertinent for above situation having strongly

confined and rough gorge walls having critical Froude number (Figure 4.47; Table 4.23).

**Table 4.23** Froude numbers at cross sectional sites

| **Site** | **flow type** | | |
|---|---|---|---|
| | Fr < 1 | Fr = 1 or close to 1 | Fr > 1 |
| Parchapada | - | - | 1.03 |
| Borvan | - | 0.93 | - |
| Ghatalbari | 0.768 | - | - |
| Kalmane | - | - | 1.96 |
| Jhiri | 0.685 | - | - |
| Chachpada | - | - | 1.08 |
| Mendha | - | 0.99 | - |
| Dhamni | 0.55 | - | - |
| Nanivahial | 0.62 | - | - |
| Panchlai | - | - | 1.13 |
| Parvas | 0.61 | - | - |
| Sudhalvada | 0.745 | - | - |
| Pardi | 0.521 | - | - |
| Umbardhe | - | - | 1.06 |
| Pendha | 0.131 | - | |
| Tamchhadi | - | - | 1.05 |

Fr > 1 = Subcritical flow; Fr = 1 or close to 1 = Critical flow; Fr < 1 = Supercritical flow. See Figure 4.19 for location of sites

**Figure 4.57** Standing wave-train upstream of Ghatalbari Knickpoint; Flow direction from top to bottom; See Figure 4.19 for location of site

**Figure 4.58** Broken standing waves upstream of Ghatalbari knickpoint; Flow direction from top to bottom; See Figure 4.19 for location of site

The hydraulic analysis of Par River indicates that the Froude number greater than 1 (highly erosive supercritical flow) have been reached on several occasions (Table 4.21; Table 4.23) e.g. at Kalmane (Fr = 1.96), Panchlai (Fr = 1.13), Chachpada (Fr = 1.08), Parchapada (Fr = 1.03), Umbardhe (Fr = 1.06; on the Nar River) and Tamchhadi (Fr = 1.05; on the Nar River) (See location of sites in Figure 4.19). In addition to this, roll waves or slug flow have been generated at steep reaches of Kalmane site as the value of Froude number is 1.96 and it exceeds 1.6 (Hjalmarson and Phillips, 1997). At knickpoints of Chikadi (Figure 4.59) and Kalmane (Figure 4.60), where water flows smoothly and rapidly down the steep slope, however, at the base of the knickpoints, the depth of water increases to 10-15 m, the flows are so deep that the formation of supercritical flow is then suppressed (Baker and Costa, 1987) and subsequently supercritical flow turns into subcritical flow (Fr > 1), forming a hydraulic jump (Figure 4.59; Figure 4.60). As depths increase in the bedrock channel the flow may remain critical, become supercritical, or revert to subcritical as downsteps and smaller knickpoints begin to drown out e.g. at Chikadi knickpoint (10.40 m elevation) (Figure 4.59).

In comparison, the supercritical and critical flows are shallower, nevertheless, faster than that of subcritical flow, and enhance sediment transport of large clasts (Hopkins, 1844). Thus, the large clasts of Par River have been transported downstream, wherever, flow remain supercritical and critical e.g. at Mendha (Figure 4.61).


**Figure 4.59** Hydraulic drop and hydraulic jump at Chikadi; Note cow inside the circle for scale; See Figure 4.19 for location of reach


**Figure 4.60** Hydraulic drop and hydraulic jump at Kalmane (40 m); See Figure 4.19 for location of reach

**(iii) Reynolds Number (Re)**

High values of Reynolds number (>2100) of the Par River indicate that the flood discharges were extremely turbulent, and thus, are capable of accomplishing a variety of geomorphic activities. The deep narrow reach at Mendha (Figure 4.4; Figure 4.46; Figure 4.47; Table 4.21) produced the highest Reynolds number, and it is likely that this may be the reach of very high and intense bedrock erosion. The turbulent flow formed at constricted reach of Mendha Gorge was one of the reasons responsible for detachment and entrainment of large rock-blocks. The material removed from gorge bed and wall, have been deposited immediately downstream of gorge in the form of expansion bar, where channel instantaneously widens (Figure 4.46; Figure 4.48). A huge rock block, having 6200 mm i-axis has been detached from gorge wall and entrained up to 410 meters further downstream (Figure 4.61). Several examples of entrainment of large boulders due to excess turbulent flow and their measures have been given in Table 4.24. The erosional power of the flood flows is also evident from the presence of scablands, knickpoints (Figure 4.41; Figure 4.43; Figure 4.57; Figure 4.58), inner channels (Figure 4.37; Figure 4.38), plunge pools, and large boulder berms (Figure 4.48) on the river. The deep and narrow gorge of Kalmane (Figure 4.37) exhibit second highest Reynolds number, the highest knickpoint (26 m) (Figure 4.41) and deepest plunge pool (14 m) of the river have been observed at this site. Reynolds number also exceeds for wide and exposed bedrock channel of Par River at Parvas (Figure 4.19; Table 4.23). It is exhibited through multiple inner channels located upstream of Parvas (Figure 4.29).

**Figure 4.61** Giant boulder with 6200 mm i-axis, downstream of Mendha Gorge; See Figure 2.20 for location of site

**(iv) Critical velocity for inception of cavitation (Vc)**

Estimates of the values of critical velocity for inception of cavitation indicate that none of the powerful floods on the Par River exceed the conditions expressed by the Equation 3.13 except at deep narrow gorges of Kalmane and Mendha where inception of cavitation is possible. The critical velocities required for inception of cavitation for Kalmane and Mendha sites are 11.54 m/s and 16.12 m/s respectively. However, the actual velocities estimated for these sites are 15.70 m/s and 16.62 m/s correspondingly (Table 4.24). This, therefore, suggests that channel adjustment produced by cavitation tend to inhibit or reduce the forces that would cause the threshold to be crossed in nature (Baker and Costa, 1987).

**Table 4.24** Critical velocity for inception of cavitation (Vc)

| **Site** | **Manning's Roughness values (n)** | **Velocity ($\bar{v}$) (m/s)** | **Vc (m/s)** |
|---|---|---|---|
| Kalmane | 0.050 | 15.70 | 11.54 |
| Mendha | 0.050 | 16.62 | 16.12 |

Vc = Critical velocity for inception of cavitation; See figure 4.19 for location of sites

Intense bedrock scouring which results from cavitating flow condition is also reflected by erosional features such as flute marks, polished rock surfaces (e.g. Figure 4.62) and pot holes (Figure 4.21; Figure 4.23; Figure 4.26; Figure 4.30; Figure 4.63).

**Figure 4.62** Polished rock surface at Parvas; See Figure 4.19 for location of site

**Figure 4.63** Huge pothole with grinding tools (sand to boulders)**;** Flow direction from top to bottom; See Figure 4.19 for location of site

**(v) Hydraulic plucking**

Highly Plucked bed of the Par River has been located 9 km away from source at Parchapada (Figure 4.64). Majority of dykes in the Par River are highly dissected due to plucking, for instance dykes at Borpada (Figure 4.61) Dhamni (Figure 4.66), Panchlai (Figure 4.67) and Parvas (Figure 4.68) are noticeable. For instance, block with i-axis of 2100 mm plucked from the Borpada dyke due to 1968 flood (evidenced by eye-witness) and deposited in boulder cluster located 76 m downstream (Table 4.25). The detachment of rock-blocks and their entrainment are tabulated below.

**Table 4.25** Detachment, entrainment and deposition of blocks

| **Sr. No.** | **Location** | **Reference Figure** | **i-axis (mm)** | **Transported distance (m)** |
|---|---|---|---|---|
| 1. | Borpada (dyke) | Figure 4.65 | 1300 | 30 |
| 4. | Mendha (gorge) | Figure 4.47 | 6200 | 410 |
| 5. | Dhamni (dyke) | Figure 4.66 | 2100 | 76 |
| 6. | Parvas (dyke) | Figure 4.68 | 2000 | 11.8 |
| 7. | Parvas (dyke) | Figure 4.68 | 1300 | 21.10 |

**Figure 4.64** Highly Plucked plain bed of Par River at Parchapada; Flow direction from bottom to top; See Figure 4.19 for location of site

**Figure 4.65** Plucked dyke (63.5 m) at Borpada; Flow direction from left to right; See Figure 4.19 for location of site

**Figure 4.66** Extremely quarried dyke (20.4 m) near Dhamni; Flow direction from right to left; See Figure 4.19 for location of site

**Figure 4.67** Remnant of plucked dyke (10.6 m) at Panchlai; Flow direction from right to left; See Figure 4.19 for location of site


**Figure 4.68** The dyke (4.9 m) cutting across the Par River at Parvas. It raises high from the bed showing prominent control on the channel due to its resistance; See Figure 4.19 for location of site

**(vi) Hydraulic wedging**

The wedging process was not observed in river channel from source to mouth. However, it was possible to locate hydraulic wedging downstream of Manjarpada Knickpoint (Figure 4.43; Figure 4.69) in the upper reaches of the river. The Figure 4.69 shows two circular boulders with intermediate-axis 300 mm and 200 mm, wedged leading to development of cracks. Since the example is found immediately downstream of the Manjarpada Knick, it is likely that the clasts are emplaced forcefully by very high flow velocities.


**Figure 4.69** Wedging process leading to development of cracks at Manjarpada; See Figure 4.19 for location of site

**(vii) Knickpoint migration and river incision**

Headward migration of a knickpoint through resistant substrate can leave behind a deep and narrow gorge, it reflects the erosional resistance of the channel boundaries, and maximizes the shear stress and stream power per unit area of a given discharge and channel gradient (Baker, 1988; Wohl, 1992, 1998; 2000a; Ikeda, 1997). Similar observations have been noted for the Par River as well as its tributaries, where, deep and narrow gorges are observed immediate downstream of knickpoints (Figure 4.70; Figure 4.71; Table 4.26).

**Table 4.26** Dimensions of knickpoints and associated gorges

| Sr. No. | Site | Elevation of Knickpoint (m) | Distance from source (km) | Length of Gorge (km) | Average Width of Gorge (m) |
|---|---|---|---|---|---|
| 1 | Manjarpada | 21.0 | 2.52 | 0.65 | 13.52 |
| 2 | Chikadi | 10.4 | 19.30 | 01.64 | 66.80 |
| 3 | Ghatalbari | 8.40 | 23.38 | 3.31 | 169.12 |
| 4 | Kalmane | 40.0 | 33.64 | | |
| 5 | Kelavan (Bhimtas River) | 51.0 | 8.80 | 04.50 | 395.0 |

See Figure 4.8 location of sites

Quantitative analysis of Stream Power Erosion Model (SPEM) reveals that the incision rate of Kalmane Gorge is 6.57 x $10^{-05}$ m/yr (0.0657 mm/yr) and that of Bhimtas Gorge is 9.66 x $10^{-05}$ m/yr (0.0966 mm/yr) (Table 4.26). The above incision rate is less when compared with the range of incision rates given by Brocard et al. (2003) for mountains landscapes (i.e. 0.149 mm/yr to 0.736 mm/yr). For instance, a study of post-glacial fluvial bedrock incision in the French Western Alps reports incision rates of about 0.8 mm/yr (Brocard et al., 2003). The comparative low rate of incision of the Par River is obvious because the incision is not associated with the mountain-building tectonic processes where the rates of upliftment are comparatively faster. It is also supported by the widespread view that the western margin of India, where the Par River flows, has undergone protracted uplift and tectonic deformation from tertiary to recent times (Widdoson and Cox, 1996; Widdoson, 1997; Widdoson and Mitchell, 1999; Sheth, 2007).

**Table 4.27** Parameters of Stream Power Erosion Model (SPEM)

| River | Lithology | A ($km^2$) | S | K | m | n | Ri (m/yr) |
|---|---|---|---|---|---|---|---|
| Par | Basalt | 201.95 | 0.0068 | $7*10^{-6}$ | 0.3 | 0.7 | 6.57 x $10^{-05}$ |
| Bhimtas | Basalt | 21.830 | 0.0304 | $7*10^{-6}$ | 0.3 | 0.7 | 9.66 x $10^{-05}$ |

A = area; S = Slope; K = coefficient of erosion; m and n are constants; Ri = Rate of incision;
See Figure 1.2 for location of rivers

The plot in Figure 4.72 indicates that the width of the gorge increases proportionately away from the knickpoint. It is, further, proved from the value of $R^2$ which is 0.96. It is assumed that the knickpoint migrated for about 4.5 km upstream. The upstream migration of the knickpoint will take place in future too. It is also likely that the width of the gorge will increase in the same proportion as it shows at present by maintaining very high value of the positive correlation coefficient (r).

**Figure 4.70** Upright knickpoint (51 m) at Kelavan on river Bhimtas (tributary of Par River); See Figure 4.71 and Figure 4.82 for location of reach

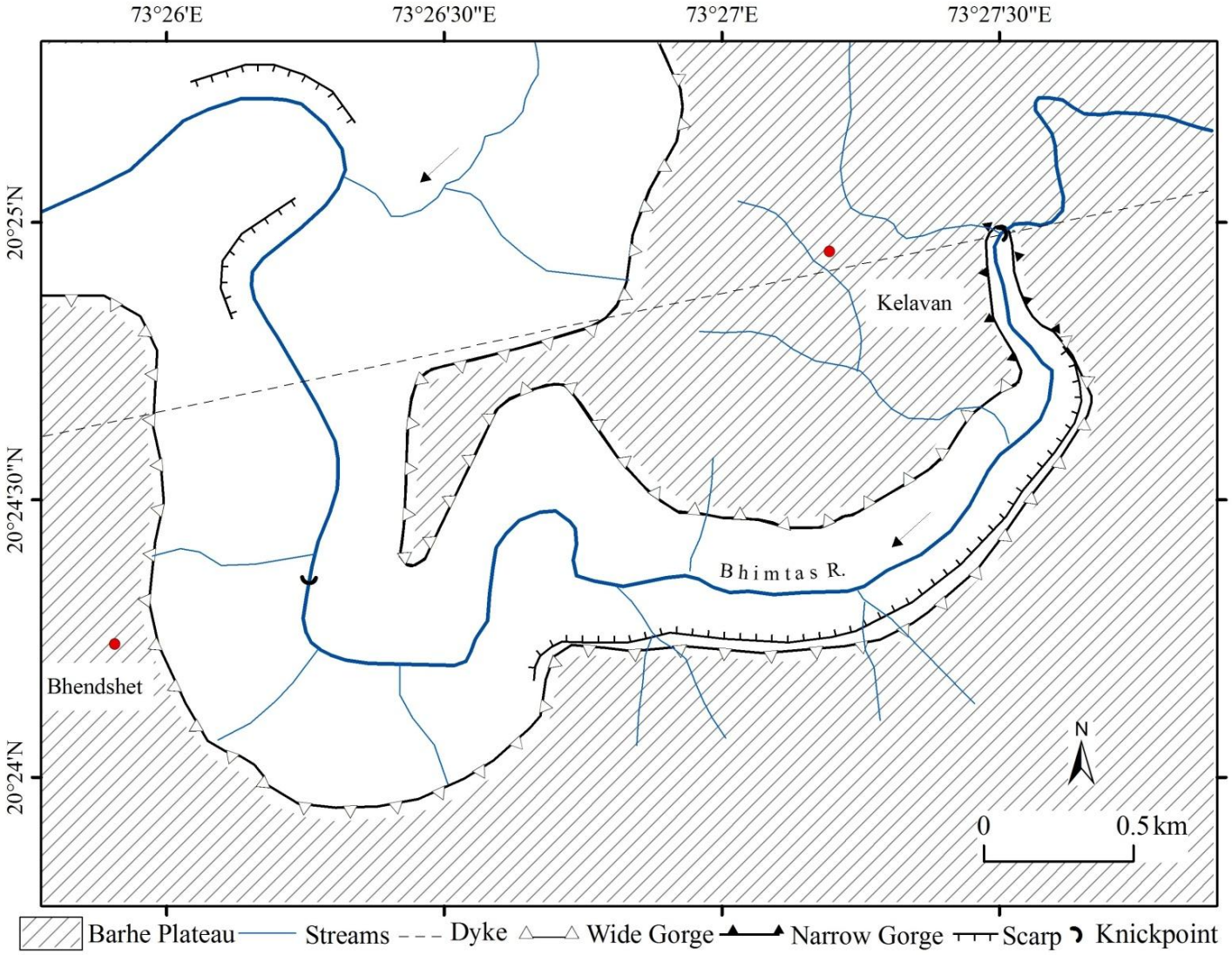


**Figure 4.71** Geomorphic map of Bhimtas Gorge; See Figure 1.2 for location of river

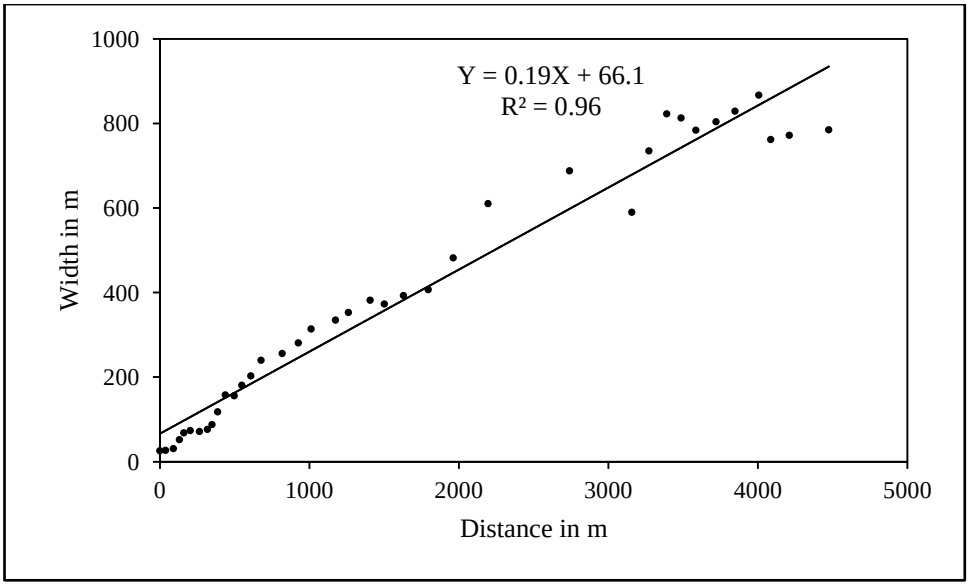


**Figure 4.72** Width(s) versus distance(s) of Bhimtas Gorge downstream of the knickpoint

### *4.3.2 Coarse sediment transport*

The minimum intermediate axis (i-axis) of a coarse sediment is 164 mm and the maximum i-axis is 6200 mm, observed immediately downstream of Mendha Gorge (Figure 4.47; Table 4.64).

**Table 4.28** Boulder dimensions

| No of Samples | Min (mm) | Max (mm) | Range |
|---|---|---|---|
| 285 | 164 | 6200 | 6036 |

The presence of large boulders along the Par River provide evidences to the competence of flows. The estimated values, when compared with the values of bed shear stress, unit stream power, and mean velocity generated by reconstructions of flows, reveal that the river flows are several orders of magnitude higher than the threshold values for the entrainment of boulders. From the calculated hydraulic data of the Par River, unit stream power and bed shear stress ranges between 616 and 52125 $W/m^2$, and 125 and 3320 $N/m^2$ respectively (Table 4.57). These values indicate unusually high ability of the river to erode and transport coarse sediment. These estimates and the hydraulic characteristics of the Par River further suggest that high flows can easily move cobbles in suspension, and large boulders as bedload. The calculated figures further propose that floods are competent enough to transport the largest ever recorded boulder present on the channel bed. According to estimated

values of flood hydraulics with respect to theoretical values, the giant boulders with 6200 mm (Figure 4.61) and 3350 mm i-axis have been transported downstream of Mendha Gorge (Figure 4.47). During 2004, discharge i.e. 35785 $m^3/s$ transported huge boulder with 1100 mm i-axis at Panchlai (Figure 4.73). In the bedrock channels, such as the Par River, the unit stream power and bed shear stress values are higher by several orders of magnitude than those that occur in the alluvial channels (Kale et al., 1994; Rajaguru et al., 1995; Baker and Kale, 1998).

**Figure 4.73** Huge transported boulder with 1100 mm i-axis at Panchlai; See Figure 4.19 for location of site

An example of collapse of a bridge across the Par River has been recorded at Dhamni. Eye-witnesses have revealed that the bridge had been damaged due to 2004 flood with the discharge of 21775 $m^3/s$. This event had produced unusually high values of bed shear stress (159 $N/m^2$) and unit stream power (1024 $W/m^2$) that has resulted into collapse of bridge and slight downstream transportation of bridge pillars with the 11900 mm X 4000 mm dimensions (Figure 4.74).

**Figure 4.74** Collapsed bridge across the Par River due to 2004 flood (21775 $m^3/s$); Note the piller with 11900 mm X 4000 mm dimensions; Flow direction from right to left

## 4.4 Role of Lithology and Tectonics

### *4.4.1 Rock mass strength of resistant boundary channel of the Par River*

As a simple tool for quick RMS assessment, Schmidt hammer has been widely used. In order to study longitudinal variability in strength of rocks, 190 N values for 12 cross sectional sites and 22 similar values for five dykes were used (Table 4.29; Table 4.31). The descriptive statistics of the values of resistance (RMS) offered by rocks in the Par River is presented in Table 4.1. With respect to above analyses, the minimum RMS is 42.18 $N/mm^2$ measured at Chikadi and greatest RMS i.e. 111.36 $N/mm^2$ measured at exposed bedrock near mouth of the Par River at Pardi. The average values of RMS range between 63.18 and 91.35 $N/mm^2$. These RMS values can be surpassed only during infrequent large magnitude floods, which occur at long intervals. According to several previous researchers, high-magnitude flows are significant to shape bedrock channels and associated erosional features as only such

flows are capable of exceeding the high boundary resistance provided by bedrock channels (Baker and Kale, 1998). The value of the coefficient of variation is 15%, which proposes less variation in the RMS of the rocks of the Par River. It further states that the formation of majority of rocks belongs to the same period. The RMS for the river under review varies spatially. Even though it does not show any specific pattern or trend in surface hardness, there is gradual increase in RMS values towards downstream direction (Figure 4.1). Selby (1993) have classified rocks into six categories on the basis of RMS values and other measures of rock strength. This classification is constructive foundation to classify rocks and to provide clear indication of a rock's character. According to classification given by Selby (1993), the rocks in association with Par River are competent igneous and comparatively strong in nature. Therefore, only high magnitude, infrequent floods are capable of making alterations in the resistant boundary channels of the Par River.

**Table 4.29** Rock Mass Strength (RMS) (in N/mm$^2$) variations between cross-sectional sites

| XS No. | XS site | No. of Samples | Mean N | Max RMS | Min RMS | Range | Mean RMS | (σ) | Cv (%) |
|---|---|---|---|---|---|---|---|---|---|
| 1 | Borvan | 25 | 49.69 | 83.06 | 60.22 | 22.84 | 68.45 | 7.12 | 10.40 |
| 2 | Chikadi | 30 | 48.73 | 92.98 | 42.18 | 50.79 | 66.92 | 16.33 | 24.40 |
| 3 | Ghatalbari | 30 | 55.20 | 60.22 | 108.65 | 48.43 | 81.61 | 14.62 | 17.92 |
| 4 | Kalmane | 30 | 55.33 | 103.32 | 73.58 | 29.74 | 81.60 | 8.45 | 10.35 |
| 5 | Mendha | 25 | 49.85 | 92.98 | 47.92 | 45.06 | 69.29 | 15.62 | 22.54 |
| 6 | Dhanmi | 25 | 59.31 | 105.97 | 80.65 | 25.33 | 91.35 | 7.85 | 8.59 |
| 7 | Nanivahial | 25 | 57.23 | 103.32 | 73.58 | 29.74 | 86.26 | 9.70 | 11.25 |
| 8 | Panchlai | 25 | 47.23 | 78.27 | 47.92 | 30.35 | 63.18 | 10.31 | 16.32 |
| 9 | Parvas | 26 | 52.29 | 92.98 | 49.89 | 43.08 | 74.72 | 13.69 | 18.32 |
| 10 | Sudhalwada | 30 | 56.33 | 105.97 | 69.01 | 36.96 | 84.07 | 9.77 | 11.63 |
| 11 | Pardi | 20 | 57.20 | 111.36 | 64.56 | 46.80 | 86.52 | 16.20 | 18.73 |
| 12 | Umbardhe | 25 | 50.54 | 85.50 | 60.22 | 25.28 | 70.42 | 8.80 | 12.49 |
| 13 | Pendha | 25 | 54.00 | 98.10 | 51.90 | 46.20 | 78.78 | 14.65 | 18.60 |
| 14 | Tamchhadi | 30 | 58.07 | 100.70 | 78.27 | 22.43 | 89.30 | 6.60 | 7.39 |
| | Minimum | | 47.23 | 60.22 | 42.18 | 22.43 | 63.18 | 6.60 | 7.39 |
| | Maximum | | 59.31 | 111.36 | 108.65 | 50.79 | 91.35 | 16.33 | 24.40 |
| | Mean | | 53.64 | 93.91 | 64.90 | 35.93 | 78.03 | 11.41 | 14.92 |

XS = cross sectional sites; N = Schmidt hammer rebound value; RMS = Rock Mass Strength; σ = Standard deviation; Cv = coefficient of variation; (See location of XS sites in Figure 4.12).

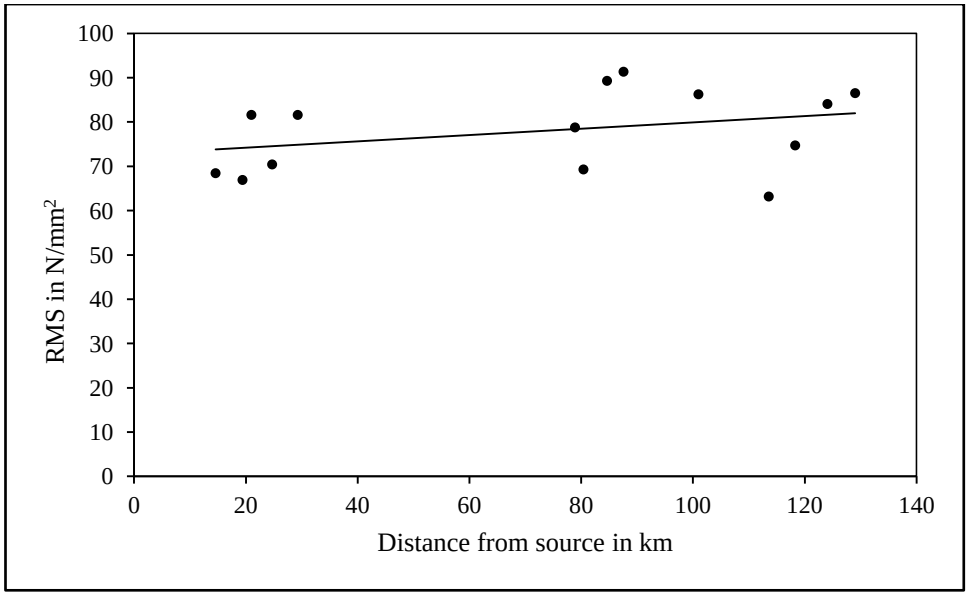


**Figure 4.75** Longitudinal variation in RMS ($N/mm^2$)

The Table 4.30 shows widths, position of dykes with respect to river and control of dykes on the path of river. The exposed width of dykes in river has been measured. It ranges between 1.5 m at Nanivahial to 63.60 m at Borpada (Figure 4.65). The orientations of dykes with regard to river channel are variable. These positions have been classified into three categories i.e. i) oblique ii) perpendicular iii) oblique to perpendicular, according to the intersection angle of dykes with river. It is been observed that only few dykes have control on the river. This situation is mainly observed at Nanivahial (Figure 4.2) and Parvas (Figure 4.68), where river has changed its path due to existence of more resistant dykes (Table 4.30). At other places dykes are extensively eroded and are in the form of outcrop in channel i.e. at Borpada (Figure 4.65), near Dhamni (Figure 4.66), at Dhamni (Figure 4.77), Makadban and Panchlai (Figure 4.67).

**Table 4.30** Dimension, position and control of dykes with regard to Par River

| Dyke. No. | Site | Width (m) | Position of dyke | Control of dyke |
|---|---|---|---|---|
| 1 | Ghatalbari | 9.00 | Oblique to river | Cut by river |
| 2 | Borpda | 63.50 | Oblique to river | Less control on river |
| 3 | Near Dhamni | 20.40 | Oblique to river | No control of dyke on river |
| 4 | Near Dhamni | 6.30 | Right angle to river | No control of dyke on river |
| 5 | Near Dhamni | 15.00 | Oblique to river | No control of dyke on river |
| 6 | Dhamni | 23.00 | Perpendicular to river | No control of dyke on river |
| 7 | Makadban | 25.20 | Parallel to channel | Outcrop in the channel |
| 8 | Makadban | 3.00 | Perpendicular to river | No control of dyke on river |
| 9 | Makadban | 30.60 | Oblique to Perpendicular | No control of dyke on river |
| 10 | Nanivahial | 21.40 | Oblique to river | Strong control of dyke on river |
| 11 | Nanivahial | 3.00 | Perpendicular to river | Control of dyke on river |
| 12 | Nanivahial | 1.50 | Oblique to Perpendicular | No control of dyke on river |
| 13 | Nanivahial | 7.00 | Oblique to river | No control of dyke on river |
| 14 | Nanivahial | 1.50 | Oblique to river | No control of dyke on river |
| 15 | Panchlai | 6.00 | Oblique to river | No control of dyke on river |
| 16 | Panchlai | 10.60 | Oblique to river | Rocky outcrop of dyke |
| 17 | Parvas | 4.20 | Oblique to Perpendicular | No control of dyke on river |
| 18 | Parvas | 6.00 | Oblique to river | No control of dyke on river |
| 19 | Parvas | 4.90 | Dyke of Y junction | Strong control of dyke on river |
| 20 | Parvas | 1.80 | Oblique to Perpendicular | No control of dyke on river |
| 21 | Parvas | 4.60 | Oblique to river | No control of dyke on river |
| 22 | Parvas | 6.40 | Parallel to river | No control of dyke on river |
| 23 | Parvas | 5.30 | Oblique to Perpendicular | No control of dyke on river |
| 24 | Parvas | 3.60 | Oblique to Perpendicular | No control of dyke on river |
| 25 | Parvas | 6.90 | Oblique to Perpendicular | No control of dyke on river |
| 26 | Parvas | 4.80 | Oblique to Perpendicular | No control of dyke on river |
| 27 | Parvas | 7.30 | Oblique to Perpendicular | No control of dyke on river |
| 28 | Parvas | 2.00 | Oblique to Perpendicular | No control of dyke on river |
| 29 | Parvas | 2.80 | Oblique to Perpendicular | No control of dyke on river |
| 30 | Parvas | 11.00 | Perpendicular to river | No control of dyke, New dyke |
| 31 | Parvas | 7.30 | Perpendicular to river | No control of dyke, old dyke |

See locations of sites in Figure 4.19

**Figure 4.76** Resistant dyke (21.4 m) at Nanivahial; Flow direction from right to left; See Figure 4.19 for location of site

**Figure 4.77** Extensively eroded dyke (23 m) in the form of outcrop at Dhamni; Flow direction from right to left; See Figure 4.19 for location of site

In order to find out control of dykes on the river, RMS values of dykes were derived. According to analysis, minimum RMS of dykes is 66.77 N/mm$^2$ and maximum RMS is 111.36 N/mm$^2$. The average RMS of dykes is 92.72 N/mm$^2$ (Table 4.31), it is greatest than that of other rocks in the river (i.e. 78.03 N/mm$^2$) mainly due to hardness of dykes in nature (Aydin and Basu, 2005). The value of the coefficient of variation (10.75%) suggests that there is very less variation in the RMS of dykes of the Par River. It further reveals that the formation of majority of dykes belongs to the same period. However, it is pertinent to mention here that the observations are based on limited number of dykes.

**Table 4.31** Rock mass strength (RMS in N/mm$^2$) for dykes

| Samples | Mean N | Max RMS | Min RMS | Range | Mean RMS | (σ) | Cv(%) |
|---|---|---|---|---|---|---|---|
| 22.00 | 59.82 | 111.36 | 66.77 | 44.59 | 92.72 | 9.97 | 10.75 |

**(i) Differences in erodibility between basalt and dykes**

It is assumed that Schmidt hammer numbers are proportional to the tensile strength, higher Schmidt hammer rebound values (N) will indicate less erodible bedrock. Therefore, an attempt has been made to find out differences in erodibility semi-quantitatively between basalt and dykes using box-whisker plots (Figure 4.78; Figure 4.79). Box-whisker plots show median value as solid line, the plus sign indicates the mean, the box ends show as 1$^{st}$ and 3$^{rd}$ quartiles and, whiskers are extending 1.5 times of the interquartile range, the points outside whiskers are outliers. The Figure 4.78 (A and B) and Figure 4.79 (A and B) indicate that there are differences in rock erodibility between basalt and dykes. It is clear from the figures that the basalt rock is comparatively weaker than dykes in terms of N and RMS. Based on the previous assumption that N and RMS measures are inversely related to erosional resistance. The results of this analysis support the hypothesis that the differences in rock erodibility are present. It is further proved by control of dykes on the channel of the Par River at few locations e.g. at Nanivahial (Figure 4.76) and Parvas (Figure 4.68). However, more detailed studies and more number of samples are necessary to strengthen the said hypothesis.

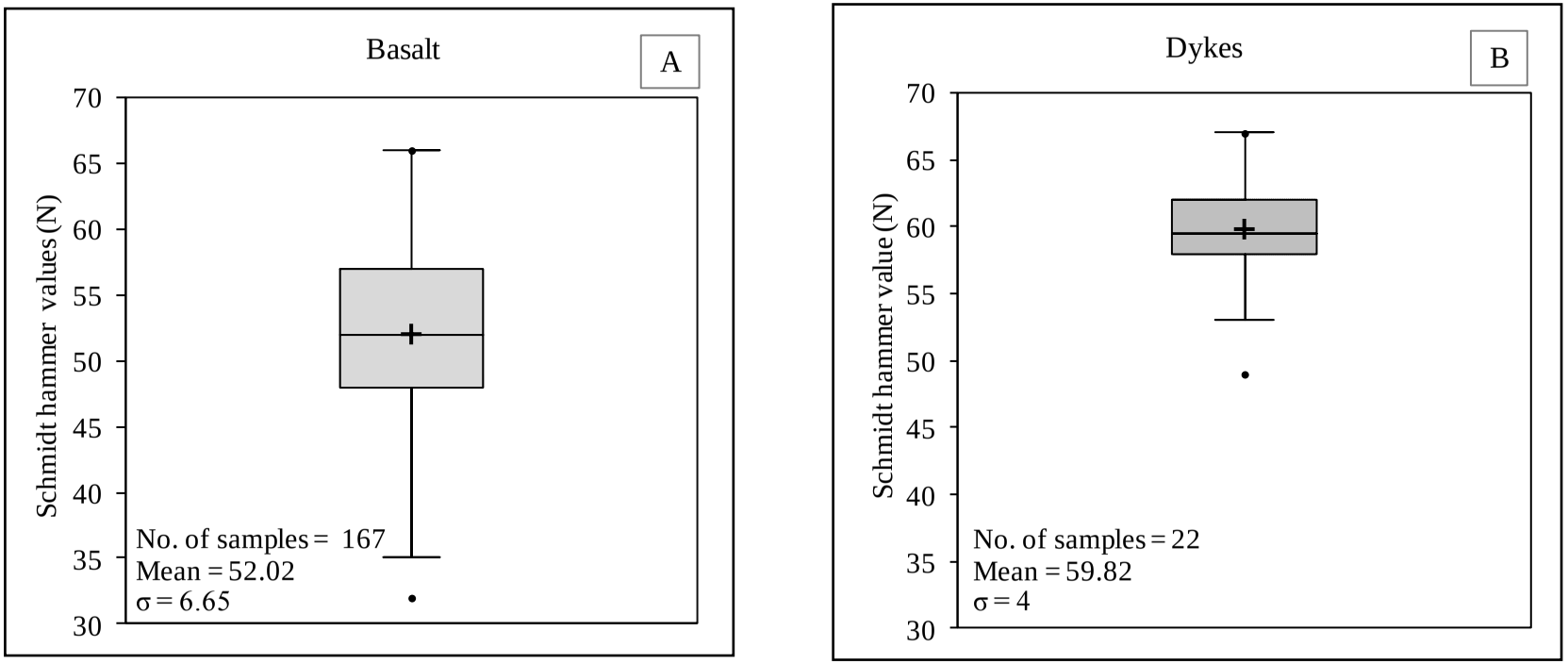


**Figure 4.78** Comparison of substrate resistance between basalt and dykes (Schmidt hammer values)

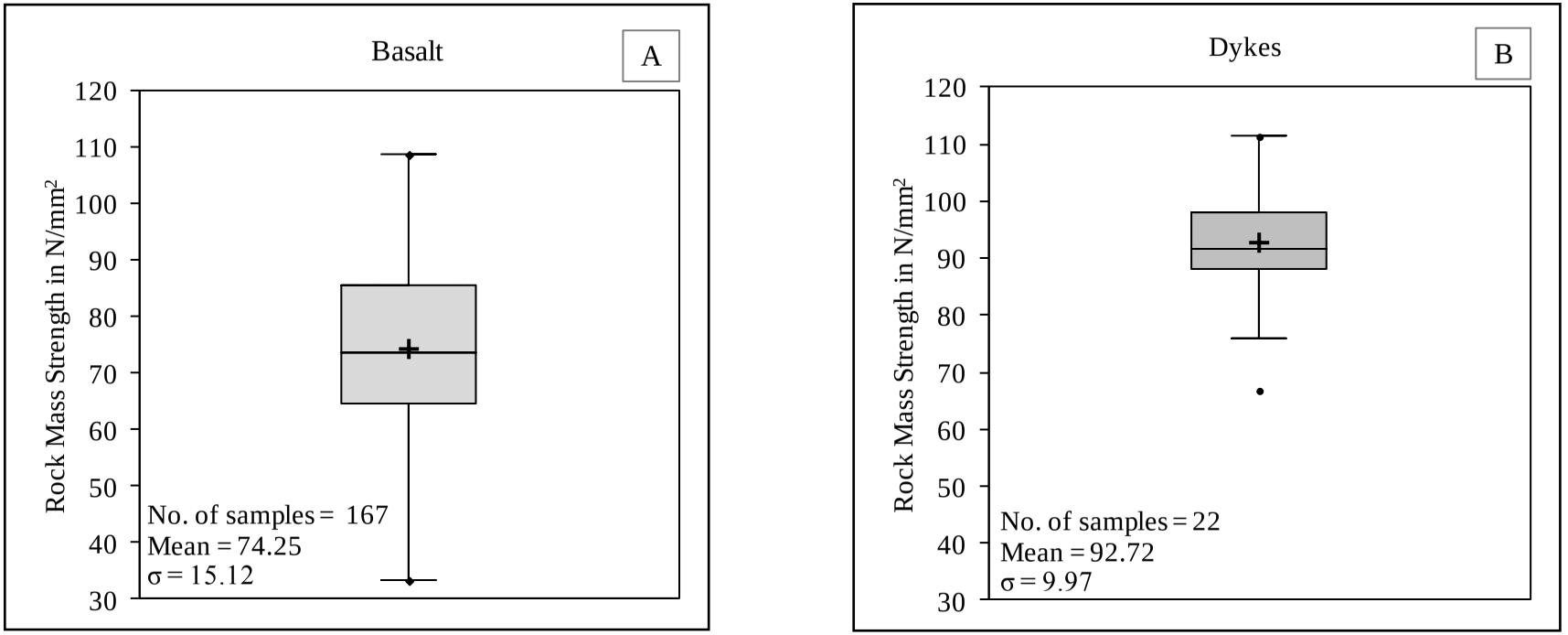


**Figure 4.79** Comparison of substrate resistance between basalt and dykes (Rock Mass Strength)

### *4.4.2 Geomorphic Indices of Active Tectonics (GAT) in morphotectonic analysis*

The results of the analysis of the geomorphic indices of active tectonics (GAT) are presented in Table 4.32. The results of the geomorphometric analysis reveal that GAT values are not very far from the values typically associated with drainage basins affected by active tectonics and deformation.

**Table 4.32** Results of geomorphic indices of active tectonics (GAT)

| Sr. No. | Index | Values | Mean | Max | Min |
|---|---|---|---|---|---|
| 1 | Hypsometric Integral (HI) | 0.30 | - | - | - |
| 2 | Valley width-height Ratio (Vf) | - | 1.18 | 2.08 | 0.44 |
| 3 | Asymmetry Factor (AF) | 60.75 % | - | - | - |
| 4 | Stream Length-Gradient Index (SL) | - | 198.14 | 795.68 | 30 |
| 5 | Basin elongation ratio (Re) | 0.49 | - | - | - |

**(i) Geomorphic indices of active tectonics (GAT)**

**a. Hypsometric integral (HI) and hypsometric curve (HC)**

The hypsometric integral value for the Par River is 0.30 (Table 4.32) which is relatively high. Kale and Shejwalkar (2008) have calculated hypsometric integral values based on ca. 90-m resolution SRTM (Shuttle Radar Topography Mission) data for adjacent river basins, including the Par Basin, namely Damanganga, Auranga, Purna, and Ambica, their calculated values are also relatively higher. The hypsometric curve of the Par Basin (Figure 4.80) is little convex-up indicating that the basin is moderately eroded.

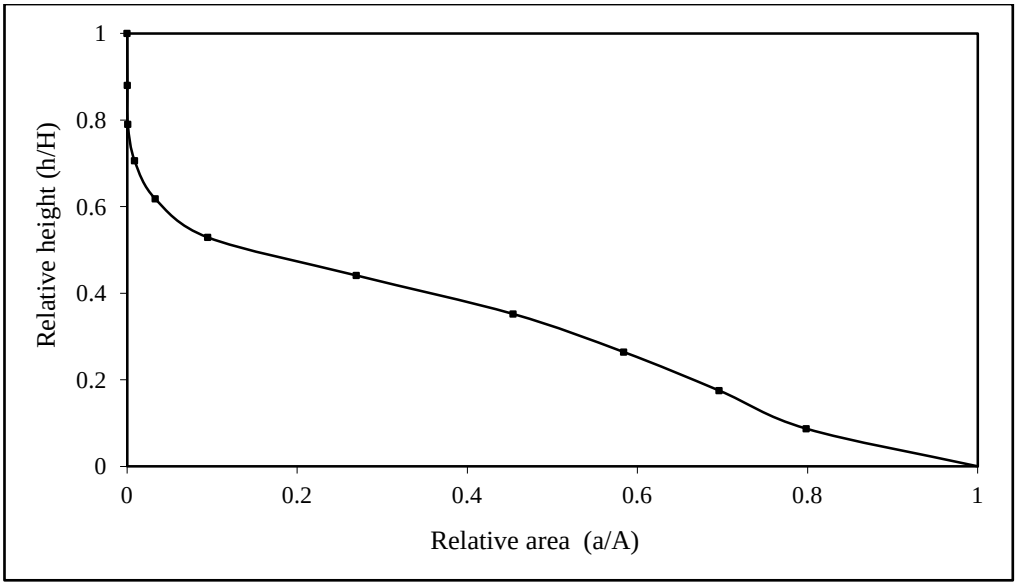


**Figure 4.80** Hypsometric curve of the Par River

**b. Valley width-height ratio (Vf)**

For the Par River, the necessary valley width and height data were obtained along 16 valley cross-sections perpendicular to the drainage basin axis, approximately up to 83 km from the source of the Par River. The average of 16 valley cross-sections was then taken as the representative of the Par Basin which is 1.18. Although the value is not less than 1.0 (Table 4.32), it reveals that Par River valley is relatively narrower and demonstrates down cutting. This further shows that the basin is experiencing certain uplift.

**c. Basin asymmetry factor (AF)**

The Par River has more basin area to the downstream right of the trunk stream (AF = 61%) (Figure 4.81; Table 4.32). Since AF is more than 50, there is tilting perpendicular to the direction of the master stream. Af is significantly greater or smaller than 50 can be attributed to active tectonics or strong lithologic control (Dehbozorgi et al., 2010).

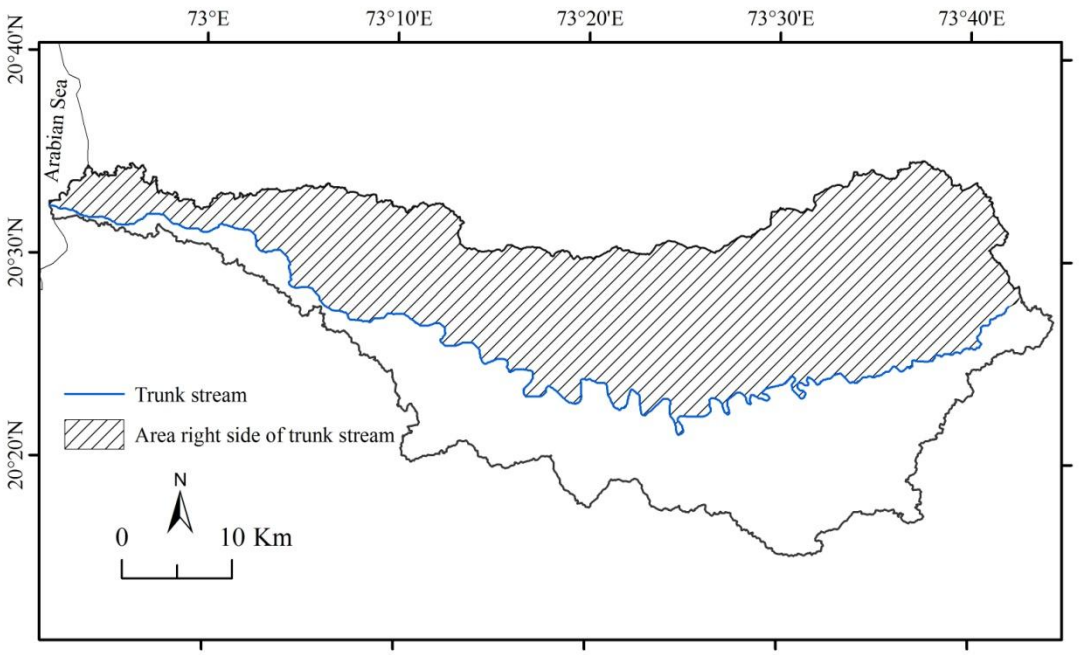


**Figure 4.81** Tectonic tilting of the Par Bain, 61% area of basin is right side to trunk stream

**d. Stream gradient-length ratio (SL)**

The average stream length-gradient index value for the Par River is 198 (Table 4.32). Nonetheless, several reaches show SL values that trend away from average value, reaching positive anomalies with the highest values up to 800. These data show that there are reaches along the channel that can be identified as the knickpoints. Such knickpoints are identified in the field and mapped (Figure 4.82). The average SL index value of the Par River is significantly higher than the average SL index values calculated by Kale and Shejwalkar (2008) for the Konkan and the Upland rivers of the western DBP, suggesting relatively high tectonic activity.

**e. Basin elongation ratio (Re)**

The elongation ratio of the Par River Basin is 0.49 suggesting that the basin is moderately elongated. This, in turn, suggests that the basin is undergoing tectonic uplift.

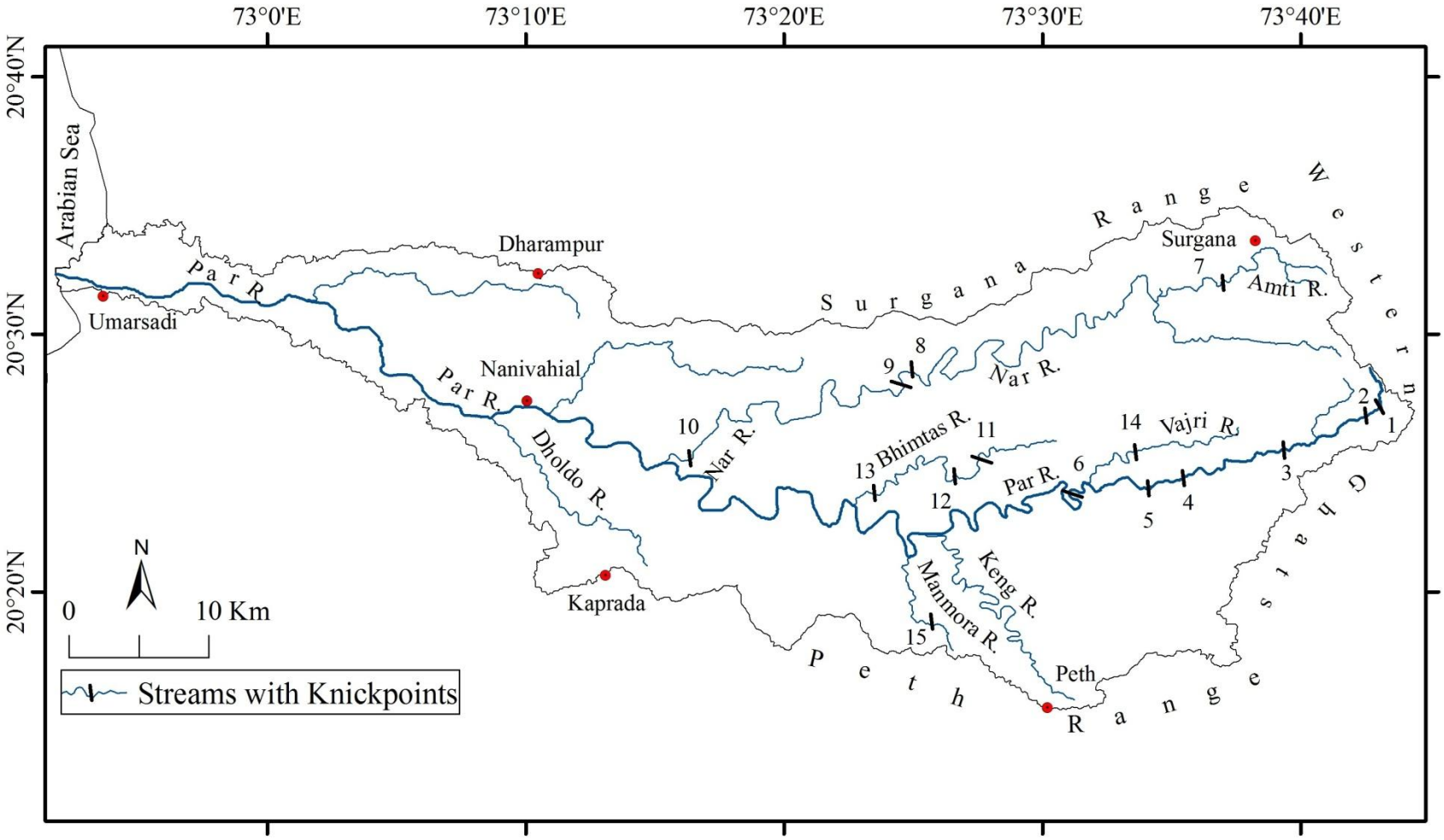


**Figure 4.82** Par Bain; Knickpoints: 1 Dongrale; 2 Manjarpada; 3 Parchapada; 4 Chikadi; 5 Ghatalbari; 6 Kalmane (Par R.); 7 Shirada (Amti R.); 8 Ranpada; 9 Chiknalpada; 10 Tamchhadi (Nar R.); 11 Kelavan; 12 Bhendshet; 13 Bhutran (Bhimtas R.); 14 Haste (Vajri R.); 15 Nalshet (Manmora Nala)

**(ii) Supporting field evidences and its interpretation**

One of the geomorphic facts evident in the field is that the river valleys in the upper and middle Par Basin are remarkably deep. Their V-shaped appearance suggests that this part of the basin is undergoing tectonic uplift. It is pertinent to mention here that the development of such narrow, V-shaped valleys (Average Vf = 1.18) are the results of the regional base which has been disturbed for a short period of time due to tectonic instability. In addition to this, many workers have postulated that the DBP was experiencing continuous and protracted uplift during Neogene and Quaternary period (Kale and Shejwalkar, 2008). Therefore, formation of such narrow, deep, V-shaped valleys are possible. It is, therefore, rational to propose that the Par Basin is undergoing tectonic uplift.

Inspection of the topographical maps, satellite images and DEM (Figure 1.1) would clearly demonstrate that the valleys carved by the Par River and its tributaries are subjected to tectonic activity. Deeply incised bedrock meanders (e.g. Figure 4.7) and a series of knickpoints (e.g. Figure 2.24; Figure 4.41; Figure 4.43; Figure 4.82) at the gorge head occur in the Par River and its tributaries. Incised or entrenched meanders and knickpoints are common phenomena in uplifted plateaux around the world and therefore, these features are considered as markers of regional or tectonic uplift (Matmon et al., 1999). The presence of these spectacular features can be accepted with sign of deeply incised bedrock channels. Logical explanation for such incised meanders and knickpoints is tectonic uplift. It is pertinent to mention here that the southern limit of the bedrock-meander-dominant area coincides with the Kurduwadi or Ghod lineament, a major regional structural feature of the DBP (Powar and Patil, 1980). The bedrock-meander-dominant Par River also lies to the north of this lineament. However, the river in its middle and lower reaches are also featured by Quaternary deposits (e.g. at Nanivahial near Dharampur).

The Par River and its tributaries are featured by knickpoints, scablands, inner channels, waterfalls and potholes at several locations. Fifteen major knickpoints in the Par Basin have been identified i.e. at Manjarpada (21 m) (Figure 4.43), Parchapada (6 m), Chikadi (10.4 m) (Figure 4.59), Ghatalbari (8.4 m) (Figure 4.23), Kalmane (41 m) (Figure 4.40; Figure 4.60) on Par River, near Shirada on Amti River, near Ranpada (5 m), Chiknalpada (10 m), Tamchhadi on Nar River, near Kelavan (50 m) (Figure

4.70), Bhendshet (10 m), Bhutran (6 m) on Bhimtas River, near Haste on Vajri R, and near Nalshet on Manmora Nala (Figure 4.82). Since waterfalls are normally associated with gorge-heads, it could be inferred that the knickpoints are migrating in upstream direction. Such prominent knickpoints (Figure 4.82) in the longitudinal profiles have been generally connected with geological or structural control or zones of uplift. However, while establishing a relation between knickpoints and faults/lineaments or lithology, one fact that is often overlooked that the breaks or knicks rapidly migrate upstream from the point of origin. Thus, the fundamental reason of knickpoint formation in most cases may often lie several hundred meters or tens of kilometers downstream and not in the vicinity of the existing inflection point (Kale and Shejwalkar, 2008 and references therein).

The inner channels are observed at Mangdhe (Figure 4.36), Shingharpada (Figure 4.37), Chikadi (Figure 4.44), Ghatalbari (Figure 4.22), Mohankavchali (Figure 4.38 and Figure 4.39), Nanivahial (Figure 4.34) and Parvas (Figure 4.29) on the Par River. Diverse potholes sites from source to around 120 km of the Par River have been identified, measured and mapped (refer chapter 2$^{nd}$ for in detail information).

Finally, the geomorphometric indices, which form the basis of the present study, are only reconnaissance tools that are used to assess the relationship between tectonics and basin morphology. Interpretation of geomorphic indices of active tectonics for the Par River along with other field geomorphic evidences provide a very good support to the widespread view that the western margin of India has undergone protracted uplift and tectonic deformation from Tertiary to recent times (Widdowson and Cox, 1996; Widdowson, 1997; Widdowson and Mitchell, 1999; Sheth, 2007). It is, therefore, evident that the Par Basin has indeed undergone significant uplift till recent times and the consequences of the tectonic activity have left noticeable imprints on the river basin under review.

## 4.5 Flood Hydrometeorology, Hydrology and Geomorphology

### *4.5.1 Flood hydrometeorology*

**(i) Rainfall regime characteristics**

The Par Basin is located in an environment typical of monsoonal tropics, with periodic high-magnitude rainfall. The monsoon rainfall is variable, both spatially as well as temporally. The spatial variation in the monsoon rainfall shows interplay of meteorology and topography characteristics. Figure 1.3 reveals the spatial variation of average annual rainfall and Figure 4.84 shows rainfall characteristics for five raingauge stations in the Par Basin. The grounds behind spatial variation are;

- The Par River and its tributaries originate in the highlands of Western Ghats. The orographic lifting of the central highlands i.e. Barhe Plateau and the Western Ghats (Figure 1.1) are responsible for enhancing the spatial variation in monsoon rainfall.
- Geographical location, orographic effect of Barhe Plateau (interflew of Par and its major tributary Nar) and the east-west trending ranges in the Par Basin, for instance, Peth Range, Surgana Range and other interfluves act as barrier for the rain bearing south-west monsoon clouds. It attributes to maximum amount of rainfall in the middle reaches of Par River (2200 mm to 2300 mm).
- Average relief of the adjacent Damanganga Basin appears to be less than that of Par Basin. Therefore, monsoon clouds easily enter in the basin and due to obstacle in the form of Peth Range orographic lifting takes place near Mandava (Figure 4.83). The above situation results into maximum amount of rainfall at Mandava (2400 mm).
- Being distant from coast, the amount of rainfall reduces towards the source of the Par and Nar Rivers. It ranges between 1700 mm and 1800 mm. However, due to proximity of coast the amount of rainfall is more at the western part of the basin (2000 mm to 2200 mm).

More than 98% of the annual rainfall is recorded during the monsoon season (Table 4.33). The average annual rainfall of the basin ranges from about 1800 mm to 2200 mm rainfall with the basin average annual rainfall 2094 mm (Table 4.38).

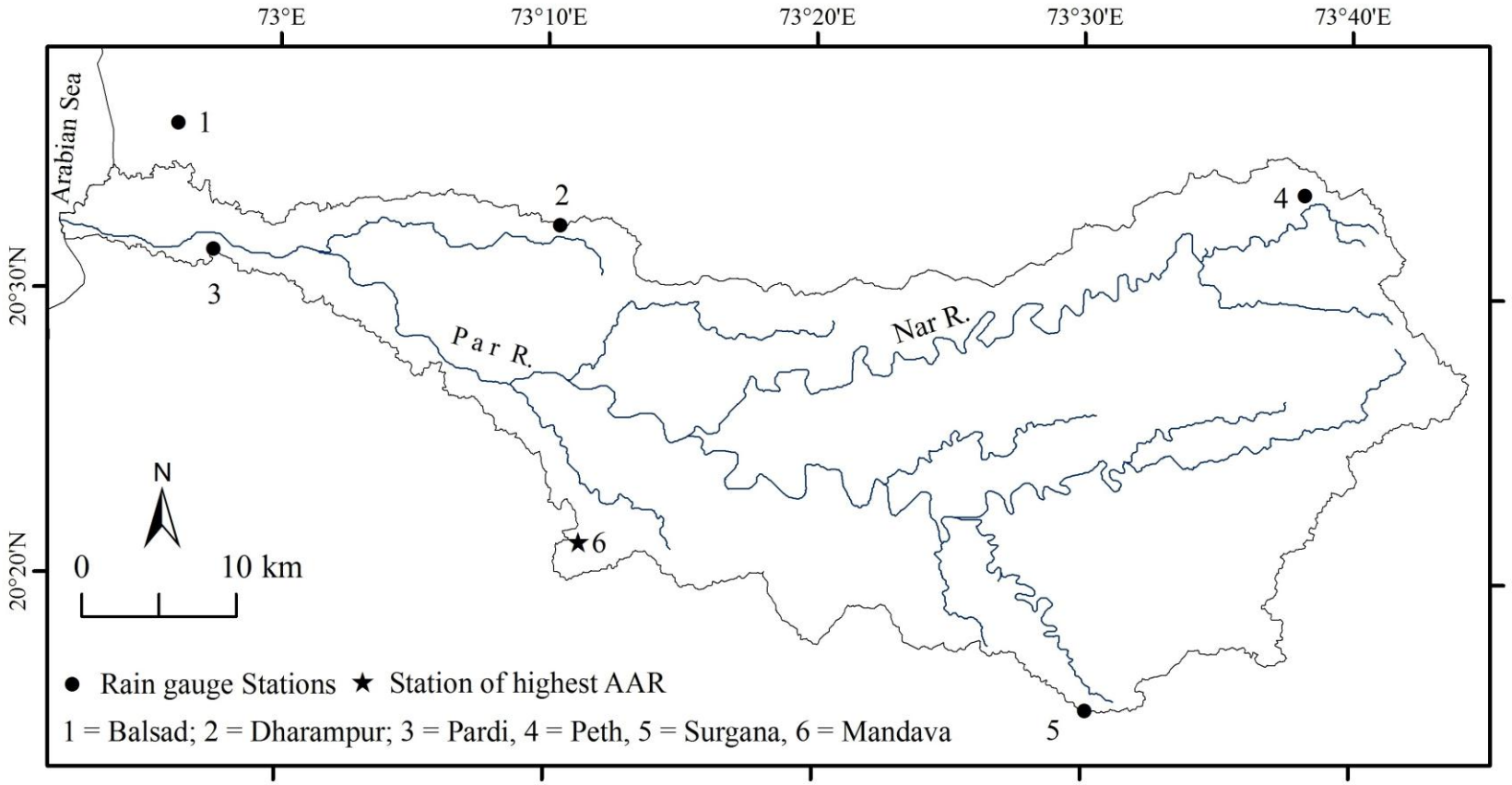


**Figure 4.83** Rain gauge stations in Par Basin

**a. Spatial and annual variability**

The annual variation in rainfall at the five sites given in Figure 4.34 indicates wide range in seasonal rainfall distribution. The southwest monsoon months account for a large proportion of the mean annual rainfall, roughly 97% to 99% occur in the monsoon months (Table 4.33). Generally, the basin receives monsoon rains from mid-June with the onset of southwest monsoon. July is the rainiest month throughout the basin followed by August (Figure 4.34) and they account for 39% and 27% the total annual rainfall of the basin respectively. The monthly rainfall totals also vary during the monsoon season. For example, at Surgana (near source of the Par River), about 67% of the rain falls in the months of July and August (Figure. 4.84; Table 4.33). On the other hand, Dharampur station, located in the lower basin, receives about 69% during the same period, however, the rainfall is, more or less well distributed in the four months (June to September) of the monsoon season (Figure. 4.84; Table 4.33).

**Table 4.33** Rainfall characteristics at selected stations in the Par Basin (Monthly and annual averages in mm)

| **Water year** | **Balsad** | **Dharampur** | **Pardi** | **Peth** | **Surgana** |
|---|---|---|---|---|---|
| June | 371.99 | 325.81 | 342.02 | 274.14 | 245.87 |
| July | 736.16 | 949.83 | 763.96 | 865.46 | 725.62 |
| August | 460.24 | 647.66 | 481.05 | 656.43 | 589.00 |
| September | 272.12 | 352.19 | 288.75 | 335.73 | 303.11 |
| October | 44.53 | 57.34 | 42.15 | 74.79 | 74.88 |
| November | 11.83 | 12.46 | 10.54 | 17.71 | 22.16 |
| December | 1.40 | 4.41 | 13.93 | 4.48 | 4.96 |
| January | 1.57 | 2.38 | 2.40 | 1.69 | 0.47 |
| February | 1.45 | 7.58 | 1.05 | 1.13 | 0.44 |
| March | 0.91 | 10.35 | 0.74 | 0.30 | 0.39 |
| April | 1.39 | 5.14 | 1.84 | 2.78 | 1.80 |
| May | 5.99 | 11.06 | 6.25 | 14.19 | 10.70 |
| AAR | 1910 | 2386 | 1955 | 2248 | 1972 |
| MR | 1885.04 | 2332.83 | 1917.93 | 2206.55 | 1931 |
| NMR | 24.55 | 53.37 | 36.75 | 42.29 | 40.93 |
| % Monsoon rainfall (Jun-Oct) | 98.71 | 97.76 | 98.12 | 98.12 | 97.92 |
| % Non-monsoon rainfall (Nov-Dec) | 1.29 | 2.24 | 1.88 | 1.88 | 2.08 |

Data source: IMD; Based on 50-130 years of record; AAR = Average annual rainfall; MR = Monsoonal rainfall; NMR = Non-monsoonal rainfall; See Figure 4.85 for location of stations

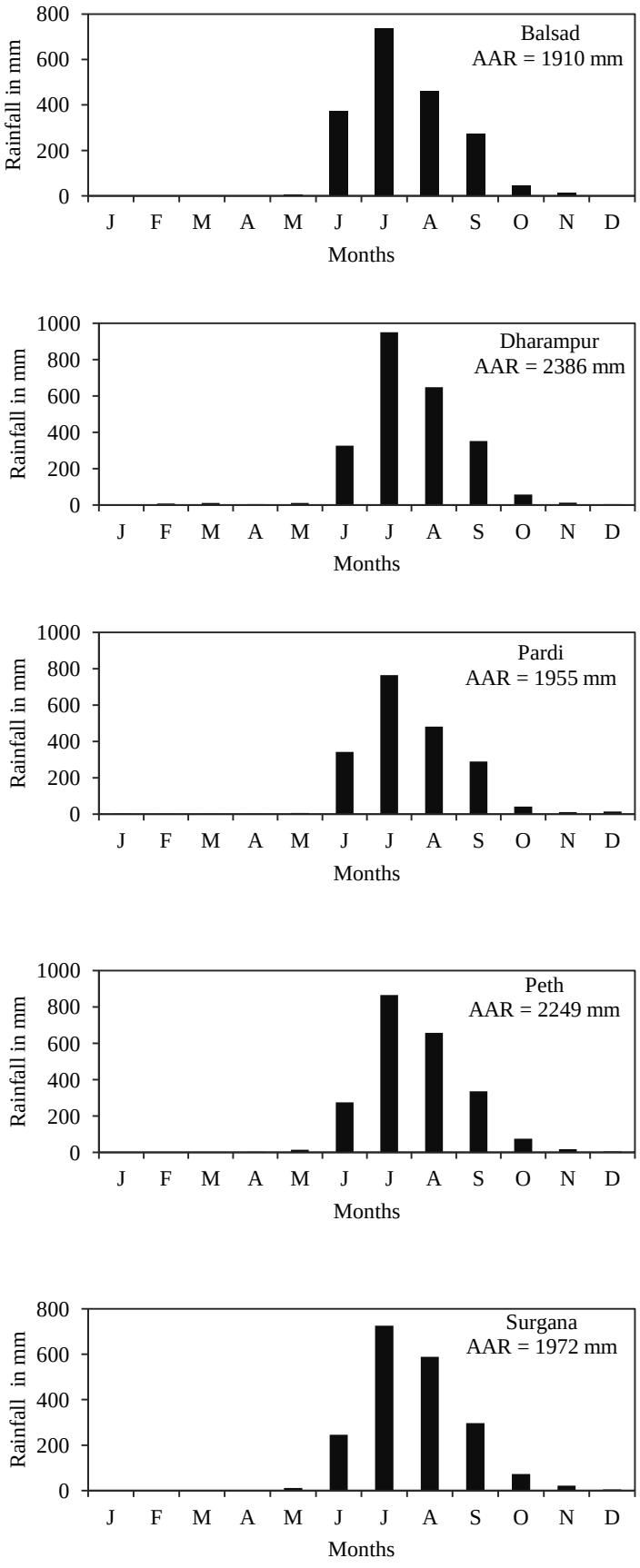


**Figure 4.84** Average annual rainfall (AAR) of five stations in the Par Basin

**b. Interannual variability**

Like other parts of the monsoon tropics, there is variability in the annual as well as monsoon rainfall between years. This variability increases, in general, with the distance from the source and the basin outlet. With climatic variability in such a region there is inevitably drought or flood. Table 4.34 lists details of the five stations with long-duration rainfall records. Mean annual rainfall increases towards the middle of the Par Basin, and ranges from 1910 mm at Balsad to 2386 mm at Dharampur. Interannual variability is not particularly high, which is proved by the less coefficient of variation (Cv) (27-33 %) of annual rainfall in most parts of the Par Basin. All the sites show very high range of annual rainfall (Table 4.34). For instance, the minimum annual rainfall recorded at the Peth station was 451 mm for the year 1982, and the maximum annual rainfall was 5470 mm for the year 1977. The values of the coefficient of skewness ($C_s$) are positive for all the sites, ranging between 0.55 and 1.08. The Pardi site reveals relatively high positive $C_s$ value. The positive $C_s$ values suggest the occurrence of a few very wet years during the gauged period. Since skewness values for the study area have been determined on the basis of more than 100 years of data, they are all statistically significant (Viessman and Lewis, 2003).

**Table 4.34** Annual rainfall characteristics at selected stations in the Par Basin (between 1901 and 2004)

| Site | Record length in years | Rmax mm (year) | Rmin mm (year) | AAR mm | σ | Cv | $C_s$ |
|---|---|---|---|---|---|---|---|
| Balsad | 103 | 3955 (1954) | 744 (1905) | 1910 | 601 | 0.31 | 0.55 |
| Dharampur | 103 | 5470 (1977) | 693 (1974) | 2386 | 778 | 0.33 | 0.87 |
| Pardi | 103 | 4376 (1963) | 916 (1911) | 1955 | 565 | 0.28 | 1.08 |
| Peth | 104 | 4673(1931) | 451 (1982) | 2248 | 608 | 0.27 | 0.75 |
| Surgana | 050 | 3440 (1981) | 1110(2000) | 1972 | 552 | 0.28 | 0.79 |

Data source: IMD; Based on 50-104 years of record; Rmax = Maximum annual rainfall; Rmin = Minimum annual rainfall; AAR = Average Annual Rainfall; σ = Standard deviation; Cv = Coefficient of variation; **$C_S$ =** Coefficient of skewness; See Figure 4.83 for location of sites

The time series of annual rainfall for five sites are illustrated in the Figure 4.85 to 4.89. The figures reveal noteworthy interannual variability in the rainfall totals. The annual rainfall series includes two discrete periods when rainfall anomalies of a particular type were most consistent. There exist two types of rainfall anomalies particularly negative rainfall anomaly (i.e. annual rainfall below the mean annual rainfall) and the positive anomaly (i.e. annual rainfall above the mean annual rainfall) (Figure 4.85 to Figure 4.89).

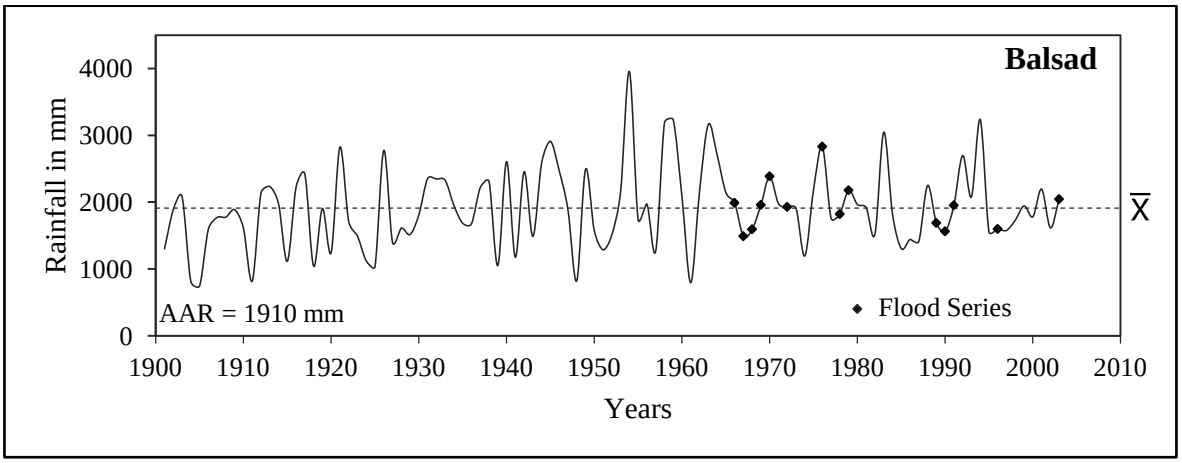


**Figure 4.85** Interannual variability of Station Balsad; See the location of station in Figure 4.83

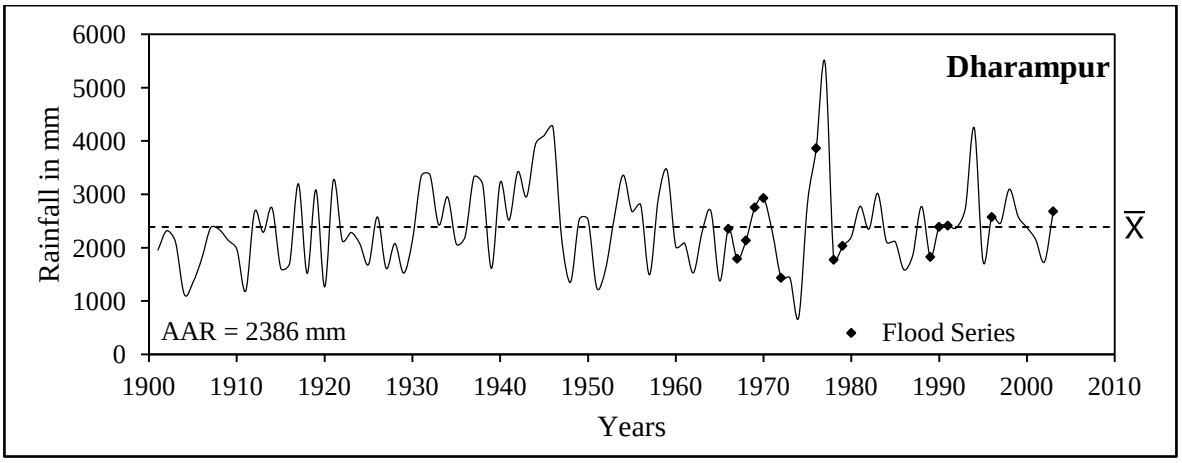


**Figure 4.86** Interannual variability of Station Dharampur; See the location of station in Figure 4.83

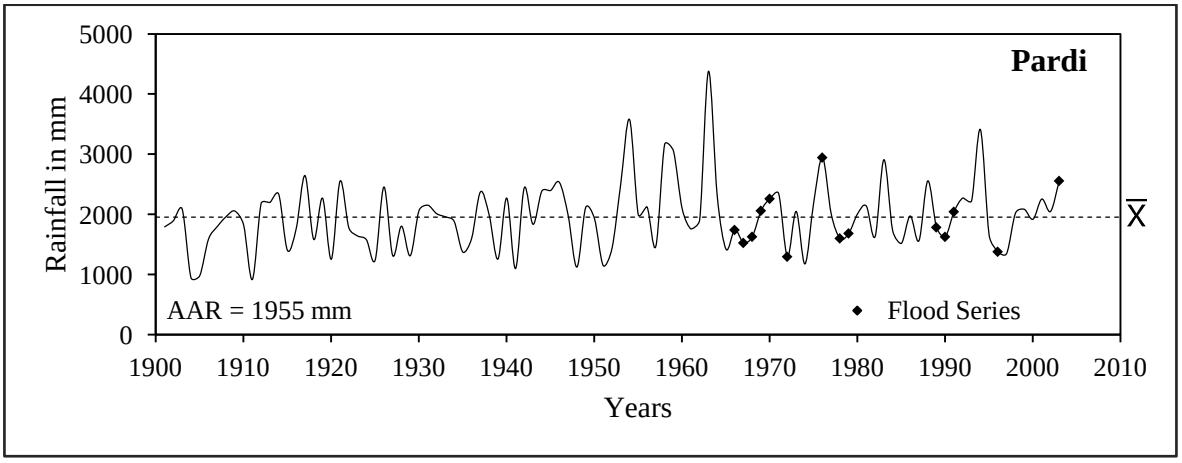


**Figure 4.87** Interannual variability of Station Pardi; See the location of station in Figure 4.83

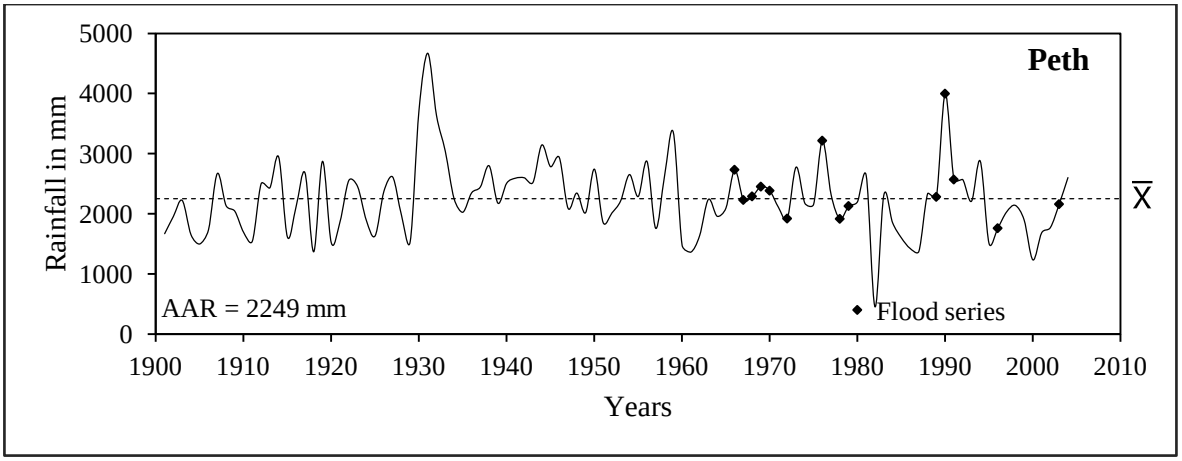


**Figure 4.88** Interannual variability of Station Peth; See the location of station in Figure 4.83

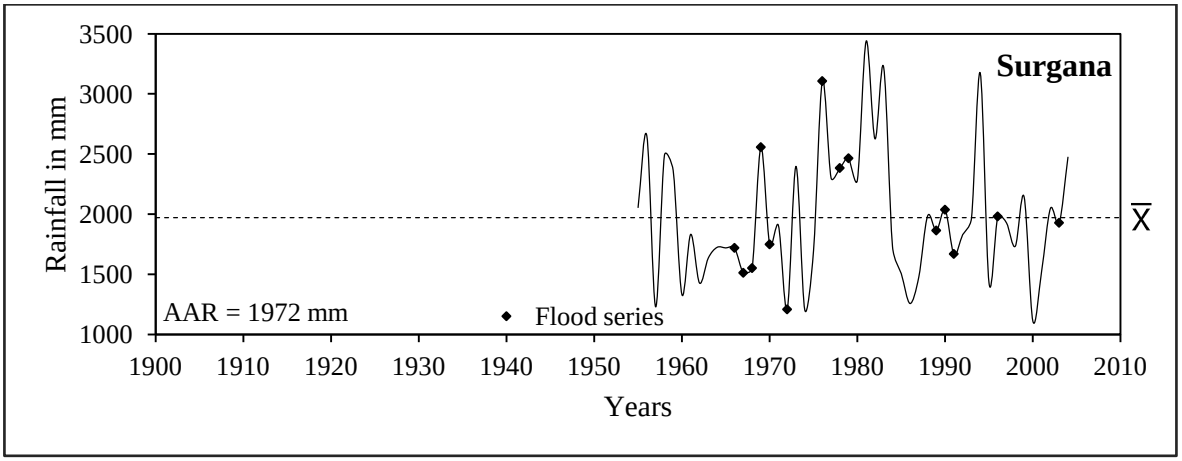


**Figure 4.89** Interannual variability of Station Surgana; See the location of station in Figure 4.83

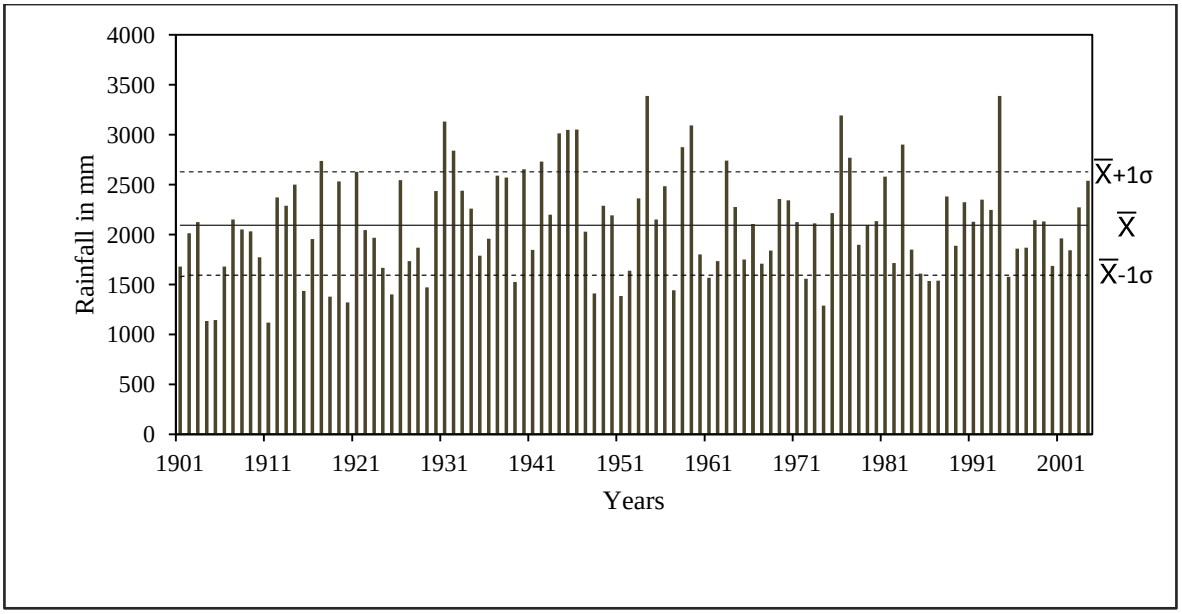


**Figure 4.90** Interannual variability for the Par Basin (from 1901 to 2004)

Examination of the Figure 4.90 indicates that, prior to 1930, the rainfall was frequently below-average, but the interannual variability was low. On the other hand, from 1930 to 2004, many years recorded above-average annual rainfall, but the interannual variability was high. Interestingly, this period of high interannual variability was characterized by increased large floods on the Par River. Summarizing it can be said that the Par Basin displays a marked concentration of rainfall within a few months of the year, episodic high-magnitude rainfalls and high intra-annual as well as inter-annual variability in rainfall. It is such events that are important from the point of view of floods. Thus, in the following section the synoptic and rainfall conditions associated with floods and large floods are discussed.

**(ii) Flood-generating meteorological conditions**

The Par Basin lies in the western part of India and within the classical monsoon region. It is in vicinity of one of two major severe rainstorm zones of India. Therefore, the principal cause of large floods on the Par River is severe rainstorms or Low Pressure System (LPS). Table 4.35 gives the important meteorological conditions associated with the large modern floods on the Par River.

**Table 4.35** Synoptic conditions associated with major floods on the Par River

| Month, date and year of flood | Annual rainfall of the basin mm | Monsoon rainfall of the basin mm | Associated LPS[1] | El Niño or La Niña year | Remark |
|---|---|---|---|---|---|
| September 6, 1966 | 2106.8 (+0.60%) | 2098.6 (+2.14%) | Bay Depression | - | Passed close to the source area |
| July 28, 1967 | 1709.5 (-18.37%) | 1677.2 (-18.37%) | Bay Depression | Weak La Niña | Path parallel to the Basin |
| August 6, 1968 | 1839 (-12.19%) | 1823.5 (-11.25%) | Bay Depression | Weak El Niño | Path parallel to the Basin |
| September 9, 1969 | 2355.9 (+12.49) | 2337.2 (+13.75%) | Bay Depression | Weak El Niño | Passed close to the source area |
| September 6, 1970 | 2341.6 (+11.81%) | 2329.6 (+13.38%) | Bay Depression | Moderate La Niño | Path parallel to the Basin |
| August 20, 1972 | 1557.2 (-25.65%) | 1552.3 (-24.45%) | Bay Depression | Strong El Niño | Passed close to the basin |
| July 31, 1976 | 3192.5 (+52.44%) | 3139.4 (+52.80%) | Land Depression | Weak El Niño | Passed close to the basin |
| August 29, 1978 | 1898.5 (-9.35%) | 1791.5 (-12.81%) | Bay Depression | - | Passed close to the basin |
| August 10, 1979 | 2097.5 (+0.15%) | 2112.3 (+2.80%) | Bay Depression | Weak El Niño | Passed close to the basin |
| July 24, 1989 | 1888.3 (-9.84%) | 1878.7 (-8.56%) | Land Depression | - | Passed close to the source area |
| August 19, 1990 | 2323.1 (+10.93%) | 2247.8 (+9.40%) | Bay Depression | - | Passed close to the basin |
| July 28, 1991 | 2129.2 (+1.67%) | 2114.7 (+2.92%) | Bay Depression | Moderate El Niño | Passed close to the basin |
| July 23, 1996 | 1858.2 (-11.27%) | 1857.4 (-9.60%) | Bay Depression | - | |
| July 27, 2003 | 2273.8 (+8.57%) | 2247.6 (+9.39%) | Bay Depression | - | Passed close to the basin |

LPS = Low Pressure Systems; Values in bracket represent percentage departure from mean

### a. Characteristics of the flood-generating low pressure systems (LPS)

Streamflow records available for a site on the Par River specify that low pressure systems (LPS) can have an immense impact. The systems, which comprise lows, depressions and cyclonic storms (Dhar and Nandargi, 1995), cause big stream rise leading to large floods (Table 4.35). The Par Basin is located at the southern margin of the zone commonly visited by low pressure systems originating over the Bay of Bengal and land. Table 4.35 indicates that all the LPS associated with floods on the Par River generally occur either in the month of July or August. By this time, on an average about 67% of the annual rainfall is received and soils are fully saturated, which in addition boosts the magnitude of floods.

The analysis reveals that precisely 217 tracks of LPS pass through the circle for 117 years (1891-2007). These tracks have been classified according to their source of origin into three categories i.e. Bay of Bengal, Arabian Sea and Land Depressions. The classification states that 96 LPS tracks originated from the Bay of Bengal, 82 tracks have their source in the Arabian Sea and 14 were land depressions. The cyclones that form over the Bay of Bengal and land are more effective in terms of producing high magnitude floods, therefore, for generation of mean tack of cyclone affecting the Par Basin, only those cyclones originated over Bay of Bengal and land were selected. The mean track reveals that the LPS travel in a west-northwest or northwest direction (Figure 4.91) to produce floods in the Par Basin.

The orientation of the track of LPS, with respect to the basin and the rate of movement of the LPS has intense influence on the severity of floods on the river. Therefore, the tracks of the LPS responsible for generation of floods on the Par River are shown in Figure 4.92. However, all these LPS were not associated with extreme floods. Analysis shows that the track and duration of the LPS over the basin determine the rainfall depths and consequently the magnitude of floods (Kale et al., 1994). Besides, majority of the large floods were associated with Bay depressions, nevertheless, two largest floods of the 20$^{th}$ Century (1968 and 1970) resulted from the land depression (Figure 4.92; Table 4.35). According to the path, two types of flood-producing LPS can be identified.

**aa. LPS that moved roughly parallel to the basin axis**

There are few LPS tracks that have moved parallel to the basin axis, and have been coupled with very large floods. The August 1968 and September 1970 LPS are excellent examples of this kind (Figure 4.92; Table 4.35). These two cyclones were responsible for heavy rainfall in the Par Basin, since the basin remained in the southwest sector of these LPS. The above tracks were responsible for high flood levels and discharges in the Par River, for instance due to passage of LPS in 1968, highest gauged discharge i.e. 23820 $m^3/s$ has occurred at Nanivahial. Sometimes, ‘antecedent precipitation’ causes large floods in the basin. Well-known example of

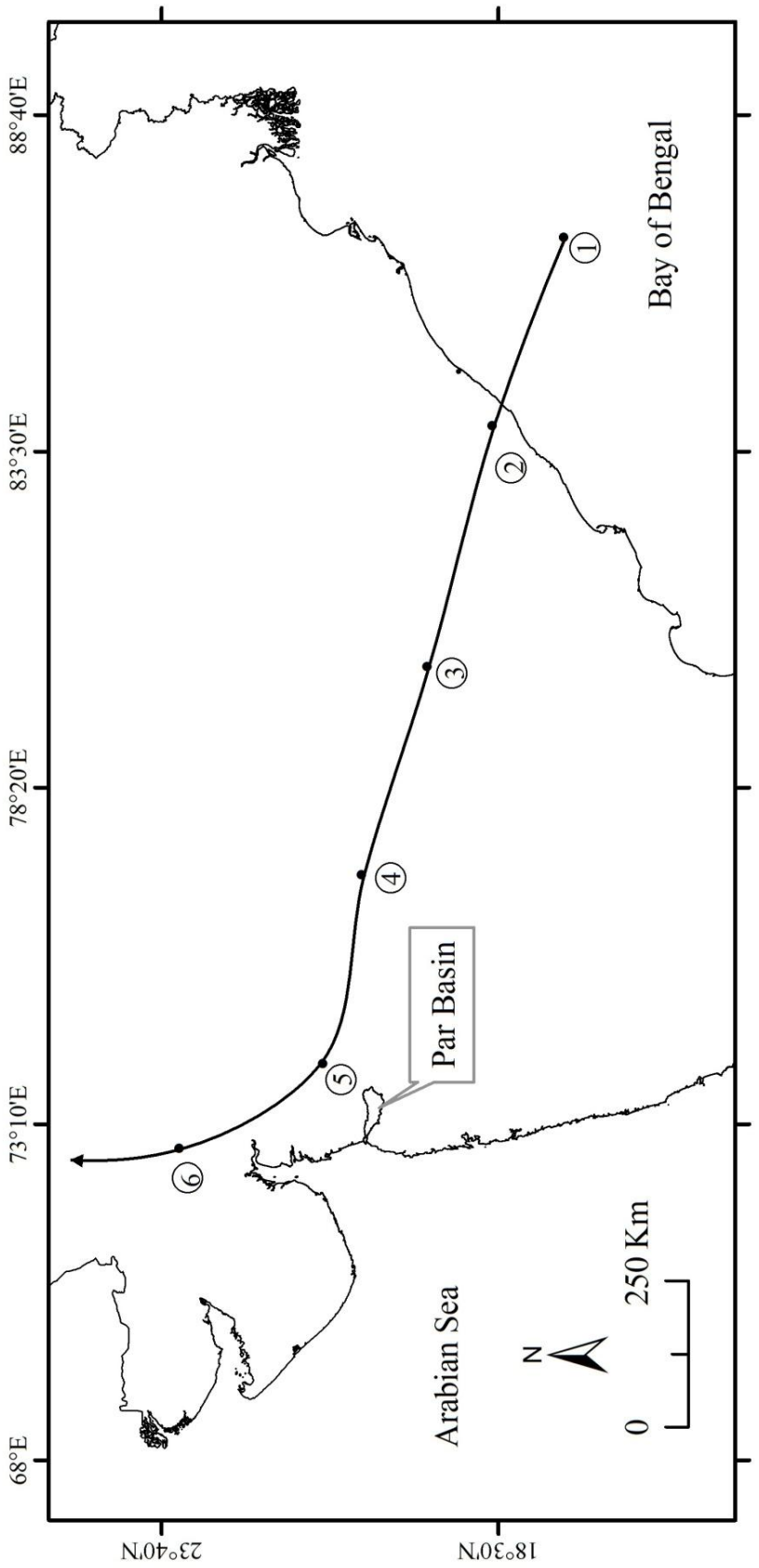


**Figure 4.91** Mean track of Low Pressure System (LPS)

above situation is that of 4-6 August, 1968 flood. It is interesting to note that the LPS that produced the largest flood of the 20$^{th}$ Century was preceded by another depression between 29$^{th}$ and 31$^{st}$ July 1968, that is about a week before the mega event. Thus, in spite of the fact that the year 1968 was a below-normal rainfall year, two rainstorms deposited large amounts of precipitation within a short period, and thus produced the largest ever recorded flood of the 20$^{th}$ Century.

**ab. LPS that passed from north-east direction of the basin**

The majority of the LPS have passed from north-east direction of the basin and it has produced high-magnitude floods in the Par Basin (Figure 4.92). The flood magnitude due to such cyclones may vary over the different reaches of the Par River. The best example of this is provided by the 1966 depression, which was responsible for high flood levels in the Par River with 8000 $m^3/s$ (>mean discharge of Nanivahial i.e. 5030 $m^3/s$) discharge at gauging site of Nanivahial. The 1966 LPS moved westward towards the river basin and it further travelled in the north direction (Figure 4.92).

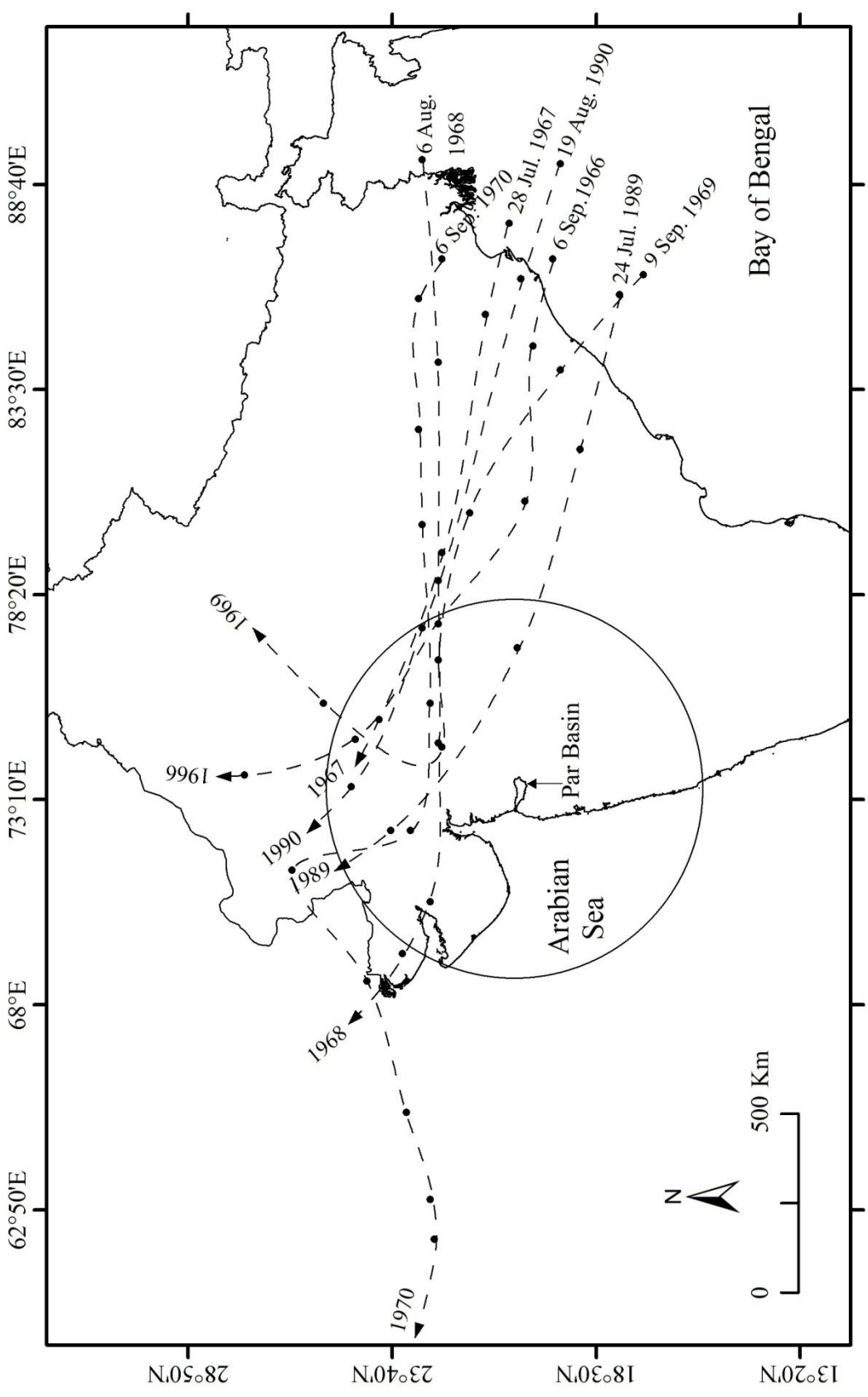


**Figure 4.92** Tracks of Low Pressure System (LPS) associated with large floods in the

**(iii) Relationship between annual rainfall totals and flood occurrences**

Figure 4.93 gives a plot of average annual rainfall (Par Basin) and discharge (Nanivahial site) departure from their respective averages. The graph clearly reveals that two major floods (1976 and 2004) recorded at Nanivahial, have occurred during the years of above-average annual rainfall. However, it is of interest to note that the 1968 flood, which was the largest flood of the 20$^{th}$ Century, occurred during a below-average rainfall year. The year 1994 has produced the highest average annual rainfall in the basin (3389 mm). However, the year 1994 did not record the peak flood in basin (Figure 4.93). It may be attributed to the well distributed rainfall throughout the monsoon season but not the intense flood producing rainfall.

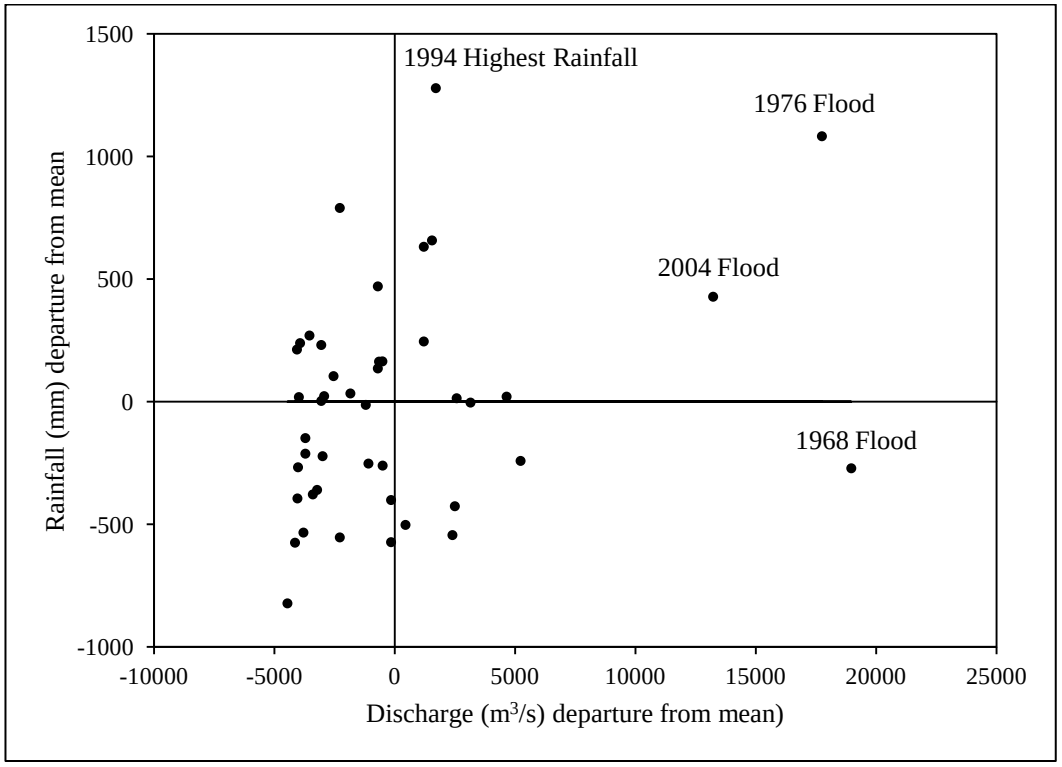


**Figure 4.93** Discharge (Nanivahial) and Rainfall (Average annual rainfall of the basin) departure from mean

**(iv) Normalized accumulated departure from mean (NADM) method**

The main purpose of the study is to detect the changes in the rainfall on the basin scale. The NADM graph given in Figure 4.94 shows the long-term trends of rainfall and it provides patterns for the Par Basin. The rising nature of NADM graph indicates above-average conditions, while, falling nature of the graph reveals the below-average conditions of rainfall. The NADM graph proposes that the rainfall amounts were below-average in the beginning of the 20$^{th}$ century i.e. up to 1930 (Figure 4.94). The middle part of the century i.e. from 1930 to 1960 is characterised by sharp rise in the graph, which specifies the period of above-average rainfall conditions. The graph shows short term rising and falling trend after 1960 (Figure 4.94), nevertheless, above average condition in general. This period has yielded the largest ever recorded floods on the river. It is, therefore, reasonable to state that the large magnitude floods on the Par River have occurred in the modern period.

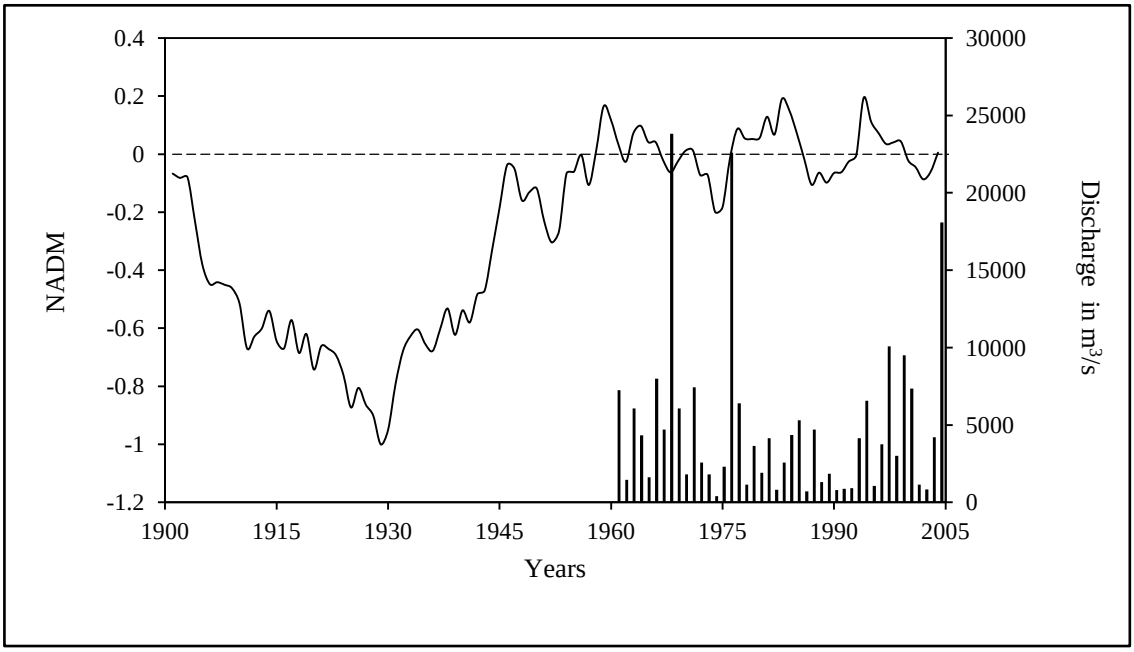


**Figure 4.94** Normalized Accumulated Departure from Mean (NADM) and Discharge (Nanivahial) Graph

It is not easy to draw general conclusion regarding the rainfall pattern of the Par Basin from the above illustrations (Figure 4.94), nonetheless, they point towards some general characteristics of the rainfall over the basin.

(i) 1901 to 1930 is associated with the below-average (low) rainfall.

(ii) Above-average (high) rainfall period is observed between 1930 and 1960.

(iii) Short term fluctuations are seen in the latter half of the 20$^{th}$ century particularly after 1960.

Consequently, the analysis of the annual rainfall data of the basin relating to the deviations in the amount clearly indicates that the major changes in the rainfall occurred around 1930 and 1960. Similar noteworthy changes have been identified by Mooley and Parthasarathy (1984); Fu and Fletcher (1988); Parthasarathy et al. (1991) and Kripalani and Kulkarni (1997) in the monsoon conditions about the same years in India. The association of all-India monsoon rainfall (Parthasarathy et al., 1991) with the rainfall of the Par Basin show remarkable similarity in their long-term fluctuations.

**(v) Long-period fluctuations in monsoon rainfall and floods**

Assessment of Figure 4.94 indicates that, although floods have occurred during the entire gauging period for Nanivahial site (1961-2004), noteworthy high magnitude floods (1968, 1976 and 2004) of 20$^{th}$ century have occurred in specific period of above-average rainfall condition with short-term fluctuations in rainfall. This, therefore, indicates that there is a relationship between long-term fluctuations in the monsoon rainfall and the frequency and magnitude of floods in the Par Basin.

The Par Basin is located in a region that is very sensitive to changes in the Indian southwest monsoon and which is foremost component of the Asian monsoon circulation. It is now a renowned fact that variations in the southwest monsoon are linked with circulation patterns across the globe through teleconnections with large-scale phenomena such as El Niño and Southern Oscillation (ENSO) (Ropelewski and Halpert, 1987; Kane, 1989; Simpson et al., 1993; Lutgens and Tarbuck, 1995).

The rainfall over the Indian subcontinent is highly susceptible to the changes in the Indian southwest monsoon which is teleconnected with the ENSO events. Therefore, an attempt has been made to recognize natural variability in annual rainfall (and therefore floods) in the Par Basin and its correlation with ENSO events. The annual

rainfall data for the period of 104 years (1901-2004) of the basin have been used to establish relationship with ENSO events. The method implemented by Eltahir (1996) for the Nile River was used for the analysis. The ENSO index published by Wright (1989) for the period 1891-1983 has been employed in the study. The SST data from 1984 were obtained from Climate Prediction Centre (CPC) of National Oceanic and Atmospheric Administration (NOAA). It is the monthly series of the mean sea surface temperature (SST) anomaly averaged over the central and eastern Pacific Ocean. The index finally applied here is averaged over the monsoon season (June-October). As recommended by Eltahir (1996), the data on SST were categorized into cold, warm and normal conditions on the basis of temperature (-0.5°C and +0.5°C). Figure 4.95 shows the categories of the annual rainfall of the Par Basin and ENSO index. To examine the relationship of the magnitude of the rainfall and the condition of the ENSO in different years, the conditional probabilities of the rainfall have been calculated and presented Table 4.36.

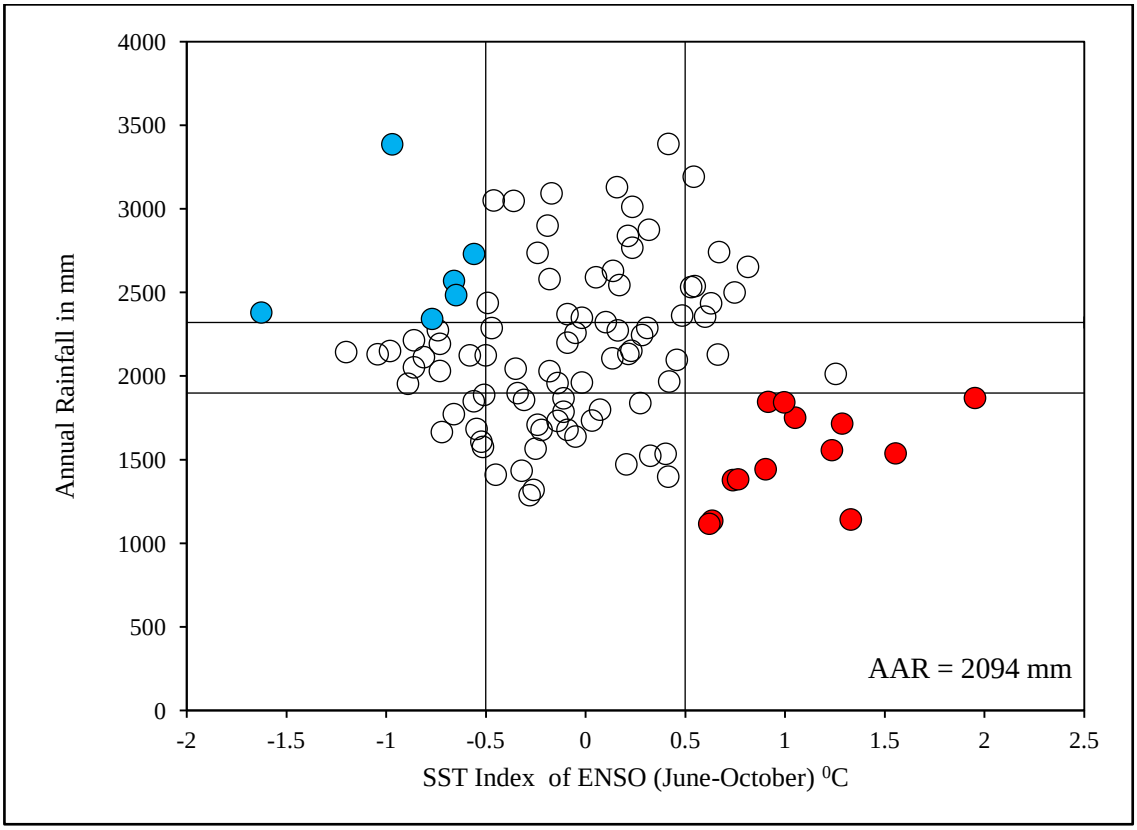


**Figure 4.95** Categories of annual rainfall and ENSO index of the Par Basin; AAR = Average Annual Rainfall; Data source: India Meteorological Department (IMD)

**Table 4.36** Conditional probabilities of the monsoon rainfall over the Par Basin given the SST index of ENSO (N = 104 years)

| Region | AAR | SST | | |
|---|---|---|---|---|
| | | Cold | Average | Warm |
| Par Basin | High | 0.25 | 0.35 | 0.35 |
| | Normal | 0.46 | 0.30 | 0.08 |
| | Low | 0.29 | 0.35 | 0.57 |

**Data source:** IMD; Low < 10% AAR and High >10% AAR; AAR = Average Annual Rainfall

The analysis shows that the probability of having high rainfall is 0.25 (25%) during La Niño/cold ENSO conditions, the probability of low rainfall is 0.57 (57%) during warm ENSO conditions. Although the probability of more rainfall during La Niño/cold ENSO is not very high, the probability of low rainfall during warm ENSO is high i.e. 0.57 (57%) (Figure 4.95; Table 4.36).

**(vi) Detection of changes in the annual rainfall**

According to Mann-Kendall test the positive (negative) sign of τ indicates increasing (decreasing) trend. Therefore, the positive value of τ i.e. 0.067 (Table 4.37) for the Par River suggests, the rainfall trend for the given period is increasing. However, whether, the trend is statistically significant or not is intended by testing the significance of Tau (τ)

**Table: 4.37** Nature of changes/trends in annual rainfall records based on Mann-Kendall test

| Station | Period | *N* | Tau (τ) | *z* score | Trend/change |
|---|---|---|---|---|---|
| Par Basin | 1901 – 2004 | 104 | 0.067 | 1.00 | No specific trend |

*N* = number of observations

The analysis of testing the significance of Tau (τ) states that the Par Basin, as a whole, does not show any noteworthy rainfall trend over the period of a century. The majority of the investigations for larger areas (all-India scale) during last few decades have given analogous results. These studies noticeably specified that the monsoon rainfall, mainly on all-India scale, is trendless and is primarily random in nature over a long period of time, (Mooley and Parthasarathy, 1984). Srivastava et al. (1998)

employed Mann-Kendall test to find the trend in rainfall over India for the period 1901-1992. His analysis concluded that more or less all-India rainfall does not show any specific trend.

**(vii) Detection of future changes in the rainfall**

Table 4.38 shows the percentage change required in the future rainfall before it can be considered to be significantly different from the historical record. As a result of its inherent nature, the rainfall over the basin shows substantial inter-annual variability in its amount, predominantly for the short-period of time. Therefore, high distinctions in the amount of rainfall can be observed for the short-period of time which ceases with the increase in the time span of the record. Thus, it is, clear that high percentage change is required in the future rainfall of the short-period of time, before considering it noticeably different from historical record. While, for the long-period of time small percentage change is necessary in the future rainfall to consider it significantly different than the previous data.

**Table 4.38** Percent change required to identify statistically significant change in AAR of the Par Basin

| **Region** | **N** | **AAR (mm)** | **σ** | **Percent change required in the AAR at 95% of confidence level, Years.** | | | |
|---|---|---|---|---|---|---|---|
| | | | | **10** | **20** | **50** | **100** |
| Par Basin | 104 | 2094 | 518 | 16 | 12 | 9 | 7 |

Data source: IMD, Pune; N = No. of observations

The results of application of the t test to the statistical parameters of the rainfall data of the Par Basin are shown in Table 4.38. It is observed that on the basin scale 16% change in the annual rainfall is required in the average rainfall of next 10 years to consider it different than the available rainfall record. Likewise, to establish the significant change in the rainfall of the next 20 and 50 years, the average rainfall should differ by 12 and 7% correspondingly than the present mean of the rainfall (Table 4.38). While, to declare the average rainfall of the present century ($21^{st}$ century) considerably different than the previous century ($20^{th}$ century), 7% change is required in the long-term mean of the rainfall of the basin (Table 4.38). The analyses

of the t test as well as other analyses accomplished in the previous sections of this chapter specify that the monsoonal rainfall of the Par Basin is highly regular and reliable. Consequently, it is probable to be the same in this as well as in the next century.

### 4.5.2 Flood hydrology

#### (i) Stage discharge curve/rating curve

The datasets of discharge and stage fit very well ($R^2 = 0.98$). By keeping this fact in view, at attempt has been made to estimate the values of AMS discharges from 2006 to 2009 (Figure 4.96). These estimated discharges have been used in statistical analyses of the AMS data.

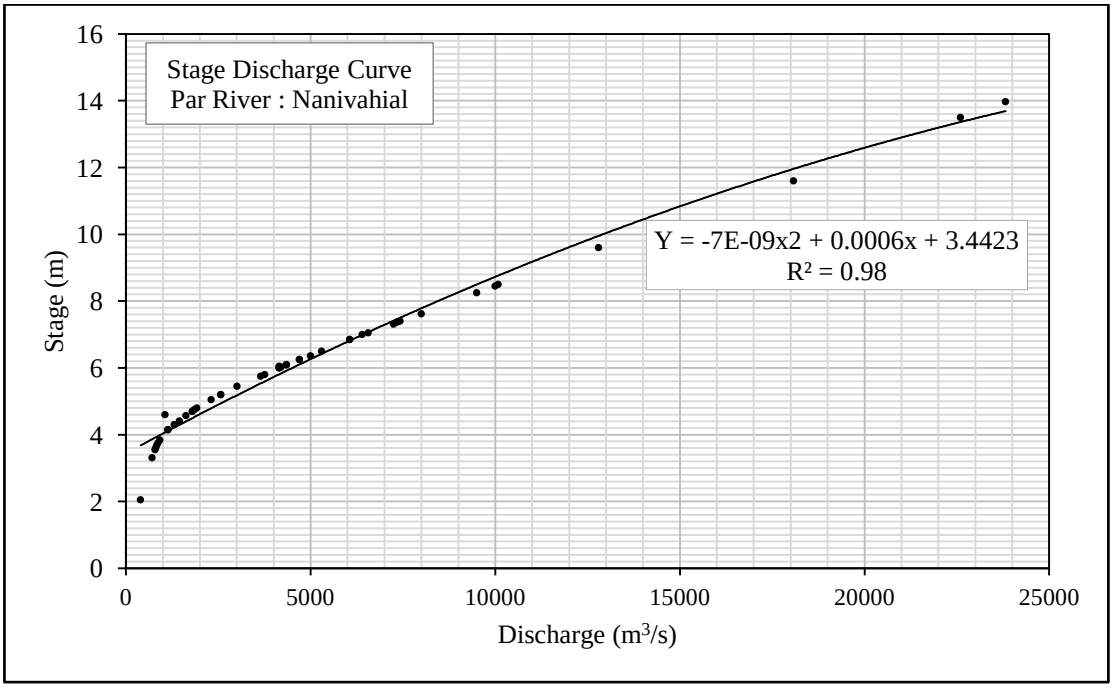


**Figure 4.96** Rating curve of the Par River at Nanivahial

**(ii) Flood regime characteristics**

The available gauged data for Nanivahial site shows that the mean discharge is 5030 $m^3/s$. The highest flood ever recorded on the Par River at Nanivahial (Figure 4.12) in 1968 was of the order of 23820 $m^3/s$ (Table 4.40). Howerver, the estimated high magnitude flood for the Par River reaches up to 38000 $m^3/s$ for site Parvas (Figure 4.12; Table 4.21), which is eighteen km downstream of Nanivahial.

**a. Interannual variability in annual peak discharges**

The temporal pattern of variation in the annual peak discharges at Nanivahial site on the Par River is demonstrated in Figure 4.97.

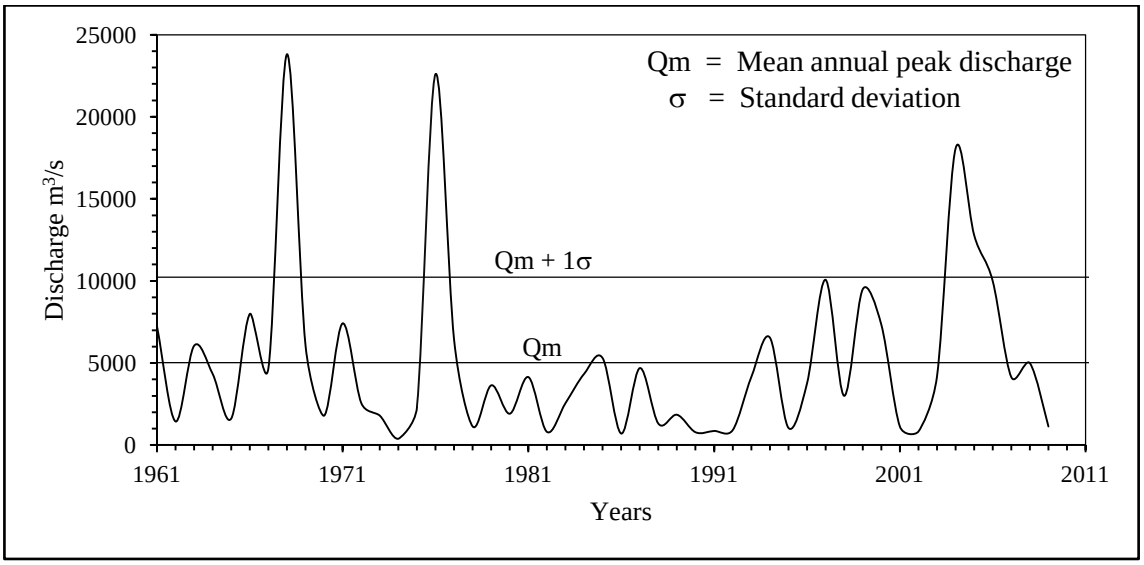


**Figure 4.97** Time series plot, Nanivahial; See Figure 4.12 for location of site

The Figure 4.97 reveals high interannual variability in the annual peak discharges. The figure also shows the occurrence of three large events i.e. in year 1968, 1976 and 2004 during the gauge period. These events, nonetheless, were entirely natural. The unusual high discharges were principally the outcome of Low Pressure System (LPS) developed over Bay of Bengal and adjacent land (Figure 4.92). The bedrock reaches of the Par River undoubtedly limit the width of the flow and consequently the increase in discharge is principally compensated by a distinct increase in the velocity and depth. Hence, it can inferred that the bedrock reaches characterize higher velocities

and therefore extremely high flood power. This situation in bedrock reaches of the Par River resulted into acceleration of geomorphic work to accomplish.

**b. Average magnitude and variability**

The mean (Qm) and range of annual peak discharges for a gauging site of Nanivahial are given in the Table 4.39.

**Table 4.39** Flood flow characteristics of the Par River at Nanivahial

| **Site** | **Nanivahial** |
|---|---|
| Area ($km^2$) | 1252 |
| Record length (Years) | 49 |
| Qmin ($m^3/s$) | 395 |
| Qmax ($m^3/s$) | 23820 |
| Qm ($m^3/s$) | 5030 |
| Flood range ($m^3/s$) | 23425 |
| Qmax /Qm | 4.74 |
| $\sigma$ ($m^3/s$) | 5190 |
| Cv ($\sigma$/Qm) | 1.03 |
| $C_s$ | 2.2 |
| $C_s$/Cv | 2.14 |
| FFMI | 0.42 |
| Unit discharges ($m^3/s/km^2$) | 19 |

Data source: Gujarah State Irrigation Department; A = Catchment area; Qmin = Minimum annual peak discharge; Qmax = Maximum annual peak discharge; Qm = Mean annual peak discharge; $\sigma$ = Standard deviation; Cv = Coefficient of variation; Cs = Coefficient of skewness; FFMI = Flash flood magnitude index

The Qmax/Qm ratio for Nanivahial site is 4.74. This, therefore, indicate that the maximum annual peak discharge (Qmax) is about 5 times higher than average peaks. Since the more variable the flow is, the more important the higher discharges become (Wolman and Miller, 1960). The effect of such extreme flows on geomorphic activity in channel is likely to be noteworthy. The Cv for Nanivahial site is 1.03 (or 103%) (Table 4.39). It proposes that the variability in peak flows at Nanivahial Site in the Par Basin is in fact higher.

Deviations from mean annual peaks have been shown graphically for Nanivahial site. The plot confirms the highly variable nature of flows at the gauging site.

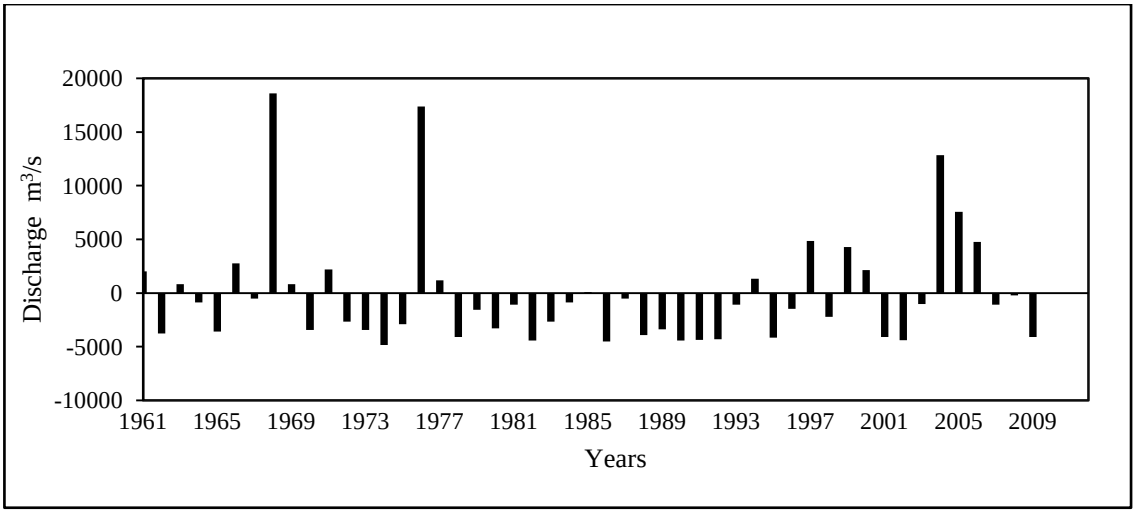


**Figure 4.98** Variability of Peak Floods, Nanivahial Site; See Figure 4.12 for location of site

An interesting fact reflected by the graph is that the positive deviations are much larger, but less frequent. This, therefore, indicates that the mean is strongly affected by a few large flows.

The FFMI values of the Nanivahial site is 0.42 (Table 4.39). The relatively higher FFMI value of Nanivahial site indicates flashy and variable nature of floods. The index further indicates that the possibility of the river experiencing noteworthy geomorphic work during large floods.

**c. Skewness ($C_s$)**

The Nanivahial site on the Par River shows high positive $C_s$ Value i.e. 2.2. The positive $C_s$ value suggests the occurrence of one or two (or a few) very large-magnitude flows during the gauge period (Figure 4.98). Nevertheless, the characteristic of skewness is doubtful when it is estimated for less than 50 years data (Viessman et al., 1989). The $C_s$/Cv ratio for gauging site is 2.14. This, therefore, proposes that the distribution of peak discharge is positively skewed and occurrence of one or two (or a few) very large-magnitude flows during the gauge period. For most large Indian rivers the values of this ratio are more than 2.0 (Shaligram and Lele, 1978).

**d. Unit discharges**

The unit discharges have been calculated for sixteen sites on the Par River (Figure 4.99). It ranges between 5.4 and 101 $m^3/s/km^2$ (Table 4.40). The average unit discharge for Par Basin is 27.77 $m^3/s/km^2$. The unit discharge of the Par Basin (27.77 $m^3/s/km^2$) is extremely higher than other world rivers with comparable drainage areas. Therefore, Par River is capable of producing large floods compared with rivers with comparable drainage areas in the world. Such larger discharges are likely to be effective in terms of geomorphic changes in the channel and valley (Costa and O'Connor, 1995).

**Table 4.40** Unit discharges for the Par River and Nar River

| **Sr. No.** | **River Site** | **A ($Km^2$)** | **Qmax ($m^3/s$)** | **Unit discharge ($m^3/s/km^2$)** |
|---|---|---|---|---|
| 1 | Parchapada | 35.64 | 3614 | 101.40 |
| 2 | Borvan | 66.50 | 2708 | 40.72 |
| 3 | Ghatalbari | 108.11 | 2427 | 22.45 |
| 4 | Kalmane | 201.95 | 9710 | 48.08 |
| 5 | Jhiri | 424.46 | 3955 | 9.32 |
| 6 | Chachpada | 628.72 | 5954 | 9.47 |
| 7 | Mendha | 655.63 | 20056 | 30.59 |
| 8 | Dhamni | 1108.85 | 21775 | 19.64 |
| 9 | Nanivahial* | 1252.31 | 23820 | 19.02 |
| 10 | Panchlai | 1354.21 | 35785 | 26.43 |
| 11 | Parvas | 1400.23 | 38006 | 27.14 |
| 12 | Sudhalvada | 1501.49 | 10699 | 7.13 |
| 13 | Pardi | 1528.07 | 25732 | 16.84 |
| 14 | Umbardhe | 177.17 | 4438 | 25.05 |
| 15 | Pendha | 387.84 | 2087.52 | 5.38 |
| 16 | Tamchhadi | 404.85 | 14414 | 35.60 |

A = Catchment area; Qmax = Maximum annual peak discharge; * = Gauging site; See Figure 4.12 for location of sites

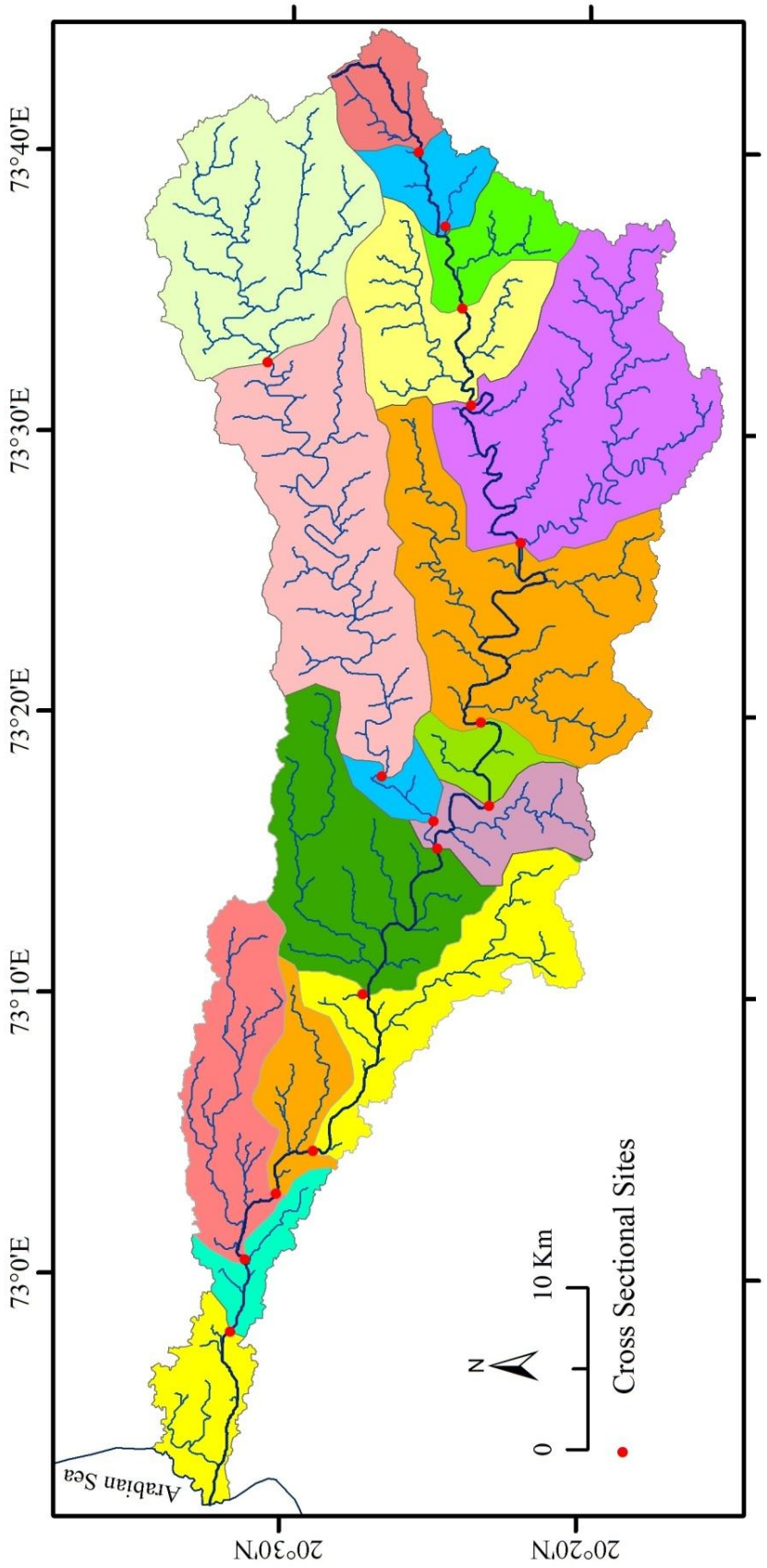


**Figure 4.99** Catchment areas upstream of cross-sectional sites

**(iii) Flood frequency analyses**

**a. Gumbel extreme value type I (GEVI) distribution**

By using GEVI probability distributions, peak flows have been estimated for different return periods such as 2, 5, 10, 25, 50, and 100 years. The estimated discharges are given in Table 4.41.

**Table 4.41** Estimated discharges in $m^3/s$ for different return periods (Based on GEVI distribution)

| River | Site | Record length | Return period (years) | | | | | |
|---|---|---|---|---|---|---|---|---|
| | | | 2 | 5 | 10 | 25 | 50 | 100 |
| Par | Nanivahial | 49 | 4200 | 8767 | 11777 | 15618 | 18576 | 21327 |

See Figure 4.12 for location of site

The distributions have also been employed to estimate the recurrence interval of mean annual peak discharge (Qm), large flood (Qlf) and actually observed maximum annual peak discharge (Qmax) (Table 4.42).

**Table 4.42** Return period of Qm, Qlf and Qmax (Based on GEVI)

| River | Site | Record length | Q $m^3/s$ | Return period (yr) |
|---|---|---|---|---|
| Par | Nanivahial | 49 | Qm = 5030 | 2.33 |
| | | | Qlf = 10220 | 6.93 |
| | | | Qmax = 23820 | 185.47 |

Qm = mean annual peak discharge; Qlf = large flood; Qmax = maximum annual peak discharge; GEVI = Gumbel Extreme Value Type I; See Figure 4.12 for location of site

In the GEVI analysis, the observed annual peak discharges have been plotted against the return period or F(X) values (plotting positions) on the Gumbel graph paper, designed for GEVI probability distribution. The plotted graph is shown in Figure 4.100 which show that, the fitted lines are fairly close to the most of the data points and, therefore, can be reliably and conveniently used to read the recurrence intervals for a given magnitude and vice versa. Interestingly, in plot of GEVI distribution, the actually observed peak on record (Qmax) falls well close to the fitted lines. This

means the return period of Qmax of Nanivahial station predicted by GEVI distribution are likely to be quite reliable.

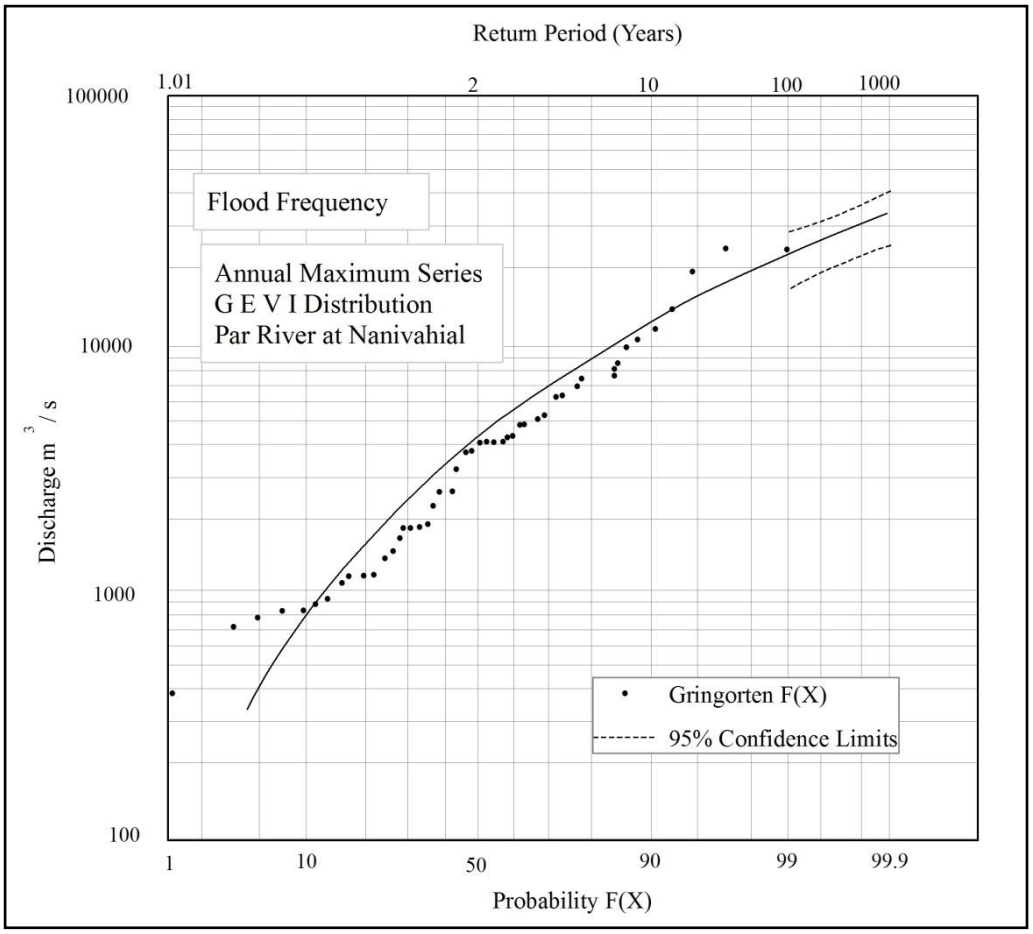


**Figure 4.100** Annual Maximum Series, GEVI distribution, Nanivahial, Par River

**b. Weibull's method**

The recurrence intervals of high-magnitude flood events that have occurred on the Par River at Nanivahial were predicted by using the Weibull method (Table 4.43).

**Table 4.43** Return periods for high floods on the Par River at Nanivahial based on Weibull's method

| Year | Q (cms) | Rank | Return period (yr) |
|---|---|---|---|
| 1968 | 23820 | 1 | 50.0 |
| 1976 | 22600 | 2 | 25.0 |
| 2004 | 18080 | 3 | 16.7 |
| 2005 | 12800 | 4 | 12.5 |
| 1997 | 10080 | 5 | 10.0 |
| 2006 | 10000 | 6 | 8.3 |
| 1999 | 9500 | 7 | 7.1 |
| 1966 | 8000 | 8 | 6.3 |
| 1971 | 7425 | 9 | 5.6 |
| 2000 | 7350 | 10 | 5.0 |
| 1961 | 7250 | 11 | 4.5 |
| 1994 | 6560 | 12 | 4.2 |
| 1977 | 6400 | 13 | 3.8 |
| 1963 | 6060 | 14 | 3.6 |
| 1969 | 6060 | 15 | 3.3 |
| 1985 | 5300 | 16 | 3.1 |
| 2008 | 5000 | 17 | 2.9 |
| 1967 | 4700 | 18 | 2.8 |
| 1987 | 4700 | 19 | 2.6 |
| 1984 | 4350 | 20 | 2.5 |
| 1964 | 4340 | 21 | 2.4 |
| 2003 | 4200 | 22 | 2.3 |
| 1981 | 4150 | 23 | 2.2 |
| 1993 | 4150 | 24 | 2.1 |
| 2007 | 4150 | 25 | 2.0 |
| 1996 | 3760 | 26 | 1.9 |
| 1979 | 3650 | 27 | 1.9 |
| 1998 | 3010 | 28 | 1.8 |
| 1972 | 2570 | 29 | 1.7 |
| 1983 | 2570 | 30 | 1.7 |
| 1975 | 2310 | 31 | 1.6 |
| 1980 | 1920 | 32 | 1.6 |
| 1989 | 1855 | 33 | 1.5 |
| 1970 | 1800 | 34 | 1.5 |
| 1973 | 1800 | 35 | 1.4 |
| 1965 | 1627 | 36 | 1.4 |
| 1962 | 1450 | 37 | 1.4 |
| 1988 | 1310 | 38 | 1.3 |
| 1978 | 1140 | 39 | 1.3 |
| 2001 | 1140 | 40 | 1.3 |
| 2009 | 1140 | 41 | 1.2 |
| 1995 | 1060 | 42 | 1.2 |
| 1992 | 920 | 43 | 1.2 |
| 1991 | 870 | 44 | 1.1 |
| 2002 | 835 | 45 | 1.1 |
| 1982 | 810 | 46 | 1.1 |
| 1990 | 790 | 47 | 1.1 |
| 1986 | 710 | 48 | 1.0 |
| 1974 | 395 | 49 | 1.0 |

Data source: Irrigation Department of Gujarat

**c. Discharge-area envelope curve**

The envelope curve prepared for the Par Basin shows that there is a rapid increase in the maximum possible discharge with an increase in drainage area. The peak gauged discharge for Nanivahial site for year 1968 lies much above the world envelope curve prepared by Baker (1995). The peak flows estimated for nine sites on the Par and a site on Nar River also lie above the world envelope curve for the respective drainage area. However, remaining sites fall below the world envelope curve. A comparison with Baker's (1995) world envelope curve indicates that Par Basin can produce relatively high flood peak discharges than some of the drainage basins with comparable basin areas in the other parts of the world. This is to say that under given climatic, hydrologic and physiographic conditions, extraordinary floods can be produced in the Par Basin and expected to generate large forces to cause enduring changes in the channel and valley morphology.

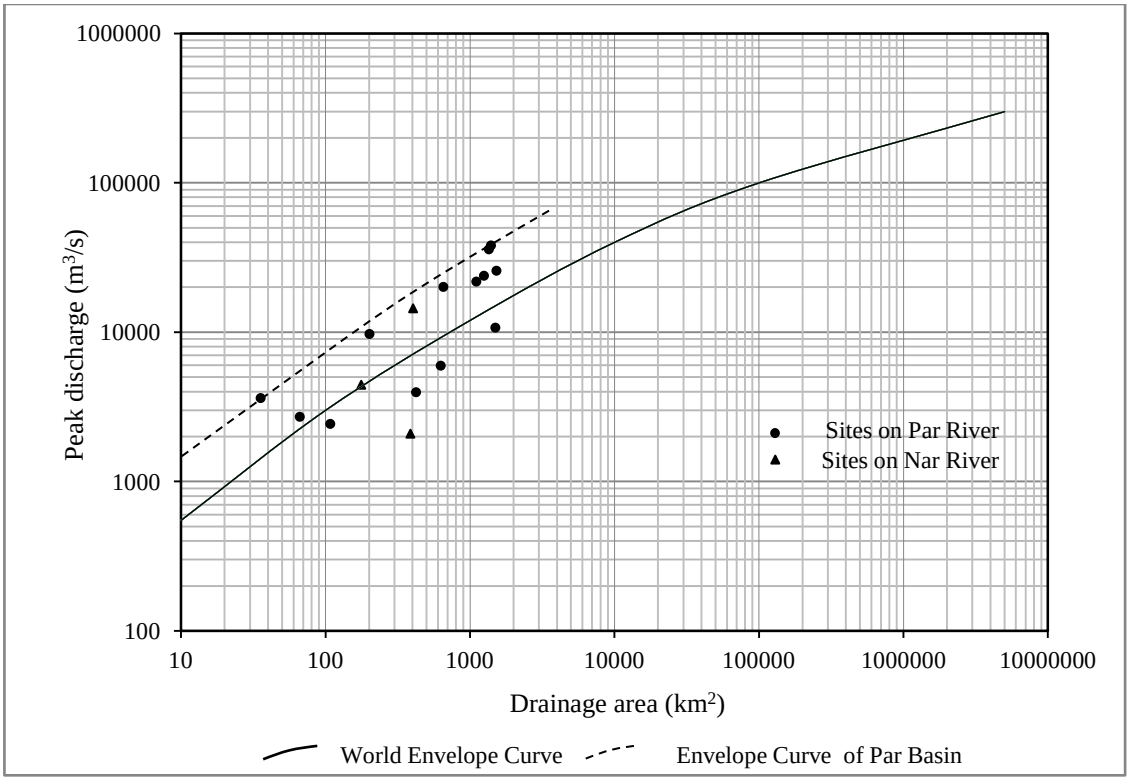


**Figure 4.101** World Envelope Curve with reference to Par Basin; Data source: Baker, 1995; Gujarat Irrigation Department; Field surveys

### *4.5.3 Flood geomorphology*

#### (i) Channel form with respect to high flood level (HFL)

The supply limited rivers such as Par, are able to move materials made available to them and the channels tend to be narrow and deep. In this chapter, an attempt has made to study the morphology of channel with respect to bankfull stage. However, due to significance of infrequent large magnitude floods in shaping the bedrock channels, in this chapter, an attempt has made to study the morphology of channel with respect to high flood level (HFL). For this purpose, cross sectional surveys were carried out at different locations from source to mouth with respect to high flood level. Thirteen cross sections on the Par and three cross sections on the Nar River (Figure 4.12) have been constructed.

#### a. Water surface width (w)

Most of the cross-sections of the Par River are generally trapezoidal and saucer shaped. The channels are narrow in the upper reaches and significantly wider in the middle and lower reaches. The average channel width of the Par River is about 230 m and it varies from approximately 42 m at constricted reach of Mendha gorge (Figure 4.47) to 600 m at Nanivahial (Figure 4.108; Figure 4.109; Table 4.45). The average width of Nar River is 114 m. In upper reaches, the rocky channel of the Par River is typically narrow where, in middle reaches, it is moderately wide. However, the channel exceptionally becomes narrow at the Mendha Gorge (42 m) (Figure 4.47). The channel width increases abruptly from the confluence of Par and Nar River at Dhamni (240 m) to Pardi (390 m) near mouth of the river. The channel is widest at Nanivahial (600 m) (Figure 4.109). In spite of the local variations in the channel width, there is a gradual increase in the width with an increase in the distance from the source (Figure 4.102).

#### b. Flow depth (D)

Channel depth is vital parameter to determine the power per unit area and boundary shear stress at a cross section. The maximum channel depth of the Par River is 29 m, 80 km away from source at Mendha Gorge (Figure 4.12; Figure 4.47). The minimum

depth is 6.3 m at Borvan (Figure 4.12; Figure 4.21). The average channel depth is 13.3 m (Table 4.44). Figure 4.102 shows that there is gradual increase in depth in the downstream direction, however, unlike width, the rate of increase in the depth is lower.

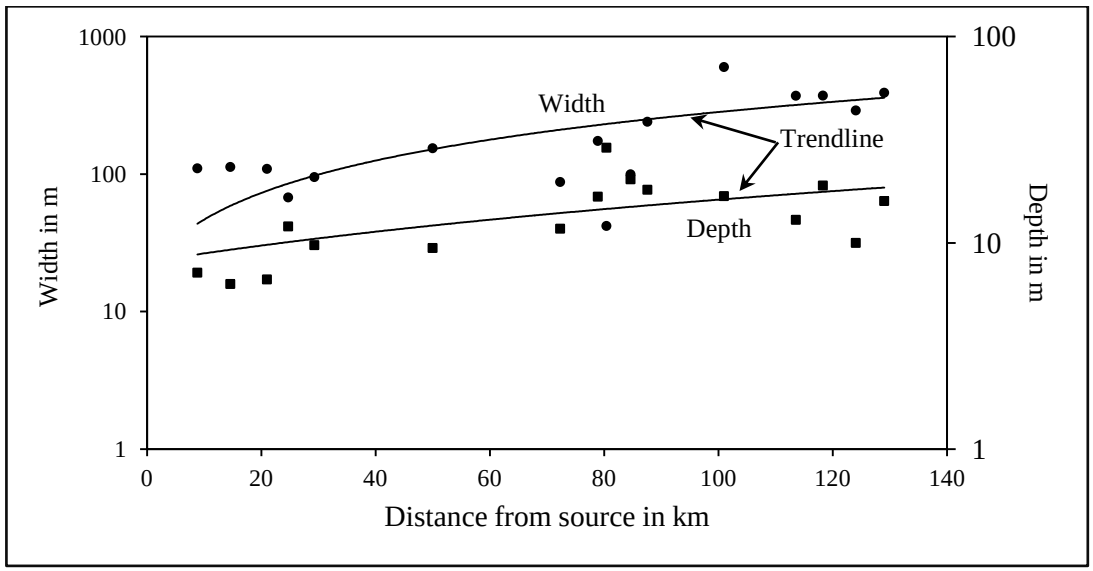


**Figure 4.102** Downstream changes in width and depth

**c. Form ratio (F)/ width-depth ratio (w/D ratio)**

The form ratio for Par River varies from 2 to 35. The width-depth ratio is highest at Nanivahial due to wide channel (Figure 4.109) and it is lowest at Mendha due to channel in the form of constricted gorge (Figure 4.47). The average width-depth ratio is about 16.03. Osborn and Stypula (1987) employed width/depth ratio to characterize channels for hydraulic relations using channel boundary shear as a function of channel shape, according to the their classification ten as of sixteen cross-sectional sites reveals moderate to high width-depth ratio (W/d ratio > 12). Rosgen's (1994) channel classification states that, the Par as well as the Nar River channel reaches at the cross sections surveyed fall in types of A to C, representing relatively straight (A) (sinuosity < 1.2; W/D ratio < 12 ), low sinuosity (B) (sinuosity > 1.2 to < 1.4; W/D ratio > 12), meandering (C) (sinuosity > 1.4; W/D ratio > 12). Accordingly three cross-sections on the Par River (Figure 4.12) namely Kalmane (P4), Chachpada (P6) and Mendha (P7) and Umbardhe (N1) Pendha (N2) and Tamchhadi (N3) on the Nar River belong to category A, representing relatively straight bedrock channels. The

rest of the channel cross-sections on both rivers fall in type B and C categories of channel classification.

**d. Change in the width-depth ratio with discharge**

Width-depth ratios for high flood level (HFL) is variable at different reaches of the Par River, ranging from deep narrow to wide open. During the dry season and during low flows the water spreads at few cross sections, and the width is greater and depth is smaller. Therefore, the width-depth ratio is high and the channel reflects all the characteristics of a shallow-wide channel. However, in response to heavy rainfall as the stage and discharge increases, there is an increase only in the depth of flow in deep-narrow channels. As a result, the width-depth ratio decreases, and the hydraulic efficiency increases dramatically. Figure 4.103 shows the plot of width-depth ratios for low flows as well as high flows for different cross-sections along the Par River. There is a noteworthy drop in the ratios in the lower reaches, because of the very wide nature of the channel of the Par River in these reaches (Figure 4.103).

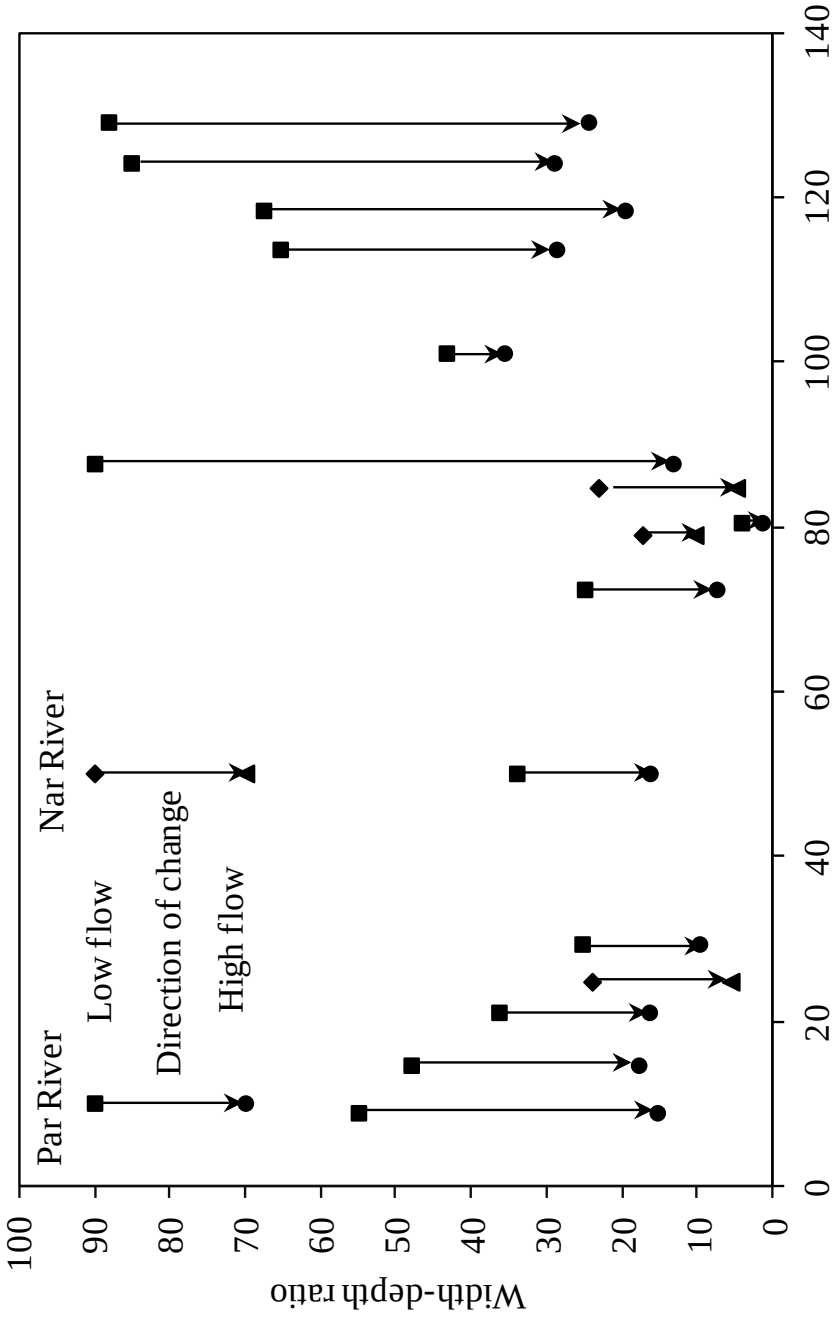


**Figure 4.103** Downstream variation in width-depth ration with discharge

**e. Mean depth (d)**

The form of a river channel affects its hydraulic efficiency rather that can be quantified by calculating the hydraulic radius. In case of Par River, hydraulic radius is replaced by mean depth for analyses. The mean depth of the Par River ranges from 4.40 to 28.8 m. The average depth is about 9.60 m. Such high value reflects the high efficiency of the channel of the Par River. Like the channel depth, the mean depth also goes on increasing with an increase in distance from the source.

**f. Channel capacity (Ca)**

The channel capacity is a fundamental scale variable and is usually defined as the cross-sectional area. It therefore, represents the amount of water and sediments, which a channel can accommodate (Petts and Foster, 1985). The channel capacity of the Par River ranges between 322 $m^2$ and 4998 $m^2$ (Figure 4.104 to 4.111; Table 4.44). The average channel capacity is 1839 $m^2$. The existing channel sizes at different reaches of the Par River indicate that the flows of sufficient magnitude have occurred in the past to create such a large channel.

**g. Channel gradient**

The channel gradient is one of the important morphological parameters dictating the unit steam power and geomorphic impact. Channel gradient decreases gradually with distance from the source (Figure 4.40). The average gradient of the Par River is 0.0691. Channel gradient, as expected, is steeper at waterfalls, rapids and in narrow bedrock reaches.

**Table 4.44** Channel morphologic variables of cross sections of the Par and Nar River

| No. | Site | W (m) | D (m) | W/D | d (m) | Ca ($m^2$) | Gradient |
|---|---|---|---|---|---|---|---|
| 1 | Parchapada | 110 | 7.16 | 15.36 | 4.7 | 322.35 | 0.01294 |
| 2 | Borvan | 112.5 | 6.31 | 17.83 | 4.40 | 387.4 | 0.008831 |
| 3 | Ghatalbari | 109 | 6.64 | 16.42 | 4.41 | 394 | 0.003266 |
| 4 | Kalmane | 95 | 9.73 | 9.76 | 6.51 | 569.5 | 0.05204 |
| 5 | Jhiri | 154 | 9.43 | 16.33 | 5.23 | 481.7 | 0.00244680 |
| 6 | Chachpada | 87.5 | 11.70 | 7.48 | 7.38 | 664.7 | 0.0056 |
| 7 | Mendha | 41.9 | 28.90 | 1.45 | 28.8 | 1206.72 | 0.00816949 |
| 8 | Dhamni | 240 | 18.07 | 13.28 | 14.045 | 3375.06 | 0.00115151 |
| 9 | Nanivahial$^{+}$ | 600 | 16.83 | 35.65 | 7.487 | 4492.2 | 0.000654 |
| 10 | Panchlai | 371 | 12.91 | 28.73 | 9.04 | 3456.1 | 0.01097 |
| 11 | Parvas | 372 | 18.94 | 19.64 | 14.19 | 4998.34 | 0.00269 |
| 12 | Sudhalvada | 290 | 9.98 | 29.05 | 6.3 | 2048 | 0.00375 |
| 13 | Pardi | 390.2 | 15.93 | 24.49 | 11.78 | 4512.8 | 0.00111 |
| 14 | Umbardhe***** | 67.55 | 12.00 | 5.63 | 7.3 | 480.63 | 0.008923 |
| 15 | Pendha***** | 174 | 16.73 | 10.40 | 9.49 | 1626.7 | 0.00007407 |
| 16 | Tamchhadi***** | 99.5 | 20.31 | 4.90 | 12.51 | 404.85 | 0.0092567 |
| | Min | 41.90 | 6.31 | 1.45 | 4.40 | 322.35 | 0.00007407 |
| | Max | 600 | 28.90 | 35.65 | 28.80 | 4998.34 | 0.05 |
| | Mean | 207.13 | 13.85 | 16.03 | 9.60 | 1838.82 | 0.01 |
| | s | 1.23 | 1.01 | | | | |
| | σ | 156.43 | 6.04 | | | | |
| | Cv % | 75.52 | 95.72 | | | | |

Sources: Field surveys and Gujarat Irrigation Department$^{+}$; XS on Nar River***;** W = Channel (HFL) width; D = Maximum depth; d = Mean depth; Ca = Channel capacity; Refer Table 4.4 for notations; See Figure 4.12 for location of the sites

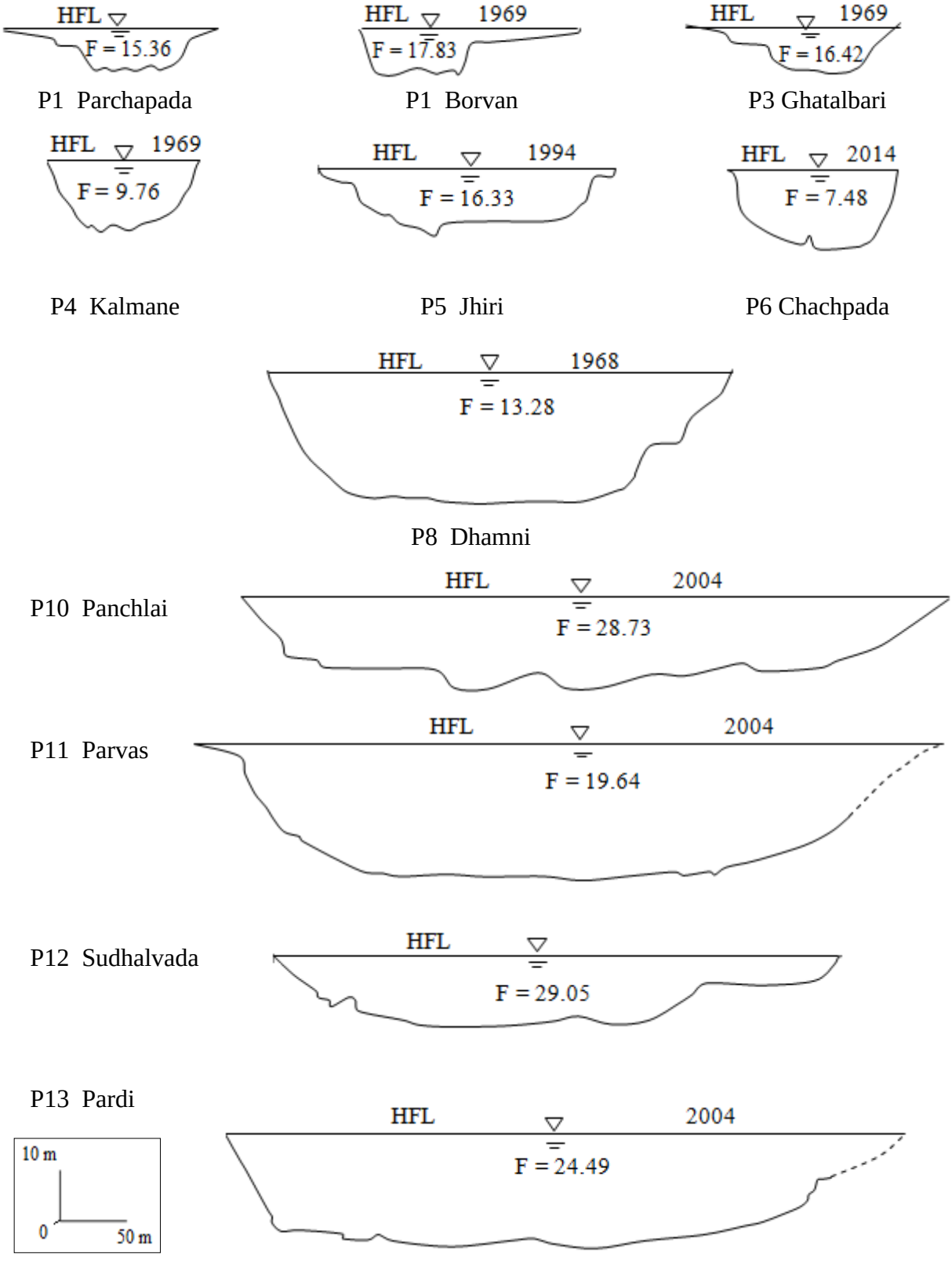


**Figure 4.104** Cross sections, Par River; See Figure 4.12 for location of sites; F = Form ratio; HFL = High flood level

**Figure 4.105** Par River at Kalmane; See Figure 4.12 for location of site

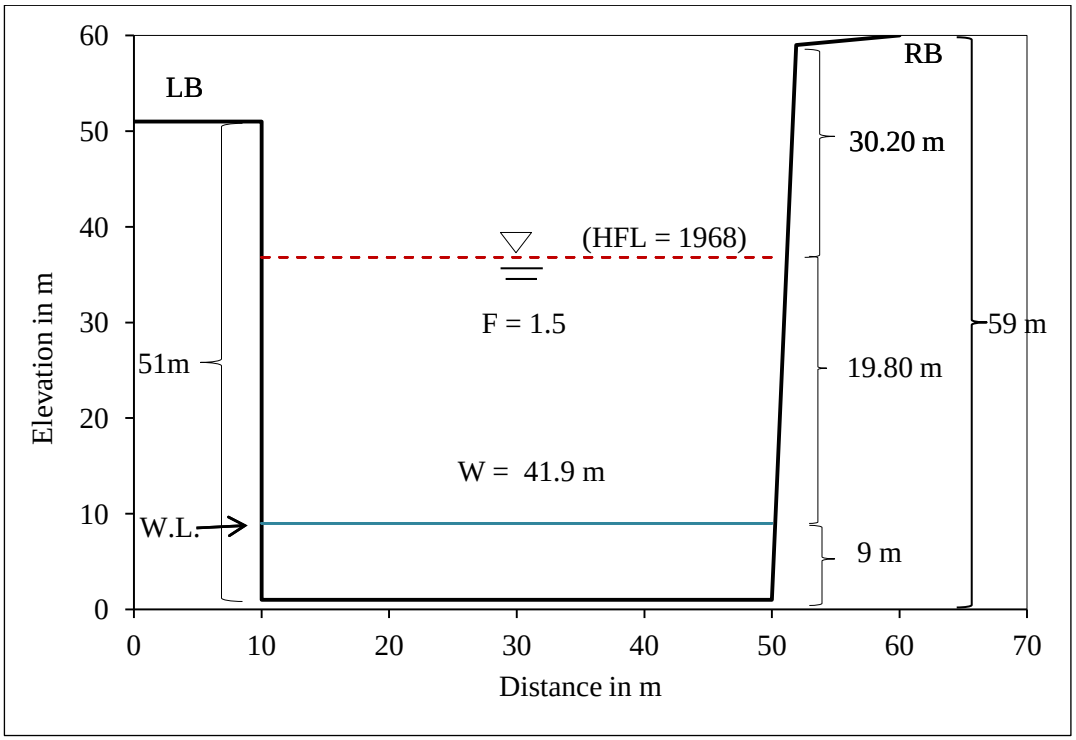


**Figure 4.106** Idealized cross-section of Par River at Mendha**;** See Figure 4.12 and 4.47 for location of site

**Figure 4.107** The Par River at Dhamni; See Figure 4.12 for location of site

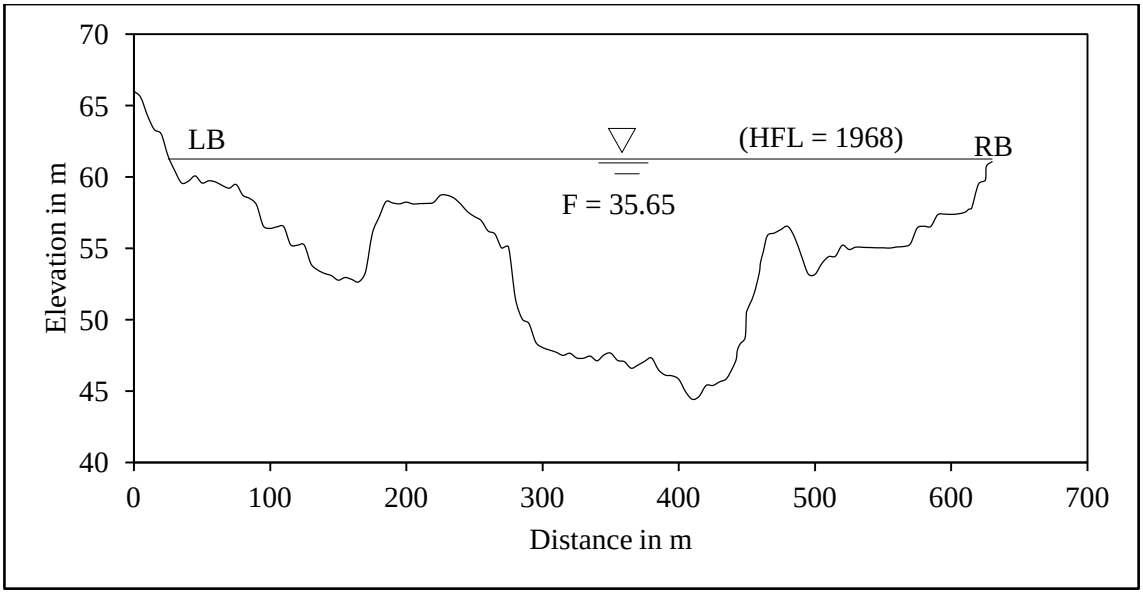


**Figure 4.108** The cross-section of Par River at Nanivahial; See Figure 4.12 for location of site

**Figure 4.109** The Par River at Nanivahial (gauging site); See Figure 4.12 for location of site

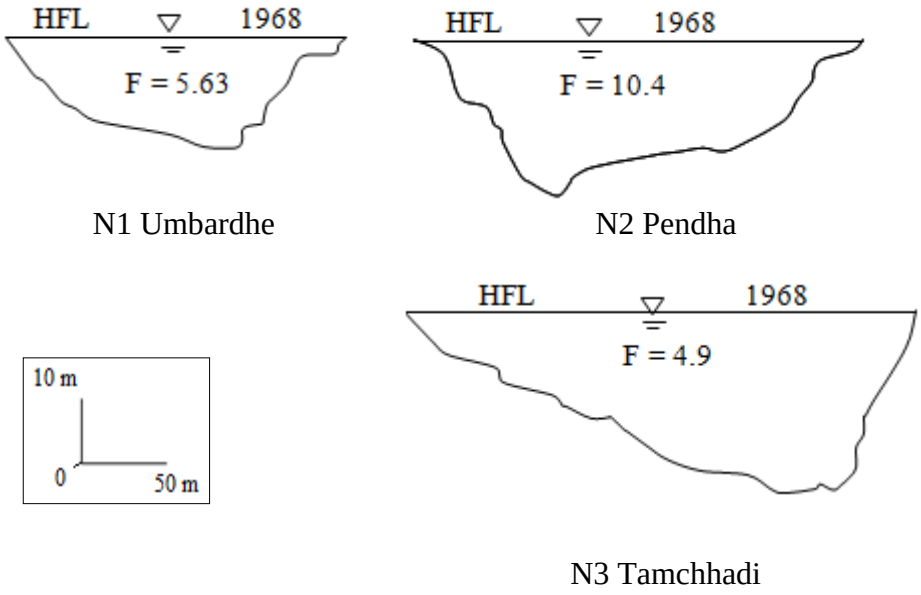


**Figure 4.110** Cross sections, Nar River; See Figure 4.12 for location of sites; F = Form ratio; HFL = High flood level

**Figure 4.111** The Nar River at Tamchhadi; See Figure 4.12 for location of site

**(ii) Changes in hydraulic variables with discharge**

The Table 4.45 and the Figure 4.112 clearly show that, the rate of change in the mean velocity (m) is greater than the rate of change in the mean depth (f) and width (b). The b/f ratio given in Table 4.45 indicates that the rate of change in width is always lower than the rate of change in mean depth. For Nanivahial site the rate of change in width is low, and b/f ratio is 0.20. This is attributed to nearly rectangular shape of the channel at this cross section. The results, therefore, confirm the inferences drawn on the basis of the changes in width-depth ratio with discharge, that the increase in the discharge is primarily compensated by a remarkable increase in depth. This has important implications for efficiency of the channel since the flood power is directly related to the flow depth.

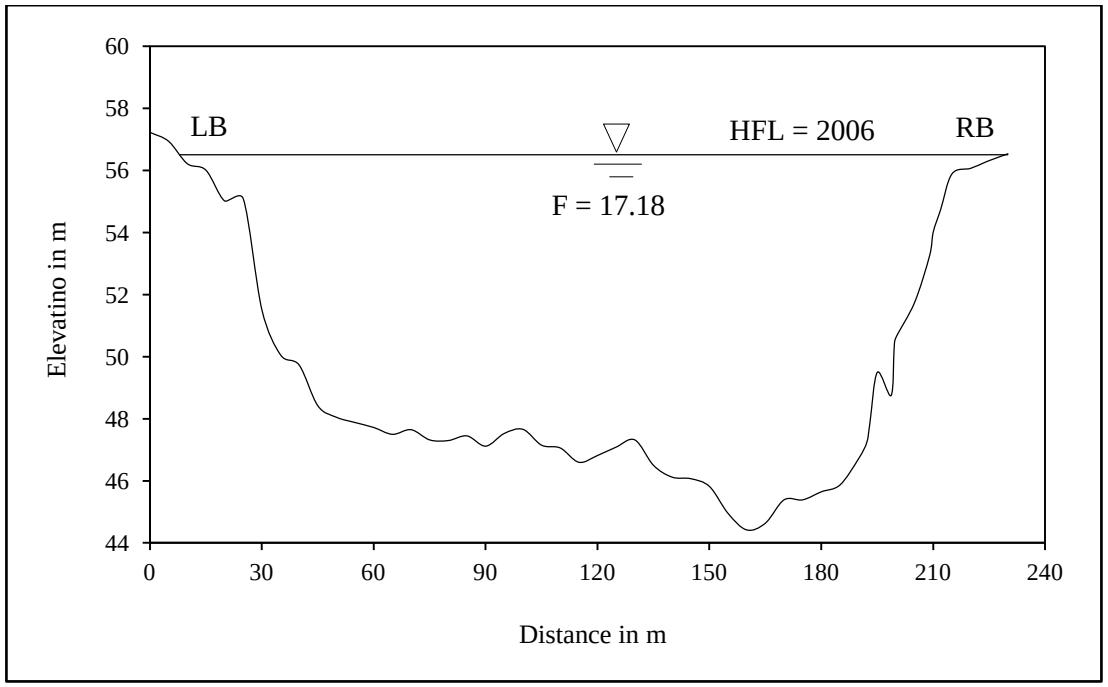


**Figure 4.112** Cross-section of Par River for bankful stage at Nanivahial, See Figure 2.13 for location of site

**Table 4.45** Exponent values of at-a-station hydraulic geometry

| No. | Site | Width (b) | Depth (f) | Velocity (m) | b/f ratio | m/f ratio | Total variance |
|---|---|---|---|---|---|---|---|
| 1 | Nanivahial | 0.048 | 0.25 | 0.71 | 0.20 | 2.93 | 0.57 |

See Figure 4.12 for location of site

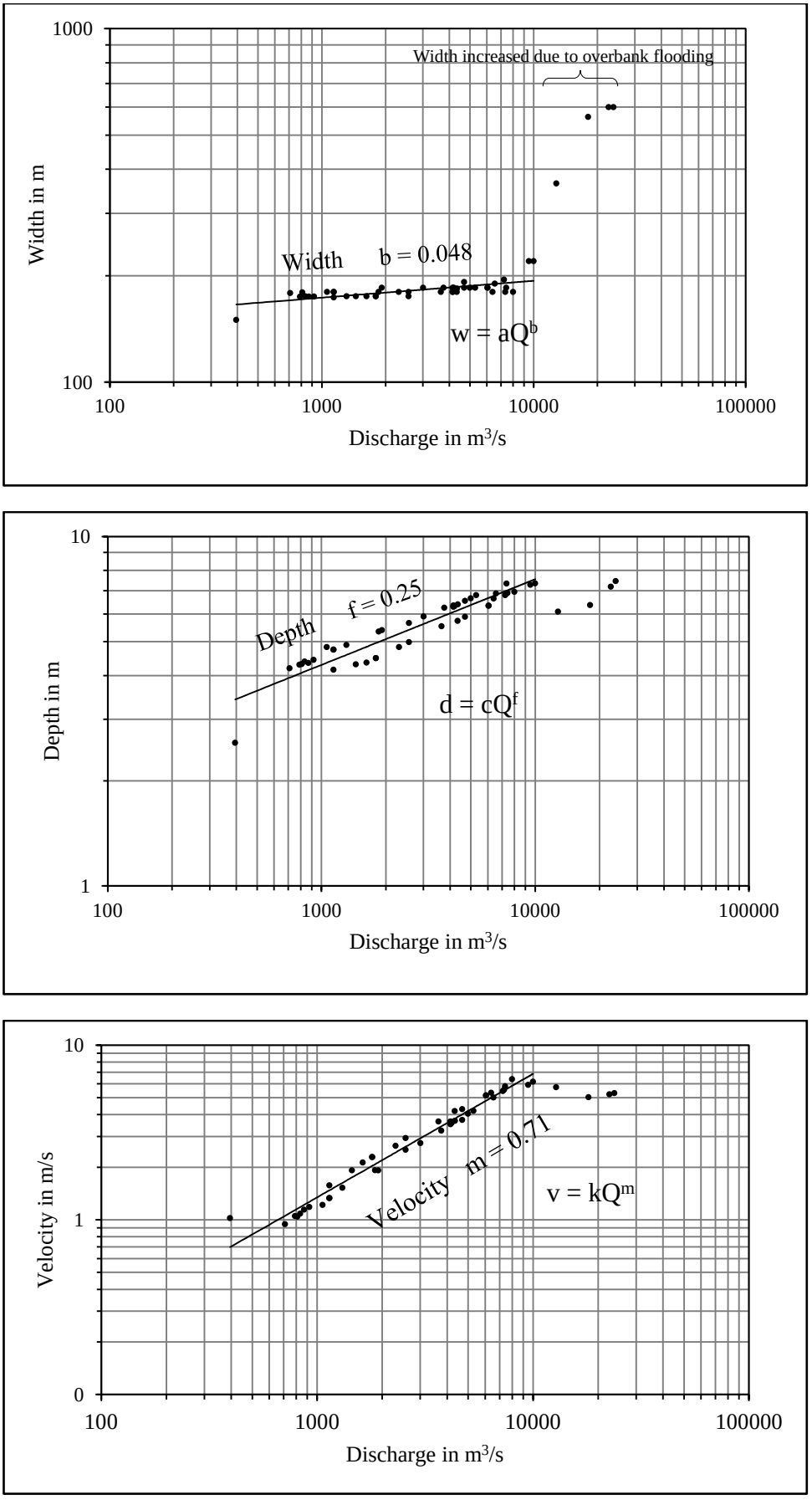


**Figure 4.113** Changes in width, mean depth and mean velocity with discharge at Nanivahial

The ratio between the rate of change in velocity and rate of change in depth (m/f) is related to the transportation of sediment load (Leopold et al., 1964). The higher the ratio, the more rapid the increase of the measured sediment load with increase of discharge (Leopold et al., 1964). Table 4.45 shows that, the value of this ratio is higher for Nanivahial. The high ratio suggests that the rate of increase of velocity with discharge much higher than the rate of increase of depth with discharge. This fact implies that high flows are associated with an increase in the transportation capacity of the channels. The ratio, therefore, suggest that the capacity of the flows to transport sediments increases rapidly with discharge.

An important concept linked with hydraulic geometry is the Langbein's concept of minimum variance (Rhodes, 1987). The total variance is the sum of the square of the hydraulic geometry exponents. Calculation of the total variance value for the Nanivahial site reveals that the value is 0.57 (Table 4.45), and thus, is away from the theoretical minimum total variance, which is 0.333 (Rhodes, 1987). This suggests that at the site the effects of changes in discharge are not equally absorbed by all the three variables, but by one or two hydraulic geometry variables (Rhodes, 1987), in this case the value of velocity (0.71) is much higher and followed by depth (0.25). This behavior of the hydraulic variables can be attributed to the box-shaped appearance of the channel and to the cohesive nature of the bank material. This fact therefore, suggests that the bedrock channel of the Par River behaves differently than alluvial channel, which is self-formed through the independent adjustment of the morphological variables (Leopold et al., 1964; Baker and Kale, 1998).

The hydraulic geometry exponents (b, f, and m) of the Nanivhahial gauging station were plotted on Rhodes (1977) ternary diagram (Figure 4.114). The point is observed at 'm-corner' i.e. velocity corner. This suggests that the primary adjustment in channel form with increase in discharge is in the mean velocity. The channel types were recognized on the basis of the location of the data points in the divisions of the ternary diagram. Figure 4.114 indicates that Nanivahial site of the Par River fall in sector 2. According to Rhodes (1977), such channel types are characterized by decrease in width-depth ratio, an increase in Froude number, and increase in velocity area ratio which in turn results in increased competence of river. This is also attributed to

rectangular form, relative stability of bed and bank material, extremely cohesive banks and compact bed, etc.

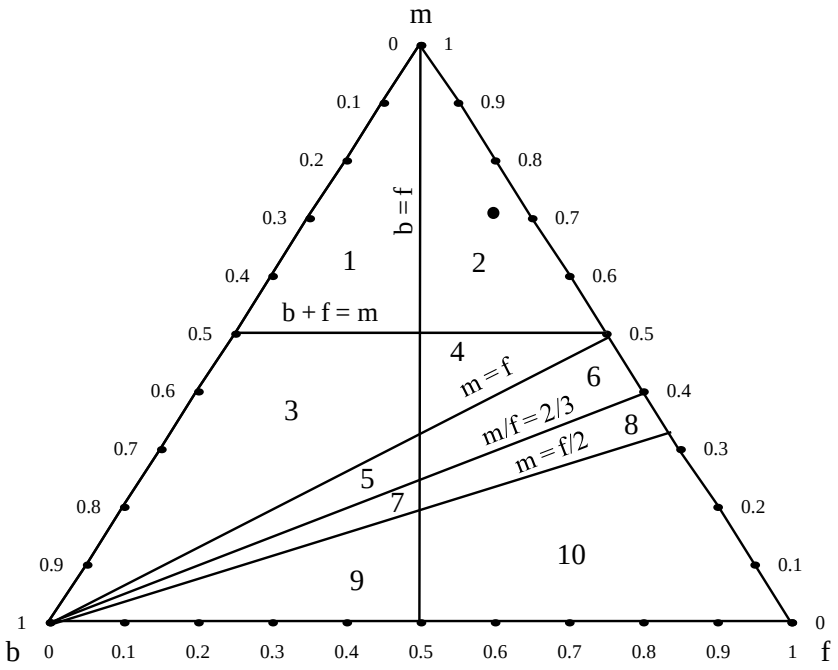


**Figure 4.114** The divided b-f-m diagram showing plotting position of at-a-station hydraulic geometry exponents for Nanivahial site

Chapter 5

# Conclusions and Major Findings

## 5.1 Introduction

The main aim of the present study is to understand fluvial forms and process of the bedrock channel of the Par River. Bedrock channel morphology reflects the interactions between erosive processes and the resistance of the channel substrate (Wohl, 1998). A variety of fluvially sculpted surfaces and erosional bedfroms were observed in bedrock channels, controlled by substrate type, flow regime and dominant erosional processes (e.g., Allen, 1971; Richardson and Carling, 2005; Springer and Wohl, 2002; Tinkler, 1997b). Bedrock rivers are predominantly erosional, however, they exhibit abundant depositional features. Infrequent large magnitude floods are associated with the processes of extensive erosion and deposition in resistant-boundary channels. In bedrock channels, erosive processes take place in the constricted reaches. These reaches of high flow energy and competence accelerate the amount of sediment transported and deposited by flood. The present study was carried out to systematically study the channel planform, different erosional and depositional landforms produced by the river.

Notably little information is available regarding the concrete processes by which bedrock channels are eroded. However, according Wohl (1998), the bedrock substrate is dominantly eroded by the processes of (i) corrosion, or chemical weathering and solution, (ii) corrasion, or abrasion by sediment in transport along the channel, and (iii) cavitation and other hydrodynamic forces associated with flow turbulence. Other processes such as shear detachment or fluid stressing, quarrying or plucking, hydraulic wedging and knickpoint migration may contribute for bedrock erosion. The bedrock channels are supply limited, therefore, coarse sediment entrainment and deposition is usually associated mainly with infrequent and extreme floods (Baker, 1988) since, energy required to transport a particle of sediment increases with its size. In present study, therefore, an attempt was made to find out the processes responsible for erosion of channel and grounds behind entrainment of coarse sediment within the channel.

The rock resistance refers to the inherent property of the rock to resist any changes in its shape or size. It is significant property of rock to find out the efficiency of various processes like weathering and erosion. In order to find out effects of rock strength/role of lithology in shaping the landforms, weathering phenomena and relative dating, the Schmidt hammer (SH) has now been adopted by Geomorphologists (e.g. Ericson, 2004). Besides lithology, tectonic uplift has also significant role in controlling the efficiency of erosional processes ultimately shaping the channels. It is well recognized, however, that the commonly-used geomorphic indices of active tectonics (GAT) have been developed as basic reconnaissance tools to assess the relationship between tectonics and basin morphology on the regional or basin scale and to identify areas experiencing tectonic deformation (Bull and McFadden, 1977; Keller, 1986; Keller and Pinter, 1996; Burbank and Anderson, 2001; Della Seta et al., 2004; Kale and Shejwalkar, 2008). The results of several geomorphic indices can be combined to provide an assessment of a relative degree of tectonic activity in an area (Keller and Pinter, 1996). The present study was, thus, carried out to study the role of lithology and tectonics in shaping the bedrock channel of the Par River.

River incision into bedrock is a significant erosion process that has an impact on the rate of landscape response to changes in rock uplift rate and climate (Howard et al., 1994). Rainfall, therefore floods, is one of the conspicuous climatic elements playing a significant role in landscape development, whose characteristics, predominantly, the distribution in space and time are important from the standpoint of flood generation in the monsoonal regions. Therefore, the present investigation has been undertaken to systematically study and assess the flood meteorological, flood hydrological and flood geomorphological characteristics of the area under review.

The major results and finding of the study are summarized below;

## 5.2 Summary of results

### *5.2.1 Morphological features of the Par River*

In order to understand the morphological features of the Par River, channel planform, the processes of channel erosion, deposition and transportation have been studied in detail and concluding remarks are given as follows;

**(i) Bedrock channel planform**

Three channel planforms namely straight, meandering and anastomoising channels have been recognized for the river under review. Thirty straight channel reaches having length more than 500 m have been identified on Par and Nar Rivers. The maximum length of perfectly straight channel reach is 2192 m at Chavra 3 and minimum length is 502 m at Payarpada 1 on Nar River. The average length of straight reaches is about 1161 m. Unfortunately, the formation processes of the straight channels are not known.

The Par River channel exhibits bedrock meanders. Analysis indicates that the average Si value for the channel is 1.74. Since the average value is greater than 1.5, the channel is said to be meandering. A constant ratio between the meander wavelength (λ) and the radius of curvature (Rc) has been constructed for the Par River. The minimum value of this ratio is three to one, maximum value is 10 to one. However, both the values are in contrast with minimum and maximum values of the ratio given by Leopold and Langbean (1966) for the alluvial rivers. It is, therefore, evident that bedrock Par River differs markedly as compared to meanders in alluvial valleys. A ratio between radius of curvature (Rc) and channel width (W) has been established. The range of values of the ratio of bedrock meanders of the Par River differ from the data given by Leopold and Wolman (1960) and Williams (1986) for alluvial rivers.

The exponent in the regression equation for the relation between meander wavelength (λ) and channel width (W) is close to unity (0.93). It shows that the relation between meander wavelength and channel width is considered linear. However, there is no radical departure from Leopold and Wolman's (1960) results for the relationship between meander wavelength (λ) and channel width (W) ($\lambda = 10.09\ W^{1.01}$) for alluvial rivers. The value of exponent for the relation between meander wavelength (λ) and mean radius of curvature ($Rc_m$) is not the unity but 0.71. This difference is perhaps due to variation in types of channel that are alluvial and bedrock. The relationship between amplitude (Am) and channel width (W) is in contract to the previous relationships established for alluvial rivers.

The extensive bedrock outcrops in the form of anastomoised/multi-thread channels were noted near Panchlai. The process of formation of bedrock anastomoised channel is attributed to insufficient channel capacity.

**(ii) Channel form/channel geometry**

Channel form/geometry has been studied in terms of width, depth and form ratio for the river under review.

By and large, in spite of the local variations in the channel width, there is a gradual increase in the width with an increase in the distance from the source. However, unlike width, the rate of increase in the depth is lower.

By using channel classification used by Rosgen (1994), the Par as well as the Nar River channel reaches at the cross sections surveyed fall in types of A to C.

There is a noteworthy drop in the width depth ratios at several locations, because of the wide nature of the channel. The drop in the ratios is medium at Kalmane, Jhiri, Chachpada and lowest at Mendha, due to narrow, deep channel. It, therefore, suggests greater hydraulic efficiency of bedrock Par River. The relation between channel width (W) and drainage area (A) suggests very good positive relations.

**(iii) Erosional features of bedrock channel**

Various erosional landforms have been identified and mapped for the Par River.

**a. Potholes**

Majority of large potholes in terms of diameter and depth have been located upstream of knickpoints thereby indicating most prominent incision and erosion in bedrock. The higher values of coefficient of variations (Cv) of all the morphometric parameters of potholes reveal greater variability in shapes and sizes of the potholes. The positive values of skewness propose the occurrence of one or two or a few very large potholes in terms of diameter, length, width and depth. The high values of kurtosis suggest that the distribution is leptokurtic thereby indicating that the morphometric parameters of the potholes of the Par River are close to the mean values. According to the categorization of potholes based on their shapes, frequency of circular and oval shaped potholes is highest than that of elongated, dumbbell and irregular shaped

potholes. The relation between diameter of potholes (K) and depth of potholes (D*) is considered linear. The relationship between Length (L) and depth of pothole (D*) is moderate.

**b. Longitudinal grooves**

The values of coefficient of variations of all the morphometric parameters of grooves indicate moderate variability in morphometry of grooves. All the values of $C_s$ are positive indicating the occurrence of one or two or a few very large grooves in terms of length, width and depth. The high values of $C_k$ for length and depth suggest that the degree of peakedness is said to be leptokurtic. However, the value of $C_k$ for the width is low suggesting that the distribution is platykurtic. It further indicates that the width of the grooves does not vary much.

**c. Inner channel**

Very high values of stream power per unit area and bed sheer stress (e.g. 52125 $W/m^2$ and 3320 $N/m^2$ respectively) must have resulted high-energy erosional processes such as cavitation and microturbulent plucking and must have formed inner channels of Par River.

**(iv) Longitudinal profile**

The longitudinal profile of the Par River shows a concave upward curve that reveals progressive decrease in gradient in the downstream direction. The channel of a Par River is characterised by five major knickpoints along its course. Such knickpoints are the locations of the higher concentration of energy dissipation along the course of the Par River. Pothole erosion at the lip of these knickpoints, are therefore, considered significant factor for headward erosion.

**(v) Depositional features of bedrock channel**

Bedrock rivers are predominantly erosional, however, they exhibit abundant depositional features as follows;

**a. Expansion bar**

Numerous expansion bars have been formed at abrupt expansions downstream of constricted reaches of the Par River.

**b. Hydraulic parameters associated with depositional features**

The estimated values of bed shear stress, unit stream power, and mean velocity generated by reconstructions of flows in the constricted reaches in vicinity of the depositional features, reveal that the river flows are several orders of magnitude higher than the threshold values for the entrainment of boulders. However, the values of hydraulic parameters associated with depositional features are much lower than the actual values estimated for rare floods in vicinity of depositional features.

### *5.2.2 Erosional processes and sediment transport*

Cavitation, shear detachment or fluid stressing, quarrying or plucking, impact erosion or abrasion, hydraulic wedging and knickpoint migration are some of the dominant processes which have incised bedrock channel of the Par River.

**(i) Flood hydraulics and hydrodynamics**

The effect of infrequent and large magnitude floods on the Par River was computed using parameters of flood hydraulics and hydrodynamics such as unit stream power, shear stress, Froude number, Reynolds number and critical velocity for inception of cavitation.

**a. Shear stress (τ)/ fluid stressing/ shear detachment and unit stream power (ω)**

From the calculated hydraulic data of the Par River, unit stream power and bed shear stress ranges between 616 and 52125 $W/m^2$, and 125 and 3320 $N/m^2$ respectively. These values indicate unusually high ability of the river to erode and transport coarse sediment. By using William's equations, thresholds of shear and entrainment have been analyzed. It is notable that the sediment transport rates and sediment entrainment are driven by excess shear stress over a threshold value (Turowski, 2012). In case of Par River the actual values of shear stress and unit stream power exceed the theoretical values, thereby indicating capability of flows to entrain largest boulders.

**b. Froude number (Fr) and Reynolds number (Re)**

The Fr numbers for the Par River range from 0.13 to 1.96. The reach upstream of Ghatalbari knickpoint shows spatial variability in hydraulics along the bedrock channel of the Par River. This reach has undulating thalweg, shows standing waves (Fr = 1) of water with critical waves system. Such reaches are incised rapidly and therefore, express very localized but persistent hydraulic forces expended on the resistant boundary channels. Broken standing waves have also been observed in channel in the form of turbulent flow with foamy water (white water) and breaking wave crests near Ghatalbari. The flow may remain critical with increasing stage and velocities may stabilize without increasing, as energy is dissipated across the entire channel width (Tinkler, 1997a; Tinkler, 1997b) or depth. This is, in particular, possible to happen if the channel boundaries at high stages (water levels) are strongly confined or are especially rough (Tinkler and Wohl, 1998). The Mendha gorge on the Par River is pertinent for above situation having strongly confined and rough gorge walls having critical Froude number. The hydraulic analysis of Par River indicates that the Froude number greater than 1 (highly erosive supercritical flow) have been reached on several occasions. In addition to this, roll waves or slug flow have been generated at steep reaches of Kalmane site as the value of Froude number is 1.96 and it exceeds 1.6. As depths increase in the bedrock channel the flow may remain critical, become supercritical, or revert to subcritical as downsteps and smaller knickpoints begin to drown out. In comparison, the supercritical and critical flows are shallower, nevertheless, faster than that of subcritical flow, and enhance sediment transport of large clasts (Hopkins, 1844). Thus, the large clasts of Par River have been transported downstream, wherever, flow remain supercritical and critical. High values of Reynolds Number (Re) (>2100) of the Par River indicate that the flood discharges were extremely turbulent, and thus, are capable of accomplishing a variety of geomorphic activities.

**c. Critical velocity for inception of cavitation (Vc)**

Estimates of the values of critical velocity for inception of cavitation indicate that none of the powerful floods on the Par River exceed the conditions expressed by the equation of critical velocity for inception of cavitation except at few deep narrow gorges where inception of cavitation is possible. The critical velocities required for

inception of cavitation for such sites are 11.54 m/s and 16.12 m/s. However, the actual velocities estimated for these sites are 15.70 m/s and 16.62 m/s. This, therefore, suggests that channel adjustment produced by cavitation tend to inhibit or reduce the forces that would cause the threshold to be crossed in nature (Baker and Costa, 1987).

**d. Hydraulic plucking**

Majority of dykes in the Par River are highly dissected due to the process of plucking.

**e. Knickpoint migration and river incision**

Headward migration of a knickpoint through resistant substrate can leave behind a deep and narrow gorge, it reflects the erosional resistance of the channel boundaries, and maximizes the shear stress and stream power per unit area of a given discharge and channel gradient (Baker, 1988; Wohl, 1992, 1998; 2000a; Ikeda, 1997). Similar observations have been noted for the Par River as well as for its tributaries, where, deep and narrow gorges are observed immediately downstream of knickpoints.

Quantitative analysis of SPEM reveals that the incision rate of Kalmane Gorge is 6.57 x $10^{-05}$ m/yr (0.0657 mm/yr) and that of Bhimtas Gorge is 9.66 x $10^{-05}$ m/yr (0.0966 mm/yr). The above incision rate is less when compared with the range of incision rates given for mountains landscapes (i.e. 0.149 mm/yr to 0.736 mm/yr). The comparatively low rate of incision of the Par River is obvious because the incision is not associated with the mountain-building tectonic processes where the rates of upliftment are reasonably faster.

**(ii) Coarse sediment transport**

The resistant-boundary channels such as channels of the Par River are supply-limited, coarse sediment entrainment and deposition is usually associated with infrequent and extreme floods. The presence of large boulders along the Par River provides evidences to the competence of flows. The estimated values, when compared with the values of bed shear stress, unit stream power, and mean velocity generated by reconstructions of flows, reveal that the river flows are several orders of magnitude higher than the threshold values for the entrainment of boulders. The values indicate unusually high ability of the river to erode and transport coarse sediment. These estimates and the hydraulic characteristics of the Par River further suggest that high

flows can easily move cobbles in suspension, and large boulders as bedload. The calculated figures further propose that floods are competent enough to transport the largest ever recorded boulder present on the channel bed. In the bedrock channels, such as the Par River, the unit stream power and bed shear stress values are higher by several orders of magnitude than those that occur in the alluvial channels.

### *5.2.3 Role of lithology and tectonics*

**(i) Rock mass strength of resistant boundary channel of the Par River**

Schmidt hammer rebound values have been analyzed to derive rock mass strength (RMS). The average values of RMS range between 63.18 and 91.35 N/mm$^2$, which can be surpassed only during infrequent large magnitude floods that occur at long intervals. According to several previous researchers, high-magnitude flows are significant to shape bedrock channels and associated erosional features as only such flows are capable of exceeding the high boundary resistance provided by bedrock channels (Baker and Kale, 1998). The value of the coefficient of variation is 15%, which proposes less variation in the RMS of the rocks of the Par River. It further states that the formation of majority of rocks belongs to the same period. The RMS for the river under review varies spatially. Even though it does not show any specific pattern or trend in surface hardness, there is gradual increase in RMS values towards downstream direction. According to classification given by Selby (1993), the rocks in association with Par River are competent igneous and comparatively strong in nature. Therefore, only high magnitude, infrequent floods are capable of making alterations in the resistant boundary channels of the Par River.

RMS values of dykes were derived to find out control of dykes on the river. According to analysis, the average RMS of dykes is 92.72 N/mm$^2$, it is greatest than that of other rocks in the river mainly due to hardness of dykes in nature. The value of the coefficient of variation (10.75%) suggests that there is very less variation in the RMS of dykes of the Par River. It further reveals that the formation of majority of dykes belongs to the same period. However, it is pertinent to mention here that the observations are based on limited number of dykes.

Box-whisker plots have been used to show the differences in erodibility semi-quantitatively between basalt and dykes. It is clear from the plots that the basalt rock

is comparatively weaker than dykes in terms of Schmidt hammer readings and RMS. Based on the previous assumption that Schmidt hammer readings and RMS measures are inversely related to erosional resistance. The results of this analysis support the hypothesis that the differences in rock erodibility are present. It is further proved by control of dykes on the channel of the Par River at few locations. However, more detailed studies and more number of samples are necessary to strengthen the said hypothesis.

**(ii) Geomorphic Indices of Active Tectonics (GAT) in morphotectonic analysis**

The present study has used five commonly used geomorphic indices (excluding mountain front sinuosity, which is one of the commonly used indices in tectonic geomorphology) as reconnaissance tools to assess the relationship between tectonics and basin morphology on basin scale and to identify areas experiencing tectonic deformation.

Combination of the results of several previous case studies shows that areas undergoing rapid tectonic uplift should exhibit the following characteristics with respect to GAT indices (Bull and McFadden, 1977; Keller and Pinter, 1996; Matmon et al., 1999; Burbank and Anderson, 2001; Silva et al., 2003; Molin et al., 2004; Della Seta et al., 2004; Peters and Van Balen, 2007; Al-Taj M. et al., 2007; Kale and Shejwalkar, 2008; Figueroa and Knott, 2010; Dehbozorgi et al., 2010; Jayappa et al., 2012).

- High hypsometric integral indicating deep incision and rugged relief.
- Asymmetry factor significantly greater or less than 50 suggesting tectonic tilt.
- Anomalously high SL index values in regions underlain by uniform lithology.
- Low values of Vf (<1) reflecting very deep, narrow V-shaped valleys occupied by actively incising streams.
- Very low elongation ratio for tectonically disturbed rivers.

Examination of the results of GAT reveals that, though not very prominently, The Par Basin shows known typical geomorphometric characteristics of an area undergoing uplift and deformation. The GAT indices values of hypsometric integral, basin asymmetry, stream gradient index, valley form and elongation ratio are associated

with drainage basins affected by active tectonics and deformation. Although the value of hypsometric integral of the Par Basin is 0.30, indicating prevalence of mature or subdued topography, the upper approximately 2/3$^{rd}$ area of the basin shows deep incision and rugged topography particularly on the Jawhar Plateau. The river valleys in the upper and middle basin are deep, narrow and V-shaped valleys occupied by actively incising streams, with average Vf value of 1.18. This value, though not less than 1, demonstrate presence of rapid valley downcutting and incision. There is also presence of basin asymmetry. The distribution of basin area with reference to the trunk stream shows tilting perpendicular to the direction of the master stream. Similarly, the elongation ratio of the Par Basin is 0.49, suggesting that the basin is moderately elongated, as expected in an uplift-dominated region. If one strictly follows Bull and McFadden's (1977) interpretation of the elongation values, then one has to conclude that elongation ratio (0.49) of the Par Basin implies that the basin is undergoing uplift. Thus, in view of the facts presented in this study, it can be stated that the Par Basin belongs to the class of relatively high tectonic activity as compared to other river basins of western DBP.

### *5.2.4 Flood hydrometeorology, hydrology and geomorphology*

Hydrometeorological, hydrological and geomorphological characteristics associated with rainfall and therefore floods on the Par River led to the following conclusions.

**(i) Flood hydrometeorology**

The spatial variation in the monsoon rainfall shows interplay of meteorology and topography characteristics. The foremost grounds behind spatial variation of the rainfall in the basin are;

- The Par River and its tributaries originate in the highlands of Western Ghats. The orographic lifting of the central highlands i.e. Barhe Plateau and the Western Ghats are responsible for enhancing the spatial variation in monsoon rainfall.
- Geographical location, orographic effect of Barhe Plateau (interflew of Par and its major tributary Nar) and the east-west trending ranges in the Par Basin, for instance, Peth Range, Surgana Range and other interfluves act as barrier for the rain bearing south-west monsoon clouds. It attributes to maximum amount of rainfall in the middle reaches of Par River (2200 mm to 2300 mm).

- Average relief of the adjacent Damanganga Basin appears to be less than that of Par Basin. Therefore, monsoon clouds easily enter in the basin and due to obstacle in the form of Peth Range orographic lifting takes place near Mandava. The above situation results into maximum amount of rainfall at Mandava (2400 mm).
- Being distant from coast, the amount of rainfall reduces towards the source of the Par and Nar Rivers. It ranges between 1700 mm and 1800 mm. However, due to proximity of coast the amount of rainfall is more at the western part of the basin (2000 mm to 2200 mm).

**a. Spatial and annual variability**

More than 98% of the annual rainfall is recorded during the monsoon season. The average annual rainfall of the basin ranges from about 1800 mm to 2200 mm rainfall with the basin average annual rainfall 2094 mm. Generally, the basin receives monsoon rains from mid-June with the onset of southwest monsoon. July is the rainiest month throughout the basin followed by August and they account for 39% and 27% the total annual rainfall of the basin respectively. The monthly rainfall totals also vary during the monsoon season.

**b. Interannual variability**

Like other parts of the monsoon tropics, there is variability in the annual as well as monsoon rainfall between years. This variability increases, in general, with the distance from the source and the basin outlet. With climatic variability in such a region there is inevitably drought or flood. Interannual variability is not particularly high, which is proved by less coefficient of variation (Cv) (27-33 %) of annual rainfall in most parts of the Par Basin. All the gauging sites show very high range of annual rainfall. The values of the coefficient of skewness ($C_s$) are positive for all the sites, ranging between 0.55 and 1.08. The Pardi site reveals relatively high positive $C_s$ value. The positive $C_s$ values suggest the occurrence of a few very wet years during the gauged period.

Interannual variability for the Par Basin, indicates that, prior to 1930, the rainfall was frequently below-average, but the interannual variability was low. On the other hand, from 1930 to 2004, many years recorded above-average annual rainfall, but the

interannual variability was high. Interestingly, this period of high interannual variability was characterized by increased large floods on the Par River. Summarizing it can be said that the Par Basin displays a marked concentration of rainfall within a few months of the year, episodic high-magnitude rainfalls and high intra-annual as well as inter-annual variability in rainfall. It is such events that are important from the point of view of floods.

**c. Flood-generating meteorological conditions**

The principal cause of large floods on the Par River is severe rainstorms or Low Pressure System (LPS). The systems, which comprise lows, depressions and cyclonic storms (Dhar and Nandargi, 1995), cause big stream rise leading to large floods. Streamflow records available for a site on the Par River specify that low pressure systems (LPS) can have an immense impact. All the LPS associated with floods on the Par River generally occur either in the month of July or August. By this time, on an average about 67% of the annual rainfall is received and soils are fully saturated, which in addition boosts the magnitude of floods. In general, during the passage of LPS, it causes heavy falls of rain along and near their tracks. The LPS (Bay or land depressions) which follow a westward track through Tapi Basin are more effective in causing heavy rainfall and floods in the Par Basin. The mean track of LPS prepared for the basin, reveals that the LPS travel in a west-northwest or northwest direction to produce floods in the Par Basin. Besides, majority of the large floods were associated with Bay depressions, nevertheless, two largest floods of the 20$^{th}$ Century (1968 and 1970) resulted from the land depression.

Two types of flood-producing LPS can be identified according to their path.

**ca. LPS that moved roughly parallel to the basin axis**

There are few LPS tracks that have moved parallel to the basin axis, and have been coupled with very large floods. The August 1968 and September 1970 LPS are excellent examples of this kind. These two cyclones were responsible for heavy rainfall in the Par Basin, since the basin remained in the southwest sector of these LPS. The above tracks were responsible for high flood levels and discharges in the Par River, for instance due to passage of LPS in 1968, highest gauged discharge i.e. 23820 $m^3/s$ has occurred at Nanivahial. Sometimes, ‘antecedent precipitation’ causes

large floods in the basin. Well-known example of above situation is that of 4-6 August, 1968 flood. It is interesting to note that the LPS that produced the largest flood of the 20th Century was preceded by another depression between 29th and 31st July 1968, that is about a week before the mega event. Thus, in spite of the fact that the year 1968 was a below-normal rainfall year, two rainstorms deposited large amounts of precipitation within a short period, and thus produced the largest ever recorded flood of the 20th Century.

**cb. LPS that passed from north-east direction of the basin**

The majority of the LPS have passed from north-east direction of the basin and it has produced high-magnitude floods in the Par Basin. The flood magnitude due to such cyclones may vary over the different reaches of the Par River. The best example of this is provided by the 1966 depression, which was responsible for high flood levels in the Par River with 8000 $m^3/s$ discharge at gauging site of Nanivahial.

**d. Relationship between annual rainfall totals and flood occurrences**

A plot of average annual rainfall (Par Basin) and discharge (Nanivahial site) departure from their respective averages has been constructed. The graph clearly reveals that two major floods (1976 and 2004) recorded at Nanivahial, have occurred during the years of above-average annual rainfall. However, it is of interest to note that the 1968 flood, which was the largest flood of the 20th Century, occurred during a below-average rainfall year. The year 1994 has produced the highest average annual rainfall in the basin (3389 mm). However, this year did not record the peak flood in basin. It may be attributed to the well distributed rainfall throughout the monsoon season but not the intense flood producing rainfall.

**e. Normalized accumulated departure from mean (NADM) method**

The NADM graph shows the long-term trends of rainfall and it provides patterns for the Par Basin. The rising natures of NADM graph indicates above-average conditions, while, falling nature of the graph reveals with the below-average conditions of rainfall. The NADM graph proposes that the rainfall amounts were below-average in the beginning of the 20th century i.e. up to 1930. The middle part of the century i.e. from 1930 to 1960 is characterized by sharp rise in the graph, which specifies the period of above-average rainfall conditions. The graph shows short term rising and

falling trend after 1960, nevertheless, above average condition in general. This period has yielded the largest ever recorded floods on the river. It is, therefore, reasonable to state that the large magnitude floods on the Par River have occurred in the modern period. Consequently, the analysis of the annual rainfall data of the basin relating to the deviations in the amount clearly indicates that the major changes in the rainfall occurred around 1930 and 1960. Similar noteworthy changes have been identified by Mooley and Parthasarathy (1984); Fu and Fletcher (1988); Parthasarathy et al. (1991) and Kripalani and Kulkarni (1997) in the monsoon conditions about the same years in India. The association of all-India monsoon rainfall (Parthasarathy et al., 1991) with the rainfall of the Par Basin show remarkable similarity in their long-term fluctuations.

**f. Long-period fluctuations in monsoon rainfall and floods**

The rainfall over the Par Basin is highly susceptible to the changes in the Indian southwest monsoon which is teleconnected with the ENSO events. To examine the relationship of the magnitude of the rainfall and the condition of the ENSO in different years, the conditional probabilities of the rainfall have been calculated. The analysis shows that the probability of having high rainfall is 0.25 (25%) during La Niño/cold ENSO conditions, the probability of low rainfall is 0.57 (57%) during warm ENSO conditions. Although the probability of more rainfall during La Niño/cold ENSO is not very high, the probability of low rainfall during warm ENSO is high i.e. 0.57 (57%).

**g. Detection of changes in the annual rainfall**

Mann-Kendall test has been used to evaluate the long-term changes/trends in the annual rainfall records of the Par Basin. The positive (negative) sign of tau ($\tau$) in analysis indicates increasing (decreasing) trend. Therefore, the positive value of $\tau$ i.e. 0.067 for the Par River suggests that the rainfall trend for the given period is increasing. However, the trend is statistically significant or not is to be tested by testing the significance of tau ($\tau$). The application of this non-parametric test to the annual rainfall data of the basin designates no significant trend at 0.01 and 0.05 level. The analysis states that the Par Basin, as a whole, does not show any noteworthy rainfall trend over the period of a century. The majority of the investigations for larger

areas (all-India scale) during last few decades have given analogous results. These studies noticeably specified that the monsoon rainfall, mainly on all-India scale, is trendless and is primarily random in nature over a long period of time, (Mooley and Parthasarathy, 1984). Srivastava et al. (1998) employed Mann-Kendall test to find the trend in rainfall over India for the period 1901-1992. His analysis concluded that more or less all-India rainfall does not show any specific trend.

**h. Detection of future changes in the rainfall**

The results of application of the t test to the statistical parameters of the rainfall data of the Par Basin shows that, on the basin scale 16% change in the annual rainfall is required in the average rainfall of next 10 years to consider it different than the available rainfall record. Likewise, to establish the significant change in the rainfall of the next 20 and 50 years, the average rainfall should differ by 12 and 7% correspondingly than the present mean of the rainfall. While, to declare the average rainfall of the present century ($21^{st}$ century) considerably different than the previous century ($20^{th}$ century), 7% change is required in the long-term mean of the rainfall of the basin. The analyses of the t test as well as other analyses accomplished in the previous sections of this chapter specify that the monsoonal rainfall of the Par Basin is highly regular and reliable. Consequently, it is probable to be the same in this as well as in the next century.

**(ii) Flood hydrology**

**a. Flood hydrology of the Par River**

It is obvious from the above discussion that monsoon regime plays an important role to determine the river regime conditions of the river under study. Therefore, on the basis of available annual peak discharge data, an attempt has been made to understand the magnitude, variability and frequency characteristics of individual high flow events or floods on the Par River and its tributaries.

**aa. Flood regime characteristics**

The available gauged data for Nanivahial site shows that the mean discharge is 5030 $m^3/s$. The highest flood ever recorded on the Par River at Nanivahial in 1968 was of the order of 23820 $m^3/s$, Nevertheless, the estimated high magnitude flood for the Par

River reaches up to 38000 $m^3/s$ for site Parvas, which is just eighteen km downstream from Nanivahial.

**aaa. Interannual variability in annual peak discharges**

The plot of interannual variability reveals high annual peak discharges. It also shows the occurrence of three large events i.e. in year 1968, 1976 and 2004 during the gauge period. These events, nonetheless, were entirely natural. The unusual high discharges were principally the outcome of Low Pressure System (LPS) developed over Bay of Bengal and adjacent land. The bedrock reaches of the Par River undoubtedly limit the width of the flow and consequently the increase in discharge is principally compensated by a distinct increase in the velocity and depth. Hence, it can inferred that the bedrock reaches characterize higher velocities and therefore extremely high flood power. This situation in bedrock reaches of the Par River resulted into acceleration of geomorphic work to accomplish.

**aab. Average magnitude and variability**

Floods that are credible to cause remarkable geomorphic change are those that generate discharges many times beyond the mean flows experienced by a river (Kochel, 1988). The Qmax/Qm ratio for Nanivahial site is 4.74. This, therefore, indicate that the maximum annual peak discharge (Qmax) is about 5 times higher than average peaks. The effect of such extreme flows on geomorphic activity in channel is likely to be noteworthy.

Besides the Qmax/Qm ratio, the coefficient of variation (Cv) is another useful measure of variability in the annual peak discharges. It is the ratio between standard deviation and the mean. The Cv for Nanivahial site is 1.03 (or 103%). It proposes that the variability in peak flows at Nanivahial Site in the Par Basin is in fact higher.

The FFMI value of the Nanivahial site is 0.42. The relatively higher FFMI value of indicates slightly flashy and variable nature of floods. The index further indicates that the possibility of the river experiencing noteworthy geomorphic work during large floods.

**aac. Skewness ($C_s$)**

The Nanivahial site on the Par River shows high positive $C_s$ Value i.e. 2.2. The positive $C_s$ value suggests the occurrence of one or two (or a few) very large-magnitude flows during the gauge period. The $C_s$/Cv ratio for gauging site is 2.14. This, therefore, proposes that the distribution of peak discharge is positively skewed.

**aad. Unit discharges**

The unit discharges for the Par Basin ranges between 5.4 and 101 $m^3/s/km^2$. The average unit discharge for Par River is 27.77 $m^3/s/km^2$. The unit discharge of the Par Basin (27.77 $m^3/s/km^2$) is extremely higher than other world rivers with comparable drainage areas. Therefore, Par River is capable of producing large floods compared with rivers with comparable drainage areas in the world. Such larger discharges are likely to be effective in terms of geomorphic changes in the channel and valley.

**ab. Flood frequency analyses**

According to GEVI probability distribution estimated peak flows for different return periods such as 2, 5, 10, 25, 50, and 100 years are 4200, 8767, 11777, 15618, 18576 and 21327 $m^3/s$ respectively. The distribution has also been employed to estimate the recurrence interval of mean annual peak discharge (Qm), large flood (Qlf) and actually observed maximum annual peak discharge (Qmax) and the recurrence interval is 2.33, 6.93 and 185.47 years respectively. In the GEVI analysis, the observed annual peak discharges have been plotted against the return period or F(X) values (plotting positions) on the Gumbel graph paper, designed for GEVI probability distribution. Interestingly, in plot of GEVI distribution, the actually observed peak on record (Qmax) falls well close to the fitted lines. This means the return period of Qmax of Nanivahial station predicted by GEVI distribution are likely to be quite reliable. In addition to above probability distribution, the recurrence interval of high-magnitude flood events that have occurred on the Par River at Nanivahial were predicted by using Weibull formula. According to that the return period for Qmax i.e. 23820 $m^2/s$ (1968) is 50 years, for Qm is 2.9 years and Qlf is 10 years.

**aba. Discharge-area envelope curve**

The envelope curve prepared for the Par Basin shows that there is a rapid increase in the maximum possible discharge with an increase in drainage area. The peak gauged discharge for Nanivahial site for year 1968 lies much above the world envelope curve prepared by Baker (1995). The peak flows estimated for nine sites on the Par and a site on Nar River also lie above the world envelope curve for the respective drainage area. However, remaining sites fall below the world envelope curve. A comparison with Baker's (1995) world envelope curve indicates that Par Basin can produce relatively high flood peak discharges than some of the drainage basins with comparable basin areas in the other parts of the world. This is to say that under given climatic, hydrologic and physiographic conditions, extraordinary floods can be produced in the Par Basin and expected to generate large forces to cause enduring changes in the channel and valley morphology.

**(iii) Flood geomorphology**

The morphological characteristics of the Par River have been described with reference to the channel reach and cross section variables.

**a. Channel form with respect to high flood level (HFL)**

Due to significance of infrequent large magnitude floods in shaping the bedrock channels, an attempt has made to study the morphology of channel with respect to high flood level (HFL).

**aa. Water surface width (w)**

Most of the cross-sections of the Par River are generally trapezoidal and saucer shaped. The channels are narrow in the upper reaches and significantly wider in the middle and lower reaches. The average channel width of the Par River is about 230 m and it varies from 42 m to 600 m. The average width of Nar River is 114 m. In upper reaches, the rocky channel of the Par River is typically narrow where, in middle reaches, it is moderately wide. However, the channel exceptionally becomes narrow at the Mendha Gorge (42 m). The channel width increases abruptly from the confluence of Par and Nar River up to mouth of the river. In spite of the local variations in the

channel width, there is a gradual increase in the width with an increase in the distance from the source.

**ab. Flow depth (D)**

The maximum channel depth of the Par River is 29 m and minimum depth is 6.3 m. The average channel depth is 13.3 m. There is gradual increase in depth in the downstream direction, however, unlike width, the rate of increase in the depth is lower.

**ac. Form ratio (F)/ width-depth ratio (w/D ratio)**

The form ratio for Par River varies from 2 to 35. The average width-depth ratio is about 16.03. Osborn and Stypula (1987) employed width/depth ratio to characterize channels for hydraulic relations using channel boundary shear as a function of channel shape, according to the their classification ten as of sixteen cross-sectional sites reveals moderate to high width-depth ratio (W/d ratio > 12). Rosgen's (1994) channel classification states that, the Par as well as the Nar River channel reaches at the cross sections surveyed fall in types of A to C, representing relatively straight (A) (sinuosity < 1.2; W/D ratio < 12 ), low sinuosity (B) (sinuosity > 1.2 to < 1.4; W/D ratio > 12), meandering (C) (sinuosity > 1.4; W/D ratio > 12).

Width-depth ratios for high flood level (HFL) is variable at different reaches of the Par River, ranging from deep narrow to wide open. During the dry season and during low flows the water spreads at few cross sections, and the width is greater and depth is smaller. Therefore, the width-depth ratio is high and the channel reflects all the characteristics of a shallow-wide channel. However, in response to heavy rainfall as the stage and discharge increases, there is an increase only in the depth of flow in deep-narrow channels. As a result, the width-depth ratio decreases, and the hydraulic efficiency increases dramatically. The plot of width-depth ratios for low flows as well as high flows for different cross-sections along the Par River shows noteworthy drop in the ratios in the lower reaches, because of the very wide nature of the channel of the Par River in these reaches.

**ad. Mean depth (d)**

The mean depth of the Par River ranges from 4.40 to 28.8 m. The average depth is about 9.60 m. Such high value reflects the high efficiency of the channel of the Par River. Like the channel depth, the mean depth also goes on increasing with an increase in distance from the source.

**ae. Channel capacity (Ca)**

The channel capacity of the Par River ranges between 322 $m^2$ and 4998 $m^2$. The average channel capacity is 1839 $m^2$. The existing channel sizes at different reaches of the Par River indicate that the flows of sufficient magnitude have occurred in the past to create such a large channel.

**af. Channel gradient**

Channel gradient decreases gradually with distance from the source. The average gradient of the Par River is 0.0691. Channel gradient, as expected, is steeper at waterfalls, rapids and in narrow bedrock reaches.

**b. Changes in hydraulic variables with discharge**

At-a-station hydraulic geometry has been established for a gauging site on the Par River. The analysis clearly shows that that, the rate of change in the mean velocity (m) is greater than the rate of change in the mean depth (f) and width (b). The b/f ratio given indicates that the rate of change in width is always lower than the rate of change in mean depth. For gauging site i.e. Nanivahial, the rate of change in width is low, and b/f ratio is 0.20. This is attributed to nearly rectangular shape of the channel at this cross section. The results, therefore, confirm the inferences drawn on the basis of the changes in width-depth ratio with discharge, that the increase in the discharge is primarily compensated by a remarkable increase in depth. This has important implications for efficiency of the channel since the flood power is directly related to the flow depth.

The ratio between the rate of change in velocity and rate of change in depth (m/f) is related to the transportation of sediment load (Leopold et al., 1964). The value of this ratio is higher for Nanivahial. The high ratio suggests that the rate of increase of velocity with discharge is much higher than the rate of increase of depth with

discharge. This fact implies that high flows are associated with an increase in the transportation capacity of the channels. The ratio, therefore, suggest that the capacity of the flows to transport sediments increases rapidly with discharge.

An important concept linked with hydraulic geometry is the Langbein's concept of minimum variance (Rhodes, 1987). The total variance is the sum of the square of the hydraulic geometry exponents. Calculation of the total variance value for the Nanivahial site reveals that the value is 0.57, and thus, is away from the theoretical minimum total variance, which is 0.333 (Rhodes, 1987). This suggests that at the site the effects of changes in discharge are not equally absorbed by all the three variables, but by one or two hydraulic geometry variables (Rhodes, 1987), in this case the value of velocity (0.71) is much higher and followed by depth (0.25). This behavior of the hydraulic variables can be attributed to the box-shaped appearance of the channel and to the cohesive nature of the bank material. This fact, therefore, suggests that the bedrock channel of the Par River behaves differently than alluvial channel, which is self-formed through the independent adjustment of the morphological variables (Leopold et al., 1964; Baker and Kale, 1998).

The hydraulic geometry exponents (b, f, and m) of the Nanivahial gauging station were plotted on Rhodes (1977) ternary diagram. The point is observed at 'm-corner' i.e. velocity corner. This suggests that the primary adjustment in channel form with increase in discharge is in the mean velocity. According to the location of the data points in the divisions of the ternary diagram, Par River falls in sector 2. In accordance with Rhodes (1977), such channel types are characterized by decrease in width-depth ratio, an increase in Froude number, and increase in velocity area ratio which in turn results in increased competence of river. This is also attributed to rectangular form, relative stability of bed and bank material, extremely cohesive banks and compact bed.

### 5.3 Limitations of the study

In the present study, every effort was made to generate the data which were not available, to collect all the available secondary data and to study all aspects of forms and processes of the bedrock channels. However, the study is not complete in all respects. Some of the major limitations of the present study have been outlined below.

1) The morphological features of bedrock channels have identified, classified and analyzed according to classification given by Wohl (1994), however, micro-scale (mm to cm) features such as abrasion, flaking or plucking of individual grains or small pieces of rock have only been observed and photographs have been obtained in the field.
2) Numerous straight reaches have been identified on Par and Nar Rivers in the field, however, reasons of formation of straight reaches have not been understood.
3) Although, wide range of literature on meander formation is available, the exact reasons of meander formation for the river under review could not be identified.
4) Large numbers of cross-sectional data are required to study channel form and other hydraulic processes systematically. However, due to strong opposition set by locals, field survey of only sixteen cross-sections could be achieved in difficult situation.
5) An ideal gorge at village Mendha have been identified on Par River, nonetheless, due to its inaccessibility, it was not possible to carry out cross-sectional survey. Although, detailed measurements were required to study this site thoroughly.
6) A huge numbers of potholes in the Par River channel have been identified from source to mouth and careful measurements of sizes and shapes of potholes have been carried out. However, due to its conspicuous quantity in the river channel, it was not possible to measure dimensions of all the potholes. The presence of grinding tools in the form of fine as well as coarse material in the potholes made difficult to measure the depth of potholes. In addition to this, sediment analysis of grinding tool of potholes has not been done. Besides, due to shape variance, it is difficult to classify potholes appropriately.
7) The longitudinal profile of the Par River has been constructed using toposheets.
8) A palaeochannel has been identified at village Mendha on Par River and mapped. It would have been more interesting if the age of the palaeochannel could be obtained.
9) Coarse sediment analysis of the Par River is mainly based on ten-largest boulders observed and measured in the field. More numbers of observations and measurements would have made it possible to understand the capacity of river to transport coarse sediment and to investigate its role in erosional processes and deposition of material.

10) The erosional processes such as abrasion and impact erosion were explained theoretically because it is most difficult task to study erosional processes of resistant channels in human time scale.
11) The analysis of the process i.e. knickpoint migration is based only on the study of two sites, however, more number of similar sites should have been analyzed to understand this process properly.
12) The Schmidt hammer was available for a very short period of time. Therefore, the resistivity of basalt as well as dyke is based on limited number of observations.
13) The hydrometeorological analysis is based on limited length of data (104 years). In addition to this, the data for the Surgana station were available only for 50 years.
14) Only one gauging site was established for the Par River at Nanivahial. Unfortunately, at present the site is out of order. Hence, the analysis of the flood hydrology of the Par River is based upon limited hydrological data (discharge) which is of very short duration i.e. forty-six years.
15) Hydraulic geometry of alluvial channel is not applicable to highly variable bedrock channels. Nonetheless, attempts have been made to establish hydraulic geometry equations for the bedrock channel of the Par River.

### 5.4 Major findings of the study

On the basis of analyses and results of the present study, following major findings can be outlined for the river under review.

1) The Par River displays all the classical morphological erosional as well as depositional features of the bedrock river.
2) The morphology of the bedrock channel reaches of the Par River dominated by erosional processes such as corrosion or abrasion, cavitation, shear detachment or fluid stressing, quarrying or plucking, hydraulic wedging and knickpoint migration. The river is supply limited, indicating unusually high ability to erode and transport coarse sediment.
3) The river shows substantial difference in erodibility between basalt and dykes. It is further proved by control of dykes on the channel of Par River. The basin, indeed, has undergone significant uplift till recent times and the consequences of tectonic activity have left noticeable imprints.

4) The Par River falls in the class of extraordinary hydrometeorological, hydrologic and geomorphic characteristics of floods which in turn results into noteworthy erosional processes, channel morphological features and bedrock incision.

**References**

Abbi, S.D.S., Jain, B.C., 1971. A study of major rainstorms of Tapi basin for evaluation of design storm. Indian Journal of Meteorology and Geophysics, 22, 203-212.

Alexander, H. S., 1932. Pothole erosion. J. Geol., 40, 305-337.

Alexander, J., 2008. Bedforms in Froude-supercritical flow. Marine and River Dune Dynamics, Leeds, United Kingdom, 1-5.

Allen, J.R.L., 1971. Transverse erosional marks of mud and rock: their physical basis and geological significance. Sediment Geology, 5,167-385.

Al-Taj, M., Shakour, F., Atallah, M., 2007. Morphotectonic indices of the Dead Sea transform, Jordan. Geogr. Fis. Dinam. Quat., 30, 5-11.

Angeby,O ., 1951. Pothole erosion in recent waterfalls. Lund Studies in Geography, Series A, Physical Geography, 2, 1951.

Aydin, A., Basu, A., 2005. The Schmidt Hammer in rock material characterization. Engineering Geology, 41, 1211-14.

Azor, A., Keller, E.A., Yeats, R.S., 2002. Geomorphic indicators of active fold growth: South Mountain-Oak Ridge anticline, Ventura basin, southern California. Geological Society of America Bulletin, 114 (6), 745-753.

Bagnold, R.A., 1980. An empirical correlation of bedload transport rates in flumes and natural rivers. Proceedings of the Royal Society of London, Series A, 372, 453-73.

Baker, V. R., Pickup, G., 1987. Flood geomorphology of the Katherine Gorge, Northern Territory, Australia, Geological Society Amer. Bull., 98, 635-646.

Baker, V.R., 1973 a. Erosional forms and processes for the catastrophic Pleistocene Missoula floods in the eastern Washington. Fluvial Geomorphology, Geomorphology publications, State University of New York, Binghamton, 123-148.

Baker, V.R., 1977. Stream channel response to floods with examples from central Texas. Geological Society of America Bulletin, 88, 1057-1070.

Baker, V.R., 1978. Large-scale erosional and depositional features of the Channeled Scabland. In: Baker., V.R., Nummedal, D. (Eds.), The Channeled Scabland. NASA, Washington D.C., 81-116.

Baker, V.R., 1984. Flood sedimentation in bedrock fluvial systems. In: Koster, E.H., Steel, R.J. (Eds.), Sedimentology of Gravels and Conglomerates, Mem. 10. Can. Soc. Pet. Geol., 87-98.

Baker, V.R., 1988. Flood erosion. In: Baker, V.R., Kochel, R.C., Patton, P.C. (Eds.), Flood Geomorphology. Wiley, New York, 81-95.

Baker, V.R., 1995. Global palaeohydrological change. Quaestiones Geographicae, 4, 27-35.

Baker, V.R., Costa, J.E., 1987. Flood power. In: Mayer, L., Nash, D. (Eds.), Catastrophic Flooding. Allen and Unwin, London, 1-21.

Baker, V.R., Kale, V.S., 1998. The role of extreme floods in shaping bedrock channels. In: Tinkler, K.J., Wohl, E.E. (Eds.), Rivers Over Rock: Fluvial Processes in Bedrock Channels, Geophysical Monograph Series. American Geophysical Union, Washington, D.C., 107, 153-165.

Barbour, R., 2008. Introducing Qualitative Research: A Student Guide to the Craft of Doing Qualitative Research. London, UK: Sage Publications Ltd.

Barnes, H.L., 1956. Caviatation as a geological agent. American General of Science, 254, 493-505.

Bates, R.E., 1939. Geomorphic history of the Kickapoo region, Wisconsin. Geol. Soc. America Bull., 50, 819-879.

Beckinsale, R.R., 1969. River regimes. In: Chorley R.J. (Ed), Water Earth and Man, London, 449-471.

Bedient, P.B., Huber, W.C., 1989. Hydrology and Floodplain Analysis. Addison-Wesley Publication Company, New York.

Bishop, P., Goldrick, G., 1992. Morphology, processes and revolution of two waterfalls near Cowra, New South Wales. Australian Geographer, 23, 116-121.

Bitter, J., 1963. A study of erosion phenomenon, Part II, Koninklijke/shell-Laboratorium, Amsterdam (Shell Internationale Research Maatschppij N.V). The Netherlands, 169-190.

Blank, H.R., 1958. Pothole grooves in the bed of the James River, Mason County, Texas. Texas J. Sci., 10, 293-301.

Bretz, J. H., 1924. The Dalles type of river channel. J. Geol., 24, 129-149.

Bretz, J.H., 1923. The Channeled Scabland of the Columbia Plateau. J. Geol., 31, 617-649.

Brice, J.C. 1964. Channel patterns and terraces of the Loup Rivers in Nebraska. U.S. Geological Survey Professional Paper 422 (D), 1-41.

Brocard, G.Y., Beek, V.D., Bourles, P.A., Siame, D.L., Mugnier, J.L., 2003. Long-term fluvial incision rates and postglacial river relaxation time in the French

Western Alps from Be-10 dating of alluvial terraces with assessment of inheritance, soil development and wind ablation effects. Earth and Planetary Science Letters, 209 (1-2), 197-214.

Bull, W., McFadden, L., 1977. Tectonic geomorphology north and south of the Garlock Fault California. In: Doehring, D.O., (Ed.), Geomorphology in Arid regions. Binghamton: State University of New York, 115-138.

Bull, W.B., 1978. Geomorphic tectonic activity classes of the south front of the San Gabriel Mountains, California. U.S. Geological Survey Contract Report, 14-08-001-G-394.

Bull, W.B., 1984. Tectonic geomorphology. Journal of Geological Education, 32, 310-324.

Burbank, D.W., Anderson, R. S., 2001. Tectonic geomorphology. Oxford, UK, Blackwell Publishing. http://dx.doi.org/10.1002/9781444345063.

Burn, D.H., Arnell, N.W., 1993. Synchronicity in global flood responses. Journal of Hydrology, 144, 381-404.

Carling, P.A., 1987. Hydrodynamic interpretation of a boulder-berm and associated debris-torrent deposits. Geomorphology, 1, 53-67.

Carling, P.A., 1989. Hydrodynamic models of boulder berm deposition. Geomorphology, 2, 319-340.

Carling, P.A., 1995. Flow-separation berms downstream of a hydraulic jump in a bedrock channel. Geomorphology, 1 (1), 245-253.

Cenderelli, D.A., Cluer , B.L., 1998. Depositional Processes and Sediment supply in Resistant-Boundary Channels: Examples from Two Case Studies. In: Tinkler, K.J., Wohl, E.E. (Eds.), Rivers Over Rock: Fluvial Processes in Bedrock Channels, Geophysical Monograph Series. American Geophysical Union, Washington, D.C., 107, 105-131.

Chatanantavet, P., Parker, G., 2009. Physically-based modelling of bedrock incision by abrasion, plucking and maco-abrasion. Journal of Geophysical Research, 114, http://F94918.doi:10.1029/2008JF001044.

Chen, Y., Sung, Q., Cheng, K., 2003. Along-strike variations of morphometric features in the western foothills of Taiwan: tectonic implications based on stream gradient and hypsometric analysis. Geomorphology, 56, 109-137.

Chiew, E., McMohan, T., 1993. Detection of trend or change in annual flow of Australian Rivers. International Journal of Climatology, 13, 643-653.

Chow, V.T., 1964. Handbook of Applied Hydrology. McGraw-Hill, New York.

Church, M., Jones, D., 1982. Channel bars in gravel-bed rivers. In: Hey, J.C., Bathurst, C.R., Thorne, C.R. (Eds.). John Wiley and Sons, London, UK. 291-324.

Cluer, B.L., 1995. Cyclic fluvial processes and bias in environmental monitoring, Colorado River in Grand Canyon. J . Geol., 103, 411-421.

Costa, J. E., 1974. Response and Recovery of a Piedmont Watershed From Tropical Storm Agnes. Water Resources Research, 10 (1), 106-112.

Costa, J.E., O'Connor, J.E., 1995. Gemorphologically effective foods. In: Natural and Anthropogenic Influences in Fluvial Geomorphology. Geophysical Monograph, 89, 45-56.

Cox, R.T., 1994. Analysis of drainage-basin symmetry as a rapid technique to identify areas of possible quaternary tilt-block tectonics: An example from Mississippi Embayment. Geological Society of America Bulletin, 106, 571-581.

Currado, C., Fredi, P., 2000. Morphometric parameters of drainage basins and morphotectonic setting of western Abruzzo. Memorie della Società Geologica Italiana, 55, 411-419.

de Jong, C., Ergenzinger, P., 1995a. The interrelations between mountain valley form and river-bed arrangement. In: Hickin E.J. (Ed), River Geomorphology. John Wiley and Sons, 55-91.

Dehbozorgi, M., Pourkermani, M., Arian, M., Matkan, A. A., Motamedi, H., Hosseiniasl, A., 2010. Quantitative analysis of relative tectonic activity in the Sarvestan area, central Zagros, Iran. Geomorphology, 121, 329-341.

Della Seta, M., 2004. Azimuthal transects of stream orientations: an advance in understanding the regional morphotectonic setting of eastern Abruzzo (Central Italy). Geografia Fisica e Dinamica Quaternaria, 27, 21-28.

Della Seta, M., Del Monte, M., Fredi, P., Lupia, P.E., 2004. Quantitative morphotectonic analysis as a tool for detecting deformation patterns in soft rock terrains: a case study from the southern Marches, Italy. Géomorphologie, 4, 267-284.

Dhar, O.N., Kulkarni, A.K., Sangam, R.B., 1984. Generalized 100-year point rainfall charts for the Narmada Basin for planning and design of medium size hydraulic structures. Proceedings of the Colloquium of 'Precipitation Analysis and Flood Forecasting'. IITM, Pune, 1-6.

Dhar, O.N., Nandargi, S., 1995. On some characteristics of sever rainstorms of India. Theoretical and Applied Climatology, 50, 205-212.

Dietrich, W.E., Smith, J.D., 1984. Bed load transportation in a river meander. Water Resourc. Res., 20, 1355-1380.

Dubinski, I.M., Wohl, E.E., 2005. Physical Model of River Erosion into Jointed Bedrock Through Quarrying. American Geophysical Union, Fall Meeting, #H53D-0516.

Duckson, D.W., Duckson, L.J., 1995. Morphology of bedrock step pool systems, Water Resour. Bull., 31(1), 43-51.

Eckley, M.S., Hinchliff, D.L., 1986. Glen Canyon Dam's quick fix. ASCE Civil Eng., 56, 46-48.

Elfstrom, A., 1987. Large boulder deposits and catastrophic floods. Geografiska Annalet, 69 (a), 101-121.

Elliot, C.M. (Ed.), 1984. River Meandering. Proceedings '83, New Orleans, Louisiana. American Society of Civil Engineers, New York.

Eltahir, E.A.B., 1996. El Niño and the natural variability in the flow of the Nile River. Water Resources Research, 32, 131-137.

Ely, L.L., Enzel, Y., Baker, V.R., Kale, V.S., Mishra, S., 1996. Changes in the magnitude and frequency of late Holocene monsoon floods on the Narmada River, central India. Geological Society of America Bulletin, 108 (9), 1134-1148. doi: 10.1130/0016-7606(1996)108<1134:CITMAF>2.3.CO;2.

Embleton, C., King, C. A. M., 1968. Glacial and periglacial geomorphology: New York. St. Martin's Press, 608.

Enzel, Y., Ely, L.L., House, P.K., Baker, V.R., 1993. Palaeoflood evidences for a natural upperbound to flood magnitudes in the Colorado Basin. Water Resources Research, 29, 2287-2297.

Ericson, K., 2004. Geomorphological surfaces of different age and origin in granite landscapes: an evaluation of the Schmidt test hammer. Earth Surface Processes and Landforms, 29, 495-509.

Ferguson, R.I., 1976. Disturbed periodic model for river meanders. Earth Surf. Process. Landforms, 1, 337-347.

Figueroa, A. M., Knott, J.R., 2010. Tectonic geomorphology of the southern Sierra Nevada Mountains (California): Evidence for uplift and basin formation. Geomorphology, 123, 34-45.

Finnegan, N.J., Roe, G., Montgomery, D.R., Hallet, B., 2005. Controls on the channel width of rivers: implications for modelling fluvial incision of bedrock. Geology, 33 (3), 229-232. http://doi:10.1130/G21171.1.

Font, M., Amorese, D., Lagarde, J.L., 2010. DEM and GIS analysis of the stream gradient index to evaluate effects of tectonics: The Normandy intra plate area (NW France). Geomorphology, 119, 172-180.

Fryirs, K., Spink, A., Brierley, G., 2009. Post-European settlement response gradients of river sensitivity and recovery across the upper Hunter catchment, Australia. Earth Surface Processes and Landforms, 25 (7), 904-928.

Fu, C., Fletcher, J., 1988. Large signals of climatic variations over the ocean in the Asian monsoon region. Adv. Atmos. Sci., 5, 389-404.

Gadgil, A., 2002. Rainfall characteristics of Maharashtra. In: Diddee, J., Jog, S. R., Kale V.S., Datye V. S. (Eds.), Geography of Maharashtra. Rawat Publications, Jaipur, 89-102.

Gannet, H. A., 1893. Manual of Topographic Methods. U. S. Geol. Surv. Monogr., 22.

Garde, R.J., Kothyari, U.C., 1990. Flood estimation in Indian catchments. Journal of Hydrology, 113, 135-146.

Gardner, T. W., 1983. Experimental study of knickpoint and longitudinal profile evolution in cohesive, homogeneous material. Geological Society of America Bulletin, 94, 664-672.

Garner, H.F., 1974. The Origin of Landscapes. Oxford University Press, New York, 734.

Garner, W. R., 1974. The processing of information and structure. Potomac, Md: Lawrence Erlbaum Associates.

Gilbert, G., 1877. Report on the geology of the Henry Mountains. Washington, D.C. U.S. Government Printing Office.

Giovanni, B., 2008. Stage–Discharge relationships in open channels: practices and problems. FORALPS Technical Report, Agency for Environmental Protection and Technical Services, Rome, Italy, 11, 2-32.

Glossary of American Meteorological Society, 1959. Link: https://www.ametsoc.org/ams/index.cfm/publications/glossary-of-meteorology/.

Goktan, R.M., Gunes, N., 2005. A comparative study of Schmidt hammer testing procedures with reference to rock cutting machine performance prediction. International Journal of Rock Mechanics and Mining Sciences, 42, 466-72.

Goode, J.R., Wohl, E., 2010. Substrate controls on the longitudinal profile of bedrock channels: implications for reach-scale roughness. Journal of Geophysical Research- Earth Surface, 115, F03018, http://dx.doi.org:10.1029/2008JF001188.

Goswami, D.C., 1985. Brahmaputra River, Assam, India: Physiography, basin denudation, and channel aggradation. Water Resources Research, 21, 959-978.

Goudie, A. S. (Ed.), 2004. Encyclopedia of Geomorphology, 1, A-I.

Goudie, A., 2006. The Schmidt hammer in Geomorphological research. Prog. Phys. Geogr., 30, 703-718.

Grant, G. E., 1997. Critical flow constrains flow hydraulics in mobile bed-streams, a new hypothesis. water Recourc. Res., 33, 349-358.

Gregory, S., 1989b. Macro-regional definition and characteristics of Indian summer monsoon rainfall, 1871-1985. International Journal of Climatology, 9, 465-483.

Güneralp, I., Abad, J.D., Zolezee, G., Hooke, J., 2012. Advances and challenges in meandering channels research. Geomorphology, 163-164, 1-9.

Gunjal, R.P., 2016. Rainfall characteristics of the Tapi basin. Unpublished Ph.D. Thesis, Tilak Maharashtra Vidyapeeth, Pune.

Gupta, A., 1983. High-Magnitude Floods and Stream Channel Response. In: Collinson, J.D., Lewin, J. (Eds.), Modern and Ancient Fluvial Systems. Blackwell Publishing Ltd., Oxford, UK. http://doi: 10.1002/9781444303773.ch17.

Gupta, A., 1988. Large floods as geomorphic events in the humid tropics. In: Baker, V.R., Kochel R.C., Patton, P.C. (Eds.), Flood Geomorphology. Wiley, New York, 301-315.

Gupta, A., 1995a. Magnitude, frequency, and special factors affecting channel form and processes in the seasonal tropics. In: Costa, J.E. Miller, A.J., Potter, K.W., Wilcock, P. (Eds), Natural and Anthropogenic influences in the Fluvial Geomorphology. American Geophysical Union, Washington, D.C., Monograph, 89, 125-136.

Gupta, A., Kale, V.S. Rajaguru, S.N., 1999. The Narmada River, India, through space and time. In: Miller, A.J., Gupta, A. (Eds.), Varieties of fluvial form. John Wiley and Sons Ltd., Chichester, 113-341.

Hack, J.T., 1973. Stream-profile analysis and stream-gradient index. U.S. Geological Survey, Journal Research 1(4), 421-429.

Hancock, G.S., Anderson, R.S., Whipple, K.X., 1998. Beyond power: bedrock river incision process and form. In: Tinkler, K.J., Wohl, E.E. (Eds.), Rivers Over Rock: Fluvial Processes in Bedrock Channels, Geophysical Monograph Series. American Geophysical Union, Washington, D.C., 107, 35-60.

Hare, P.W., Gardner, T.W., 1985. Geomorphic indicators of vertical neotectonism along converging plate margins, Nicoya Peninsula, Costa Rica. In: Morisawa, M., Hack, J.T. (Eds.), Tectonic Geomorphology. Proceedings of the 15th Annual Binghamton Geomorphology Symposium. Allen and Unwin, Boston, 123-134.

Hartshorn, K., Hovius, N., Dade, W.B., Slingerland, R., 2002. Climate driven bedrock incision in an active mountain belt. Science, 297, 2036-2038.

Heritage, G. L., Charlton, M. E., Regan, S. O., 2000. Morphological Classification of Fluvial Environments: An Investigation of the Continuum of Channel Types. Institute of Environmental Systems, Department of Geography, University of Salford, Greater Manchester M5 4WT, United Kingdom.

Hey, R.D., 1982. Design equations for mobile gravel-bed rivers. Gravel-bed rivers. John Wiley and Sons, Inc., New York, N.Y. 553-580.

Hirano, A., Welch, R., Lang, H., 2003. Mapping from ASTER stereo image data: DEM validation and accuracy assessment. ISPRS Journal of Photogrammetry and Remote Sensing, 57, 356-370.

Hire, P.S., 2000. Geomorphic and hydrologic studies of floods in the Tapi Basin. Unpublished Ph.D. Thesis, University of Pune, Pune, India.

Hire, P.S., Kale, V.S., 2006. Geomorphic effectiveness of high-magnitude floods on the Tapi River: Evaluation based on flood hydrographs and stream-power graphs. Transactions. Institute of Indian Geographers, 28(2), 175-182.

Hirschboeck, K.K., 1991. Hydrology of floods and droughts. National water summary 1988-1989 - Floods and droughts: Hydrology. U.S. Geological Survey Water-Supply paper, 2375, 76-88.

Hjalmarson, H. W., Phillips, J.V., 1997. Potential effect of translator waves on estimation of peak flow. J. Hyd. Eng., 123(6), 571-575.

Hjulstrøm, F., 1935. Studies of the morphological activity of rivers as illustrated by the River Fryis. Bulletin of the Geological Institute of Uppsala, 25, 221–527.

Holland, W. N., Pickup, G., 1976. Flume study of knickpoint development in stratified sediment. Geol. Soc. Amer. Bull., 87, 76-82.

Hollander, M., Wolfe, D.A., 1973. Nonparamentric Statistical Methods. John Wiley and Sons, New York. 192.

Hopkins, W., 1844. On the transport of erratic blocks. Trans. Cambridge Phil. Soc., 8(2), 220-240.

Hovius, N., Stark, C., 2001. Actively meandering bedrock rivers. American Geophysical Union, Fall Meeting, abstract #H52B-0389.

Howard, A.D., 1980. Thresholds in river regime, In: Coates, D.R., Vitek, J.D. (Eds.), Threshold in Geomorphology. Allen and Unwin, Winchester, 227-258.

Howard, A.D., 1987. Modelling fluvial systems: rock-, gravel- and sand-bed channels. In: Richards, K. (Ed.), River channels: environment and process, Basil Blackwell, Oxford, 69-94.

Howard, A.D., 1998. Long Profile Development of Bedrock Channels: Interaction of Weathering, Mass Wasting, Bed Erosion, and Sediment Transport. In: Tinkler, K.J., Wohl, E.E. (Eds.), Rivers Over Rock: Fluvial Processes in Bedrock Channels, Geophysical Monograph Series. American Geophysical Union, Washington, D.C., 107, 297-319. http://dx.doi.org/10.1029/GM107p0297.

Howard, A.D., Dietrich, W.E., Seidl, M.A., 1994. Modeling fluvial erosion on regional to continental scales. Journal of Geophysical Research, 99, 13971-13986.

Howard, A.D., Kerby, G., 1983. Channel changes in badlands. GSA Bulletin, 94(6), 739.

Husam, A.A., 2008. A test of the validity of morphometric analysis in determining tectonic activity from ASTER derived DEMs in the Jordan Dead Sea transform zone. Unpublished Ph.D. Thesis, University of Arkansas, USA.

Ihara, C., Kushnir, Y., Cane, M.A., De La Peña, V.H., 2007. Indian summer monsoon rainfall and its link with ENSO and Indian Ocean climate indices. International Journal of Climatology, 27(2), 179-187.

Inglis, C.C., 1937. The relationships between meander belts, distance between meanders on axis of stream, width, and discharge of rivers in flood plains and incised rivers: Ann. Rept. (Tech.), Central Board of Irrigation (India), 49, 1938-39.

Inglis, C.C., 1947. Meanders and their bearing on river training. Inst. Civ. Eng. (London), Mar. Waterways Eng. Div., Session 47 (7), 3-54.

Inglis, C.C., 1949. The behavior and control of rivers and canals: Central Waterpower Irrigation and Navigation Res. Sta., Poona, Res. Pub.13, 1and 2, 486.

International Society for Rock Mechanics (ISRM), 1978. Commission on standardization of laboratory and field tests. Suggested methods for determining hardness and abrasiveness of rocks. International Journal of Rock Mechanics and Mining Sciences Geomechanical Abstracts, 15, 89-97.

Jayappa, K.S., Markose V.J., Nagaraju, M., 2012. Identification of Geomorphic signatures of Neotectonic activity using DEM in the Precambrian Terrain of Western Ghats, India. International Archives of the Photogrammetry, Remote Sensing and Spatial Information Sciences, XXXIX-B8, XXII ISPRS Congress, Melbourne, Australia.

Jefferson, M., 1902. Limiting width of meander belts. Nat. Geog. Mag., 13, 373-384.

Kale V.S. and Gadgil, A., 1997. Evaluation of the flood hydrology in the upper Tapi Basin. Department of Science and Technology, report.

Kale, V.S., 1998. Monsoon floods in India: a hydro-geomorphic perspective. In: Kale, V.S. (Ed.), Flood studies in India. Geological Society of India, Memoir, 41, 229-256.

Kale, V.S., 1999b. Long-period fluctuations in Monsoon floods in the Deccan Peninsula, India. Journal of Geological Society of India, 53, 5-15.

Kale, V.S., 2005. The sinuous bedrock channel of the Tapi River, Central India: Its form and processes. Geomorphology, 70, 296-310.

Kale, V.S., Ely, L.L., Enzel, Y. Baker, V.R., 1994. Geomorphic and hydrologic aspects of monsoon floods on the Narmada and Tapi Rivers in central India. Geomorphology, 10, 157-168.

Kale, V.S., Ely, L.L., Enzel, Y., Baker, V.R., 1996. Palaeo and historical flood hydrology, Indian Peninsula. In: Branson, J. Brown, J.A., Gregory, K.J. (Eds.), Global Continental Changes: the context of Palaeohydrology. Geological Society Special Publication, London, 115, 155-163.

Kale, V.S., Gupta, A., 2001. Introduction to Geomorphology, Orient Longman Limited, Calcutta.

Kale, V.S., Hire, P. S., 2004. Effectiveness of monsoon floods on the Tapi River, India: Role of channel geometry and hydrologic regime. Geomorphology, 57, 275-291.

Kale, V.S., Hire, P.S., 2007. Temporal variations in the specific steam power and total energy expenditure of a monsoonal river: The Tapi River, India. Geomorphology, 92, 134-146.

Kale, V.S., Hire, P.S., 2007. Temporal variations in the specific stream power and total energy expenditure of a monsoonal river: the Tapi River, India. Geomorphology, 92, 134-146.

Kale, V.S., Mishra, S. Baker, V.R, Rajaguru, S.N., Enzel, Y. Ely, L., 1993b. Prehistoric flood deposits on the Choral River, central Narmada Basin, India. Current Sci., 65, 877-878.

Kale, V.S., Mishra, S., Baker, V.R., 2003. Sedimentary records of palaeofloods in the bedrock gorges of the Tapi and Narmada rivers, central India. Current Science, 84 (8), 1072-1079.

Kale, V.S., Shejwalkar, N., 2007. Western Ghat escarpment evolution in the Deccan Basalt Province: Geomorphic observations based on DEM analysis. Journal of Geological Society of India, 70, 459-473.

Kale, V.S., Shejwalkar, N., 2008. Uplift along the western margin of the Deccan Basalt Province: Is there any geomorphometric evidence? J. Earth Syst. Sci., 117(6), 959-971.

Kale, V.S., Shingade, B.S., 1987. A morphological study of potholes of Indrayani knick-point (Maharashtra). In: Datye, V.S., Diddee, J., Jog, S.R., Patil, C., (Eds.), Explorations in Tropics, Dr. Dikshit Felicitation Volume, Pune, 206-214.

Kane, R.P., 1989. Relationship between southern oscillation/El Niño and rainfall in some tropical and midlatitude regions. Proceedings of Indian Academy of science, 98, 223-235.

Katz, O., Reches, Z., Roegiers, J. C., 2000. Evaluation of mechanical rock properties using a Schmidt Hammer. International Journal of Rock Mechanics and Mining Sciences, 37, 723-28.

Kay, M., 1998. Practical Hydraulics. E. & F.N. Spon, London.

Kelkar, R.R., 2009. Monsoon Prediction. B S Publications, Hyderabad, India.

Keller, E.A., 1986. Investigation of active tectonics: use of surficial Earth processes. In: Wallace, R.E. (Ed.), Active tectonics. Studies in Geophysics. National Academy Press, Washington DC, 136-147.

Keller, E.A., Bonkowski, M.S., Korsch, R.J., Shlemon, R.J., 1982. Tectonic geomorphology of the San Andreas Fault zone in the southern Indio Hills, Coachella Valley, California. Geological Society of America Bulletin, 93, 46-56.

Keller, E.A., Pinter, N., 2002. Active Tectonics: Earthquakes, Uplift, and Landscape (2nd Ed.). Prentice Hall, New Jersey.

Kendall, M.G., 1955. Rank Correlation Methods. Hafner, New York. 54.

Khandekar, M.L., 1979. Climatic teleconnections from the equatorial Pacific to the Indian monsoon, analysis and implications. Arch. Meteor. Geophys. Biokal., A 28, 159-168.

Khole, M., 2004. Tele-connections between Indian summer monsoon rainfall on regional scale and sea surface temperature over equatorial Pacific Ocean. Mausam, 55(2), 293-304.

Kirby, E., Whipple, K., 2001. Quantifying differential rock-uplift rates via stream profile anaylsis. Geology, 29 (5), 415-418.

Knighton, D., 1998. Fluvial Forms and Processes. Edward Arnold, UK, 218.

Kobor, J.S., Roering, J.J., 2004, Systematic variation of bedrock channel gradients in the central Oregon Coast Range: implications for rock uplift and shallow landsliding. Geomorphology, 62 (3 to 4), 239-256.

Kochel, R.C., 1988. Geomorphic impact of large floods: review and new perspectives on magnitude and frequency. In: Baker, V.R., Kochel, R.C., Patton, P.C. (Eds), Flood Geomorphology. Wiley, New York, 169-187.

Korup, O., 2006. Rock-slope failure and the river long profile. Geology, 34(1), 45-48.

Kripalani, R.H., Kulkarni, A., 1997. Climatic impact of El Niño/La Niña on the Indian monsoon: A new perspective. Weather, 52, 39-46.

Krishnakumar, K.N., Prasada Rao G.S.L.H.V., Gopakumar, C.S., 2009. Rainfall trends in twentieth century over Kerala, India. Atmospheric environment, 43, 1940-1944.

Krishnan, R., Sugi, M., 2003. Pacific decadal oscillation and variability of the Indian summer monsoon rainfall. Climate Dynamics, 21, 233-242.

Lal, B., Lakshmanaswamy, B. Meena, L.R., 1993. Trends and periodicities of winter, monsoon and annual rainfall of districts of hills of west Uttar Pradesh. Vayu Mandal, 1, 28-34.

Lang, H., Welch, R., 1999. ATDB-AST-08 Algorithm Theoretical Basis Document for ASTER Digital Elevation Models (Standard Product AST14). Version 3.0. Jet Propulsion Laboratory (JPL), Pasadena, CA, 69.

Leopold, L. B., Langbein, W.B., 1966. River Meanders. Scientific American, 214, 60-70.

Leopold, L.B., Maddock, T. 1953. The hydraulic geometry of stream channels and some physiographic implications. United States Geological Survey Professional Paper, 252, 1-57.

Leopold, L.B., Maddock, T., Thomas, J. R., 1953. Hydraulic geometry of stream channels and some physiographic implications. U.S. Geo. Survey Prof. Paper, 252, 57.

Leopold, L.B., Wolman, G.M., 1957. River channel patterns: Braided, Meandering and Straight. Physiographic and hydraulic studies of rivers. Geological Survey Professional Paper, 288(B), 53.

Leopold, L.B., Wolman, M.G., 1960. River meanders. Geological Society of America Bulletin, 71, 769-793.

Leopold, L.B., Wolman, M.G., Miller, J.P., 1964. Fluvial processes in Geomorphology. Dover publications, INC. New York.

Lupia, P. E., Ciccacci, S., Civitelli, G., Corda, L., D'Alessandro, L., Del Monte, M., Fredi, P., Pugliese, F., 1995. Geomorfologia quantitativa e morfodinamica del territorio abruzzese. I. Il Bacino del Fiume Sinello. Geografia Fisica e Dinamica Quaternaria 18, 31-46.

Lupia, P.E., Biasini, A., Caputo, C., Centamore, E., Ciccacci, S., Del Monte, M., Fredi, P., Pugliese, F., 2001. Quantitative Geomorphology and Morphodynamics of the Abruzzo Region, Italy: III The drainage basin of the River Saline. Geogr. Fis. Dinam. Quat., 24, 157-176.

Lutgens, F.K., Tarbuck, E.J., 1995. The Atmosphere. Prentice Hall, Englewood Cliffs, New Jersey. USA.

Lutgens, F.K., Tarbuck, E.J., 2007. The Atmosphere. Prentice Hall, Englewood Cliffs, New Jersey, USA.

Maddock, T., 1976 III. A Primer on flood plain dynamics, Journal of Soil and Water Conservation, 31, 44-47.

Marengo, J.A., 1995. Variations and change in South American streamflow. Climate Change, 31, 99-117.

Martini, I.P., 1977. Gravelly flood deposits of Irvine Creek, Ontario, Canada, sedimentology 2 (4), 603-622.

Matmon, A., Enzel, Y., Zilberman, E., Heimann., 1999. Late Pliocene and Pleistocene reversal of drainage systems in northern Israel: Tectonic implications. Geomorphology, 28, 43-49.

Matthews, J.A., Shakesby, R.A., 1984. The status of the 'Little Ice Age' in southern Norway: relative age dating of Neoglacial moraines with Schmidt Hammer and lichenometry. Boreas, 13, 333-46.

Mayer, L., 1990. Introduction to quantitative geomorphology. An exercise manual. Englewood Cliff, Prentice Hall, New Jersey.

Merritts, D.J., Vincent K.R., Wohl, E.E., 1994. Long river profiles, tectonism, and estuary: a guide to interpreting fluvial terraces. J. Geophys. Res. (Special Issue on Tectonics and Topography), 99(B7), 14031-14050.

Merritts, D.J., Vincent, K.R., 1989. Geomorphic response of coastal streams to low, intermediate, and high rates of uplift, Mendocino triple junction region, northern California. Geological Society of America Bulletin, 101 (11), 1373-1388.

Miller, A.J., Cluer, B.L., 1998. Modeling considerations for simulation of flow in bedrock channels. In: Tinkler, K.J., Wohl, E.E. (Eds.), Rivers Over Rock: Fluvial Processes in Bedrock Channels, Geophysical Monograph Series. American Geophysical Union, Washington, D.C., 107, 61-104.

Miller, J. R., 1991. The influence of bedrock geology on knickpoint development and channel-bed degradation along downcutting streams in south-central Indiana, J. Geol., 99 (4), 591-605. https://doi.org/10.1086/629519.

Molin, P., Pazzaglia, F.J., Dramis, F., 2004. Geomorphic expression of active tectonics in a rapidly-deforming forearc. Sila Massif, Calabria, Southern Italy; American Journal of Science 304, 559-589.

Molnar, P., England, P., 1990. Late Cenozoic uplift of mountain ranges and global climate change: Chicken or egg?. Nature, 346, 29-34.

Monteiro, K.A., Missura, R., Correa, A.C.B., 2010. Application of the Hack Index-Or Stream Length-Gradient Index (SL Index)- to the Tracunhaem River Watershed, Pernambuco, Brazil, São Paulo, UNESP, Geociências, 29 (4), 533-539.

Montgomery, D.R., Abbe, T.B., Buffington, J.M., Peterson, N.P., Schmidt, K.M., Stock, J.D., 1996. Distribution of bedrock and alluvial channels in forested mountain drainage areas. Nature, 381.

Montgomery, D.R., Gran, K.B., 2001. Downstream variations in the width of bedrock channels. Water Resources Research, 37 (6), 1841-1846.

Mooley, D.A., Parthasarthy, B., 1984. Fluctuation of all-India summer monsoon rainfall during 1871-1978. Climatic Change, 6, 287-301.

Mooley, D.A., Shukla, J.M., 1987. Characteristics of the west-ward moving summer monsoon low pressure systems over the Indian region and their relationship with the monsoon rainfall. Center for Ocean-Land-Atmosphere Interactions. University of Maryland. USA, 1-47.

Moore, R. C., 1926. Origin of inclosed meanders on streams of the Colorado Plateau, Journal of Geology, 4, 29-57.

Morisawa, M.E., 1962. Quantitative geomorphology of some watersheds in the Appalachian Plateau. Geological Society of American Bulletin, 73, 1025-1046.

Morisawa, M.E., 1968. Streams: their Dynamics and Morphology. McGraw-Hill, New York.

Morisawa, M.E., 1985. Rivers: Forms and Processes. Longman, New York.

Mutreja, K.N., 1995. Applied Hydrology. Tata McGraw-Hill Publishing Company Ltd., New Delhi.

National Oceanic and Atmospheric Administration (NOAA), Climate Prediction Centre (CPC), http://www.cpc.ncep.noaa.geov/data/indices.

O'Connor, J. E., Webb, R.H., Baker, V.R., 1986. Paleohydrology of pool-riffle pattern development: Boulder Cr.eek, Utah. Geol. Soc. Amer. Bull., 97, 410-420.

O'Connor, J.E., 1993. Hydrology, hydraulics and geomorphology of the Bonneville Flood, Special Paper. Geol. Soc. Am., 274, 83.

Osborn, J.F., Stypula, J.M., 1987. New models of hydrological and stream channel relationships. In: Erosion and sedimentation in the Pacific Rim. IAHS, Oregon State Univ., Corvallis, 165.

Parthasarathy, B., Rupa Kumar, K., Munot, A.A., 1991. Evidence of secular variations in Indian monsoon rainfall-circulation relationship. Journal of Climatology, 4, 927-938.

Pazzaglia, F.J., Pederson, J.L., Koning, A.D., Toya, C., 1998. Geologic map and report of the Jemez Pueblo quadrangle, New Mexico, by U.S. Geological Survey. Open File Map, 000.

Peters, G., Van Balen, R.T., 2007. Tectonic geomorphology of the northern Upper Rhine Graben Germany. Global and Planetary Change, 58, 310-334.

Petts, G.E., Foster, I.D.L., 1985. Rivers and Landscape. Edward Arnold, London.

Pickup, G., Rieger, W.A., 1979. A conceptual model of the relationship between channel characteristics and discharge. Earth Surface Processes, 4, 37-42.

Pike, R.J., 2002. A bibliography of terrain modeling (geomorphometry), the quantitative representation of Topography. U.S. Geological Survey, Menlo Park, California, 02-465.

Powar, K.B., Patil, D.N., 1980. Structural evolution of the Deccan Volcanic Province: A study based on LANDSAT-1 imageries. Indian Geology Congress (Proceedings 3rd), Poona, 235-253.

Probst, J.I. Tardy, Y., 1987. Long range stream flow and world continental runoff fluctuations since the beginning of this century. Journal of Hydrology, 94, 289-311.

Rajaguru, S.N., Gupta, A., Kale, V.S., Mishtra. S., Ganjoo, R.K., Ely, L.L., Enzel, Y., Baker, V.R., 1995. Channel form and process of flood-dominated Narmada River, India. Earth Surface Processes and Landforms, 20, 407-421.

Rakhecha, P.R., 2002. Highest Floods in India. The Extremes of the Extremes: Extraordinary Floods (Proceedings of a symposium held at Reykjavik. Iceland). IAIIS 271, 167-172.

Ramaswamy, C., 1985. Meteorological aspects of sever floods in India (1923-1979). India Meteorological Department, New Delhi, 10 (MMH).

Rasmussen, E.M., Carpenter, T.H., 1983. The relationships between eastern equatorial Pacific sea surface temperature and rainfall over India and Sri Lanka. Monsoon Weather Review, 111, 517-528.

Rhodes, D.D., 1977. The b-m-f diagram: Graphical representation and interpretation of at-a-station hydraulic geometry. American Journal of Science, 277, 73-96.

Rhodes, D.D., 1987. The b-m-f diagram for downstream hydraulic geometry. Geografiska Annaler, 69(A), 147-161.

Richards, K., 2004. Rivers: Form and Process in Alluvial Channels. Caldwell, NJ: Blackburn Press.

Richardson, K., Carling, P.A., 2005. A Typology of Sculpted Forms in Open Bedrock Rivers. Geological Society of America, Special Paper 392. Geological Society of America: Washington, DC., 1-108.

Richardson, K., Carling, P.A., 2006. The hydraulics of a straight bedrock channel: Insights from solute dispersion studies. Geomorphology, 82 (1-2), 98-125.

Riehl, H., El-Bakry, M., Meitin, J., 1979. Nile River discharge. Mon.Weather Rev., 107. 1546-1553.

Robert, A., 2003. River Processes: An Introduction to Fluvial Dynamics. Arnold, London.

Rockwell, T.K., Keller, E.A., Johnson, D.L., 1985. Tectonic geomorphology of alluvial fans and mountain fronts near Ventura, California. In: Morisawa, M., Hack, J.T. (Eds.), Binghampton Symposia in Geomorphology International Series, NY: Tectonic geomorphology, 183-207.

Ropelewski, C.F., Halpert, M.S., 1987. Global and regional scale precipitation patterns associated with the El Niño/Southern Oscillation. Monthly Weather Review, 111, 517-528.

Rosgen, D.L., 1994. A classification of natural rivers. Catena, 22, 169-99.

Rosgen, D.L., 1996. Applied river morphology. Pagosa springs, colo, wildland, Hydrology.

Rostvedt, J.O., and Others, 1968. Summary of floods in the United States during 1963. Water Supply Paper, USGS, 120.

Saha, G.N., Sen Roy, S., Rajeswara Rao, V., 2007. Contrasting behaviour of Indian monsoon convection during ENSO years. Vayu Mandal, 33 (1-4), 87-93.

Sahu, M.L., 2004. Variation in annual rainfall of Vidarbha during the last century (1901-2003). Mausam, 55 (3), 497-502.

Schmidt, J.C., 1990. Recirculating flow and sedimentation in the Colorado River in Grand Canyon, Arizona. J. Geol., 98, 709-724.

Schumm, S.A., 1956. Evolution of drainage systems and slopes in Badlands at Perth Amboy, New Jersey. Bull. Geol. Soc. Amer., 67, 597-646.

Schumm, S.A., 1960. The shape of alluvial channels in relation to sediment type. U.S.G.S. Prof. Paper 3, 52 (B), 17-30.

Schumm, S.A., 1977. The Fluvial System. John Wiley & Sons, New York.

Schumm, S.A., Winkely, B.R., 1994.The character of large alluvial rivers. In: Schumm, S.A., Winkely, B.R. (Eds.), The variability of large Alluvial Rivers. American Society of Civil Engineering, New York, 1-9.

Seetharam, K., 2003. Inter annual and intra decadal behavior of monsoon rainfall over Jalpaiguri. Mausam, 54 (2), 539-560.

Seidl, M. A., 1993. Form and process in channel incision of bedrock. Ph.D. Thesis, University of California, Berkeley, California.

Seidl, M. A., Dietrich, W.E., 1992. The problem of channel erosion into bedrock. In: Schmidt, K.H., de Ploey, J. (Eds.). Functional Geomorphology. Catena Suppl., 23, 101-124.

Seidl, M.A., Finkel, R.C., Caffee, M.W., Hudson G.B., Dietrich, W.E., 1997. Cosmogenic isotope analyses applied to river longitudinal profile evolution: problems and interpretations. Earth Surf. Proc. Land., 22, 195-209.

Selby, M.J., 1993. Hillslope materials and processes. Oxford: Oxford University Press.

Sengupta, S., Kale, V. S., 2011. Evaluation of the role of rock properties in the development of potholes: A case study of the Indrayani knickpoint, Maharashtra. Journal of Earthsystem Science, 120, 157-165. http://dx.doi.org/10.1007/s12040-011-0005-5

Shaligram, V.M., Lele, V.S., 1978. Analysis of hydrologic data using Pearson Type III distribution. Nordic Hydrology, 9, 31-42.

Shaw, E.M., 1988. Hydrology in Practice. Van Nostrand Reibhold Int. Co. Ltd., London. 263-293.

Shepherd, R.G., 1979. River channel and sediment responses to bedrock lithology and stream capture, Sandy Creek drainage, central Texas. In: Rhodes, D.D., Williams, G.P. (Eds.). Adjustments of the Fluvial System, Kendall/Hunt, Iowa, 255-275.

Shepherd, R.G., Schumm, S.A., 1974. Experimental Study of river incision. Geol. Soc. Amer. Bull., 85, 257-268.

Sheth, H.C., 2007. Plume-related regional pre-volcanic uplift in the Deccan Traps: Absence of evidence, evidence of absence. In: Foulger, G.R., Jurdy, D.M. (Eds.), Plates, Plumes, and Planetary Processes. Geol. Soc. Am. Spec. Pap., 430, 785-813.

Shukla, J., Paolino, D.A., 1983. The Southern Oscillation and the Long-range forecasting of summer monsoon rainfall over India. Mon. Wea. Rev., 111, 1830-1853.

Sikka, D.R., 1980. Some aspects of large scale fluctuations of summer monsoon rainfall over India in relation to fluctuations in planetary and regional scale circulation parameters. Indian Acad. Sci. (Earth Planetary Sci.), 89, 179-185.

Silva, P.G., Goy, J.L., Zazo, C., Bardaj´I, T., 2003. Fault generated mountain fronts in southeast Spain: Geomorphologic assessment of tectonic and seismic activity. Geomorphology, 50, 203-225.

Simpson, H.J., Cane, S.K., Zebiak, S.E., 1993. Forecasting annual discharge of river Murray, Australia, from a geophysical model of ENSO. Journal of Climatology, 6, 386-390.

Sklar, L., Dietrich, W.E., 1998. River longitudinal profiles and bedrock incision models: Streampower and the influence of sediment supply. In: Tinkler, K.J., Wohl, E.E. (Eds.), Rivers Over Rock: Fluvial Processes in Bedrock Channels, Geophysical Monograph Series. American Geophysical Union, Washington, D.C., 107, 237-260.

Skylar, L. S., Dietrich, W. E., 2001, Sediment and rock strength controls on river incision into bedrock. Geology, 29(12), 1087-1090.

Springer, G. S., Tooth, S., Wohl, E. E., 2006. Theoretical modelling of stream potholes based upon empirical observations from the Orange River, Republic of South Africa. Geomorphology, 82, 160-176.

Springer, G.S., Wohl, E.E., 2002. Empirical and theoretical investigations of sculpted forms in Buckeye Creek Cave, West Virginia. Journal of Geology, 110, 469-481.

Srivastava, H.N., Sinha Ray., Dikshit, S.K., Mukhopadhyay., 1998. Trends in rainfall and radiation over India. Vayu Mandal, 28(2), 41-45.

Stark, C.P., 2006. A self-regulating model of bedrock river channel geometry. Geophysical Research Letters, 33. L04402. doi: 10.1029/2005GL023193.

Stock, J. D., Montgomery, D.R., 1999. Geological constraints on bedrock river incision using stream power law. J. Geophys. Res., 104(B3), 4983-4993.

Strahler, A.N., 1952. Hypsometric (area-altitude) analysis of erosional topography. Geological Society of America Bulletin, 63, 1117-1142.

Strahler, A.N., 1958. Dimensional analysis applied to fluvially eroded landforms. Geological Society of America Bulletin, 69 (3), 279-299.

Strahler, A.N., 1964. Quantitative Geomorphology of Drainage Basins and Channel Networks. In: Chow, V.T. (Ed.), Handbook of Applied Hydrology, McGraw Hill Book Company, New York, Section 4.II. Survey Journal of Research, 1, 421-429.

Subramanian, S.K., Palande, S.V., Dewan, B.N., Dikshit, S.K., Joseph, L., 1992. Trends and periodicities in sub-divisional rainfall. Mausam, 43 (1), 77-86.

Suresh, R., Mistry, R.D., Bhan, S.C., 1998. Variability of rainfall between Colaba and Santacruz. Vayu mandal, 28 (1), 18-24.

Thomas, R.G., 1993. Rome rainfall and sunspot numbers. Journal of Atmospheric and Terrestrial Physics, 55 (2), 155-164.

Tinkler, K.J., 1971. Active valley meanders in South-Central Texas and their wider significance. Geological Society of American Bulletin, 15, 1783-1800.

Tinkler, K.J., 1997a. Critical flow in rockbed streams with estimated values for Manning's n. Geomorphology, 20, 147-164.

Tinkler, K.J., 1997b. Indirect velocity measurement from standing waves in rockbed streams. J. Hyd. Eng., 123(10), 918-921.

Tinkler, K.J., Parish, J., 1998. Recent adjustments to the long profile of Cooksville Creek, an urbanized bedrock channel in Mississauga, Ontario. In: Tinkler, K.J., Wohl, E.E. (Eds.), Rivers Over Rock: Fluvial Processes in Bedrock Channels, Geophysical Monograph Series. American Geophysical Union, Washington, D.C., 107, 167-188.

Tinkler, K.J., Wohl, E. E., 1998. A primer of bedrock channels. In: Tinkler, K.J., Wohl, E.E. (Eds.), Rivers Over Rock: Fluvial Processes in Bedrock Channels, Geophysical Monograph Series. American Geophysical Union, Washington, D.C., 107, 1-18.

Toda, M., 1994. Bedrock channel erosion on the upper Obitsu, Boso Peninsula. A field experiment on the influence of a fissure on erosion, Geographical Review of Japan, 67A(1), 14-25.

Troiani, F., Della Seta M., 2008. The use of the Stream Length-Gradient index in morphotectonic analysis of small catchments: A case study from Central Italy. Geomorphology, 102, 159-168.

Turowski, J.M., 2010. Probability distributions of bedload transport rates: A new derivation and comparison with field data. Water Resour. Res., 46, W08501, http://doi:10.1029/2009WR008488.

Turowski, J.M., 2011. Probability distributions for bed form–dominated bed load transport: The Hamamori distribution revisited. Journal of Geophysical Research, 116: doi: 10.1029/2010JF001803.

Turowski, J.M., 2012. Semi-alluvial channel and sediment-flux-driven bedrock erosion. In: Churt, M., Biron, P.M., Roy, A.G. (Eds.), Gravel bed river: processes, tools, environments. Oxford, UK: John Wiley and Sons, Ltda Published, 401-416. http://dx.doi.org/10.1002/9781119952497.ch29.

Turowski, J.M., Hovius, N., Meng-Long, H., Lague, D., Men-Chiang, C., 2008. Distribution of erosion across bedrock channels. Earth Surf. Proc. Land., 33, 353-363.

Velázquez, V.F., Portela, V.D.A., Sobrinho, J.M.A., Guedes, A.C.M., Pletsch, M.A. J.S., 2016. Fluvial Erosion Characterisation in the Juqueriquerê River Channel, Caraguatatuba, Brazil. Earth Science Research, 5(2), 119-134.

Verrios, S., Zygouri, V., Kokkalas, S., 2004. Morphotectonic analysis in the Eliki fault zone (Gulf of Corinth, Greece). Bulletin of the Geological Society of Greece, 36, 1706-1715.

Viessman, W., Lewis, G.L., 2003. Introduction to Hydrology. Happer and Row Publishers, Singapore.

Viessman, W., Lewis, G.L., Knapp, J.W., 1989. Introduction to Hydrology. Happer and Row Publishers, Singapore.

Walker, G.T., 1924. Correlation in seasonal variation of weather. Further study of world weather, Memoirs. India Meteorological Department, 24 (IX-A), 275-332.

Ward, R., 1978. Floods: A Geographical Perspective. The MacMillan Press Ltd., London.

Weissel, J.K., Seidl, M.A., 1998. Inland propagation of erosional escarpments and river profile evolution across the southeast Australian passive continental margin. In: Tinkler, K.J., Wohl, E.E. (Eds.), Rivers Over Rock: Fluvial Processes in Bedrock Channels, Geophysical Monograph Series. American Geophysical Union, Washington, D.C., 107, 189-206.

Wells, S.G., Bullar, T.F., Menges, C.M., Drake, P.G., Kara, P.A., Kelson, K.I., Ritter, J.B., Wesling, J.R., 1988. Regional variations in tectonic geomorphology along a segmented convergent plate boundary, Pacific coast of Costa Rica. Geomorphology, 1, 239-365.

Whipple, K. X., 2001. Fluvial landscape response time: how plausible is steady state denudation?. American Journal of Science, 301, 313-325.

Whipple, K.X., 2004. Bedrock Rivers and the Geomorphology of Active Orogens. Annual Review of Earth and Planetary Sciences, 32, 151-185. http://DOI: 10.1146/annurev.earth.32.101802.120356.

Whipple, K.X., Hancock, G.S., Anderson, R.S., 2000a. River incision into bedrock: Mechanics and relative efficacy of plucking, abrasion and cavitation. Geological Society of America Bulletin, 112(3), 490-503.

Whipple, K.X., Snyder, N.H., Dollenmayer, K., 2000 b. Rates and processes of bedrock incision by the Upper Ukak River since the 1912 Novarupta ash flow in the Valley of Ten Thousand Smokes, Alaska. Geology, 28 (9), 835-838.

Whipple, K.X., Tucker, G.E., 1999. Dynamics of the stream-power river incision model; implications for height limits of mountain ranges, landscape response timescales, and research needs. Journal of Geophysical Research, 104 (B8), 17661-17674.

Whipple, K.X., Tucker, G.E., 2002. Implications of sediment-flux dependent river incision models for landscape evolution. J. Geophys. Res., 107(B2), 2039, http://doi:10.1029/2000JB000044.

Whittaker, A.C., Cowie, P.A., Attal, M., Tucker, G.E., Roberts, G.P., 2007. Bedrock channel adjustment to tectonic forcing: implications for predicting river incision rates. Geology, 35, 103-106. http://doi:10.1130/G23106A.1.

Widdowson, M., Mitchell, C., 1999. Large-scale stratigraphical, structural, geomorphological constraints for earthquakes in the southern Deccan Traps India: The case for denudationally driven seismicity. In: Subbarao, K.V. (Ed.), Deccan Volcanic Province, Bangalore. Geol. Soc. India Memoir, 43, 245-274.

Widdowson, M., 1997. Tertiary palaeosurfaces of the SW Deccan western India: Implications for passive margin uplift; In: Widdowson, M. (Ed.), Palaeosurfaces: Recognition reconstruction and palaeoenvironmental interpretation. Geol. Soc. Spec. Publ., London, 120, 221-248.

Widdowson, M., Cox, K. G., 1996. Uplift and erosional history of the Deccan Traps India: Evidence from laterites and drainage patterns of the Western Ghats and Konkan coast. Earth Planet. Sci. Lett., 137, 57-69.

Wiejaczka, L., Bucała, A., Sarkar, S., 2014. Human role in shaping the hydromorphology of Himalayan rivers: study of the Tista River in Darjeeling Himalaya. CURRENT SCIENCE, 106 (5).

Willett, S.D., 1999. Orogeny and orography: the effects of erosion on the structure of mountain belts. Journal of Geophysical Research. Solid Earth, 104 (B12), 28957-28981.

Williams, G. P., 1986. River meanders and channel size. Journal of Hydrology, 88, 147-164.

Williams, G.P., 1983. Paleohydrological methods and some examples from Swedish fluvial environments. I. Cobble and boulder deposits. Geografiska Annaler, 65(A), 227-243.

Wilson, A., 2009. Fluvial bedrock abrasion by bedload: process and form. PhD Thesis, University of Cambridge.

Wiltschko, D.V., Hassler, L., Hung, J., Liao, H., 2010. From accretion to collision: Motion and evolution of the Chaochou Fault, southern Taiwan. Tectonics, 29, TC2015, . http://doi:10.1029/2008TC002398.

Wobus, C.W., Crosby, B.T., Whipple, K.X., 2006a. Hanging valleys in fluvial systems: controls on occurrence and implications for landscape evolution. J. Geophys. Res. 111, F02017. . http://doi:10.1029/2005JF000406.

Wobus, C.W., Tucker, G.E., Anderson, R.S., 2006b. Self-formed bedrock channels. Geophys. Res. Lett. 33, L18408. http://doi:10.1029/2006GL027182.

Wohl, E. E., 2000. Substrate influences on step-pool influences in the Christopher Creek drainage, Arizona. J. Geol., 108, 121-129. doi:10.1086/314385.

Wohl, E.E., 1992a. Gradient irregularity in the Herbert Gorge of northeastern Australia. Earth Surface Processes and Landforms, 17, 69-84.

Wohl, E.E., 1992b. Bedrock benches and boulder bars: Floods in the Burdekin Gorge of Australia. Geological Society of America Bulletin, 104, 770-778. doi: 10.1130/0016-7606(1992)1042.3.CO;2.

Wohl, E.E., 1993. Bedrock channel incision along Piccaninny Creek, Australia. J. Geol., 101, 749-761.

Wohl, E.E., 1998. Bedrock channel morphology in relation to erosional processes, In: Tinkler, K.J., Wohl, E.E. (Eds.), Rivers Over Rock: Fluvial Processes in Bedrock Channels, Geophysical Monograph Series. American Geophysical Union, Washington, D.C., 107, 133-151.

Wohl, E.E., Achyuthan, H., 2002. Substrate Influences on Incised-Channel Morphology. The Journal of Geology, 110(1), 115-120.

Wohl, E.E., David, G.C.L., 2008. Consistency of scaling relations among bedrock and alluvial channels. Journal of Geophysical Research Earth Surface, 113, F04013.

Wohl, E.E., Grodek, T., 1994. Channel bed-steps along Nahal Yael, Negev desert, Israel. Geomorphology, 9, 117-126.

Wohl, E.E., Ikeda, H., 1997. Experimental simulation of channel incision into a cohesive substrate at varying gradients. Geology, 25, 295–298.

Wohl, E.E., Legleiter, C.J., 2003. Controls on pool characteristics along a resistant boundary channel. Journal of Geology, 111(1), 103-114.

Wohl, E.E., Merritt, D.M., 2001a. Bedrock channel morphology. Geol. Soc. Am. Bull., 113, 1205-1212. http://doi:10. 1130/0016-7606(2001)113<1205: BCM>2.0.CO;2.

Wohl, E.E., Thompson, D.M., Miller, A.J., 1999. Canyons with undulating walls. Geol. Soc.Am.Bull.,111, 949-959. http://doi:10.1130/00167606(1999)111<0949:CWUW>2.3.CO;2.

Wohl, E.E., Webb, R.H., Baker, V.R., Pickup, G., 1994. Sedimentary flood records in the bedrock canyons of rivers in the monsoonal region of Australia. Colorado State University. Water Resources Paper, 107, 102.

Wolman, M.G., Gerson, R., 1978. Relative scales of time and effectiveness of climate in watershed geomorphology. Earth Surface Processes, 3,189-208.

Wolman, M.G., Miller, J.P., 1960. Magnitude and frequency of forces in geomorphic process. Journal of Geology, 68, 54-74.

Wright, P.B., 1989. Homogenized long-period Southern Oscillation indices. International Journal of Climatology, 9, 33-54.

Yasar, E., Erdogan, E., 2004. Estimation of rock physicomechanical properties using hardness methods. Engineering Geology, 71, Elsevier, 281-288.

Zaprowski, B.J., Evenson, E.B., Pazzaglia, F.J., Epstein, J.B., 2001. Knickzone propagation in the Black Hills and northern High Plains: A different perspective on the late Cenozoic exhumation of the Laramide Rocky Mountains. Geology, 29(6), 547-550.

Zovoili, E., Konstantinidi, E., Koukouvelas, I.K., 2004, Tectonic geomorphology of escarpments: the cases of Kompotadses and Nea Anchialos faults. Bulletin of the Geological Society of Greece, 36, 1716-1725.